`

UNIVERSITY OF SOUTHAMPTON

NATURAL AND ENVIRONMENTAL SCIENCE

National Oceanography Centre

Diversity and extinction in Aepyornithidae

by

James Peter Hansford

A dissertation submitted to the University of Southampton in accordance with the requirements for award of the degree of Doctor of Philosophy in the Department of Ocean and Earth Science

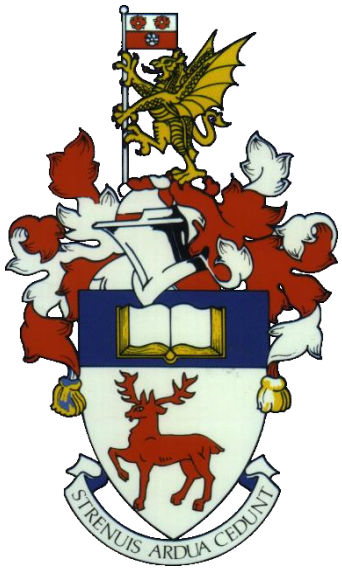

September 2017

`

UNIVERISTY OF SOUTHAMPTON

ABSTRACT

NATURAL AND ENVIRONMENTAL SCIENCE

Ocean and Earth Science

Thesis for the degree of Doctor of Philosophy

DIVERSITY AND EXTINCTION IN AEPYORNITHIDAE

by James Peter Hansford

The Aepyornithidae are an insular radiation of giant birds from the late Quaternary of Madagascar which have been extinct for c. 1000 years. Complex and conflicting historical taxonomic hypotheses have limited study into these charismatic megafauna and they have been subject to little modern study in comparison to other avian megafauna and the mammalian megafauna of Madagascar. This thesis is the first modern study of Aepyornithidae to quantify the diversity and biogeography of skeletal remains in comparison to putative taxonomic hypotheses. Clarifying the convoluted history of historically proposed taxa underpins a modern framework for studying these enigmatic birds. A novel chronological sequence of high-quality radiocarbon dates provides the most reliable evidence for their species-specific extinction timings. Late survival of these birds contrasts markedly with rapid extinction processes observed in avian megafauna and presents an extended period of co-occurrence with human colonists suggesting complex and poorly understood interactions. Recording and dating evidence of butchery to modern osteological standards has provided unique and extraordinary evidence of human settlement 6000 years earlier than any other evidence suggests, and is the first verifiable information on direct impacts of butchery and hunting of Aepyornithidae. Dietary analysis demonstrates that these morphologically diverse species fulfilled different ecological niches, including extensive grazing behaviour in the central highlands. This promotes the need for new discussions into the pristine landscape of Madagascar, including more expansive investigations into aepyornithid ecosystem functions and the pre-human distribution of grassland savannah versus forested regions. It is hoped that this thesis will lead to novel research into Aepyornithidae and develop understanding of their role in defining the natural state of one of the worlds most threatened ecosystems.

`

Table of contents

`

`

`

List of tables

Chapter one

Chapter two

`

Chapter three

Chapter four

Chapter five

`

List of figures

Chapter one

Chapter two

Chapter three

Chapter four

`

Chapter five

`

List of accompanying materials

`

DECLARATION OF AUTHORSHIP

I, JAMES PETER HANSFORD declare that this thesis “Diversity and extinction in Aepyornithidae” and work presented in it are my own and has been generated by me as a result of my own original research.

I confirm that:

1. This work was done wholly or mainly while in candidature for a research degree at this University;

2. Where any part of this thesis has previously been submitted for a degree or any other qualification at this University or any other institution, this has been clearly stated;

3. Where I have consulted the published work of others, this is always clearly attributed;

4. Where I have quoted from the work of others, the source is always given. With the exception of such quotations, this thesis is entirely my own work;

5. I have acknowledged all main sources of help;

6. Where the thesis is based on work done by myself jointly with others, I have made clear exactly what was done by others and what I have contributed myself.

Signed: ……

Date: ……

`

Acknowledgements

Firstly, I would like to thank my external supervisor Dr. Samuel Turvey, for giving me the support and guidance necessary to complete this thesis. Sam and I developed this project together in close collaboration and he has been my primary inspiration to study vertebrates of the late Quaternary. His enthusiasm, knowledge and critical perspective of taxonomy and evolution will stay with me for the remainder of my scientific career, for which I am truly grateful. I also wish to thank my previous supervisor Dr. Gareth Dyke, for creating the opportunity for me to study at the University of Southampton when all other doors were closed to me. I would like to extend my gratitude to my co-students at the University of Southampton (E. Martin-Silverstone, A. Roberts, J. Lawrence-Wujek and R. Gandola) and at the Institute of Zoology (J. Taylor and S. Dures); their support during the complications of conducting this PhD research project and thesis writing has been invaluable.

I would like to express thanks to Dr. David Errickson and Prof. Tim Thompson from Teesside University as well as Dr. Ventura Perez from the University of Massachusetts for their training and assistance in collecting osteoarchaeological data of butchery and hunting practices. Prof. Patricia Wright from the Stony Brook University and Prof. Laurie Godfrey from the University of Massachusetts have provided invaluable advice and critical review of some of the unexpected result of my thesis. Additionally, I would like to thank Prof. Armand Rasoamiaramanana from the University of Antananarivo for his support in obtaining destructive permissions for key specimens used in this thesis and making sure these specimens are available for future study in a secure museum collection.

This project was funded by the Institute of Zoology (Zoological Society of London) through core funds and a Daisy Balough travel award, the University of Southampton through core funds and a one year Mayflower scholarship. Funding for radiometric carbon dating was supported by a NERC Radiocarbon Facility grant.

I want to thank all of the institutions visited during this thesis and their curators for hosting me and supplying me with supporting information: NHM (Lorna Steele and Sandra Chapman), MNHN (Ronan Allain), PMO (Jorn Hurum), PMU (Benjamin Kear), MFN (Thomas Schossleitner), NHMW (Ursula Gohlrich), UA (Armand Rasoamiaramanana), CVB (Patricia Wright), NMNH (Mark Florence), AMNH (Carl Mehling), OUMNH (Mark Carnall).

`

I would like to extend special thanks to my Mother, Linda Hansford for her financial and motivational support as well as commissioning original artwork based upon my findings. Both of my parents, Linda and Stephen Hansford encouraged me to undertake a challenging career path, and without this advice I would not have undertaken this project. Without the concessions of my mother-in-law Mrs Felicitas Taylor I would not have been able to live and work in London and she deserves considerable thanks for this contribution.

Finally, I wish to dedicate this thesis to my wife, Kuki Taylor. Ms Taylor's ever present and incredible efforts to keep me alive, motivated and sane have been the driving force behind this thesis and as such, she has my undying gratitude.

`

Institutional abbreviations

AMNH: American Museum of Natural History, Washington DC, United States of America

CVB: Centre ValBio, Madagascar, Ranomafana, Madagascar

MFN: Museum für Naturkunde, Berlin, Germany

MNHN: Museum National d'Histoire Naturelle, Paris, France

MNZ: Museum of New Zealand Te Papa, Wellington, New Zealand

NHM: Natural History Museum, London, United Kingdom

NHMW: Naturhistorisches Museum, Vienna, Austria

OUMNH: Oxford University Museum, Oxford, United Kingdom

UA: University of Antananarivo, Madagascar

UIO/ PMO: Natural History Museum, University of Oslo, Norway

USNM: United States National Museum, New York, United States of America

ZIUU/ PMU: Zoologiska Museum, Uppsala University, Sweden

`

Chapter one

`

`

1.1 Late Quaternary Madagascar

Madagascar is one of the most intriguing and biologically diverse island ecosystems in the world. With numerous expansive interconnected biomes including montane, savannah, rainforest, semi-arid desert and wetland regions, it can be described as both an isolated island which separated from the Gondwanan super continent 100-130 million years ago and as a mini-continent, driving numerous scientific investigations into the biogeography and evolutionary history of its unique biota (Goodman et al. 2003).

Figure 1. Ecological zones and topography of Madagascar

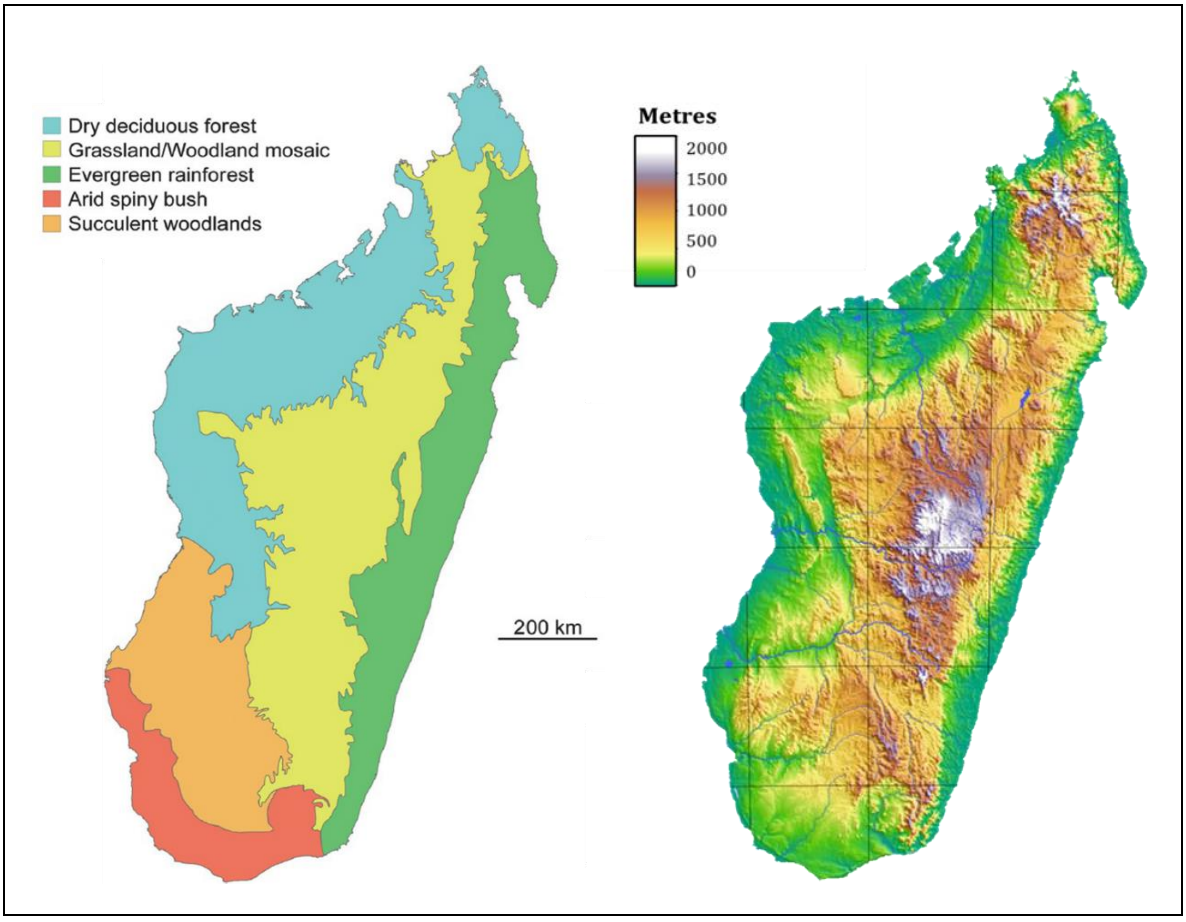

Adapted from (Yoder et al. 2016) Adapted from (Godfrey and Crowley 2016)

Current patterns of regional endemicity in floral and faunal communities are congruent with geographic barriers, including major rivers, indicating that hydrological conditions drive diversification of species. Regional hydrological differences act as a nutrient limitation of plant species, which in turn drives major differences in faunal communities. Regional hydrological regimes are created by the disparity of annual average precipitation levels, averaging 3500mm per annum in the tropical forests of the east and just 350mm in the semi-arid desert conditions

`

of the south. Seasonal rains arriving from the Indian Ocean disperse predominantly across the eastern mountain range and the central highland regions. The eastern side of the mountain range descends rapidly into the Indian Ocean, creating an intense hydrological regime which can support its dense rainforest. The western side of the island has a much shallower slope creating much slower flowing rivers that support a shifting matrix of succulent low-density forest and savannah ecosystems. The semi-arid desert of the south receives very little annual rainfall and an extremely limited wet-season (Dewar et al. 2007) (Figure 1).

With Madagascar's incredibly high endemic vascular plant diversity per km^2 (10,000-12,000 species) versus continental Africa (30,000-35,000 species) (Goodman and Benstead 2003) there are numerous floral communities that have been exploited by and have co-evolved with terrestrial vertebrate species (Guimarães et al. 2008; Midgley et al. 2009; Andriansaralaxa et al. 2013; Crowley et al. 2013). Following the focussed efforts of primatologists, the most well-known and studied of Madagascar's vertebrates are the extremely diverse lemurs, which are dispersed across modern forest remnants in all ecoregions. Whilst there are numerous other unique terrestrial vertebrate species still found in Madagascar such as fossa, tenrecs and crocodiles, the reality is that these represent only a fragment of the Quaternary vertebrate community in an ecosystem that has lost much of its interspecific functionality (Goodman et al.1997; Goodman et al. 2014).

The extraordinary and now extinct Quaternary vertebrate community of Madagascar is predominantly a subset of African taxa. The arrival of these taxa from continental Africa has often assumed to be through "rafting" colonization across the Mozambique channel (Krause et al. 1997). However, recent analysis of possible dispersal via this vector indicates that wind and current conditions are very unlikely to support this process, leading to uncertainty over the "rafting" hypothesis (Stankiewicz et al. 2006). It includes three families of lemurs (Palaeopropitecidae, Archaeolemuridae, Megaladapidae) including much larger animals such as *Archaeoindris fontoynontii* which is comparable to the size of a gorilla; three species of hippopotami, giant tortoises; and a family of ratites (Aepyornithidae) or "elephant birds" including the world's largest bird, *Vorombe titan* (Chapter 2). These animals arrived, adapted and dispersed across the landscape of the island in a staggered process, with the elephant birds being amongst the earliest known representatives of the "modern" Holocene community of the last 11,500 years within Cenozoic strata (Krause et al. 1997; Mitchell et al. 2014). Many of these species evolved unique ecological interactions to fulfil dietary niches that would otherwise be

`

occupied by African fauna that have not colonised the island, and constitute an important and missing part of this unique ecological network that remains poorly understood.

Following the onset of the widespread human colonisation, Madagascar has seen radical habitat transformations, through transformation of floral communities into agricultural pasture using fire, extensive deforestation, and exploitation of the native fauna through hunting (Goodman et al. 1997; Godfrey et al. 2016). The narrative of conservation and restoration of Madagascar's habitats has focussed on the impact of deforestation due to the success of primatologists in promoting the restoration of forest habitats and the use of lemurs as flagship species (Godfrey and Crowley 2016). The prevalence of the forested-island hypothesis has sparked continuing debate as to the "natural" ecological composition of the island as this hypothesis contrasts with much of the palynological record, which includes endemic grasses dating to the Miocene, and a sequence of stratified species consistent with a dynamic matrix of successional savannah, scrubland and forest communities throughout the late Quaternary (Goodman et al. 1997; Virah-Sawmy et al. 2008; Quéméré et al. 2012; Needham et al. 2015).

The dynamic succession of floral communities (pollen) and a low "natural" fire regime (charcoal particulates) in sedimentary records informs a hypothesis of regulation of plant matter by herbivores (Burney et al. 2003; Burney et al. 2004; Crowley et al. 2010). Faunal regulation of floral communities would likely have been dominated by megaherbivores (i.e. body mass of ≥44Kg) such as hippos, tortoises, elephant birds and the giant lemurs as larger bodied animals have a disproportionate impact on landscapes (Malhi et al. 2016). Hippos and giant tortoises have seen little ecological reconstruction as compared to the extinct lemur families (Godfrey et al. 2016), and due to extreme confusion of their diversity, distribution and ecology the elephant birds have been subject to extremely limited modern research. Clarification of the ecological dynamics of this megaherbivorous community is fundamental in interpreting pristine environmental conditions and determining restoration objectives for Madagascar.

Understanding the timing and tempo of extinction of these keystone species is also a vital component of interpreting ecosystem restoration targets through framing the decline of floral limitation and dispersal via herbivores (Guimarães et al. 2008; Wolf et al. 2013; Pires et al. 2014). Whilst generic dates for extinction starting at 1700 CE based upon the accounts of early European colonists have been widely reported, radiocarbon dating of palaeontological evidence suggests that many of these species were extinct hundreds of years earlier and some may have

`

survived as relictual populations into the European colonial or even post-colonial eras (Turvey 2009). With rapidly growing information on the presence and impact of humans in Madagascar throughout the Holocene (Dewar and Radimilahy 2013; Douglass 2016a) (also see Chapter 2), investigations into the causes and consequences of the decline of Malagasy megafauna requires the synthesis of palaeontological, palynological, archaeological and ecological data (Battistini et al. 1963). The majority of palaeontological data used to interpret this pattern currently concerns the extinct lemurs and omits other megafauna that were likely keystone species, and may have had different extinction dynamics and trajectories (Turvey 2009; Hansen et al. 2009; Crowley et al. 2011; Crowley et al. 2012).

This thesis aims to discuss the avian megafauna of Madagascar; the elephant birds. Despite the enormous interest created in this radiation of extinct ratites, there has been remarkably little modern research into their systematics, ecology and interactions with humans. This introduction aims to summarise the early research into these charismatic avian megafauna and to explain how their complex and poorly recorded taxonomy has restricted insights into their relevance to the Quaternary and contemporary ecosystems of Madagascar.

`

1.2 Madagascar's terrestrial avian megafauna: The elephant birds

During the early Cenozoic, the flying ancestors of elephant birds colonised the island of Madagascar (Mitchell et al. 2014). These birds diversified following the shift of hydrological and floral turnover in the mid-late Cenozoic (Grealy et al. 2017). By the late Quaternary these birds had evolved into a family of terrestrial ratites including species with enormous body sizes (>500 Kg) that produced the most massive eggs on record for any species at approximately 8-9 litres in volume (Saint-Hilaire 1851). They persisted into the second millennium of the Common Era, co-occurring on the island with human settlers for several thousand years (Goodman and Jungers 2014). By the time natural historians reached Madagascar from the Middle East and Europe, these avian megafauna had disappeared (Strickland 1849; Kay 2004). Their eggshell and skeletal remains were found and traded across the Indian Ocean and are likely to have inspired literature and art pertaining to mythical creatures, namely Sinbad's "Rukh".

1.2.1 Scientific discovery

The first published records of animals and remains that are likely to be elephant birds are from second-hand descriptions. Whilst it is difficult to verify these accounts, they are interesting points of anecdotal evidence that demonstrate that there was folk-knowledge of large birds and large eggs in Madagascar in the last few hundred years.

The first recorded account detailing a large bird comes from French colonial commandant of Madagascar, Etienne Flacourt (1607-1660) who was resident in Fort Dauphin in the extreme South of the island. His 1648 publication *"Histoire de la Grande Isle Madagascar"* details a second-hand account of the "Vorounpatra" (Vouron = bird, patra=Ampartes or the Mandrare basin of the Androy region). This bird was described as having keen vision, being too fast for men to catch and when approached "sought the loneliest of places" (Kay 2004).

A written description extracted from the diary of Mr. John Joliffe from 1848 (surgeon on the HMS Geyser) details an encounter by M. Dumarele with an enormous egg being used to transport rum on a boat in Port Leven. Dumarele was not able to purchase the egg but did purchase the contents and measured the liquid inside, finding it to be "13 wine quarts" in volume (over 9 litres by modern standards). The Sakalava who owned the egg stated that they were found extremely rarely, and seeing the forest dwelling birds that laid them was an even rarer occurrence (Strickland 1849).

`

The first remains to be studied by scientists were reported by Saint-Hilaire in 1851. A distal fragment of an avian tarsometatarsus and three eggs purchased recovered separately from the south coast of Madagascar by merchant captain M. Abadie were presented in France and the UK. Saint-Hilaire named these birds *Aepyornis maximus* (or "Greatest high-bird") and made note that these eggs were the largest example from any known species and the hind limbs were of similar but more robust morphology to moa (*Dinornis*). Coupled with both Flacourt's and Dumarele's accounts, he described these remains to be recently deposited in sand dunes and wetlands, indicating that at least some birds may have been alive in unexplored regions at that time (Saint-Hilaire 1851).

Saint Hillarie's hypothesis that the birds may not be extinct prompted several competing European expeditions to discover if there were any living examples (Last 1894; Major and Robert 1896). Whilst unsuccessful in finding a surviving individual or any viable eggs, these expeditions also incorporated archaeological and palaeontological investigations, yielding further examples of subfossil remains. As these specimens arrived in museum collections across Europe, scientists sought to describe the various morphotypes in their individual collections, describing new species and publishing comparative measurements to support their diagnoses. The majority of these species were described as distinct taxonomic units on the basis of the commonly preserved hind-limb elements, femora, tibiotarsi and tarsometarsi. However, as European collections were extremely limited in the mid-late 19th century, species were raised on that basis of unequivocal solitary elements (i.e. an eggshell fragment, a tarsometatarsus, or a femur) (Milne-Edwards and Grandidier 1869; Burckhardt 1893; Andrews 1894a; Milne-Edwards and Grandidier 1894).

Towards the end of the 19th century the proliferation of European missionaries in Madagascar and their construction of large buildings, led to the discovery of numerous examples of Quaternary megafauna including these giant birds (Rosaas 1893). With much larger collections available for study scientists in Germany, the United Kingdom and France described two new genera and a number of species. A "conflict of authority" arose between British scientist Andrews, and the French anatomists Milne-Edwards and Grandidier to describe the largest of these birds (Anderson 2013). It should be noted that Andrews' 1894 description of *Aepyornis titan*, preceded the more expansive review of aepyornithid diversity of Milne-Edwards and Grandidier by just a few weeks (Andrews 1894b; Milne-Edwards and Grandidier 1894).

`

1.2.2 Taxonomic revisions and confusion

In the early 20th century three studies examined the relevance of putative taxa, again using comparative measurements (Monnier 1913; Lamberton 1934), perceived ontogenetic stages (Lambrecht 1933), and size classes (Monnier 1913) perceived from distinct cranial specimens that had been accrued in collections. These revisions synonymised several taxa, reducing the known diversity to three species of the largest birds (*Aepyornis*) and four species of the more gracile birds (*Mullerornis*). Crucially, the original type specimen of *Aepyornis maximus* was not incorporated into these reviews, either as the specimen was missing from the Museum National d'Histoire Naturelle collection (MNHN, Paris) (as it is today) or it was deemed to be missing too many features to be of diagnostic value.

Modern understanding of elephant bird diversity and biogeography is commonly based upon these 20th century reclassifications, compiled by Pierce Brodkorb in 1963 (Brodkorb 1963). Brodkorb's published taxonomy and distribution data, was the aggregation of the conclusions of Monnier and Lambrecht, but excluded Lamberton's work on *Mullerornis grandis*. Whilst he did provide a well-supported assessment, he did not include any morphometric or descriptive data to diagnose the taxa. Consequently, most modern taxonomic frameworks including aepyornithids have been based on the broad size differences of genera, *Aepyornis* being very large and robust, and *Mullerornis* being much smaller and gracile.

Elephant birds and moa were the two 19th century popular-science rivals for the title of the "world's largest bird" with elephant birds being more broad but moa being slightly taller in stature (Owen 1852; Anderson 2013). Whilst systematic research continued on moa in the late 20th and early 21st centuries, through multivariate statistics, ontogenetic growth series, consideration of sexual dimorphism and eventually DNA sequences (Cracraft 1976b; Worthy and Scofield 2012), elephant bird systematics were subject to no further quantitative or qualitative review. Radical departures from 19th century systematics and taxonomy, demonstrating both a reduction in species diversity and an increase in the number of recognised genera, has cast doubt on the validity of the antiquated understanding of elephant bird diversity.

The cool climate of New Zealand degrades ancient DNA sequences slowly; contrastingly the tropical environment of Madagascar has provided a challenging environment for DNA preservation (Oskam et al. 2010). Through persistence and recent advances in analytical

`

methods, a small and highly fragmented series of DNA sequences are available for study and have been used to clarify ratite evolutionary patterns and dispersal to Madagascar (Mitchell et al. 2014). These recent efforts are impeded by the lack of knowledge of elephant bird diversity and the lack of capacity to differentiate morphotypes, again only referring to the two recognised genera, based upon large size differences. Furthermore, this bimodal taxonomy is inferred on the eggshell (thick = *Aepyornis*, thin = *Mullerornis*) used in comparative DNA studies (Oskam et al. 2010; Michael Parker Pearson 2010; Grealy et al. 2017), based on Saint Hillarie's original description of a skeletal element and multiple large eggs, which may not represent the same species (Saint-Hilaire 1851).

The poorly understood and complex taxonomic history of elephant birds has slowed progress in reconstructing their evolutionary history and ecological significance. The largest collection of their remains, including Lamberton's comparative series was held in the Queens Palace in Antananarivo, Madagascar (Fig. 2). Whilst there are a large number of specimens held in collections across Europe and the USA, and the University of Antananarivo, including several type specimens, their poor accession has left confusion as to the number in existence, where they were collected and their appropriate taxonomy.

Figure 2 : Aepyornithidae skeletons from the Queens palace, Antananarivo, Madagascar

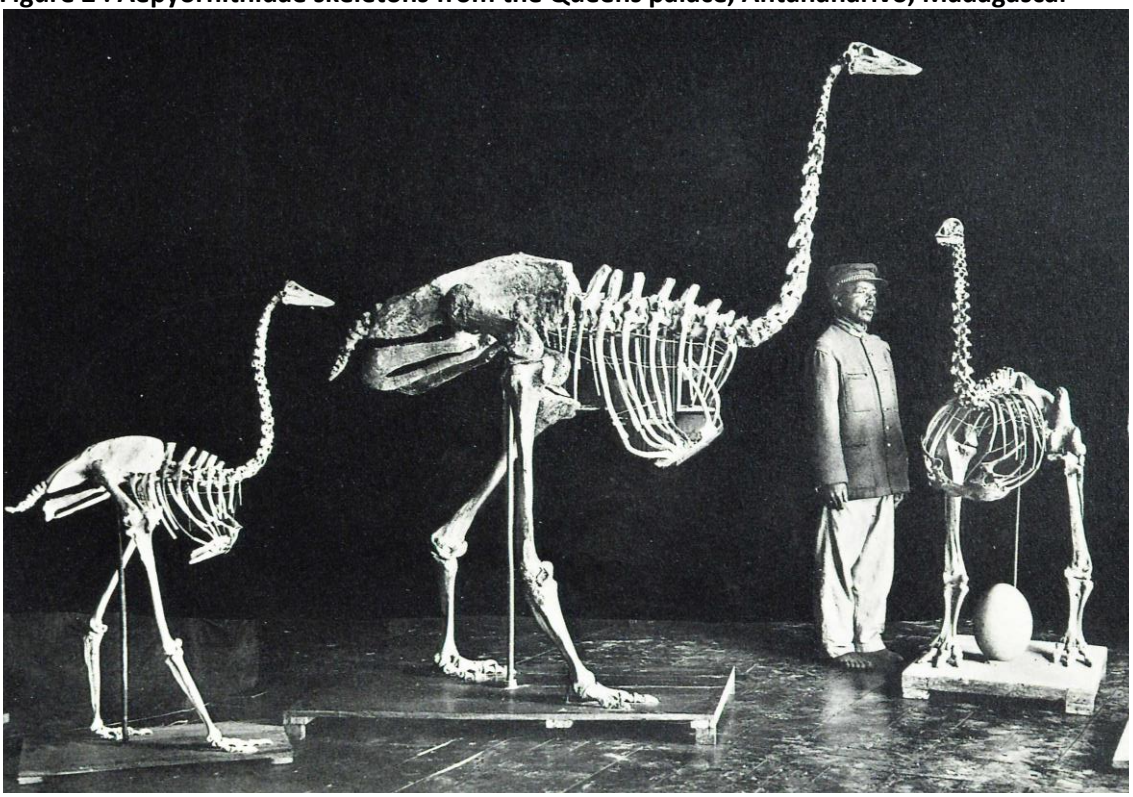

From left to right, *Mullerornis agilis, Aepyornis maximus, Aepyornis hildebrandti.* These specimens were destroyed during a fire in 1995.

`

1.3 19th and 20th century taxonomy of Aepyornithdae

Section 1.3 is a summary of the historically reported Aepyornithidae taxa, including brief descriptions of putative taxa as well as the linear measurements used in their diagnosis, published as part of their original descriptions, in chronological order. No accession details are included within the original publications and are therefore not recorded in this chapter.

Aepyornis maximus Saint-Hiliaire, 1851

Syntype specimens: 2 eggs, lower fragment of a left tarsometatarsus with 3 trochlear apophyses. (Specimens are unlabelled in the MNHN and mixed with other, similar egg specimens)

Location: Recovered from South Coast. Purchased from Merchant Captain M. Abadie.

Saint Hiliaire's description: Eggs and bone morphology appear to belong to an extremely large bird. (Table 1)

Table 1: Saint-Hiliarie's 1851 egg measurements

Measurement (mm)	Specimen 1	Specimen 2
Long diameter	340	320
Transverse diameter	225	230
Large circumference	850	840
Small circumference	710	720
Thickness	3	3
Volume (Litres)	N/A	8.88

In 1852, Richard Owen provided an additional description of the specimens providing comparison to the similarly sized *Dinornis* of New Zealand (Owen 1852). He noted that there was no rugose tract on the tarsometatarsus for the attachment of a hallux and an increasing concavity of the shaft similar to Cassowaries, but having a much narrower lateral margin. The width of the shaft was large in proportion to the trochleae and Owen noted this was a feature more similar to Cassowaries (*Casuarius* sp.) than Moa species known at the time. (Table 2)

Table 2: Owen's 1852 measurements of *Aepyornis maximus* tarsometatarsus vs. other ratites

Measurement (mm)	*Aepyornis maximus*	*Dinornis giganteus*	*Casuarius*
Extreme breadth across the trochlear condyles	127	142.2	58.42
Transverse diameter of shaft 6 inches above lower end	73.66	58.42	29.21
Antero-posterior diameter of shaft 6 inches above lower end	33.02	38.1	17.78

Family: *Aepyornithidae* Bonaparte, 1853

Charles Lucien Bonaparte lists *Aepyornis* within a novel family

`

Aepyornis grandidieri Rowley, 1867

Syntype specimens: 9 eggshell fragments. Excavated by Grandidier

Location: Cap Sainte Marie

Rowley's description: Air pores on *A. maximus* eggshell specimens have a "comet like tail". Specimens presented by Rowley have only small indentations with "no tail". The eggshell thickness is approximately half that of the *A. maximus* examples. Rowley describes *A. grandidieri* as a much smaller and delicate bird than *A. maximus.*

Aepyornis modestus (Milne-Edwards & Grandidier, 1869)

Type specimen: Portion of femur

Location: Amboulisatre, West Madagascar

Aepyornis medius Milne-Edwards & Grandidier, 1869

Type specimen: Femur

Location: Amboulisatre, West Madagascar

A. modestus and *A. medius* were described at the same time by Milne-Edwards and Grandidier. They distinguished these specimens as separate species as they were significantly smaller and had a narrower medial facia between the trochanter and the femoral neck than material that had been identified as *A. maximus*. *A. medius* is described as having a weakly defined intermuscular line. (Table 3)

Table 3: Milne-Edwards and Grandidier's femora measurements for *A. medius* *A. modestus* and *A. maximus* type specimens

Measurement (mm)	*A. medius*	*A. maximus*	*A. modestus*
Shaft circumference	215	270	120
Width at nutrient foramen	115	123	
Height of popliteal fossa	255	300	
Narrowest head width	50	58	
Width of the front fascia	76	90	
Width of the rear fascia	73	88	

`

Aepyornis hildebrandti Burckhardt, 1893

Syntype specimens: Tarsometatarsus, Tibiotarsus and Femur

Location: Central highlands/Antsirabe

Hildebrandt's description: Tarsometatarsus appears slim with a broad proximal articular surface. Specimens found by T.G Rosaas, donated to Hildebrandt and examined by Burckhardt, show dimensions that are not consistent with previously recognised material. *A. hildebrandti* measurements are in table 4. Tables 5 and 6 shows Burckhardt's comparative datasets.

Table 4 : Burckhardt's *A. hildebrandti* hind-limb bone measurements

Tarsometatarsus dimensions	**mm**
Length	275
Narrowest width of proximal end	110
Width of the proximal articular surface	95
Width of the distal articular surface	100
Narrowest width of the diaphysis	45
Middle trochlea width	43
Tibiotarsus dimensions	**mm**
Length	485
Shaft circumference	110
Width of the distal condyle	82
Width of the proximal condyle	130
Circumference of the distal condyle	240
Circumference of the proximal condyle	335
Femur dimensions	**mm**
Narrowest circumference of diaphysis	158
Nutrient foramen to base of the popliteal fossa	90
Width of the diaphysis	50
Width of the distal end	100

Table 5: Burckhardt's *Aepyornis* comparative femora measurements

Measurement (mm)	***A. maximus***	***A. medius***	***A. modestus***	***A. hildebrandti***
Shaft circumference	270	215	120	158
Nutrient foramen to base of the popliteal fossa	123	115		90
Width of the diaphysis at the narrowest point	90	76		50

NB: *A. modestus*, *A. medius* and *A. hildebrandti* measurements are from type specimens, whereas *A. maximus* femora was subsequently assigned to this taxon.

Table 6: Burckhardt's *Aepyornis* comparative tibiotarsus measurements

Measurement (mm)	***A. maximus***	***A. hildebrandti***
Length	640	485
Shaft circumference	155	110
Width of the proximal condyle	190	130
Width of the distal condyle	135	82

NB: *A. hildebrandti* measurements are from the syntype, whereas the *A. maximus* femora was subsequently assigned to this taxon

`

Aepyornis titan (Andrews, 1894)

Syntype specimens: Tibiotarsus, Femur (Upper part of trochanter and the anterior part of the condyles missing)

Location: Itampulu Ve

Andrew's description: Tibiotarsus diaphysis has slight inwards concavity. Anterior surface of distal 2/3 is flat and bounded by ridges on either side, medial ridge is stronger separating it from the lateral facia. Upper 1/3 is traversed by continuous lines aspersa to the lower end of the ecto-cnemial crest. Closely resembles *A. maximus* at fibula surface of attachment. The intercondylar surface is only slightly depressed and though faintly convex from side to side does not show the strong ridge as in *A. hildebrandti*. Femur neck is short and thick, anterior surface rugose. Upper articular surface of trochanter is flat and continuous with that of the head from which it slopes steeply upwards and outwards, widening. The trochanter projects considerably from the head, but does not form a crest strongly oriented forwards as in *Dinornis*. The articulation for the fibula is narrower than in *Dinornis.* Andrews' measurements for *A. titan* and his comparative material can be seen in Tables 7 and 8.

Table 7: Andrews' *Aepyornis* comparative tibiotarsus measurements

Measurement (mm)	***A. titan***	***A. maximus***	***A. hildebrandti***
Length	800	640	485
Width of distal end	170	135	82
Width of shaft at narrowest point	75	-	-
Circumference of shaft at narrowest point	207	155	110
Shortest antero-posterior diameter	45	-	-

NB: *A.titan measurements are taken from the syntype. A. hildebrandti* and *A. maximus* measurements are from Burckahrdt's published data (Table 6)

Table 8: Andrews' *Aepyornis* comparative femora measurements

Measurement (mm)	***A. titan***	***A. maximus***	***A. hildebrandti***
Length	415	320 (?true length)	-
Circumference of shaft at narrowest point	273	270	158
Width of shaft at narrowest point	92	91 (from cast)	50
Width of distal end (approx.)	210	190	100
Neck circumference	230	-	-

NB: *A.titan measurements are taken from the syntype. A. hildebrandti* measurements are from Burckahrdt's published data (Table 5) and *A. maxmimus* measurements are from a NHM cast of a specimen assigned to this taxon.

`

Aepyornis ingens Milne-Edwards & Grandidier, 1894

Syntype specimens: Tarsometatarsus, Tibiotarsus and Femur

Location: Unknown

Milne-Edwards and Grandidier's description: The largest *Aepyornis*, greatly exceeding the proportions of *A. maximus. A. ingens* likely shares an affinity with Andrews' *A. titan*. The tarsometatarsus has wide condyles. (Table 9)

Table 9: Milne-Edwards and Grandidier's *A. ingens* hind-limb bone measurements

Tarsometatarsus dimensions	**mm**
Length	420
Proximal width	180
Minimum shaft circumference	210
Tibiotarsus dimensions	**mm**
Length	910
Minimum shaft circumference	200
Femur dimensions	**mm**
Narrowest measurement	290
Circumference of ball	100

Aepyornis cursor Milne-Edwards & Grandidier, 1894

Type specimen: Tarsometatarsus

Location: Unknown

Milne-Edwards and Grandidier's description: Almost as large as material determined to be *A. grandidieri* but more slender. (Table 10)

Table 10: Milne-Edwards and Grandidier's *A. cursor tarsometatarsus* measurements

Tarsometatarsus dimensions	**mm**
Length	380
Width of proximal end	140
Width of distal end	120
Circumference of shaft	155
Width of shaft	68

`

Aepyornis lentus Milne-Edwards & Grandidier, 1894

Type specimen: Tarsometatarsus

Location: Unknown

Milne-Edwards and Grandidier's description: Short and massive feet. Measurements *A. lentus* are presented in table 11.

Table 11: Milne-Edwards and Grandidier's *A. lentus tarsometatarsus* measurements

Tarsometatarsus dimensions	mm
Length	360
Width of proximal end	150
Circumference of shaft	170
Width of shaft	68

Aepyornis mulleri Milne-Edwards & Grandidier, 1894

Syntype specimens: Skull, mandible, vertebrae, ribs; sternum, a part of the pelvis, the leg bones, and a few phalanges of the pes. Collected by M.G. Muller (MNHN)

Location: Antsirabe, Central Madagascar

Milne-Edwards and Grandidier's description: A smaller species than *A. ingens*, *A. cursor* or *A. lentus* but larger than *A. hildebrandti.* The skull is less flattened than *Dinornis* and much longer and narrower. Temporal pits are deep, but narrow. The hole on each side of the basiphenoid has a well-marked pterygoidal apophysis. The lower beak is straight, robust, similar to that of a Rhea, but the maxillary branches are higher and robust. The sternum is similar to that of *Apteryx*; it's a thin and flattened plastron. The coracoidal scapulars (shoulder girdles) are small and carry a very light joint indicating the presence of rudimentary forelimbs. The legs, although of different proportion are similar to *A. titan.*

`

Mullerornis Milne-Edwards & Grandidier, 1894

Genus description: Birds of medium size, not having the heavy and massive build of *Aepyornis*. They appear most similar to *Casuariidae.*

Mullerornis betsilei Milne-Edwards & Grandidier 1894

Syntype specimens: Tibiotarsus, Tarsometatarsus

Location: Antsirabe, Central Madagascar

Milne-Edwards and Grandidier's description: Tarsometatarsus is not as large as *Aepyornis* and the shaft has a triangular cross-section. Milne-Edwards and Grandidier's Measurements are presented in table 12. The bones are comparable in size and proportion to *Dromaius*.

Table 12: Milne-Edwards and Grandidier's *M. betsilei* hind-limb bone measurements

Tarsometatarsus dimensions	**mm**
Length of tarsometatarsus	310
Circumference of tarsometatarsus	80
Width of shaft of tarsometatarsus	27
Width of proximal end	70
Tibiotarsus dimensions	**mm**
Length of tibiotarsus	390
Circumference of tibiotarsus	90
Width of tibiotarsus	30
Width of proximal end	75
Width of distal end	60

Mullerornis agilis Milne-Edwards & Grandidier 1894

Type specimen: Tibiotarsus

Location: South-west Madagascar

Milne-Edwards and Grandidier's description: The tibiotarsus is remarkable for the marking of the intermuscular bony ridges and tendon grooves. The exterior border of the bone above the lower articular surface has developed into a pronounced crista. Measurements are presented in table 13.

Table 13: Milne-Edwards and Grandidier's *M. agilis* tibiotarsus measurements

Tibiotarsus dimensions	**mm**
Length of tibiotarsus	440
Circumference of tibiotarsus	97
Width of tibiotarsus	34
Width at proximal end	65
Width at distal end	70

`

Mullerornis rudis Milne-Edwards & Grandidier 1894

Type specimen: Tibiotarsus recovered by M. Greve. (MNHN)

Location: West Coast

Milne-Edwards and Grandidier's description: Similar length as *M. betsilei* but more massive with an enlarged distal end. The digital blocks are very large. There is a sluice between the central and lateral digits for the adductor tendon. Measurements are presented in table 14.

Table 14 : Milne-Edwards and Grandidier's *M. rudis* tibiotarsus measurements

Tibiotarsus dimensions	mm
Length of tibiotarsus	400
Circumference of tibiotarsus	100
Width of tibiotarsus	35
Width at proximal end	N/A
Width at distal end	75

Flacourtia Andrews, 1895

Differs from *Mullerornis* in having a completely ossified bony bridge over the lower end of the groove for the adductor of the outer digit in the tarsometatarsus.

Flacourtia rudis (Andrews, 1895)

Type specimen: Tarsometatarsus (NHM)

Location: Unknown

Andrews' Description: A **l**ong, slender right sided tarsometatarsus, which is perhaps that of *Mullerornis agilis*. 1: Anterior depression seems to disappear rather higher up the shaft than in the metatarsus of *Aepyornis* 2: The tubercule for the insertion of the tendon of the tibialis anticus is not very prominent, but the depression above it into which the foramina interossea opens is very deep. 3: the intermuscular ridges on the posterior surface are strongly marked, especially towards the distal end. A completely ossified bony bridge is present over the lower end of the groove for the adductor of the outer digit, a character absent in the tarsometatarsi of known *Aepyornis* species. This is present in *Mullerornis rudis* but not *M. betsilei* or *M. agilis.* Andrews proposed the generic name *Flacourtia for this specimen and for M. rudis specimens. Flacourtia* was characterised by greater proportionate stoutness and more powerful articulations of its limb bones. Measurements are presented in table 15.

Table 15: Andrews' *F. rudis* tibiotarsus measurements

Tarsometatarsus dimensions	mm
Length	280
Circumference of tarsometatarsus	85

`

Monnier and the revision of *Aepyornis*

In 1913, taxonomist L. Monnier (Monnier 1913) noted an extreme confusion in the nomenclature of *Aepyornis* due to the competitive nature of 19th century researchers and a poor understanding of morphological variance between individuals, ontogenetic stage and across populations. Monnier based his revisions on the most commonly available and best-preserved material, the hind limb bones of aepyornithid species. As seen above, these also included most of the comparative material from which species were originally described. Having excavated both left and right tarsometatarsi from what was reported to be a single *Aepyornis* sp. individual, he was able to record a 20mm difference in the total length from left to right. This led to the conclusion that if these extraordinarily large bones were scaled to the proportions of a chicken, then the putative morphometric delineation of several aepyornithid taxa would appear to be of no significance. He also went on to describe a new species, based upon a much more slender femur than had previously been described: *Aepyornis gracilis.*

Monnier reclassified specific groups based upon a more parsimonious model of broad size classes. *Aepyornis modestus* was transferred to *Mullerornis* as it was implicitly assumed to be conspecific to the genus *Mullerornis* based on circumference of femur shaft being 12cm, but the species name *modestus* was subsequently neglected as the femur could not be assessed against the holotypes of existing taxa (tarsometatarsi and tibiotarsi). *A. grandidieri* was revised to a junior synonym of *A. maximus* as it has only been described through egg-shell fragments and no comparison could be drawn against skeletal material. Monnier also attributed crania and their mandible material to these species. These skulls are pictured in figure 3 and Monnier's measurements are presented in tables 16-18 as the species based upon size to which he assigned them. Figure 4 is Monnier's sketch of the morphotypes of femora in the collection.

`

Summary of Monnier's taxonomic conclusions

Aepyornis maximus Saint-Hiliaire, 1851

Junior synonyms: *Aepyornis titan* (Andrews, 1894); *Aepyornis ingens* Milne-Edwards & Grandidier, 1894

Justification: Variation likely represents a continuous, normal distribution of size rather than delineated species.

Aepyornis medius Milne-Edwards and Grandidier 1869

Junior synonyms: *Aepyornis cursor* Milne-Edwards & Grandidier, 1894; *Aepyornis lentus* Milne-Edwards & Grandidier, 1894

Justification: Femur fragment of *A. medius* is clearly a different size distribution *to A. maximus (i.e. outside of natural variation)*. The tarsometatarsus from which *A. maximus* is originally described (Saint-Hilaire, 1851) is most likely an *A. medius.* The femurs of *A. lentus* and *A. cursor* fall into the continuous size distribution of *A. medius* and such are recorded as junior synonyms.

Monnier (1913, p. 138) also notes the possibility of geographic variation of *A. maximus* morphotypes. "Large and slightly more slender varieties are more frequent in lowland areas rich in limestone while in the central highlands, the size is generally stockier."

Aepyornis hildebrandti Burckhardt 1893

Junior synonyms: *Aepyornis mulleri* Milne-Edwards and Grandidier, 1894; *Aepyornis* sp.? Andrews, 1894

Justification: *Aepyornis mulleri* and Andrews's speculative species are considered as part of a continuous distribution as they are only slightly larger than *A. hildebrandti* and have no further basis of delineation.

`

Figure 3: Photographs of Aepyornis crania From Monnier 1913

1: *Aepyornis hildebrandti*, 2: *Aepyornis medius*, 3: *Aepyornis maximus*. Scale not given.

Table 16: Cranial measurements of *Aepyornis* species made by Monnier

Measurement (mm)	***A. maximus***	***A. medius***	***A. hildebrandti***
Maximum height of occipital foramen	22	19	16
Minimum width of occipital foramen	19	15	13
Width of occipital condyle	16	N/A	11
Height of occipital condyle	13	N/A	10
Distance between the two internal angles of the paraoccipital processes	60	50	43
Distance between the two external angles of the paraoccipital processes	110	100	76/78
Distance from the top of the occipital hole to the top of the skull	55	45	50
Distance from the center of the occipital condyles to the top of the skull	85	N/A	70
Width of the skull at the postorbital processes	125	108	83
Distance between the end of the beak and the occipital	325?	280	208
Height of the basal plane at the top of the skull	86	70	70
Length of branches of the lower mandible	280	257	176/191
Height of the mandible in the anterior third	23	17	14
Height of the mandible in the posterior third	34	30	24
Height from mandible to articular condyle	40	30	293
Angle made by the mandible	20°	20°	30°
Interval separating the optical holes	12	N/A	80

`

Table 17 : Tibiotarsi measurements of *Aepyornis* species made by Monnier

Measurement (mm)	*A. maximus*		*A. medius*		*A. hildebrandti*	
	Min	**Max**	**Min**	**Max**	**Min**	**Max**
Length	730	810	572	680	485	580
Circumference of the diaphysis	180	205	155	168	110	140
Width of the lower extremity	160	170	120	145	82	114
Width of upper extremity	210	255	158	195	130	170
Circumference of the lower extremity	470	490	365	425	260	350
Circumference of the upper extremity	545	595	412	490	310	430

Table 18: Tarsometatarsi measurements of *Aepyornis* species made by Monnier

Measurement (mm)	*A. maximus*		*A. medius*		*A. hildebrandti*	
	Min	**Max**	**Min**	**Max**	**Min**	**Max**
Length	420	480	330	380	275	303
Circumference of the diaphysis	190	215	160	180	110	140
Width of the lower extremity	175	185	120	135	95	115
Width of upper extremity	164	170	130	140	100	113
Width of middle trochlea	60	63	47	50	40	43

`

Aepyornis gracilis Monnier, 1913

Material: Femur

Location: Unknown

Monnier's description: The length is similar to *A. medius* but is more slender. It has many similarities with *A. hildebrandti.* The triangle formed by the popliteal fossa is more acute and elongated isosceles triangle with the height exceeding the base. Measurements are presented in table 19.

Table 19: Femora measurements of *Aepyornis* species made by Monnier

Measurement (mm)	*A. maximus*		*A. medius*		*A. hildebrandti*		*A. gracilis*
	Min	**Max**	**Min**	**Max**	**Min**	**Max**	
Length	410	465	330	368	240	320	322
Shaft circumference	270	285	210	240	158	195	170
Shaft width	78	92	58	77	50	60	51
Width of the lower extremity of the knee joint	188	210	150	168	101	130	130
Circumference of head	220	230	180	190	170	175	172

Figure 4: Monnier's sketches of femoral morphotypes of *Aepyornis*

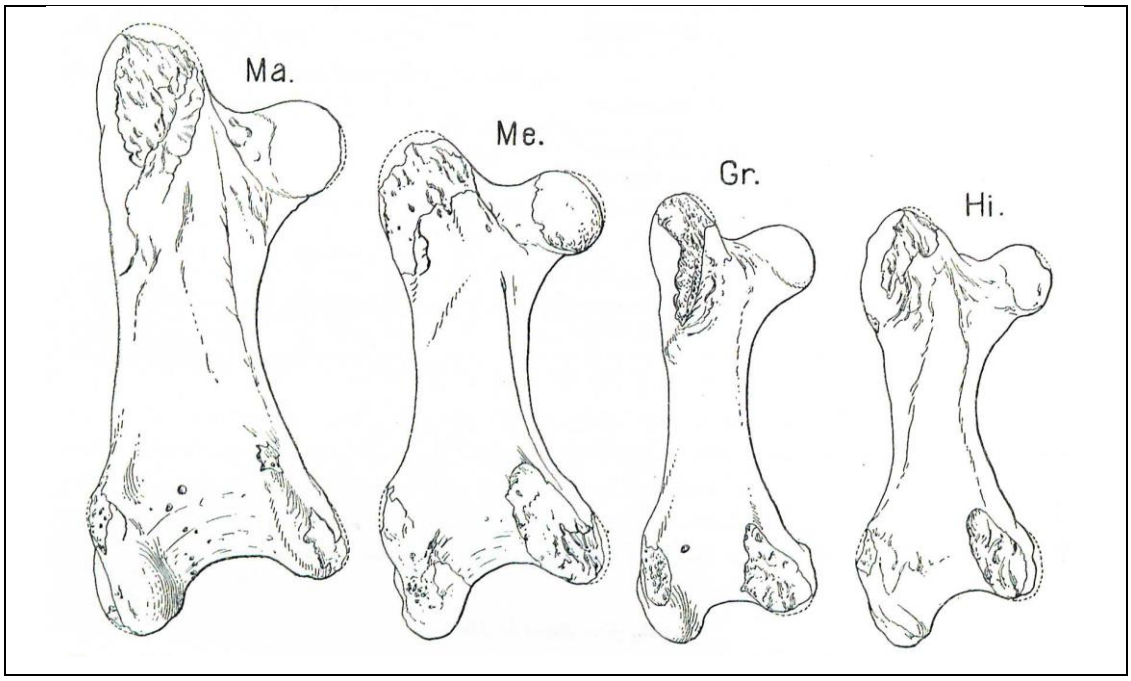

Ma.: *Aepyornis maximus*, Me.: *Aepyornis medius*, Gr.: *Aepyornis gracilis*, Hi: *Aepyornis hildebrandti*

`

Lamberton's *Aepyornis hildebrandti* crania

In 1930, Charles Lamberton described an aepyornithid skull recovered from Antsirabe which he associated with *A. hildebrandti* (Fig. 5). Whilst photographs of palaeontological specimens can be misleading, the cranium which Lamberton photographed and published appears to be a different morphotype to Monnier's example of *A. hildebrandti* (Fig. 3). As Monnier's association of crania to *A. maximus, A. medius* and *A. hildebrandti* based upon their relative size matching his delineated size classes from appendicular remains there is no evidence to accurately attribute any valid taxonomy. As both Monnier's and Lamberton's specimens are lost in the MNHN and to a fire respectively, we cannot assess the identity of these specimens. It is however important to note that there may be four different morphotypes of crania previously recorded, if not identified.

Figure 5: Lamberton's *Aepyornis hildebrandti* skull

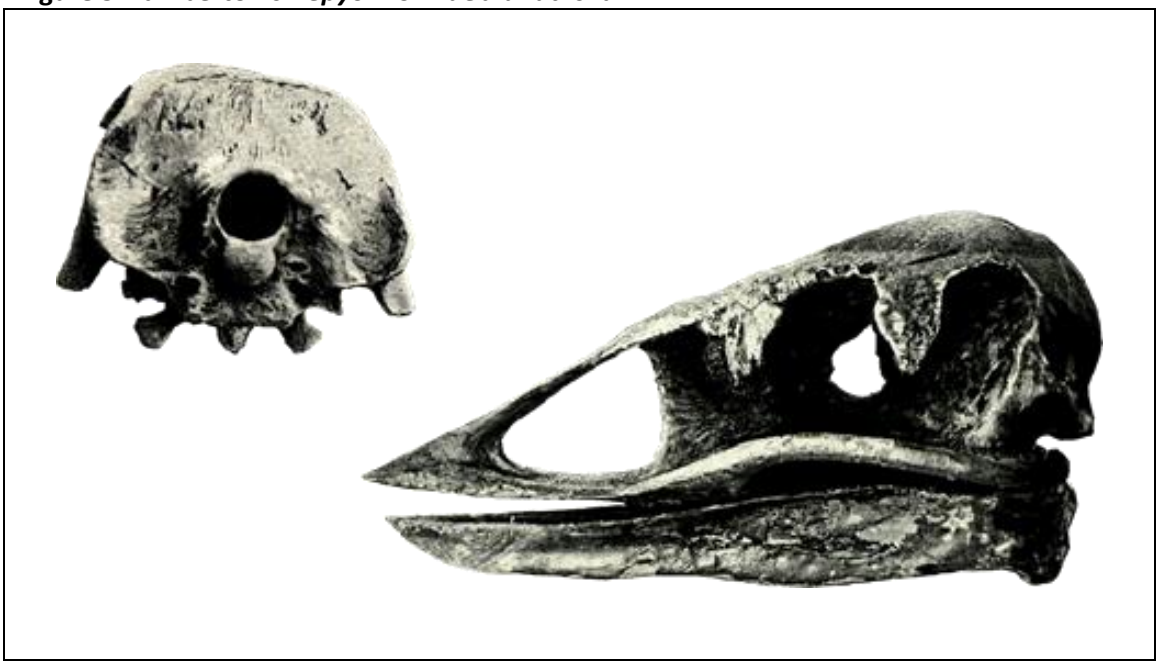

Scale not given.

`

Lambrecht and ontogenetic growth stages

In 1933, Kalman Lambrecht used European collections of *Aepyornis*, *Mullerornis* and *Flacourtia* in an attempt to develop the ontogenetic sequence of elephant bird hind limb bones. He used his findings to assess the validity of all described species and Monnier's revisions based upon size classes and their association with cranial specimens. As Lambrecht did not identify any accession numbers or other identifiers with his data, it remains unclear as to where his reported *Mullerornis agilis* skull came from or is currently stored.

Lambrecht assessed that Monnier was correct to highlight three size classes of *Aepyornis*, and the association of these to the sizes cranial specimens available at the time. However, he proposed that the type specimen of *Aepyornis modestus was* a juvenile and a subjective synonym of *Aepyornis maximus.* He also determined that the intercondylar ossified bridge on the tibiotarsus of *Flacourtia* was a common feature amongst *Mullerornis* species, and determined *F. rudis* to be a subjective synonym of *Mullerornis agilis.* Lambrecht's comparative measurements are presented in table 20.

Table 20: Lambrecht's comparative measurements of Aepyornithidae

Measurements (mm and degrees	***A. maximus***	***A. medius***	***A. hildebrandti***	***A. gracilis***	***M. betsilei***	***M. agilis***	***M. rudis***
Skull length	325	280	208			172	
Mandible angle	20^{o}	20^{o}	30^{o}				
Humerus length	92	72	67				
Femur length	410-470	330-368	240-320	322	235	270	270
Shaft circumference	270-285	210-240	158-195	170			
Tibiotarsus length	730-810	572-680	485-588		390	440	400
Shaft circumference	180-205	155-168	110-140				
Tarsometatarsus length	420-480	330-380	275-303		310? 273	300	

NB: Includes data collected by Monnier (1913)

`

Mullerornis grandis: Lamberton 1934

Material: Femur and tibiotarsi

Location: Central highlands/Antsirabe

Lamberton's description: Similar in morphology but considerably larger and more robust than other *Mullerornis* species.

Lamberton used specimens available in Madagascar, held at the Queen's palace, Antananarivo. This was perhaps the largest collection of aepyornithid remains in the world and was lost to a fire in 1995. Examples of Lamberton's comparative collection of ratites is pictured in figure 6 below. Lamberton's comparative measurements are presented in tables 21 and 22.

Table 21: Lamberton's comparative femora measurements of aepyornithids

Femora measurements (mm)	*Mullerornis grandis*			*Mullerornis agilis*			*Aepyornis hildebrandti*
	Max	**Min**	**Mean**	**Max**	**Min**	**Mean**	
Length of the top of the trochanter at the base of the external condyle	295	270	283	275	247	257	290
Length of the top of the head at the base of the internal condyle	231	210	225	214	181	203	234
Width of the proximal epiphysis	113	97	105	111	91	96	130
Width of the distal epiphysis	113	97	103	100	90	94	
Diameter of the head	39	35	37	39	32	35	45
Circumference of the diaphysis in the middle part	145	125	134	135	105	126	
Circumference of the diaphysis in the middle							105
Width of the lower epiphysis							130

Table 22: Lamberton's comparative tibiotarsi measurements of aepyornithids

Tibiotarsi measurements (mm)	*Mullerornis grandis*			*Mullerornis agilis*		
	Max	**Min**	**Mean**	**Max**	**Min**	**Mean**
Maximum length taken from the top of the spine	523	462	493	535	422	475
Length taken from the top of the table	486	430	459	497	397	445
Width of upper epiphysis	85	76	80.7	85	74	79.2
Width of the lower epiphysis	78	71	74.5	83	62	70.4
Minimum transverse diameter	41	35	37.1	42	32	31.9
Antero-posterior diameter at the same level	29	25	26.9	29	23	25.6
Circumference of the diaphysis at the same level	117	100	107.2	110	92	99

`

Figure 6: Photograph of examples from Lamberton's comparative material from (Lamberton 1934)

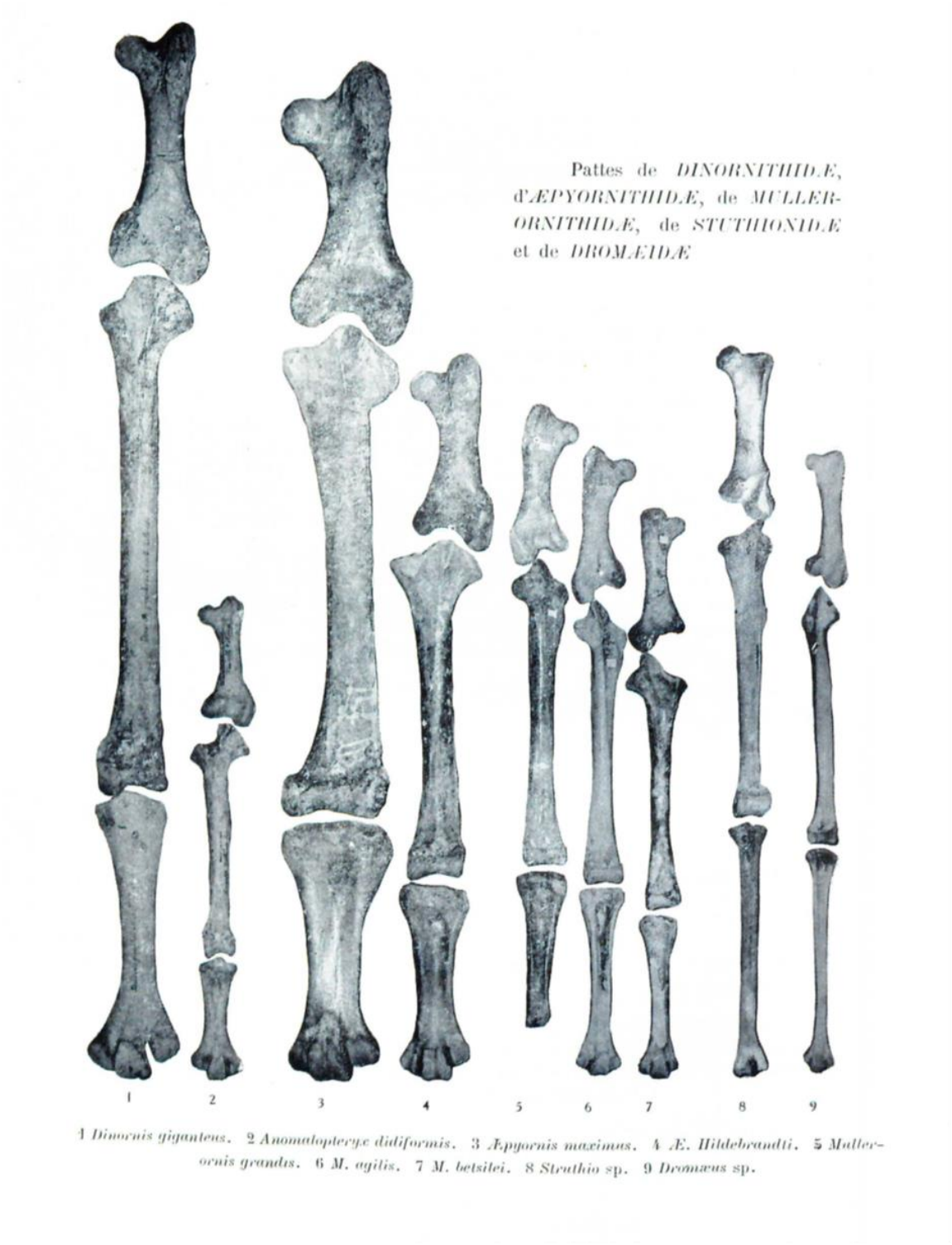

`

1.4 The biogeography of Aepyornithdae

Pierce Brodkorb's summary of Aepyornithidae taxonomy in 1963 included collected locations for type specimens and their synonymised junior taxa, based upon the revised descriptions by Monnier and Lambrecht. The collected locations indicate that *A. maximus* and *A. medius* are sympatrically distributed across the south and south west, and *A. hildebrandti* is restricted to the central highlands, near Antsirabe. *Aepyornis gracilis* is recognised by Brodkorb but has no known location data. Brodkorb's data showed that *M. agilis* and *M. rudis* were only present on the west coast, near Belo-sur-mer. *Mullerornis betsilei* is restricted to the central highlands near Antsirabe. *Mullerornis grandis* was not included in this review (Brodkorb 1963). Below are Brodkorb's summary of *Aepyornis* and *Mullerornis* as published in 1963.

***Aepyornis* (type *A. maximus*)**
A. maximus = *A. modestus* = *A. titan* = *A. ingens* (Ambolisatra, Masikoro, Mouroundava, between Belo-sur-mer and Moroundava, Itampulu Vé, Lamboharana)
A. medius = *A. grandidieri* = *A. cursor* = *A. lentus* (Cape Sainte-Marie; Belo-sur-mer and Moroundava)
A. hildebrandti = *A. mulleri* (Antsirabé)
A. gracilis (No precise localities)

***Mullerornis* (type *M. betsilei*)** = *Flacourtia* (type *F. rudis*)
M. betsilei (Antsirabé)
M. agilis (near Mouroundava)
M. rudis (Belo-sur-mer and Moroundava)

Material excavated after this review has extended the geographical range for *Mullerornis* to include eggshell fragments characterised as thin (~2mm thickness), found within the dry dune networks of the extreme south and south west. Fragments of both thick (*Aepyornis* sp. ~4mm thickness) and thin shell, found in these coastal dune networks are the most frequently studied remains of elephant bird. Archaeologists have sought to understand their significance through examining the age, preservation their chemical composition and anthropogenic modification. Whilst these formations of thousands of fragments were initially described as mass exploitation of eggs by humans (Saint-Hilaire 1851), most modern authors now consider them to be natural nesting sites and assume their autochthonous deposition following hatching (Oskam et al. 2010; Parker Pearson 2010; Douglass 2017).

`

1.5 Co-occurrence and conflict with humans

The timing and causes of extinction in elephant birds and other Malagasy megafauna has been a source of debate throughout their study, with scientists seeking to use evidence of human arrival and settlement to frame extinction hypotheses of anthropogenic modification of habitat and direct exploitation through hunting (Goodman et al. 1997; Burney et al. 2004; Goodman and Jungers 2014; Bakker et al. 2016). Understanding the distribution and contemporary habitats of elephant birds also defines our capacity to understand their ecological function (Clarke et al. 2006), environmental pressures (Mahe et al. 1972; Crowley et al. 2016), and the consequences of the loss of their interspecific interactions with floral and faunal communities (Bond and Silander 2007; Midgley et al. 2009). Recent years have seen a radical shift in our understanding of human arrival in Madagascar, extending the archaeological record into the mid-late Holocene (Dewar and Radimilahy 2013; Douglass 2016a). The extended overlap of human activity and survival of megafauna indicate a complex, and poorly understood extinction process. Examination of this extinction process must incorporate this new chronological sequence of events and requires a nuanced understanding of geological records, species distributions, and human activity (Battistini et al. 1963).

Reliable evidence for mid-Holocene human presence is restricted to just one archaeological site in the north west where the stratigraphic context of stone tools found in Lakatoni Anja cave were OSL (Optically Stimulated Luminescence) dated to c.4500 BP (R. Dewar and Radimilahy 2013). The earliest known signs of prolonged use of a rock shelter dates to c. 3000 BP on the south west coast at Velondriake, with middens indicating subsistence on coastal and marine resources (Douglass 2016b). Whilst knowledge of this early period is incomplete, current evidence shows no signs of agriculture or major habitat transformations (Burney, et al. 2003; Burney et al. 2004; Crowley et al. 2010).

Prior to the discovery of the stone tools from Lakatoni Anja, human arrival was determined to be c. 2400 BP, based upon direct radiocarbon dating of a *Palaeopropithecus ingens* femur from Taolambiby in the dry southern forest bearing tool marks with clear signs of anthropogenic modification during butchery. This hypothesis of recent and rapid human settlement was formerly supported by a shift in the charcoal records, just a few hundred years later (c. 1300-900 BP), as evidence of increased human activity associated with using fire to modify forest

`

habitats into agricultural pasture (Goodman et al. 1997; Burney et al. 2004; Crowley et al. 2010).

Recent analysis of human DNA collected from all regions of Madagascar indicates that the modern Malagasy people are the combination of mariners from Indonesia with an undefined arrival time and a later colonisation by African Bantu settlers c. 1500-1000 BP (Pierron et al. 2017). Widespread networks of human settlement appear in the archaeological record c.1000 BP onwards, with subsistence heavily reliant upon agricultural pasture (Crowley et al. 2010).

The accounts of Flacourt and Dumarele have driven ideas of extremely late survival of elephant birds in relictual populations surviving in deep forested areas after the arrival of European colonists c. 500 BP. As these accounts cannot be used as reliable sources of evidence for a contemporary sighting, the most reliable estimate for their extinction timing is based upon radiometric carbon dating of their subfossil remains. In 1963, Battistini produced the most recent evidence of their presence through a radiocarbon age estimate of c. 840 BP taken from a piece of thick eggshell (*Aepyornis maximus*), but this may be unreliable due to the poor sample preparation methods used at the time (Battistini et al. 1963). More reliable published aepyornithid radiocarbon dates are only slightly older than this estimate, indicating that at least some elephant birds were alive c. 1000 BP (Parker-Pearson et al. 1995; Parker-Pearson 2010). With at least 3500 years of co-occurrence of humans and elephant birds on Madagascar, interpretation of their extinction process cannot rely on the separation of two periods during the Holocene, before and after initial colonisation by humans (Goodman et al. 2014).

Although a record of past exploitation of subfossil lemurs has been compiled (Godfrey et al. 2016), the elephant birds have had little scrutiny of butchery impacts on bones indicating hunting pressures. Several radiocarbon dated examples of anthropogenically modified skeletal remains of elephant birds have been discussed in literature reviews of Madagascar's Holocene environment, but have not been recorded with photographic evidence or descriptions of modifications and are not available for examination in museum collections (Goodman et al. 1997; Burney et al. 2004).

With clear evidence of exploitation of complete eggshells being utilised as liquid carrying devices (Strickland 1849), discussion of elephant bird direct exploitation has focussed on the harvesting of eggs as a food source (Parker-Pearson et al. 1995; Parker-Pearson 2010; Douglass

`

2016a). The coastal dune systems of the south and south west are littered with aepyornithid eggshell fragments and these were initially interpreted to be vast archaeological midden sites (Saint-Hilaire 1851). However, due to the prodigious nature of these eggshells in the dune networks, they are now commonly interpreted as communal nesting sites and fragments have no evidence of being exploited as viable eggs (Parker-Pearson 2010; Goodman and Jungers 2014). Eggshell is found in archaeological midden sites and have been modified into beads, however radiocarbon dates from these specimens demonstrates that they are hundreds or even thousands of years older than the settlements themselves (Michael Parker Pearson 2010; Douglass 2016).

The lack of review of subfossil collections of elephant birds has led to confusion over the role of direct exploitation in their extinction process and has supported previous hypotheses of natural climate change being dominant extinction pressures (Parker Pearson 2010; Goodman and Jungers 2014). Developing a database of the morphology and age of anthropogenic modifications of elephant bird remains will clarify the role of humans in their extinction process and will contribute to the wider understanding of human presence and impact in Madagascar.

1.5.1 Sinbad's Rukh: Cryptic evidence for Madagascar's avian megafauna?

Throughout the history of research into elephant birds, from Etienne Flacourt to modern syntheses of Madagascar's megafauna, the enormous eggs of aepyornithids have been proposed to be the basis of stories of avian megafauna in fictional literature by comparison to the "Rukh" or "Roc" described in the Sinbad story cycle and reported in the accounts of Marco Polo (1254-1324)(Kay 2004; Goodman 2014). Polo describes a giant eagle type bird he personally witnessed on a trip to Madagascar "coming from the south", and details the gift of an impossibly large Rukh feather to Kublai-Khan. As Polo's expeditions to Madagascar may not have occurred, this account cannot be accepted as reliable evidence of avian megafauna. Although fictional accounts of animals will not hold up against even superficial scientific rigour, it is interesting to discuss the possibility that stories of humans interacting with giant birds may have influenced concepts of mythical animals and continue to promote intrigue in these poorly understood birds.

The earliest widely distributed version of the Sinbad story cycle was included in an iteration of the *kitāb ʾalf layla wa-layla* (The Arabian Nights) translated into French by Antoine Galland in 1701 (Muhawi 2005). The story cycle was an addition to the Middle Eastern compendium of

`

stories following the discovery of an unnamed manuscript in Constantinople reported to have been submitted in 1637 and is thought to be a Persian folk tale. The Rukh features in both the second and fifth voyages in the story cycle. The second voyage describes the Rukh as a giant bird big enough to carry an elephant within its talons and its enormous eggs the size of a house. The fifth voyage describes the Rukh from a desert island with giant eggs on its shores and flying birds that sank their ship by dropping large boulders carried in their talons. Whilst the origin of the use of "elephant bird" to describe Aepyornithidae is unclear, it is almost certainly drawn from the association of their giant eggs and skeletons to this work of fiction.

"An egg the size of a house" cannot be used as an accurate description of an elephant bird egg or any animal. However, elephant bird eggs are the largest example of any egg on record for any species alive or extinct, and their inclusion in this fictional tale may be exaggeration of a factual account of eggs in the sand dune networks of Madagascar where their fragments can still be found today. The description of an adult, flying, eagle-like bird, does not match the morphology and terrestrial ecology of adult aepyornithids, but perhaps is again an exaggeration in the size of the giant Malagasy crowned eagle *Stephanoaetus mahery* which had a four-metre wing span and was much larger than any eagle alive today (Goodman 1994).

Whilst the description of the Rukh has clearly inspired research into the intriguing avian megafauna of Madagascar, these accounts are clearly inaccurate and cannot be attributed to any subfossil or extant animal with certainty. Middle Eastern trade networks were active in Madagascar up to the 13th century and this may account for the origin of the avian megafauna narrative in Sinbad's voyages. It is perhaps more interesting to examine the lack of description of an adult elephant bird, indicating that this narrative may have started after their extinction, as their eggs remained important cultural artefacts. Unfortunately, whilst the *Kitab al-Hayawan* (The Book of Animals) describes and depicts images of many East-African fauna, neither contemporary or extinct animals from Madagascar are included as early middle eastern natural historians did not visit the island (al-Jahiz and Kopf 1953).

`

1.6 Thesis aims

Now extinct Pleistocene megafauna had a disproportionately large impact on ecological networks in pristine, pre-Anthropocene continental and insular ecosystems. The island of Madagascar is recognised to be one of the most biologically diverse and threatened ecosystems in the world, driving international interest in the conservation and restoration of its unique flora and fauna. The islands radiation of giant birds, Aepyornithidae were a topic of interest to academics and popular scientists during the 19th century but have seen remarkably little modern research into their ecological significance in comparison to avian and mammalian megafauna.

Attempts at modern research into Aepyornithidae have been heavily restricted by the complex and poorly understood historical taxonomy associated with skeletal and eggshell remains. Without an accurate systematic framework to explain the diversity of aepyornithid taxa, we cannot progress the narrative of their subsistence strategies that have co-evolved with numerous plant species and environmental change.

This thesis aims to review and evaluate long standing hypotheses of aepyornithid familial systematics, comparing distinct morphotypes with type specimens and series of putative taxa. Location data associated with distinct morphotypes will be collated and used to support novel understanding of the distribution of these birds across Madagascar.

Creating a chronological record for the persistence and extinction of Aepyornithidae underpins our capacity to understand their contemporary environments and to compare their extinction timing with natural and anthropogenic pressures.

This thesis aims to understand the contemporary environments of Aepyornithidae by providing accurate estimates of their age and their extinction timing by reviewing pre-existing data and creating novel datasets. Comparing this data with records of environmental and anthropogenic change throughout the Holocene will provide insight into their ecology, extinction processes, and promote new studies into quantifying the contemporary ecological consequences of the extinction of these avian megafauna.

`

`

Chapter two

`

`

Chapter two

Unexpected diversity within the extinct elephant birds (Aves: Aepyornithidae), and a new identity for the world's largest bird

2.1 Abstract

Madagascar's now-extinct radiation of large-bodied ratites, the elephant birds (Aepyornithidae), has been subject to little modern research compared to the island's mammalian megafauna and other late Quaternary giant birds. The family's convoluted and conflicting taxonomic history has hindered accurate interpretation of morphological diversity, and has restricted modern research into their evolutionary history, biogeography and ecology. We present a new quantitative analysis of patterns of morphological diversity of aepyornithid skeletal elements, including material from all major global collections of aepyornithid skeletal remains, and constituting the first taxonomic reassessment of the family for over 50 years. Linear morphometric data collected from appendicular limb elements, and including nearly all type specimens, were examined using multivariate cluster analysis and the Bayesian Information Criterion, and with estimation of missing data using multiple imputation and expectation maximisation algorithms. These analyses recover three distinct skeletal morphotypes within the Aepyornithidae. Two of these morphotypes are associated with the type specimens of the existing genera *Mullerornis* and *Aepyornis*, and represent small-bodied and medium-bodied aepyornithids respectively. *Aepyornis* contains two distinct morphometric subgroups, which are identified as the largely allopatric species *A. hildebrandti* and *A. maximus.* The third morphotype, which has not previously been recognised as a distinct genus, is described as the novel taxon *Vorombe titan*. *Vorombe* represents the largest-bodied aepyornithid and is the world's largest bird, with a mean body mass of almost 650 kg. This new taxonomic framework for the Aepyornithidae provides an important new baseline for future studies of avian evolution and the Quaternary ecology of Madagascar.

`

2.2 Introduction

"*When they found an Aepyornis with a thigh a yard long, they thought they had reached the top of the scale, and called him Aepyornis maximus. Then someone turned up another thigh-bone four feet six or more, and that they called Aepyornis titan…if they get any more Aepyornises, he reckons some scientific swell will go and burst a blood-vessel*." H.G. Wells, *Aepyornis* Island (Wells 1894)

An accurate understanding of taxonomy and diversity in recently extinct groups is necessary in order to understand evolutionary processes that have contributed to the functioning of past ecosystems, patterns of regional biogeography, and ecological disruption caused by humans in prehistory (Malhi et al. 2016; TH Worthy and Scofield 2012). However, current understanding of past diversity is often based on now-outdated and qualitative approaches, and as specimens on which original descriptions are based are often limited in number, they may not provide an accurate reflection of morphological diversity within and between extinct taxa (Hansford et al. 2012; Worthy and Scofield 2012). Instability of nomenclature leads to taxonomic confusion and has serious implications for estimating past diversity and diversity change. Modern systematic approaches, using up-to-date quantitative methods, are necessary to review putative taxa and establish stable diversity estimates (Hansford et al. 2012; Turvey et al. 2015; Turvey et al. 2016).

The Quaternary faunal record of Madagascar contains a unique and extraordinary megafauna, including giant lemurs, hippopotami, giant tortoises, and the world's largest birds, the elephant birds. These taxa all survived into the late Holocene and became extinct following the arrival of prehistoric human settlers, with available radiometric data suggesting that elephant birds persisted until around 1000 years ago (Goodman and Patterson 1997). Studies of the Malagasy megafauna have been dominated by the efforts of anthropologists investigating subfossil lemurs in tandem with studies of extant lemurs. Both giant tortoises and hippopotami have also been included in recent ecological reconstructions of Quaternary environments (Godfrey and Crowley 2016), but in comparison the radiation of elephant birds has seen remarkably little study since the advent of quantitative taxonomic methods, so that the relationship between observed morphological diversity and number of valid taxa within the group remains unclear.

`

2.2.1 History of research on elephant birds

Following the presentation and description of the world's largest egg and enormous avian skeletal remains from Madagascar in 1851 (Saint-Hilaire 1851), the elephant birds (Aves: Aepyornithidae) (Bonaparte 1853) have excited debate in palaeontologists, archaeologists and zoologists ever since. These first specimens were reported to have a young geological age, which led to a series of 19th century expeditions to find further subfossil remains of these giant birds and if possible extant individuals (LeMoine 1902). Although no living elephant birds were found, many additional skeletal and eggshell remains were discovered by subsequent researchers. Initial collections came from the extreme south and southwest of Madagascar, in swamp sites, coastal river sites, and as part of alluvial deposition from rivers, and vast deposits of highly fragmented eggshells were found within coastal dune systems (Saint-Hilaire 1851; Saint-Hilaire 1856). Towards the end of the 19th century, T.G. Rosaas collected further subfossil remains of elephant birds, hippopotami, giant tortoises, and giant lemurs from Antsirabe, and passed these remains onto museum collections in Berlin, Sweden, Norway, the UK, and Austria (Goodman and Jungers 2014).

Richard Owen investigated diversity within another extinct insular radiation of giant island-endemic ratites, the moa (Aves: Dinornithiformes) of New Zealand, through a series of linear measurements of leg bones (femora, tarsometatarsi and tibiotarsi) that allowed separation and diagnosis of moa taxa (e.g. total length; widths at proximal end, midshaft, and distal end) (Owen 1846). These rudimentary linear morphometrics were subsequently used by other scientists studying elephant birds to establish an initial taxonomic framework for the Aepyornithidae during this early discovery period, but this was conducted through comparison of univariate measurements of incomparable elements (femur versus tarsometatarsus versus eggshell; (Rowley 1867)). These early attempts at taxonomic quantification, focused on allometric scaling, also had no realistic consideration of natural variation within taxa, and often interpreted marginally observable differences as being taxonomically important.

Throughout this initial discovery period, scientists in France, Britain and Germany erected 13 elephant bird species across three genera: *Aepyornis* Saint-Hilaire, 1851 (nine species), *Mullerornis* Milne-Edwards and Grandidier, 1894 (three species), and *Flacourtia* Andrews, 1895 (one species) (table 1). Published descriptions of these taxa were based almost entirely upon the most common elements found, the robust leg bones, as well as upon major size differences between the two most widely accepted genera, *Aepyornis* (c. 400 kg) and *Mullerornis* (c. 100 kg). Differentiation of species was based largely upon linear measurements of the limited

`

remains then available for study in respective national collections and via inter-museum loans of casts. Most of these taxa were erected between 1893 and 1895, and authors attempted to demonstrate their authority by synonymising "competing" taxa, often focusing on laying claim to the largest birds (with *A. maximus*, *A. ingens* and *A. titan* all variously reported as being the largest in size). This "conflict of authority" (Anderson 2013) led to extreme confusion over diversity within the family, and also over biogeographic patterns shown by aepyornithids across the vast and highly variable ecological regions of Madagascar. Whilst most (although not all) of the referred type series associated with proposed taxa can be identified for study today, few holotypes were identified, further adding to taxonomic confusion.

In the early 20th century, further attempts to clarify the taxonomic diversity of the Aepyornithidae were made by Monnier (Monnier 1913), Lambrecht (Lambrecht 1933), and Lamberton (Lamberton 1934). These later researchers had access to large collections in France and Madagascar to help describe taxa more accurately, including cranial series and articulated skeletons, but they still failed to consider variation within species adequately, as their definitions were limited by the small series of adult specimens of femora, tibiotarsi and tarsometatarsi available for study for many taxa. Whilst Monnier and Lamberton both erected new putative elephant bird species during their reviews, bringing the total number of named species to 15 by 1934, the results of these efforts saw several taxa originally described from incomparable elements and based upon approximate size comparisons to now become reduced to the status of junior synonyms. This framework of reduced elephant bird diversity (two genera, seven species: *Aepyornis*, four species; *Mullerornis*, three species) was summarised by Brodkorb (Brodkorb 1963). Although his review did not include all previously described elephant bird taxa (*M. grandis*, based on material then curated in Madagascar, was not considered), it is still the most commonly cited framework for species-level nomenclature of aepyornithids in modern literature, biogeographic studies and phylogenetic analysis (Goodman and Jungers 2014; Mitchell et al. 2014; Grealy et al. 2017; Yonezawa et al. 2017a) (table 1). Brodkorb's qualitative assessment of species distributions within *Aepyornis* recognised geographical co-occurrence of *A. maximus* and *A. medius* in both the central west coast region and the extreme south of Madagascar, with *A. hildebrandti* found in the central highlands. *Mullerornis* was also considered to contain two geographically co-occurring species, *M. agilis* and *M. rudis*, with the area of their spatial overlap limited to the central west coast region near Belo-sur-mer and Morondava, and with a third recognised species, *M. betsilei*, restricted to the central highlands.

`

The elephant birds have been the focus of remarkably little study during the late 20th and early 21st centuries in comparison to moa and many other Quaternary megafaunal vertebrates. Following the recent development of methods of evolutionary and ecological analysis using ancient biomolecules, elephant bird material has been studied in efforts to reconstruct their evolutionary history and phylogenetic relationships (Oskam et al. 2010), dietary ecology (Clarke, Miller, and Fogel 2006), and causes of extinction (Michael Parker Pearson 2010). In particular, aepyornithid ancient DNA sequence data have been used to infer the timing of divergences between sampled taxa, estimated to be 27.6 million years ago between material assigned to *Mullerornis agilis* and *Aepyornis hildebrandti*, and 3.3 million years ago between *A. hildebrandti* and *A. maximus* (Mitchell et al. 2014; Grealy et al. 2017). However, this research has been conducted using either skeletal samples of uncertain taxonomic identification (Mitchell et al. 2014), or eggshell fragments from coastal dune sites and archaeological assemblages which are typically not associated with adult or juvenile skeletal remains (Oskam et al. 2010; Yonezawa et al. 2017a; Grealy et al. 2017). Aepyornithid eggshell fragments exhibit differences in thickness that are interpreted as representing two distinct size categories, which have been associated with the two currently recognised genera *Aepyornis* (~4 mm thick) and *Mullerornis* (~2 mm thick) (Grealy et al. 2017). These phylogenetic assumptions are therefore difficult to interpret in the context of aepyornithid taxonomy, which is based almost entirely upon morphology of skeletal elements rather than eggshell.

2.2.2 Towards a modern morphometric framework for elephant bird taxonomy

Multivariate analysis of morphometric data derived from skeletal elements constitutes a significantly more powerful diagnostic tool for delimiting taxa than the univariate and bivariate methods utilised in historical aepyornithid systematic studies. However, multivariate methods require data frames with no missing values. As aepyornithid remains are rarely found completely intact, attempts to quantify multivariate morphometric data inclusive of all available specimens must compensate for these data gaps (Freeman and Jackson 1990; Willig and Owen 1987; Strauss and Atanassov 2006).

Omission of characters and specimens from analysis is a common method for addressing the problem of missing data (Strauss and Atanassov 2006; Hansford et al. 2012; Turvey et al. 2016). However, this approach can lead to underrepresentation of the morphological diversity present in specimen assemblages, and can also affect statistical robustness of analyses. Maximization of

`

datasets through a stepped process of incrementally omitting specimens or characters with the largest number of missing data points can also produce alternate datasets with the same quantity of data, but may omit specimens that represent cryptic taxa, or key diagnostic features (Strauss and Atanassov 2006; Arbour and Brown 2014).

The alternative to omitting data is to estimate missing values whilst preserving natural variation of characters within taxa. One approach, imputation based upon the means of observed variables, can create conservative models that can underrepresent natural variation within the morphological range for a given taxon (Arbour and Brown 2014), and may generate composite means from data that combine separate morphologically distinct taxa. In comparison, multiple imputation (MI) methods are robust to these potential sources of error, and even against anatomically and taxonomically biased data gaps in morphometric analyses (Clavel, Merceron, and Escarguel 2014). Comparative analysis of available methods indicates that MI using expectation maximisation (EM) algorithms constitutes an effective compromise between accuracy of imputation and coverage probability (Arbour and Brown 2014).

Many studies that aim to test the validity of a given taxonomic hypothesis using morphometric data are supported by a well-delimited higher-order nomenclature and good geographical provenance of specimens (Cracraft 1976; Trevor Worthy and Holdaway 2002; Oskam et al. 2010). Conversely, the poorly defined taxonomy of the Aepyornithidae necessitates an unsupervised, objective exploration of morphotype clusters within the multidimensional shape-space generated from multiple linear measurements, to identify the most parsimonious solution for clustering morphotypes in order to determine specimen group assignment.

In order to clarify the confused state of elephant bird taxonomy, and to assess how many taxonomic units represented by distinct morphological clusters can be identified within a rigorously determined quantitative framework, we performed a series of morphometric analyses on linear size data from almost all of the specimens of aepyornithid appendicular limb elements available for study in global museum collections. We used an iterative modelling approach to permit comparison between models alternately assigning specimens to a varying number of clusters (Fraley and Raftery 1998). This study constitutes the first detailed revision of elephant bird taxonomy for over half a century and the first rigorous quantitative study of intraspecific variation and diagnostic morphological characters within aepyornithids, and permits formal reassessment of taxonomic diversity within this evolutionarily important but under-studied extinct avian family.

`

Table 1. Historically proposed species of elephant birds. Note: *M. rudis* was subsequently designated as the type species of *Flacourtia* by Andrews (1895).

Putative species	**Author**	**Revised species (after Brodkorb)**	**Distribution (after Brodkorb)**
A. maximus	Saint-Hilaire, 1851	*A. maximus*	Ambolisatra, Masikoro, between Belo-sur-Mer and Morondava, Itampulu Vé, Lamboharana
A. modestus	Milne-Edwards and Grandidier, 1869	*A. maximus*	
A. titan	Andrews, 1894	*A. maximus*	
A. ingens	Milne-Edwards and Grandidier, 1894	*A. maximus*	
A. grandidieri	Rowley, 1867	*A. medius*	Cape Sainte-Marie, between Belo-sur-Mer and Morondava
A. medius	Milne-Edwards and Grandidier, 1869	*A. medius*	
A. cursor	Milne-Edwards and Grandidier, 1894	*A. medius*	
A. lentus	Milne-Edwards and Grandidier, 1894	*A. medius*	
A. hildebrandti	Burckhardt, 1893	*A. hildebrandti*	Antsirabé
A. mulleri	Milne-Edwards and Grandidier, 1894	*A. hildebrandti*	
A. gracilis	Monnier, 1913	*A. gracilis*	Unknown
M. betsilei	Milne-Edwards and Grandidier, 1894	*M. betsilei*	Antsirabé
M. agilis	Milne-Edwards and Grandidier, 1894	*M. agilis*	near Morondava
M. rudis	Milne-Edwards and Grandidier, 1894	*M. rudis*	between Belo-sur-Mer and Morondava
M. grandis	Lamberton, 1934	N/A	N/A
Total: 3 genera, 15 species		**Total: 2 genera, 7 species**	

`

2.3 Methods

2.3.1 Specimens and measurements

Aepyornithid femora (n=97), tibiotarsi (n=162) and tarsometatarsi (n=87) of adult individuals (defined on the basis of full fusion of epiphyses) were studied from the following collections: American Museum of Natural History, USA (AMNH), Centre ValBio, Madagascar (CVB), Museum für Naturkunde, Germany (MfN), Museum National d'Histoire Naturelle, France (MNHN), Natural History Museum, UK (NHM), Naturhistorisches Museum, Austria (NHMW), Oxford University Museum, UK (OUMNH), Université d'Antananarivo, Madagascar (UA), Natural History Museum, University of Oslo, Norway (UIO), United States National Museum, USA (USNM), and Zoologiska Museum, Uppsala Universitet, Sweden (ZIUU) (Appendix one). A standard series of 20 femoral, 20 tibiotarsal, and 44 tarsometatarsal measurements were taken where possible (figure 1). Measurements up to 150mm were taken using dial callipers accurate to 0.02mm. Circumference and >150mm measurements were made using a measuring tape accurate to 1mm.

2.3.2 Missing data imputation

Of the total dataset of 346 specimens, only 82 specimens (19 femora, 42 tibiotarsi, 21 tarsometatarsi) were completely intact and undamaged (electronic supplementary information, Appendix one). As some taxa might only be represented by broken specimens, proportions of missing linear measurements from broken specimens were examined in 5% stepped increments. Selection of first-round data frames was defined by the inclusion of ~50% of available specimens to minimise imputation and maximise potential taxonomic inclusion. Skeletal elements with greater than 25% of linear measurements missing were omitted from the first round of imputation calculations and taxonomic assessments. The first-round data frames included 48 femora (49% of specimens, 11.6% imputed data), 73 tibiotarsi (45% of specimens, 7.8% imputed data) and 46 tarsometatarsi (53% of specimens, 5.8% imputed data; Appendix one).

All statistical analysis was performed in R 3.1.3 (R Development Core Team 2011). MI methods using EM algorithms were used to estimate the linear measurements of missing portions of elements to create a complete data frame using the "ImputePCA" function of the MissMDA package. The first round of the algorithm imputed missing data using the mean of the variable across the observed values, and a principal component analysis (PCA) was performed on this imputed data frame. Values fitted by the PCA were then used to predict new values for missing

`

data, whilst retaining observed values. The process of parameter estimation via PCA and refitting of imputed values was then repeated until the predicted missing values converged. This method provides good estimations of the missing data as there were very strong correlations between observed variables, and in the first round the number of missing values was small. However, to remove the problem of overfitting through EM algorithms, we used k-fold cross validation as a regulation mechanism to remove noise and improve prediction quality. The "tuned parameters" were determined by five-fold cross validation to find the PCA loadings that produced the smallest mean square error of predictions, using the "estim_ncpPCA" function of the MissMDA package (Josse and Husson 2016). All measurement data used in Principle Component Analysis was "scaled" by dividing by the standard deviation for that measurement in order to remove the dominance of total size in the calculation of eigenvalues.

2.3.3 Cluster analysis

PCA was conducted on observed and imputed data derived from the first round of EM imputation, to investigate whether morphometric measurement data are able to identify discrete clusters of elephant bird specimens that are likely to correspond with taxonomically distinct groups. This approach extracts and summarizes the major features of morphometric shape variation and reduces high dimensionality to examine the distribution of different taxonomic groups in shape space, without making any prior assumptions about the pattern of clustering of specimens.

The package "MClust" (Fraley et al. 2012) was used to perform hierarchical model-based classification cluster analysis, based upon PCA loadings derived from the first-round observed and imputed datasets. Selection of the most likely model was based upon Schwarz's Bayesian Information Criterion (BIC) (Schwarz 1978). BIC is determined by the value of the maximized log-likelihood model, penalised by increasing number of model parameters, and allowing the comparison of models with differing numbers of clusters and representation in morphospace (equal and unequal variance; Spherical, diagonal and ellipsoidal shape; and equal and varying volume). PCA loadings included in the cluster model were introduced in a stepped sequence until BIC was able to identify a distinct pattern. Specimens demonstrating high levels of classification uncertainty (≥0.05) were removed from the first-round dataset and added to the dataset with >25% missing data. As BIC weights against an increasing number of groups, we first obtained the highest number of clusters from each element (unsupervised clustering) and then if necessary re-clustered the data based upon fixed numbers of clusters obtained for other limb elements (supervised clustering) to determine whether a stable result could be observed.

`

Inclusion of specimens with >25% missing data

A second dataset was generated to include all data with >25% missing data, any available type specimens that had not yet been included in cluster models, and all specimens with location data. Missing data point imputation, clustering, and removal of specimens demonstrating high levels of classification uncertainty was then performed. Clustering was performed using the same method as above, but the number of clusters was limited to the number observed from the first round of analysis.

The large amount of missing data included in this second phase of imputation means that cluster assignment of these poorer-quality specimens must be interpreted with caution; however, this represents the only quantitative framework for identifying distinct morphological forms from incomplete remains of elephant birds. Where accession data were available for specimens, their cluster and geographic location was recorded to examine any potential pattern of spatial distributions. This second dataset included 64 femora (26.9% missing datapoints), 95 tibiotarsi (22.8% missing datapoints) and 70 tarsometatarsi (27.0% missing datapoints) (Appendix two).

2.3.4 Summary statistics

ANOVAs were performed on individual measurements for each morphological cluster of femora, tibiotarsi and tarsometatarsi, in order to describe the measurement parameters of each cluster and therefore define the taxonomic groupings represented by each cluster. Mass estimations were calculated using the Campbell and Marcus algorithm for estimating body mass in birds from femoral least-shaft circumference (LogM=2.411*LogLCF-0.065) (Campbell and Marcus 1992). Mean mass and standard deviation were determined for each cluster, based upon observed data only.

`

Figure 1. Diagram of linear measurements taken on aepyornithid leg bones

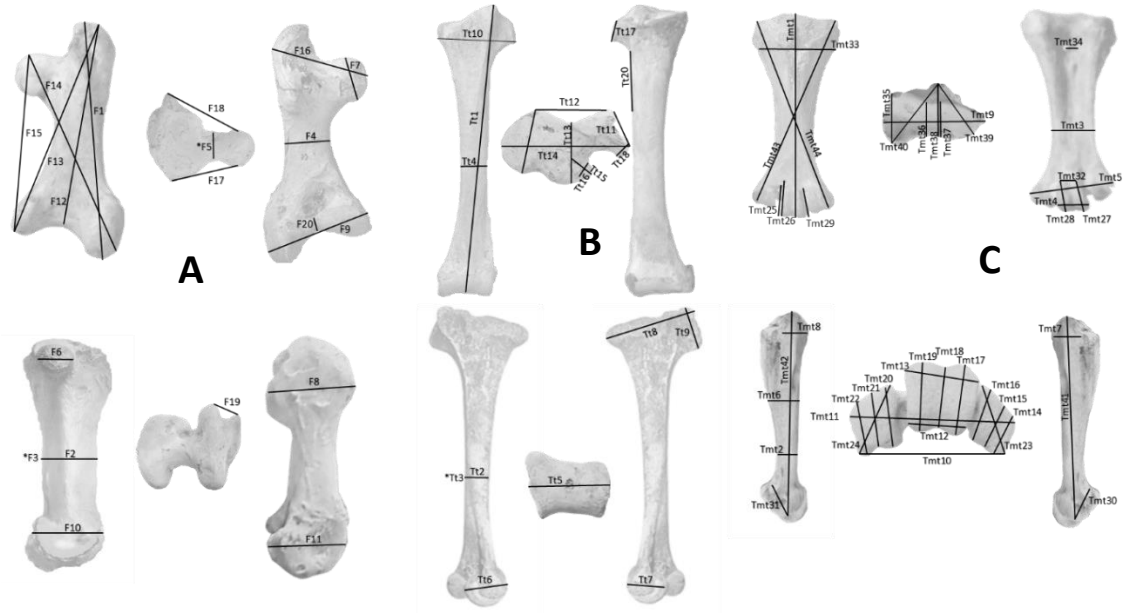

A, Femoral measurements. F1: Total length; F2: Minimum midshaft width; F3: Circumference at minimum midshaft width; F4: Maximum midshaft width; F5: Circumference of neck of ball; F6: Dorsoventral diameter of ball; F7: Proximodistal diameter of ball; F8: Dorsoventral thickness of head; F9: Maximum mediolateral thickness of head; F10: Maximum width of distal condyles; F11: Maximum height of medial condyle; F12: Maximum height of lateral condyle; F13: Trochanter to medial condyle; F14: Proximal-medial extreme of ball to lateral condyle; F15: Length of condyle gap to head; F16: Angular length, lateral head to medial condyle; F17: Maximum width of head; F18: Angular femur head width (anterior); F19: Angular femur head width (posterior); F20: Distance between medial and lateral condyles. **B**, Tibiotarsal measurements. Tt1: Total length; Tt2: Minimum midshaft width; Tt3: Circumference at Tt2; Tt4: Maximum midshaft width; Tt5: Width of condyles; Tt6: Maximum height, medial condyle; Tt7: Maximum height, lateral condyle; Tt8: Maximum width of head, including crest; Tt9: Width of crest, including ectocnemial ridge; Tt10: Width of head; Tt11: Distance between ectocnemial crests; Tt12: Extreme width of posterior groove; Tt13: Posterior groove to external condyle; Tt14: Posterior groove height to external condyle; Tt15: External condyle width; Tt16: External condyle height; Tt17: Outer cnemial crest width; Tt18: Outer cnemial crest height; Tt19: Total outer cnemial ridge length; Tt20: Tibia scar. **C**, Tarsometatarsal measurements. Tmt1: Length; Tmt2: Minimum shaft thickness (not midshaft); Tmt3: Shaft width at Tmt2; Tmt4: Middle toe width; Tmt5: Foot width (all toes); Tmt6: Head height at midpoint, including ridge; Tmt7: Maximum height, medial condyle; Tmt8: Maximum height, lateral condyle; Tmt9: Head width; Tmt10: Inside curve (bottom) across three toes; Tmt11: Outside curve (top) across three toes; Tmt12: Middle toe, bottom width; Tmt13: Middle toe, top width; Tmt14: Medial toe, medial thickness; Tmt15: Medial toe, centre thickness; Tmt16: Medial toe, lateral thickness; Tmt17: Centre toe, medial thickness; Tmt18: Centre toe, centre thickness; Tmt19: Centre toe, lateral thickness; Tmt20: Lateral toe, medial thickness; Tmt21: Lateral toe, centre thickness; Tmt22: Lateral toe, lateral thickness; Tmt23: Medial toe, diagonal length; Tmt24: Lateral toe, diagonal length; Tmt25: Centre toe, medial length, outside to notch; Tmt26: Centre toe, medial length, outside with notch; Tmt27: Centre toe, medial Length; Tmt28: Centre toe, lateral length; Tmt29: Centre toe, lateral length, outside; Tmt30: Medial toe length; Tmt31: Lateral toe length; Tmt32: Centre toe, top (peak to peak) notch width; Tmt33: Total width at foramina; Tmt34: Foramina width; Tmt35: Maximum anterior-posterior depth of external cotyle; Tmt36: Minimum depth of head; Tmt37: Maximum depth at hypotarsal ridge (no ridge); Tmt38: Maximum depth at hypotarsal ridge (inclusive of ridge); Tmt39: Proximal-lateral extreme of head to hypotarsal ridge extreme; Tmt40: Proximal-medial extreme of head to hypotarsal ridge extreme; Tmt41: Length, medial toe to head; Tmt42: Length, lateral toe to head; Tmt43: Diagonal length, medial toe to head; Tmt44: Diagonal length, lateral toe to head.

`

2.4 Results

2.4.1 Morphometric analysis

From our sample, 41 femora, 83 tibiotarsi and 41 tarsometatarsi were excluded from the first round of analysis due to exceeding the >25% missing marker criterion for taxonomic assessment. The percentage of total imputed data generated in this round was 11.6% for femora, 9.1% for tibiotarsi and 5.5% for tarsometatarsi. Five femora, 49 tibiotarsi and one tarsometatarsus were excluded from taxonomic classification through clustering due to high uncertainty in classification (>5% uncertainty). Four femora, 43 tibiotarsi and 12 tarsometatarsi were excluded from subsequent biogeographic analysis, again due to >5% uncertainty of classification. For the biogeographic assessment dataset, 26.9% of femoral markers, 23.0% of tibiotarsal markers and 27.0% of tarsometatarsal markers were not observed and so were imputed.

Cluster analysis performed separately on PCA weightings created from each specimen's linear measurements from all three limb bones revealed that the comprehensive sample of elephant bird specimens analysed in this study fall into multiple distinct morphometric groups, defined as a stable result by BIC differentiation between cluster models of >2 (Appendix two). Femora (figure 2) and tibiotarsi (figure 3) both demonstrated stable clustering into three distinct groups. Femora required two principal components to achieve a stable cluster model, whereas tibiotarsi required only one principal component. The tarsometatarsal dataset required four principal components to achieve a stable result and clustered into four distinct groups (figure 4). As BIC weights against increasing numbers of groups, supervised clustering based upon four possible groups (as determined by tarsometatarsal clustering) was then applied to both the femoral and tibiotarsal data, to investigate whether further subclustering could also be identified within the three primary clusters for these elements. The femoral dataset subdivided cluster 2 into two further subgroups (figure 2), but the tibiotarsal dataset was unable to identify any further subdivision within its sample. The tibiotarsal dataset had poorly defined clusters and the weakest predictive power for defining morphotypes.

In all taxonomic PCA clusters, PC1 was highly correlated (>0.75) with almost all measurements from each skeletal element (although not with TT5 or TT20), which could be superficially interpreted as a separation of clusters based on overall size (Appendix two) despite scaling of linear measurements. However, these clusters overlap in overall size ranges (shaft circumference), yet can be differentiated by other patterns of distinctive morphotype variation

`

through this multivariate analysis demonstrating that the distinct clusters are not mere scaling of the same morphotype.

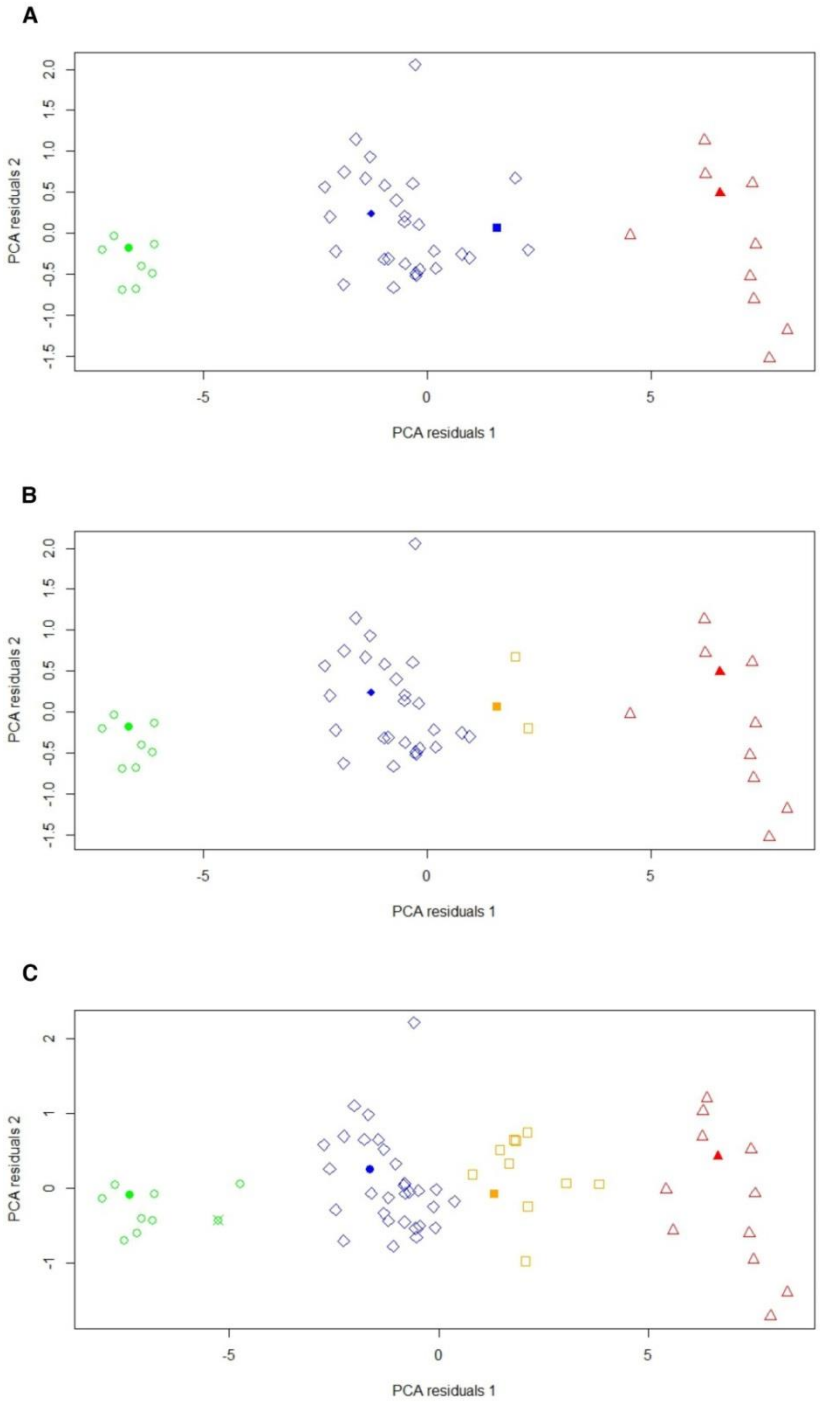

Figure 2. A, Unsupervised clusters of femora, <25% missing data. PCA axis 1, 90.8%; PCA axis 2, 2.1%. Cluster 1 = circles, cluster 2a = diamonds, cluster 2b = squares, cluster 3 = triangles. Type specimens/series: filled circle, *A. modestus*; filled diamond, *A. gracilis*; filled square, *A. medius*; filled triangle, *A. titan.* **B,** Supervised clusters of femora (four possible groups only), <25% missing data. PCA axis 1, 90.8%; PCA axis 2, 2.1%. Cluster 1 = circles, cluster 2a = diamonds, cluster 2b = squares, cluster 3 = triangles. Type specimens/series: filled circle, *A. modestus*; filled diamond, *A. gracilis*; filled square, *A. medius*; filled triangle, *A. titan.* **C,** Unsupervised clusters of femora, >25% missing data. PCA axis 1, 91.4%; PCA axis 2, 2.1%. Cluster 1 = circles, cluster 2a = diamonds, cluster 2b = squares, cluster 3 = triangles. Type specimens/series: filled circle, *A. modestus*; quartered circle, *A. hildebrandti*; filled diamond, *A. gracilis*; filled square, *A. medius*; filled triangle, *A. titan*

`

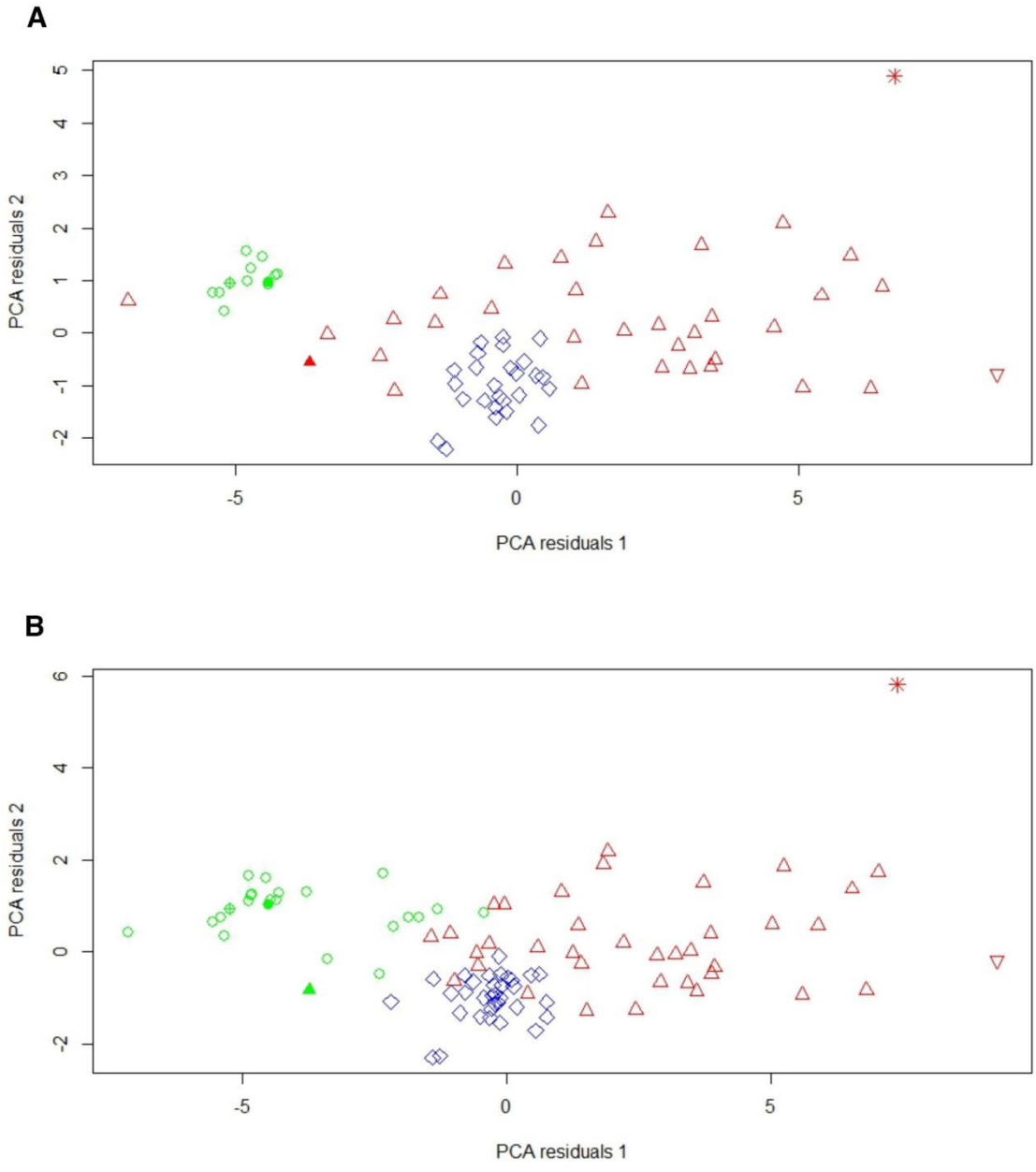

Figure 3. A, Unsupervised clusters of tibiotarsi, <25% missing data. PCA axis 1, 53.7%; PCA axis 2, 7.4%. Cluster 1 = circles, cluster 2 = diamonds, cluster 3 = triangles. Type specimens/series: filled circle, *M. agilis*; crossed-circle, *M. rudis*; filled triangle, *A. hildebrandti*; upside-down triangle, *A. ingens*; star, *A. titan*. **B,** Unsupervised clusters of tibiotarsi, >25% missing data. PCA axis 1, 67.2%; PCA axis 2, 6.6%. Cluster 1 = circles, cluster 2 = diamonds, cluster 3 = triangles. Type specimens/series: filled circle, *M. agilis*; crossed circle, *M. rudis*; filled triangle, *A. hildebrandti*; upside-down triangle, *A. ingens*; star, *A. titan*.

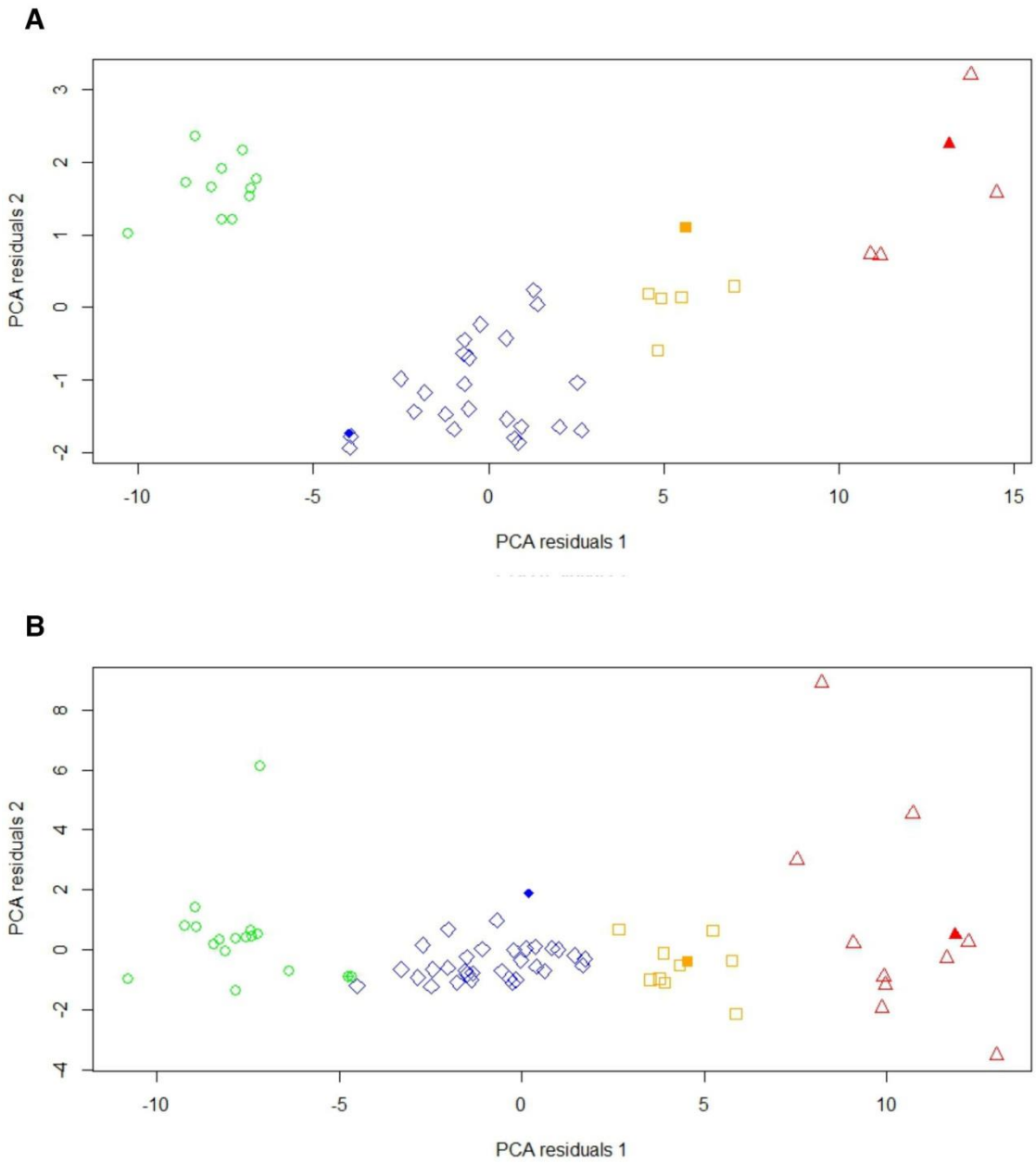

Figure 4. A, Unsupervised clusters of tarsometatarsi, <25% missing data. PCA axis 1, 86.8%; PCA axis 2, 4.6%. Cluster 1 = circles, cluster 2a = diamonds, cluster 2b = squares, cluster 3 = triangles. Type specimens/series: filled circle, *A. hildebrandti*; filled square *A. cursor*; filled triangle, *A. ingens*. **B,** Unsupervised clusters of tarsometatarsi, >25% missing data. PCA axis 1, 82.7%; PCA axis 2, 6.6%. Cluster 1 = circles, cluster 2a = diamonds, cluster 2b = squares, cluster 3 = triangles. Type specimens/series: crossed-circle, *A. hildebrandti*; filled diamond, *A. lentus*; filled square, *A. cursor*; filled triangle, *A. ingens*.

`

2.4.2 Taxonomy of morphometric clusters

Tarsometatarsal data provide the best-resolved assessment of morphological diversity within aepyornithids, as the four clusters based on data for this limb bone resolve well and group membership is the most stable (figure 4). Femoral data predict three groups as the most parsimonious result of clustering analysis, but also demonstrate well-resolved clusters and stable group membership when restricted to four possible clusters (figure 2). Tibiotarsal data also only predict three clusters, although morphological diversity on the basis of tibiotarsal data is not represented well by our current measurement framework, and the only consistent differences that can be established between samples are upon extremely large size differences when large amounts of data are compared (figure 3).

We interpret the three clusters identified using femoral and tarsometatarsal data as representing genus-level differentiation, and the two consistent and stable sub-groups within cluster 2 shown by femora and tarsometatarsi as representing further species-level differentiation within this cluster. Three existing generic names are available in the published literature that may correspond to the three clusters identified in this analysis: *Aepyornis* Saint-Hilaire, 1851 (type species *Aepyornis maximus*), *Mullerornis* Milne-Edwards and Grandidier, 1894 (type species *Aepyornis modestus*), and *Flacourtia* Andrews, 1895 (type species *Mullerornis rudis*). The type specimens or type series of 10 of the 15 species that have been assigned to these genera can still be located in museum collections, and were included within the clustering analysis. The taxonomic identity of each morphometric cluster was established by determining which type specimens were included within which clusters, and which of these type specimens represented the oldest available taxonomic name (table 2). Specimens that demonstrated high probability of conflicting cluster classification (high uncertainty) were excluded from taxonomic conclusions.

Cluster 1 represents the smallest specimens across all skeletal element datasets, and contains the type material of *Aepyornis modestus* Milne-Edwards and Grandidier, 1869 (femur), *Mullerornis agilis* Milne-Edwards and Grandidier, 1894 (tibiotarsus) and *Mullerornis rudis* Milne-Edwards and Grandidier, 1894 (tibiotarsus). Cluster 2 contains the intermediate-sized specimens across all skeletal element datasets, and contains well-predicted type material of *Aepyornis hildebrandti* Burckhardt, 1893 (tarsometatarsus within type series), *Aepyornis medius* Milne-Edwards and Grandidier, 1869 (femur), *Aepyornis cursor* Milne-Edwards and Grandidier, 1894 (tarsometatarsus), *Aepyornis lentus* Milne-Edwards and Grandidier, 1894 (tarsometatarsus) and *Aepyornis gracilis* Monnier, 1913 (femur). When subdivided by supervised cluster classification

`

(four groups), cluster 2a contains the type material of *Aepyornis hildebrandti* (tarsometatarsus within type series)*, Aepyornis lentus* and *Aepyornis gracilis*. The femur of the type series of *Aepyornis hildebrandti* was also assigned to cluster 2a, but this specimen is incomplete and cluster assignment was poorly predicted due to high uncertainty, so taxonomic assignment of the name *Aepyornis hildebrandti* was based solely on the type tarsometatarsus. Cluster 2b contained the type material of *Aepyornis medius* and *Aepyornis cursor.* All tibiotarsi that fell within cluster 2 demonstrated high uncertainty of cluster classification and were therefore not used for taxonomic assessment. Cluster 3 contains the largest specimens of all skeletal elements, and contains the type material of *Aepyornis titan* Andrews, 1894 (femur and tibiotarsus) and *Aepyornis ingens* Milne-Edwards and Grandidier, 1894 (tibiotarsus and tarsometatarsus).

Five described species could not be included directly in this analysis. The type material of *Mullerornis grandis* Lamberton, 1934 was lost in a fire in 1995, and the skeletal type material of *Aepyornis maximus* Saint-Hilaire, 1851, *Mullerornis betsilei* Milne-Edwards and Grandidier, 1894 and *Aepyornis mulleri* Milne-Edwards and Grandidier, 1894 cannot now be located in museum collections, meaning that type specimens for these species could not be included in the long bone measurement dataset. *Aepyornis grandidieri* Rowley, 1867 was described from eggshell remains only and therefore cannot be compared to other taxa.

Only eggshell measurements are available from the original description of *Aepyornis maximus* by Saint-Hilaire (Saint-Hilaire 1851). However, Owen (Owen 1852) published a small number of measurements of the incomplete tarsometatarsus originally reported as part of the type series for this species by Saint-Hilaire [9]. Other measurement ranges for this taxon are available in Monnier (Monnier 1913), but are based on a range of specimens that Monnier regarded as constituting the same species, rather than the type series. The only measurement provided by Owen (Owen 1852) that can be compared to our dataset is the extreme breadth across the trochlear condyles. This is a discrete (non-overlapping) measurement for the clusters presented here (cluster 1: 65-79.24 mm, cluster 2a: 105-118 mm, cluster 2b: 127-140 mm, cluster 3: 164-178 mm). The measurement value for *A. maximus* as reported by Owen [40] is 127 mm, indicating that the type series of this species falls within the range of cluster 2b.

The original published description of the *Mullerornis betsilei* type series by Milne-Edwards and Grandidier (1894) (Milne-Edwards and Grandidier 1894) includes four measurements from the tarsometatarsus (length, circumference, width of shaft, proximal width), and five from the tibiotarsus (length, shaft circumference, width, proximal width, distal width). Tarsometatarsal

`

length cannot be used alone to diagnose taxa, as there is considerable overlap in this measurement between clusters. Using the proximal width of the tarsometatarsus, which exhibits discrete measurement values between clusters (cluster 1: 65.8-81.46 mm, cluster 2a: 99.7-125.04 mm, cluster 2b: 140.3-150.5 mm, cluster 3: 173-182 mm), the value reported for *M. betsilei* (70 mm) falls within the range of cluster 1.

Lamberton (1934) included ranges for six femoral and seven tibiotarsal measurements in the description of *Mullerornis grandis*. Here we use the minimum femoral shaft circumference, which shows discrete measurement values between clusters (cluster 1: 114-131 mm, cluster 2a: 172-210 mm, cluster 2b: 223-237 mm, cluster 3: 253-288 mm). The minimum shaft circumference range reported for *M. grandis* (125-145 mm) falls within the upper range of cluster 1.

Aepyornis mulleri was described on the basis of a skull, mandible, vertebrae, ribs, sternum, part of pelvis, “the leg bones” and phalanges. No published measurement data exist for the “leg bones”, and so this species cannot be assigned to any of our clusters based on comparative measurements.

The genus *Aepyornis* Saint-Hilaire, 1851 was first used to describe *Aepyornis maximus*, which our data demonstrate can be assigned to cluster 2b, and this name can therefore be interpreted as the senior synonym for all of cluster 2. The genus *Mullerornis* Milne-Edwards and Grandidier, 1894 was first used to describe *Mullerornis betsilei*, which is assigned to cluster 1. As two of our clusters correspond to different genera previously defined by earlier authors on the basis of qualitative or univariate assessment of variation within the Aepyornithidae, this supports our interpretation of all three primary clusters in our analysis as representing genus-level differentiation. Cluster 3, which contains specimens that were originally assigned to two species of *Aepyornis* in 1894, represents a further distinct morphotype which on this basis also needs to be recognised as distinct at the genus level. A third aepyornithid genus name, *Flacourtia* Andrews, 1895, is also available, but the holotype tibiotarsus of the type species *Mullerornis rudis* clusters reliably within cluster 1, and so the name *Flacourtia* represents a junior synonym of *Mullerornis* and cannot be used to describe cluster 3. There is therefore no available genus name that can be applied to cluster 3.

Our analysis does not distinguish distinct morphotypes within cluster 1 (*Mullerornis*), and so we apply the oldest formally described species name available for this cluster, *Aepyornis modestus*, to name the single species that can be recognised in this genus. Cluster 2 (*Aepyornis*) can be

`

separated into two distinct morphological groups on the basis of both tarsometatarsal and femoral data, and we interpret these groups as representing separate species within the same genus: the oldest available species names within each cluster are *Aepyornis hildebrandti* (cluster 2a) and *Aepyornis maximus* (cluster 2b). No morphological differentiation can be demonstrated within cluster 3 (unnamed genus). Within this cluster, the two species names *Aepyornis titan* and *Aepyornis ingens* were both published in 1894, but *titan* (published January 1894) predates *ingens* (published February 1894) by one month, so that the oldest available species name for this group is *Aepyornis titan.* Body mass estimates for these four recognised aepyornithid taxa are given in table 3.

2.4.3 Biogeography of Aepyornithidae

Due to the poorly resolved clustering of tibiotarsal data, we selected only femoral and tarsometatarsal geographic location data to reconstruct distributions of newly defined elephant bird taxa. Specimens with high uncertainty were also removed from the pooled location dataset. Locality data associated with well-resolved specimens in our analysis (Appendix two) are plotted by species in figure 5. Our data demonstrate that *Mullerornis modestus, Aepyornis maximus* and *Vorombe titan* were widely distributed across Madagascar, and occurred sympatrically across three major ecogeographic zones: arid spiny bush in the south, succulent woodlands in the south-west, and grassland/woodland mosaic in the central highlands (Goodman and Benstead 2003). Almost all specimens of *Aepyornis hildebrandti* are restricted to the central highlands near Antsirabe and Masinandreina, except for one tarsometatarsus found at Belo-sur-Mer (MNHN MAD 388). This specimen is the type specimen for *Aepyornis lentus* and is missing >25% of measurement data, leading to potential unreliability of cluster assignment.

`

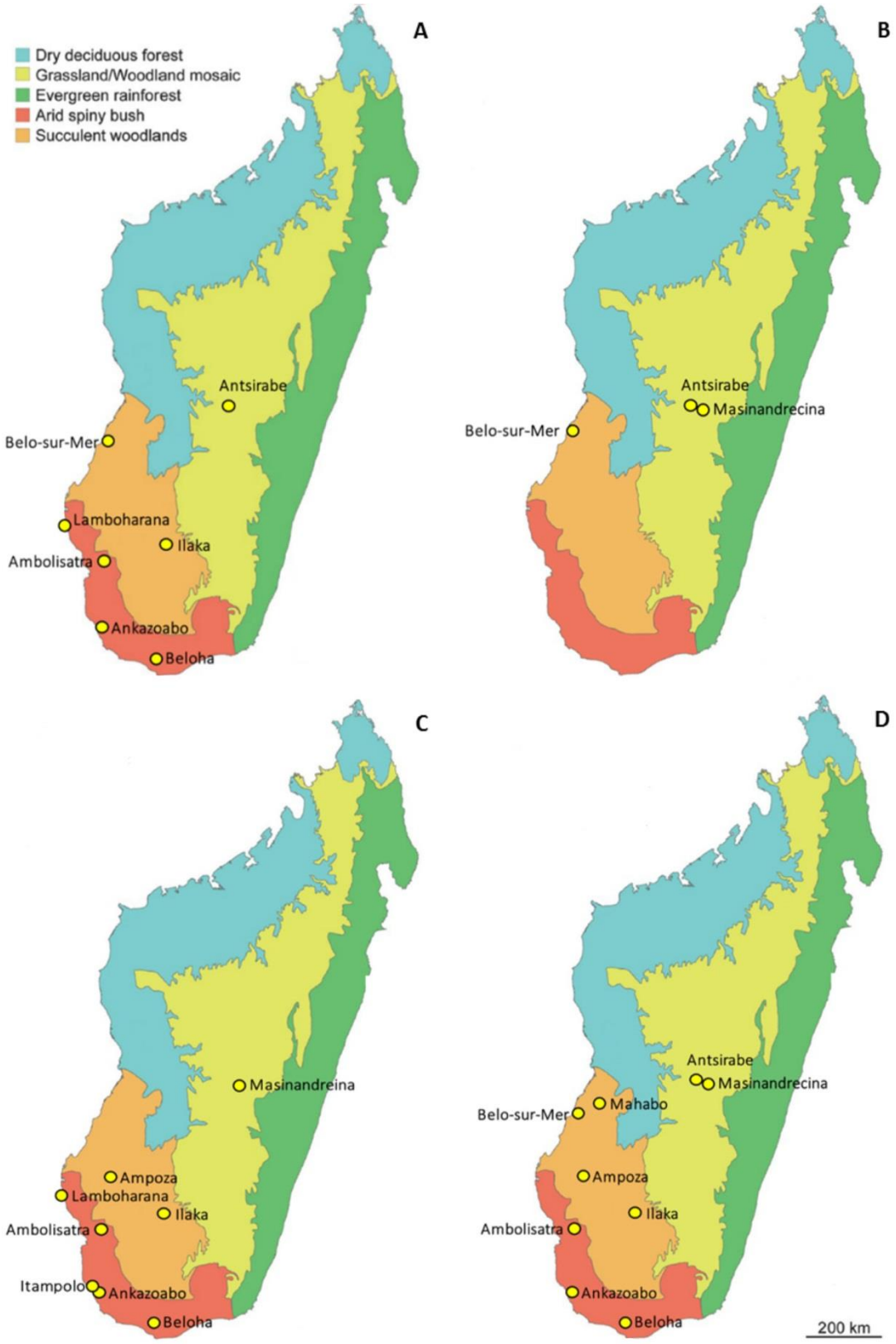

Figure 5. Distribution across Madagascar of identified specimens of elephant bird species recognised in this study. A, *Mullerornis modestus*; B, *Aepyornis hildebrandti*; C, *Aepyornis maximus*; D, *Vorombe titan*.

`

Table 2. Taxonomic matrix describing morphometric assignment and taxonomic seniority of type material of named elephant bird species to the morphometric clusters identified in this study.

Cluster	Type specimens included within each cluster			Other type specimens referable to cluster based on published measurements	Senior synonym for cluster	Available senior genus name for cluster	Name assigned to taxon
	Femur	Tibiotarsus	Tarsometatarsus				
1	(1) *Aepyornis modestus* 1869, (2) *Aepyornis hildebrandti* 1893* (part of type series)	(1) *Mullerornis agilis* 1894, (2) *Mullerornis rudis* 1894	—	(1) *Mullerornis betsilei* 1894	*Aepyornis modestus* 1869	*Mullerornis* 1894	*Mullerornis modestus* 1869
2a	(1) *Aepyornis hildebrandti* 1893* (part of type series), (2) *Aepyornis gracilis* 1912	—	(1) *Aepyornis hildebrandti* 1893 (part of type series), (2) *Aepyornis lentus* 1894		*Aepyornis hildebrandti* 1893 (based on well-predicted tarsometatarsus, not poorly predicted femur)	*Aepyornis* 1851 (name available for entirety of Cluster 2, with reference to assessment of data for Cluster 2b)	*Aepyornis hildebrandti* 1893
2b	(1) *Aepyornis medius* 1869	—	(1) *Aepyornis cursor* 1894	(1) *Aepyornis maximus* 1851	*Aepyornis maximus* 1851	*Aepyornis* 1851	*Aepyornis maximus* 1851
3	(1) *Aepyornis titan* 1894 (part of type series)	(1) *Aepyornis titan* 1894 (part of type series), (2) *Aepyornis ingens* 1894 (part of type series)	(1) *Aepyornis ingens* 1894 (part of type series)		*Aepyornis titan* 1894	None available; new genus name *Vorombe* erected to describe this cluster (see text)	*Vorombe titan* 1894

`

2.5 SYSTEMATIC PALAEONTOLOGY

Order Struthioniformes Latham, 1790

Family Aepyornithidae Bonaparte, 1853

Genus *Aepyornis* Saint-Hilaire, 1851

Type species: *Aepyornis maximus* Saint-Hilaire, 1851 (by monotypy).

Valid species recognised within genus: *Aepyornis maximus* Saint-Hilaire, 1851; *Aepyornis hildebrandti* Burckhardt, 1893.

Revised diagnosis:

Femur: Broad and robust, but to a lesser extent than that of *Vorombe*. The antitrochanter has a convex articular surface transitioning in a continuous straight line to the lateral surface of the trochanter. The proximal epiphysis is enlarged, transitioning smoothly into the neck of the ball. The distal view of the neck of the ball has a strong concave curvature that extends smoothly into the shaft, which is tapered and expands into the enlarged and robust distal condyles. Significantly larger than *Mullerornis* in the following measurements: F1–F4, F6, F10–F12, F16 (after Bonferroni correction of p-values, alpha=0.0026). Significantly smaller than *Vorombe* in the following measurements: F1–F14, F16–F17, F19–F20 (after Bonferroni correction of p-values, alpha=0.0026).

Tibiotarsus: Smaller tibiotarsi (*A. hildebrandti*) are of similar length to *Mullerornis* but are considerably more robust, with larger shaft diameters and more rounded epiphyseal features. The proximal end is enlarged, particularly medio-laterally. The angle of the ectocnemial ridge and the ventral support is ≥90^{o}. The enlarged procnemial crest extends into a ridge, leading into a prominent, straight intermuscular line that terminates on the medial side of the shaft, just before the distal condyle.

Tarsometatarsus: Smaller tarsometatarsi (*A. hildebrandti*) are similar in length to *Mullerornis* but are medio-laterally broader and have a much shallower triangular cross-section. A large, flattened hypotarsal ridge extends into the shaft for approximately 50% of its length. Nutrient foramina are widely separated by the hypotarsal ridge in posterior view, oriented away from the midline of the shaft. In anterior view, the foramina are more closely spaced inside an anterior cotyle, within a metatarsal groove formed by the flattened-triangular orientation of the metatarsi. The proximal epiphysis and trochleae are enlarged, with large intertrochlear notches.

`

The medial trochlea terminates proximal to the lateral trochlea. Significantly larger than *Mullerornis* in the following measurements: Tmt2–Tmt6, Tmt9–Tmt11, Tmt13–Tmt25, Tmt27–Tmt31, Tmt33–Tmt39 (after Bonferroni correction of p-values, alpha=0.001). Significantly smaller than *Vorombe* in the following measurements: Tmt1, Tmt3–Tmt6, Tmt10–Tmt11, Tmt13–Tmt22, Tmt27–Tmt28, Tmt31, Tmt33, Tmt35–Tmt36, Tmt38–Tmt41, Tmt43–Tmt44 (after Bonferroni correction of p-values, alpha=0.001).

***Aepyornis maximus* Saint-Hilaire, 1851**

Junior synonyms: *Aepyornis medius* Milne-Edwards and Grandidier, 1869; *Aepyornis cursor* Milne-Edwards and Grandidier, 1894.

Original syntype series: Tarsometatarsus of adult individual and two eggs (no specific holotype given), from "the south coast" of Madagascar, purchased from Merchant Captain M. Abadie. Original tarsometatarsus now cannot be located and eggs cannot be distinguished from other collections in MNHN.

Neotype: Tarsometatarsus (USNM A65208), Ilaka, Ambositra, Madagascar (figure 6A); newly designated.

Conspecific specimen: Tibiotarsus (USNM A65209), Ilaka, Ambositra, Madagascar; associated with neotype and almost certainly from the same individual (figure 6B); newly designated.

Revised diagnosis:

Femur: Has similar length and width of epiphyses but has a markedly more robust appearance in comparison to *A. hildebrandti*. The proximal epiphyses are enlarged, transitioning smoothly into the neck of the ball, which is also enlarged. The shaft is curved, tapering in the middle and leading into the enlarged and robust distal condyles. The markedly large distal pneumatic foramen is a pointed arch marginally proximal to the ectecondylar fossa. Significantly larger than *Aepyornis hildebrandti* in F15 (after Bonferroni correction of p-values, alpha=0.0026).

Tibiotarsus: Similar in total proportion and morphology to that of *A. hildebrandti*, but larger. The proximal epiphysis is more markedly expanded and has a more pronounced ectocnemial crest and procnemial crest; the latter crest leads into a more pronounced intermuscular line and is more expanded at the distal condyles.

`

Tarsometatarsus: Medio-laterally broad with a much flatter proximal epiphysis than in *A. hildebrandti*, and with metatarsi of roughly equal height. The pronounced intercondylar ridge is on the midline above the central distal trochlea. The proximal epiphysis is enlarged, and the shaft limits are straight, tapering slowly towards the distal portion before expanding sharply into the much-enlarged trochleae. Significantly larger than *Aepyornis hildebrandti* in the following measurements: Tmt9, Tmt14, Tmt19, Tmt33, Tmt35–Tmt36, Tmt40, Tmt43 (after Bonferroni correction of p-values, alpha=0.0012).

Revised description:

Femur: Large and robust, with enlarged epiphyses. The antitrochanter has a convex articular surface, with the proximal epiphyseal surface transitioning rapidly into the shaft. Proximal epiphyses are enlarged, especially anterio-posteriorly. The head transitions smoothly into the neck of the ball, which is enlarged, particularly proximo-ventrally; the distal view of the neck of the ball has a shallow and broad concave curvature. The shaft is robust and broad, and curved on the medial facia, tapering slightly in the middle, and leading into the enlarged distal condyles with a broad and deep intercondylar groove. The markedly large distal pneumatic foramen is a wide pointed arch, with its proximal point biased towards the medial portion of the shaft. Measurements given in table 4.

Tibiotarsus: Large and robust. The proximal end is enlarged, particularly medio-laterally. The angle of the ectocnemial ridge and the ventral support is ≥90°. The enlarged procnemial crest extends into a ridge, leading into a prominent, straight intermuscular line that terminates on the medial side of the shaft just before the distal condyle. Measurements given in table 5.

Tarsometatarsus: Medio-laterally broad. The pronounced intercondylar ridge is on the midline above the central distal trochlea. In posterior view a large, flattened hypotarsal ridge extends into the shaft for approximately 50% of its length. Nutrient foramina are widely separated by the hypotarsal ridge in posterior view, oriented away from the midline of the shaft. In anterior view, the foramina are inside a metatarsal groove formed by the flattened-triangular orientation of the metatarsi. The proximal epiphysis is enlarged, and the shaft limits are straight, tapering slowly towards the distal portion before expanding sharply into greatly enlarged trochleae with large intertrochlear notches. The medial trochlea terminates proximally to the lateral trochleae. Measurements given in table 6.

Figure 6. Newly designated type series of *Aepyornis maximus*. A, Neotype (tarsometatarsus, USNM A65208), Ilaka, Ambositra, Madagascar. **B,** Conspecific specimen (tibiotarsus, USNM A65209), Ilaka, Ambositra, Madagascar.

`

***Aepyornis hildebrandti* Burckhardt, 1893**

Junior synonyms: *Aepyornis lentus* Milne-Edwards and Grandidier, 1894; *Aepyornis gracilis* Monnier, 1913.

Original syntype series: Femur (MfN MB.AV.73), tibiotarsus (MfN MB.AV.70) and tarsometatarsus (MfN MB.AV.67), from Antsirabe, Madagascar.

Lectotype: Tarsometatarsus (MfN MB.AV.67), designated by Brodkorb (Brodkorb 1963).

Revised diagnosis:

Femur: Has similar length and width of distal epiphyses but a markedly more slender appearance in comparison to *A. maximus,* with a slender head and distinctly narrower shaft. The shaft is tapered, becoming straight and expanding into the markedly enlarged distal condyles. The distal pneumatic foramen is a shallow and broad arch. Significantly smaller than *A. maximus* in F15 (after Bonferroni correction of p-values, alpha=0.0026).

Tibiotarsus: Similar in total proportion and morphology to that of *A. maximus*, but smaller. The proximal epiphysis has a less well-defined ectocnemial crest and procnemial crest, which leads into a weaker intermuscular line. The distal condyles are expanded but to a lesser extent than that of *A. maximus*.

Tarsometatarsus: Medio-laterally broad at the epiphyses, and has a slender midshaft with a more proximally expanded lateral metatarsal than in *A. maximus*. The proximal epiphysis is enlarged, and the shaft limits are tapered towards the distal portion before expanding sharply into the enlarged trochleae**.** Significantly smaller than *A. maximus* in the following measurements: Tmt9, Tmt14, Tmt19, Tmt33, Tmt35–Tmt36, Tmt40, Tmt43 (after Bonferroni correction of p-values, alpha=0.0012).

Revised description:

Femur: The antitrochanter has a convex articular surface transitioning in a continuous straight line to the lateral surface of the trochanter. The proximal epiphyses are enlarged, transitioning smoothly into the neck of the ball. The distal view of the neck of the ball has a strongly concave curvature. The shaft is tapered, becoming straight towards the mid-shaft, and expanding into markedly enlarged and robust distal condyles with a broad and deep intercondylar groove. The distal pneumatic foramen is a shallow and broad arch. Measurements given in table 4.

`

Tibiotarsus: Robust, with an enlarged proximal epiphysis, particularly medio-laterally. The angle of the ectocnemial ridge and the ventral support is ≥90°. The enlarged procnemial crest extends into a ridge, leading into a straight intermuscular line that terminates on the medial side of the shaft, just before the expanded distal condyle. Measurements given in table 5.

Tarsometatarsus: Medio-laterally broad at the epiphysis, and with a slender midshaft. In posterior view a large, flattened hypotarsal ridge extends into the shaft for approximately 50% of its length. Nutrient foramina are widely separated by the hypotarsal ridge in posterior view, oriented away from the midline of the shaft. In anterior view, the foramina are more closely spaced inside an anterior cotyle located inside the metatarsal groove formed by the flattened-triangular orientation of the metatarsi. The proximal epiphysis is enlarged, and the shaft limits are tapered towards the distal portion before expanding sharply into enlarged trochleae with large intertrochlear notches. The medial trochlea terminates proximally to the lateral trochleae. Measurements given in table 6.

Genus *Mullerornis* Milne-Edwards and Grandidier, 1894

Type species: *Mullerornis betsilei* Milne-Edwards and Grandidier, 1894; designated by Richmond (Richmond 1902).

Valid species recognised within genus: *Mullerornis modestus* (Milne-Edwards and Grandidier, 1869).

Revised diagnosis:

Femur: Small and slender in comparison to other genera, with medio-laterally enlarged epiphyses. The antitrochanter transitions at a sharp angle into the shaft. The proximal epiphyses are enlarged, transitioning smoothly into the neck of the ball, which is not greatly enlarged from the neck. The shaft is slender and curved. The pneumatic foramina are markedly large in proportion to the size of the femur. Significantly smaller than *Aepyornis* in the following measurements: F1–F4, F6, F10–F12, F16 (after Bonferroni correction of p-values, alpha=0.0026). Significantly smaller than *Vorombe* in the following measurements: F1–F14, F16–F17, F19–F20 (after Bonferroni correction of p-values, alpha=0.0026).

Tibiotarsus: Similar in total length to *Aepyornis hildebrandti*, but has a more slender shaft. The prominent procnemial crest is expanded markedly in medial and lateral dimensions, terminating lateral to the lateral distal condyle. The crest extends into a strong ridge, followed by a well-

`

defined intermuscular line that spans the width of the anterior facia, terminating on the medial facia after approximately 60% of the length of the shaft. The angle of the ectocnemial ridge and the ventral support is >90^{o}. The straight shaft tapers sharply from the enlarged proximal head with a moderately pronounced enlargement at the distal end.

Tarsometatarsus: Similar in length to *Aepyornis hildebrandti*, but is markedly narrower, with the tarsal bones forming a deep triangular cross-sectional shaft. In posterior view a large, flattened hypotarsal ridge extends into the shaft, leading into marked medial and lateral intermuscular ridges, which curve outwards to the medial and lateral trochleae. Nutrient foramina are widely separated by the hypotarsal ridge in posterior view. In anterior view, the foramina are closely spaced inside an anterior cotyle located inside the deep metatarsal groove formed by the triangular orientation of the metatarsi. The proximal epiphysis is enlarged, especially the medial condyle, and the shaft limits are concave, tapering towards the distal portion before expanding sharply into greatly enlarged trochleae with large intertrochlear notches. An ossified bridge is present on the anterior facia between the medial and central trochleae. Significantly smaller than *Vorombe* in the following measurements: Tmt1–Tmt6, Tmt9–Tmt36, Tmt38–Tmt41, Tmt43–Tmt44 (after Bonferroni correction of p-values, alpha=0.001).

Revised description: As for *Mullerornis modestus* (see below).

`

***Mullerornis modestus* (Milne-Edwards and Grandidier, 1869)**

Junior synonyms: *Mullerornis agilis* Milne-Edwards and Grandidier, 1894; *Mullerornis betsilei* Milne-Edwards and Grandidier, 1894; *Mullerornis rudis* Milne-Edwards and Grandidier, 1894.

Holotype: Femur (MNHN 1908-5), from Ambolisatra, Madagascar.

Revised diagnosis: As for genus.

Revised description:

Femur: Has a slender appearance with medio-laterally enlarged epiphyses. The antitrochanter has a convex articular surface, with the epiphyseal surface transitioning rapidly into the shaft. The proximal epiphysis is enlarged, transitioning smoothly into the neck of the ball, which is not greatly enlarged from the neck; the distal view of the neck of the ball has a strongly concave curvature. The shaft is slender and curved, tapering in the middle and leading into the enlarged distal condyles with a broad and deep intercondylar groove. The markedly large distal pneumatic foramen is a pointed arch with its proximal point directed towards the medial portion of the shaft. Measurements given in table 4.

Tibiotarsus: The prominent procnemial crest is expanded markedly in a lateral direction, terminating beyond the lateral distal condyle. The crest extends into a strong ridge, followed by a well-defined intermuscular line that spans the width of the anterior facia and terminates on the medial facia after approximately 60% of the length of the shaft. The angle of the ectocnemial ridge and the ventral support is >90^{o}. The straight shaft tapers sharply from the enlarged proximal head, which is moderately enlarged at the distal end. Measurements given in table 5.

Tarsometatarsus: Long and narrow, with the tarsal bones forming a triangular cross-sectional shaft. In posterior view a large, flattened hypotarsal ridge extends into the shaft, leading into marked medial and lateral intermuscular ridges that curve outwards to the medial and lateral trochleae. Nutrient foramina are widely separated by the hypotarsal ridge in posterior view. In anterior view, the foramina are more closely spaced inside an anterior cotyle located inside the deep metatarsal groove formed by the triangular orientation of the metatarsi. The proximal epiphysis is enlarged, especially the medial condyle, and the shaft limits are concave, tapering towards the distal portion before expanding sharply into greatly enlarged trochleae with large intertrochlear notches. An ossified bridge is present on the anterior facia between the medial and central trochleae. Measurements given in table 6.

`

Genus *Vorombe* gen. nov.

Etymology: From the Malagasy for “big bird”.

Type species: *Aepyornis titan* Andrews, 1894.

Valid species recognised within genus: *Vorombe titan* (Andrews, 1894).

Diagnosis:

Femur: Extremely large and robust in comparison to other genera, with enlarged epiphyses. The head transitions smoothly into the neck of the ball, which is enlarged, particularly proximo-ventrally; the distal view of the neck of the ball has a shallow and broad concave curvature. The shaft is robust and broad, and curved on the medial facia, tapering slightly in the middle and leading into enlarged distal condyles with a broad and deep intercondylar groove. The very large distal pneumatic foramen is a wide pointed arch, with its proximal point directed towards the medial portion of the shaft. Significantly larger than both *Aepyornis* and *Mullerornis* in all measurements, F1–F20 (after Bonferroni correction of p-values, alpha=0.0026).

Tibiotarsus: Extremely large and robust in comparison to other genera. The proximal end is enlarged, particularly medio-laterally. The angle of the ectocnemial ridge and the ventral support is ≥90°. The enlarged procnemial crest extends into a ridge, leading into a prominent, straight intermuscular line that terminates on the medial side of the shaft close to the distal condyle.

Tarsometatarsus: Considerably larger and more robust than other genera. The expanded intercondylar ridge is oriented above the medial trochlea. In posterior view a very large, flattened hypotarsal ridge extends into the shaft, leading into marked medial and lateral edges which merge into trochlear ridges extending from the outer condyles of the trochleae. Nutrient foramina are widely separated by the hypotarsal ridge in posterior view. In anterior view, the foramina are more closely spaced inside a shallow anterior cotyle located within a broad metatarsal groove. The proximal epiphysis is enlarged, especially the medial condyle, tapering into a straight and parallel middle shaft before expanding sharply into greatly enlarged trochleae with large intertrochlear notches. The medial trochlea terminates distal to the lateral trochleae. Significantly larger than *Mullerornis* in the following measurements: Tmt1–Tmt6, Tmt9–Tmt36, Tmt38–Tmt41, Tmt43–Tmt44 (after Bonferroni correction of p-values, alpha=0.001). Significantly larger than *Aepyornis* in the following measurements: Tmt1, Tmt3–

`

Tmt6, Tmt10–Tmt11, Tmt13–Tmt22, Tmt27–Tmt28, Tmt31, Tmt33, Tmt35–Tmt36, Tmt38–Tmt41, Tmt43–Tmt44 (after Bonferroni correction of p-values, alpha=0.001).

Description: As for *Vorombe titan* (see below).

***Vorombe titan* (Andrews 1894)**

Junior synonyms: *Aepyornis ingens* Milne-Edwards and Grandidier, 1894.

Original syntype series: Femur (NHM A439) and tibiotarsus (NHM A437), from Itampulu Vé, Madagascar (figures 7–8).

Lectotype: Femur (NHM A439); newly designated (figure 7).

Diagnosis: As for genus.

Description:

Femur: Extremely large and robust, with enlarged epiphyses. The head transitions smoothly into the neck of the ball, which is enlarged, particularly proximo-ventrally; the distal view of the neck of the ball has a shallow and broad concave curvature. The shaft is robust and broad, and curved on the medial facia, tapering slightly in the middle, leading into the enlarged distal condyles with a broad and deep intercondylar groove. The markedly large distal pneumatic foramen is a wide pointed arch, with its proximal point directed towards the medial portion of the shaft. Measurements given in table 4.

Tibiotarsus: Extremely large and robust. The proximal end is enlarged, particularly medio-laterally. The angle of the ectocnemial ridge and the ventral support is ≥90°. The enlarged procnemial crest extends into a ridge, leading into a prominent, straight intermuscular line that terminates on the medial side of the shaft close to the distal condyle. The lateral distal condyle terminates markedly distal to the medial condyle. Measurements given in table 5.

Tarsometatarsus: Extremely large and robust with enlarged epiphyses. The medio-proximal epiphysis is particularly enlarged and extends proximally. The latero-proximal epiphysis is rounded and expanded latero-distally. The expanded intercondylar ridge is oriented above the medial trochlea. In posterior view a very large, rugose, flattened hypotarsal ridge extends into the shaft, leading into marked medial and lateral edges which merge into trochlear ridges extending from the outer condyles of the trochleae. Nutrient foramina are widely separated by

`

the hypotarsal ridge in posterior view. In anterior view, the foramina are more closely spaced inside a shallow anterior cotyle located within a broad metatarsal groove. The enlarged proximal epiphysis tapers into the nearly straight and parallel middle shaft, before expanding sharply into greatly enlarged and robust trochleae with large intertrochlear notches. The medial trochlea terminates distal to the lateral trochleae. Measurements given in table 6.

Figure 7. *Vorombe titan*, lectotype (femur, NHM A439), Itampulu Vé, Madagascar.

`

Figure 8. Vorombe titan, tibiotarsus (NHM A437), Itampulu Vé, Madagascar; part of original syntype series

`

Table 3. Mass estimates for elephant bird species recognised in this study

Femoral mass estimation (kg)	*Mullerornis modestus*	*Aepyornis hildebrandti*	*Aepyornis maximus*	*Vorombe titan*
Maximum	172	342	541	732
Minimum	78	211	334	536
Mean	107.7	283.15	409.5	642.9
Standard deviation	33.2	34.1	71.8	62.6
Sample size	10	29	8	10

Table 4. Femoral measurement ranges for elephant bird species recognised in this study

Measurement	*Mullerornis modestus*		*Aepyornis hildebrandti*		*Aepyornis maximus*		*Vorombe titan*	
	Range (mm)	**N**	**Range (mm)**	**N**	**Range (mm)**	**N**	**Range (mm)**	**N**
F1	245.0-268.0	5	307.0-347.0	18	354.0-383.0	5	437.0-490.0	8
F2	28.4-37.6	12	45.9-57.7	31	51.3-69.5	10	64.4-94.1	12
F3	114.0-135.0	12	172.0-210.0	31	208.0-254.0	10	253.0-288.0	10
F4	35.2-46.7	12	56.0-69.9	31	68.7-89.6	10	66.8-99.5	12
F5	107.0-118.0	11	147.0-180.0	28	181.0-220.0	9	212.0-276.0	8
F6	31.3-37.2	10	45.9-57.3	29	51.4-67.6	7	66.3-79.2	8
F7	32.5-37.2	11	46.6-56.5	29	56.8-69.9	8	67.1-79.9	9
F8	63.8-78.8	8	90.6-140.8	20	112.5-135.5	3	139.2-181.0	6
F9	90.7-100.0	10	87.3-142.2	26	117.3-167.0	5	182.0-207.0	8
F10	50.9-71.0	6	79.4-136.0	18	56.7-86.5	2	79.9-126.0	5
F11	56.6-70.6	8	82.7-105.3	23	107.9-118.0	5	118.9-149.0	9
F12	221.0-233.0	5	233.0-309.0	17	312.0-329.0	4	374.0-426.0	8
F13	228.0-265.0	4	250.0-327.0	16	328.0-358.0	4	392.0-445.0	8
F14	231.0-256.0	9	232.0-326.0	25	332.0-364.0	4	399.0-453.0	8
F15	196.0-211.0	9	244.0-282.0	23	287.0-350.0	5	325.0-375.0	9
F16	87.2-101.4	10	121.4-151.6	24	114.0-151.0	4	177.0-202.0	8
F17	74.1-82.8	9	89.7-147.6	24	130.4-132.6	3	156.0-171.0	6
F18	86.5-99.2	9	102.8-148.6	26	143.6-166.0	4	143.0-210.0	7
F19	18.9-27.8	7	20.5-34.8	26	26.3-35.9	7	32.0-44.0	9
F20	8.4-12.2	11	12.7-29.2	27	13.7-23.5	10	18.5-29.6	11

`

Table 5. Tibiotarsal measurements (in mm) for elephant bird species recognised in this study

Measurement	*Mullerornis modestus*, NHM A676	*Aepyornis hildebrandti*, MfN MB.AV.70	*Aepyornis maximus*, USNM A605209	*Vorombe titan*, NHM A437
Tt1	435.0	473.0	614.0	—
Tt2	20.5	39.3	60.5	44.3
Tt3	85.0	110.0	165.0	206
Tt4	28.2	26.8	39.8	75.8
Tt5	61.0	90.1	129.0	162.0
Tt6	45.5	59.3	84.6	112.5
Tt7	51.0	72.7	100.4	134.5
Tt8	91.0	128.8	184.0	—
Tt9	57.0	85.5	96.5	—
Tt10	65.0	93.9	196.0	—
Tt11	48.0	30.4	55.6	—
Tt12	40.8	65.6	111.9	—
Tt13	57.2	59.2	90.2	—
Tt14	59.8	70.9	105.4	—
Tt16	34.0	53.5	78.9	—
Tt17	28.0	28.0	45.2	—
Tt18	15.2	18.6	30.9	—
Tt19	25.0	43.3	49.7	—
Tt20	63.0	71.6	105.0	—
Tt21	96.0	153.0	225.0	263.0

`

Table 6. Tarsometatarsal measurement ranges for elephant bird species recognised in this study.

Measurement	*Mullerornis modestus*		*Aepyornis hildebrandti*		*Aepyornis maximus*		*Vorombe titan*	
	Range (mm)	N	Range (mm)	N	Range (mm)	N	Range (mm)	N
Tmt1	271.0-324.0	11	266.0-346.0	24	352.0-385.0	5	419.0-486.0	5
Tmt2	15.0-20.3	11	21.0-29.4	24	27.0-34.7	5	32.0-39.0	5
Tmt3	27.0-32.3	11	43.0-65.0	24	63.3-69.2	5	76.9-87.2	5
Tmt4	27.2-37.6	11	39.2-50.9	23	48.3-54.5	5	59.8-62.7	5
Tmt5	65.0-79.3	11	94.9-126.4	24	125.2-140.2	5	164.0-178.0	5
Tmt6	27.9-39.5	11	34.1-61.1	21	46.4-58.6	5	61.6-67.8	5
Tmt7	24.0-30.4	11	28.7-69.3	23	46.4-54.7	5	52.9-68.0	4
Tmt8	26.3-44.7	10	24.5-69.7	24	71.8-87.8	5	74.7-95.3	4
Tmt9	65.8-81.5	11	97.1-125.0	23	140.3-150.5	4	173.0-184.0	5
Tmt10	54.0-67.3	11	68.9-110.6	23	108.3-118.7	4	131.1-153.0	5
Tmt11	64.0-75.3	11	89.2-123.4	24	120.5-140.1	5	161.0-173.0	5
Tmt12	17.6-25.9	11	21.9-33.3	22	32.5-36.8	5	33.9-48.9	5
Tmt13	26.4-34.2	11	35.6-50.3	23	44.6-54.2	5	54.8-61.7	5
Tmt14	21.3-27.4	10	32.8-47.5	23	44.8-55.5	5	59.1-81.6	4
Tmt15	19.7-27.6	11	31.8-42.4	23	43.7-50.7	4	54.9-73.7	4
Tmt16	21.3-27.9	10	36.0-48.6	23	49.8-53.9	4	57.3-66.7	4
Tmt17	30.0-37.2	11	41.5-58.9	22	61.0-66.1	5	64.1-83.1	4
Tmt18	28.0-34.2	11	36.4-50.5	22	50.7-62.1	5	68.8-76.8	4
Tmt19	26.2-38.2	11	41.9-55.0	22	62.2-68.0	5	76.4-88.1	4
Tmt20	25.4-31.0	11	36.2-52.6	24	50.3-56.2	5	63.7-80.4	4
Tmt21	22.0-25.8	10	31.0-45.8	24	45.4-50.6	5	55.4-89.8	4
Tmt22	19.0-29.9	10	33.8-44.6	23	48.0-53.5	5	55.2-70.0	4
Tmt23	20.0-34.6	9	42.3-61.3	23	55.6-70.6	5	61.5-81.4	5
Tmt24	23.0-36.3	10	40.2-56.7	23	52.9-61.7	5	65.2-73.5	5
Tmt25	24.6-33.4	11	35.0-56.2	24	47.5-58.1	5	59.2-65.3	5
Tmt26	35.0-47.5	9	42.3-61.5	23	55.8-65.1	5	68.6-85.5	5
Tmt27	34.0-68.8	11	44.6-66.4	24	64.6-71.3	5	80.1-96.2	5
Tmt28	24.0-45.6	10	45.1-66.1	23	53.6-73.4	5	77.2-100.1	5
Tmt29	20.5-30.3	10	33.5-55.4	23	43.4-66.1	5	54.2-59.1	5
Tmt30	26.1-33.2	11	37.7-53.6	24	51.1-56.4	5	53.6-70.6	5
Tmt31	26.8-35.3	11	35.6-48.1	24	49.2-58.9	5	62.4-67.6	5
Tmt32	6.8-12.8	10	8.8-24.9	23	14.5-20.2	5	14.1-24.6	5
Tmt33	56.0-67.4	10	80.3-110.0	24	121.6-135.3	4	151.9-167.0	4
Tmt34	10.2-19.9	8	7.9-25.2	21	21.14-33.4	5	26.1-36.4	3
Tmt35	32.6-45.6	11	52.8-72.6	23	73.2-79.6	4	88.2-99.7	5
Tmt36	19.0-34.2	11	38.4-52.5	23	45.1-53.1	5	50.8-69.8	5
Tmt37	18.2-33.6	8	36.7-56.7	22	37.8-49.0	4	52.3-82.0	5
Tmt38	38.5-49.0	9	54.8-71.4	22	72.5-76.9	5	73.4-93.0	3
Tmt39	44.0-53.8	9	58.6-79.5	22	84.1-91.7	5	76.5-110.7	4
Tmt40	53.8-65.2	9	80.1-101.9	22	112.0-120.2	4	127.0-137.0	4
Tmt41	271.0-300.0	11	242.0-310.0	23	326.0-357.0	5	391.0-440.0	4
Tmt42	261.0-313.0	10	237.0-333.0	22	356.0-372.0	4	380.0-447.0	5
Tmt43	263.0-317.0	10	261.0-329.0	22	363.0-372.0	4	415.0-457.0	5
Tmt44	265.0-312.0	10	256.0-334.0	23	312.0-381.0	5	414.0-459.0	4

`

2.6 Discussion

Our study provides the first rigorous quantitative analysis of morphometric variation within elephant birds, using data from almost all of the specimens available for study in global museum collections, and employing multivariate analysis of morphometric data with methods for estimating missing values that are robust to potential sources of error. This exhaustive analysis fundamentally revises the taxonomic framework for understanding diversity and variation within elephant birds, compared to historical taxonomic reviews that were based largely upon qualitative assessment of much smaller sample sizes of specimens. We demonstrate that three main morphometric clusters can be identified within measurement data for elephant bird appendicular elements, with one cluster further divisible into two separate subclusters. As two of these main clusters correspond to different genera previously defined by earlier authors on the basis of qualitative or univariate assessment of variation within the Aepyornithidae, we interpret this primary separation of morphotypes as representing genus-level differentiation, with further subdivision within one cluster interpreted as representing species-level differentiation. We therefore identify three valid elephant bird genera, two of which are monotypic, and one of which contains two species.

Our new data-driven taxonomic revision, which follows the rules of seniority for available taxonomic names, recognizes both different numbers and different identities of elephant bird taxa compared to previous assessments. Our taxonomic framework recognises only four elephant bird species, substantially reducing the number of valid species recognised by earlier authors, who identified between seven and 15 species (tables 1–2). As our revision is based upon multivariate analysis of the distribution of variation within and between morphotype clusters in multidimensional shape-space, we consider our taxonomic conclusions to be substantially more robust than previous studies. However, we note that it is possible our taxonomic hypothesis may represent a conservative estimate of elephant bird species richness based upon the limitations of what morphology-based quantitative analysis can resolve, and we encourage further investigation of variation across elephant birds using alternative approaches, such as ancient DNA analysis of well-provenanced material associated with different morphometric clusters, an approach that led to a revision of morphology-based taxonomy in moa (Huynen et al. 2003).

The four valid elephant bird taxa that we recognise in this study also represent different taxonomic concepts to those recognised by previous authors. The small-bodied genus

`

Mullerornis has generally been interpreted in recent decades as comprising three species, *M. agilis*, *M. betsilei* and *M. rudis*. However, not only do we synonymise these three taxa as representing a single species on the basis of morphometric analysis, but we also identify the name *M. modestus* as the senior synonym for all three taxa; this name was previously considered to be a junior synonym of *Aepyornis maximus* (Brodkorb 1963). *Aepyornis maximus* has traditionally been interpreted as the largest elephant bird, both in older taxonomic reviews and also in popular culture, but the type material of this first elephant bird to be described has rarely been considered since its original description, with the species concept of *A. maximus* instead becoming associated with later collections of very large elephant bird bones that have been erroneously assigned to the taxon. Our analysis demonstrates that the name *Aepyornis* is in fact not associated with the largest known elephant bird material, but instead represents the medium-sized genus-level cluster in our morphometric analysis, with this genus containing only two diagnosable species (*A. hildebrandti* and *A. maximus*) compared to previous assumptions of four or more valid congeners (table 1).

As the name *Aepyornis* cannot be applied to the largest-bodied genus-level cluster recognised in our analysis, we reveal that the largest of the elephant birds, which we name in this study as *Vorombe titan*, has never previously been identified as constituting a distinct genus. All body mass estimates for giant extinct birds should be interpreted with caution as they fall outside the range of extant birds used in model construction; however, our newly derived mass estimates for elephant birds based on least femoral shaft circumference measurements (Table 3) demonstrate that the mass of *Vorombe* (mean = 642.9 kg, range = 536-732 kg) exceeds estimates based on comparable data for other extinct Quaternary giant birds such as *Dinornis* (Dinornithiformes: range = 61-275 kg) and *Dromornis* (Gastornithiformes: male mean = 583.6 kg, range = 439.3-727.8 kg; female mean = 440.7 kg, range = 316.6-560.0 kg) (Worthy et al 2005, Handley et al. 2016) giving it the largest estimated body mass of any bird on record. Indeed, the largest elephant bird femur measured for this study (MNHN MAD 368) was incomplete and therefore could not formally be assigned to a cluster due to our conservative analytic framework, but must also be referable to *Vorombe* on the basis of size; this specimen had a least shaft circumference of 308 mm and a corresponding mass estimate of 860 kg, making this the largest known bird individual ever recorded. However, prior to our study, the world's largest birds have rarely even been recognised as a distinct species let alone as a separate genus, and have instead been generally misinterpreted as merely representing the upper end of variation within *Aepyornis maximus* based upon broad, qualitative size ranges assumed for this

`

"wastebasket taxon", leading to underestimation of the true size of the largest elephant birds by previous authors (Handley et al. 2016).

Morphological variation in the giant moa *Dinornis*, which was formerly interpreted as representing taxonomic variation, has been shown instead to constitute extreme reversed sexual size dimorphism (Huynen et al. 2003; Michael Bunce et al. 2003), and most extant ratites also exhibit varying levels of sexual size dimorphism (Olson and Turvey 2013). Several authors have hypothesised that elephant birds might have also exhibited sexual size dimorphism, and it has even been suggested that *Aepyornis maximus* and *A*. *medius*, two formerly recognised species that were considered to be distinguishable only by size, could represent male and female morphs of the same species (Handley et al. 2016). Our quantitative assessment demonstrates that these two putative species are in fact better interpreted as representing natural variation (potentially sexual variation) within a single morphotype. Our results do not exclude the possibility that elephant birds exhibited sexual size dimorphism, but we consider that any such variation is likely to be captured as within-cluster variation in our analysis, as our clusters are differentiated not only by discrete size/allometric scaling but also by more complex patterns of variation across a large series of characters that would not be expected from sexual size dimorphism, and so they are better interpreted as representing distinct taxonomic units. Indeed, the cluster of specimens that we refer to *Aepyornis maximus* (cluster 2b) includes some adult individuals with medullary tissue present inside the long bones, demonstrating that these individuals were sexually mature females, and other adult individuals lacking medullary tissue. However, we encourage further research to test our new morphotype-based taxonomic framework for aepyornithids, especially through the use of ancient biomolecular techniques, to investigate whether any observed variation can be associated with sexual dimorphism (Michael Bunce et al. 2003; Handley et al. 2016).

Biogeographic assessment of locality data associated with elephant bird specimens included in distinct morphometric clusters demonstrates the sympatric co-occurrence of *M. modestus, A. maximus* and *V. titan* in the south and south west of Madagascar and into the central highlands. The substantial disparity in size between these different taxa suggests that these birds were able to coexist by exploiting distinct dietary niches and floral interactions. However, if the incomplete holotype tarsometarsus of "*Aepyornis lentus*" is excluded from biogeographic consideration due to potential unreliability of cluster assignment, all of the specimens assigned to *A. hildebrandti* in our analysis are restricted to the highest elevations of the central highlands at Antsirabe and Masinandreina. This biogeographic pattern suggests that, whereas different

`

elephant bird genera were morphologically and ecologically distinct enough to be able to coexist in the same landscapes, different species within the same genus (*Aepyornis*) displayed largely allopatric differentiation between different ecoregions, a spatial pattern also shown in many other vertebrate taxa across Madagascar today (Goodman and Benstead 2003). This spatial distribution pattern between different recognised species of *Aepyornis* also provides further support for our interpretation of clusters 2a and 2b as representing taxonomic variation rather than sexual dimorphism.

Previous assumptions of elephant bird species richness (between seven and 15 valid species; table 1) are similar to species richness in the other late Quaternary insular radiation of now-extinct ratites, the moa of New Zealand, in which nine valid species in six genera are currently recognised from Holocene deposits (Bunce et al. 2009). Moa taxa were ecologically differentiated by environmental factors including habitat type and elevation (Trevor Worthy and Holdaway 2002). However, the revised levels of elephant bird species richness presented in this study are substantially lower than for moa. This disparity may partly reflect variation in collection effort and number of available specimens between these two island systems. Madagascar's considerably larger area and greater range of ecoregions might be expected to have driven greater local endemism and diversification in ratites than in New Zealand (Goodman and Benstead 2003), but available elephant bird collections are largely restricted to material from southern Madagascar and the central highlands; however, eggshell remains from archaeological and palaeontological deposits in the extreme north of the island, not associated with skeletal material, indicate that elephant birds were more widely distributed in other ecoregions across the island that are known to contain other locally endemic taxa (Grealy et al. 2017). Conversely, New Zealand's ecosystems experienced specific geological disruptions during the Cenozoic that are likely to have driven increased diversification in moa, including separation of landmasses, glacial progression and recession, and tectonic activity (M. Bunce et al. 2009). Whereas birds were the only large-bodied terrestrial vertebrates in New Zealand before human arrival, Madagascar's Quaternary ecosystems also contained a series of other large-bodied non-avian terrestrial herbivores (giant lemurs, giant tortoises and hippos), which are likely to have limited the range of niches that elephant birds could occupy and therefore probably restricted diversification in the group.

We encourage further investigation of elephant bird systematics and taxonomy, employing complementary data and methods to those presented in this study. In particular, the suggested bimodality in thickness of elephant bird eggshell (Grealy et al. 2017) was consistent with

`

previous recognition of two size-differentiated elephant bird genera, but becomes more difficult to interpret taxonomically following recognition of three distinct genera, and necessitates rigorous quantitative assessment of patterns of eggshell thickness together with more detailed consideration of eggshell pore morphology and other characters, and efforts to link ancient DNA from eggshells and skeletal remains. We also encourage new investigation of variation in elephant bird cranial characters to test whether our taxonomic hypotheses based on postcranial skeletal elements are borne out by other available skeletal data. However, the new taxonomic framework for the Aepyornithidae that we present here provides an important baseline for future studies of avian evolution and Quaternary ecology, and represents a new framework for understanding Madagascar's past ecosystems and reconstructing extinction chronologies for the island's unique and fascinating megafauna.

`

Chapter three

`

`

Chapter three

Early Holocene human presence in Madagascar evidenced by exploitation of avian megafauna

3.1 Abstract

Recent genomic analyses suggest that people first arrived on Madagascar from Austronesia by c. 2500 BP and then from Africa by 1,500 BP (Pierron et al. 2017). This hypothesis is consistent with butchery marks on extinct lemur bones c. 2,400 BP (Perez et al. 2005), and perhaps with archaeological evidence of human presence as early as 3,000-4,000 BP (Dewar and Radimilahy 2013). Here we report the earliest dated human-modified bones for the extinct Madagascar elephant bird genera *Aepyornis* and *Mullerornis*, which show perimortem chop marks, cut marks, and depression fractures matching expectations for immobilization and dismemberment for consumption. AMS dating provides evidence for the exploitation of elephant birds from c.10,500 BP onward. Butchery traces have been used to understand human impacts on naïve faunas and to document the spread of prehistoric humans (Pitulko et al. 2016; Dowd and Carden 2016; Hockett and Jenkins 2013; McPherron et al. 2010). Our evidence for anthropogenic perimortem modification of directly dated elephant bird bones represents the earliest known indication of human presence in Madagascar, pre-dating all other archaeological and genetic evidence by approximately 6,000 years, radically extending the island's known archaeological period and changing our understanding of the earliest inhabitants of Madagascar. This revision of Madagascar's prehistory suggests prolonged human-megafaunal coexistence with limited biodiversity loss, rather than rapid overkill.

`

3.2 Introduction

Madagascar's Holocene vertebrate megafauna included giant lemurs, hippopotami, giant tortoises, and the world's largest birds, the elephant birds (Aepyornithidae, up to 500 kg (Campbell and Marcus 1992)). This megafauna is now completely extinct, with the largest surviving endemic vertebrates less than 10 kg in body mass (Goodman and Jungers 2014). Representatives of all of Madagascar's extinct megafauna are known to have survived into the Holocene (Goodman and Jungers 2014), with last-occurrence dates for all genera between ~2400-500 BP, suggesting that human activities rather than climatic shifts were responsible for the extinction of this fauna. However, the dynamics of the Malagasy megafaunal extinction process, and the nature of human involvement in driving prehistoric biodiversity loss (e.g. overkill versus population attrition, possibly through indirect processes such as habitat degradation), remain poorly understood due to limited data on human interactions with megafauna and the duration of temporal overlap between humans and now-extinct species.

Researchers have sought to understand the process of Holocene biodiversity loss in Madagascar by comparing pre- and post-human eras (Goodman and Jungers 2014). Archaeological evidence for settled villages dates from 1,300 BP onwards, with occupation of most of Madagascar's coasts by 900 BP (Crowther et al. 2016). Archaeological, genetic and linguistic data all indicate that these colonists were of both Austronesian and East African heritage (Pierron et al. 2017; Kusuma et al. 2015; Parker-Pearson 2010; Brucato 2016; Blench and Walsh 2010). Lake sediment cores indicate substantial ecological change associated with Madagascar's known late Holocene archaeological period; precipitous drops of the dung fungus *Sporormiella* demonstrate a significant loss of megafaunal endemic biomass (Burney et al. 2003), followed by the expansion of grassland savannah evidenced by pollen shifts from C3 to C4 plants and sharp rises in charcoal microparticulates (Burney et al. 2004; Crowley et al. 2010; Crowley and Samonds 2013; Burns et al. 2016).

The model of first human arrival in Madagascar during the late Holocene informs how researchers define "pristine" ecosystems, frameworks for understanding ecological succession and resilience, and conservation objectives for Madagascar's threatened biodiversity (Burns et al. 2016; Bond et al. 2008; Vorontsova et al. 2016), and suggests that megafaunal population crashes occurred rapidly (possibly within centuries) following first human arrival. However, several lines of evidence have been proposed to suggest a longer period of prehistoric human occupation of Madagascar across the middle to late Holocene. Western coastal rock shelters

`

provide support for regional human presence from ~3000 BP onwards, through evidence of protracted subsistence on endemic coastal and marine fauna (Douglass 2017). Bones of extinct megafaunal mammals with butchery cut marks but lacking any associated artefacts are also known to pre-date the widely accepted archaeological settlement period. A *Palaeopropithecus ingens* radius with cut marks from Taolambiby, southwest Madagascar, has been dated to ~2,400 BP (Perez et al. 2005), and bones of *Hippopotamus lemerlei* from northwest Madagascar that are reported to show cut marks date to 4,288-4,035 BP (Gommery et al. 2011). The paradigm of late human arrival in Madagascar has recently been challenged further by discovery of small assemblages of microlithic tools at sites indicating transient occupation in northern Madagascar (Lakaton'i Anja, Ambohiposa), which have also been dated to up to 4,000 BP (Dewar and Radimilahy 2013). These microlithic tools are similar to those used in composite projectiles, and their morphology is consistent with designs from southern and eastern Africa. These two independent lines of evidence suggest a considerably older but poorly understood period of human presence on Madagascar, with important implications for understanding the resilience of island megafauna to prehistoric human activity. However, the age of the microlithic tools is based on AMS and OSL dating on associated substrate rather than direct dates on the artefacts themselves, and supposed cut marks on the *H. lemerlei* bones do not exhibit a pattern associated with butchery (Goodman and Jungers 2014).

Madagascar's elephant birds have been the focus of remarkably little modern research in comparison to the island's extinct endemic mammals, beyond recent attempts to extract ancient DNA (Grealy et al. 2017; Yonezawa et al. 2017b; Oskam et al. 2010; Mitchell et al. 2014), and little is known about prehistoric human interactions with these giant birds. Two proposed examples of human modification of elephant bird bones have both been rejected as evidence of anthropogenic exploitation. An undated, unidentified leg element of *Mullerornis* sp. recovered from an archaeological context from Ampasambazimba (Fontoynont 1909;Dewar 1984) exhibits modification that may represent natural processes(Barthere 1915; MacPhee, Burney and Wells 1985), and an *Aepyornis* sp. tibiotarsus from Itampolo, dated to the pre-settlement period (1,297–1,590 BP (MacPhee 1999)), exhibits postmortem rather than perimortem modification. Reworked elephant bird eggshell fragments have been reported from archaeological contexts in coastal rock shelters and settlements, but radiometric dating has shown that these are substantially older than the phase of human activity at the sites(Michael Parker Pearson 2010; Douglass 2017).

`

3.3 Methods

Aepyornithid pelvic limb specimens held in museum collections in Europe, USA, and Madagascar were investigated for anthropogenic marks. Length and width measurements of each mark were taken by hand using digital callipers. Length was defined using two points for each mark including origin and termination of the mark, following standards in cut mark morphology at multiple magnifications (Galán and Domínguez-Rodrigo 2013). Width is defined as the widest point of modified bone, with termination points at the unmodified bone surface perpendicular to the long axis of the mark.

When possible, measurements were taken using a Keyence VHX5000 microscope with built-in visualization software, allowing measurements to be taken without moulding. Cut mark depth can be measured at the deepest point of the mark directly from the scan. We assessed cut mark depth at magnifications between 20X and 150X. If cut mark length extended beyond the field of view at this magnification, Keyence's stitch function was used to combine measurements along the mark's length axis. The stitch function creates a 3-D composite image from several image planes and overlapping focus levels. The visualization software then creates a true focus reproduction of the scanned bone surface. When access to the Keyence microscope was not possible, xantopren-L blue putty was used to generate casts of affected areas (Dittmar et al. 2015) where there would be no possibility of causing further damage. These casts were observed and measured using a Hitachi TM3000 tabletop Scanning Electron Microscope (SEM).

Impact marks were compared to the morphology and position of tool marks previously reported from late Holocene Madagascar(Perez et al. 2005; MacPhee and Burney 1991), modern assessments of meat utility and butchery of emu, archaeological records of tool marks on rhea, and modern frameworks of archaeological exploitation analysis(Garvey et al. 2011; Galán et al. 2013).

Here the conservative frameworks of Corron (Corron et al. 2017) and Perez (Perez et al. 2005) are applied in determining evidence for butchery practices: 1, Patterning or redundancy through multiple marks in the same region; and 2, Purposefulness, a bioarchaeological explanation of why the cut marks are present. The authors recognize that this framework underestimates butchery practices, as signs of exploitation through tool marks are rare due to false negative or type II errors, where flesh is sufficiently thick that tools do not cut all the way through it.

`

New AMS radiocarbon dates were obtained by extracting 0.5g aliquots of bone using a Dremel 4000 rotary tool with a diamond cutting wheel, with analysis at the 14CHRONO Centre (Belfast, UK) and the Oxford Radiocarbon Accelerator Unit (Oxford, UK) through a NRCF grant (NF/2015/1/4). All radiocarbon data used were calibrated using OxCal version 4.2 (Bronk Ramsey 2009) and the southern hemisphere curve SHCal13 (Hogg et al. 2013).

Figure 1. Sites containing butchered elephant bird bones and AMS radiocarbon dates

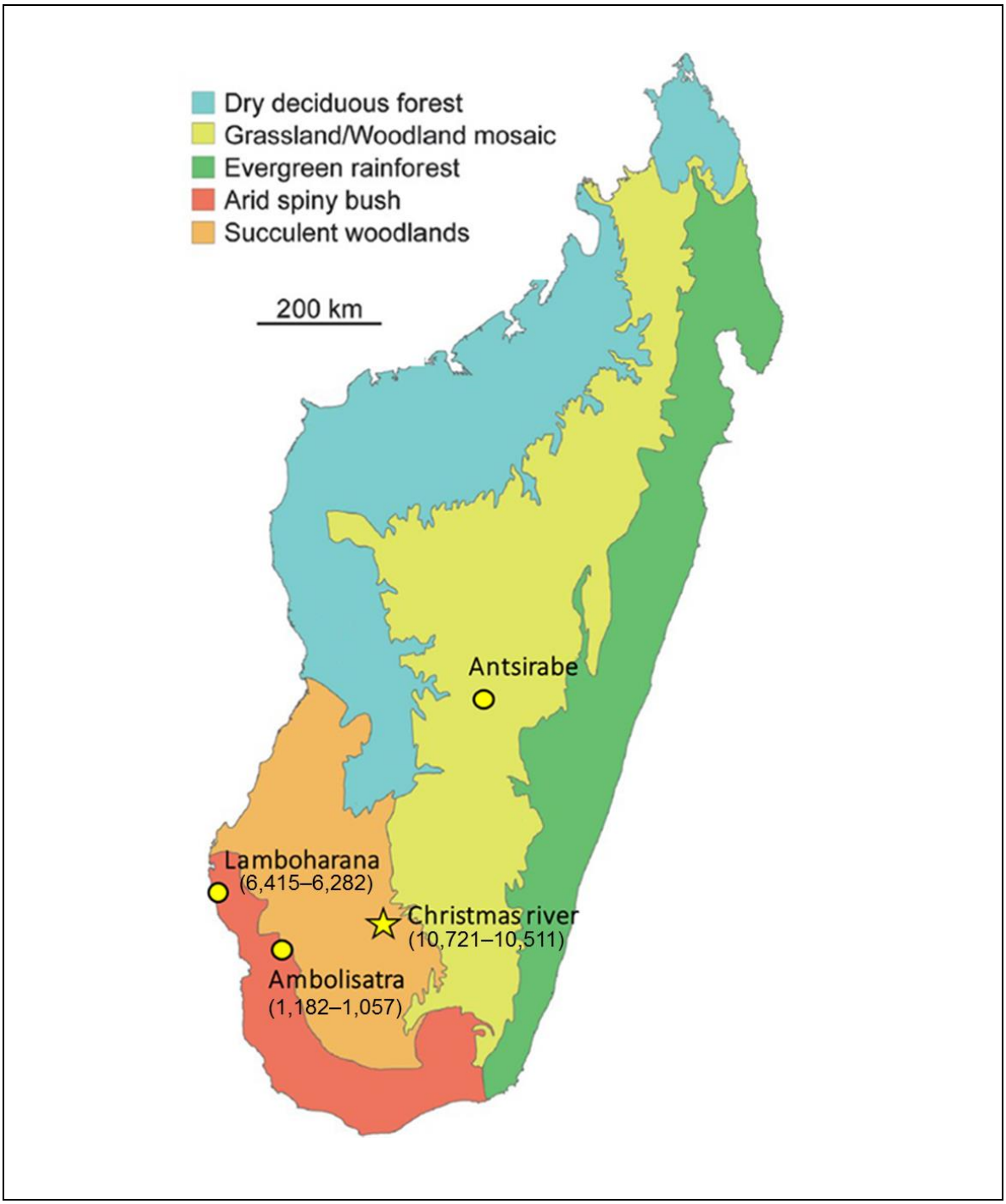

`

3.4 Results

Presented here is new evidence of prehistoric human modification of multiple elephant bird postcranial elements, representing both currently recognised genera. Pathological and taphonomic damage is distinguished from anthropogenic marks using the empirical classification of Corron et al., comparison to experimental frameworks of Galan, and the conservative criteria of Perez et al. (Corron et al. 2017; Galán et al. 2013; Godfrey et al. 2016). Anthropogenic marks described here as clefts (chop mark depression) or kerfs (cut mark depression) differ in morphology and orientation from traces resulting from natural processes (Corron et al. 2017). Clefts and kerfs are consistent with patterns of butchery in ratites through disarticulation as evidenced by marks at interarticular epiphyses of long bones (Galán et al. 2013) and phalanges (Salemme and Frontini 2011), associated with hyperextension of limb joints followed by chopping and cutting through connective tissues on their exposed fascia, leaving comparatively few anthropogenic marks on the surfaces of the diaphysis (Garvey et al. 2011).

The Christmas River (or Ilaka) site (Figure 1) is a wetland ecosystem from early Holocene Madagascar containing a well-preserved megafaunal assemblage (Muldoon and Crowley 2012). It is located on the east of the southernmost region of the Isalo sandstone massif near a tributary of the Ihazofotsy River and Ilakakabe village (S 22° 46’ 257,” E 45° 21’ 802”). The bedrock of the region is Permian and Triassic in age and belongs to the Karroo group of the Lower Sakamena formation of the Morondava basins. The bedrock is overlain by recent sediments that include layers of beige sandy soil, black clay, and a highly fossiliferous 13-15m deep layer of slate grey clay. Previously published AMS dates from multiple vertebrate taxa and from wood present in the bone bed indicate a wet phase between ~11,000–9,000 BP, and strata directly above the bone bed are consistent with increased regional aridity later in the Holocene (Muldoon and Crowley 2012). Two skeletal elements from a single *Aepyornis maximus* individual from the slate grey clay layer, described by Muldoon et al., show perimortem anthropogenic modification (Figure 2; Table 1). Bone collagen samples from these specimens were directly dated at two separate AMS radiocarbon facilities, with a combined calibrated date range of 10,721–10,511 BP (Table 2).

`

Table 1: Dimensions of tool marks on *Aepyornis maximus*, USNM A605209

Mark Number	Modification	Maximum length (mm)	Maximum width (mm)	Maximum depth (mm)
TM-1	Cut mark	16.7	5.3	1.6
TM-2	Cut mark	11.0	4.7	1.3
TM-3	Cut mark	12.4	3.3	1.3
TM-4	Cut mark	14.7	5.4	3.3
TM-5	Cut mark	5.7	4.4	3.8
TT-1	Depression Fracture	18.4	17.3	6.8
TT-2	Depression Fracture	52.1	16.6	7.6
TT-3	Chop Mark	44.5	7.8	5.1
TT-4	Cut mark	18.1	4.2	2.0

Figure 2. *Aepyornis maximus* skeletal reconstruction

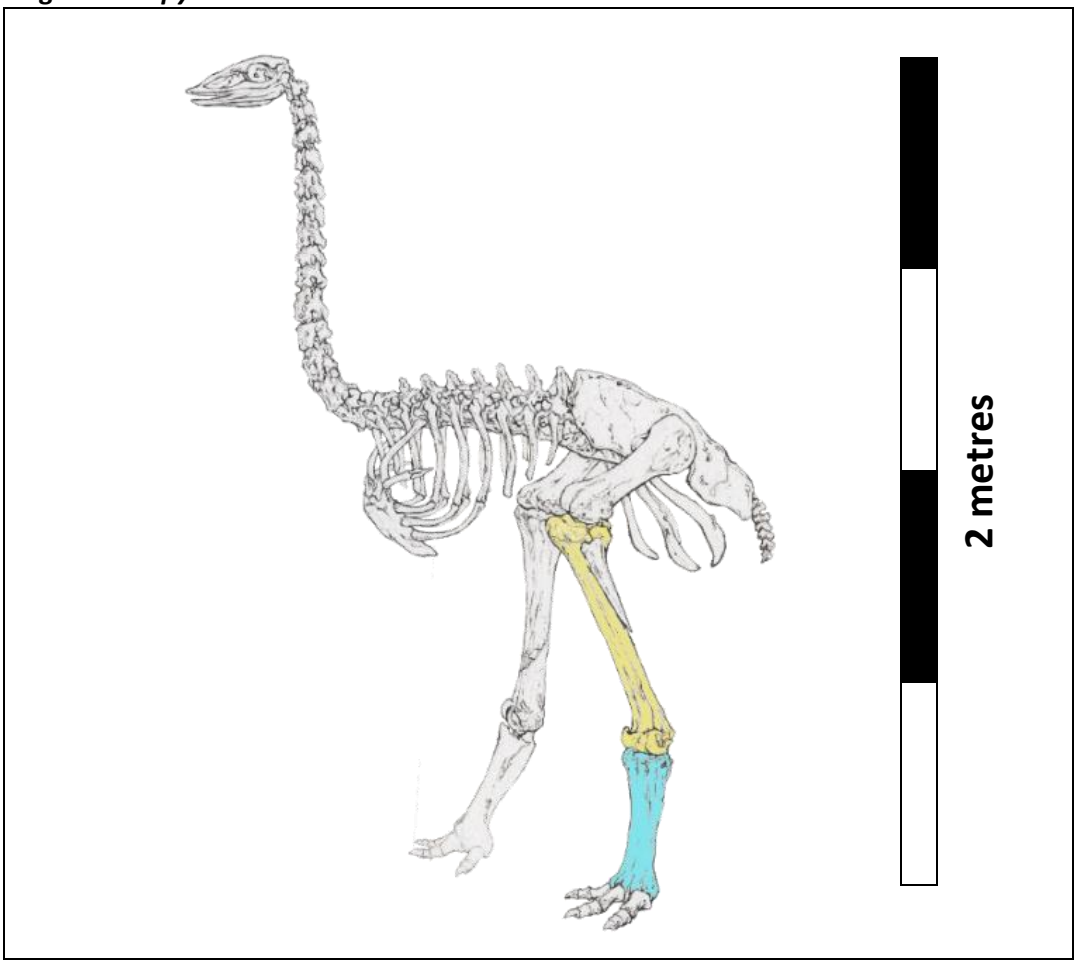

Highlighted elements correspond to Figs. 3 (blue) and 4 (yellow).

`

A tarsometatarsus (USNM A605209; Figure 3) exhibits two linear grooves on the distal aspect of the lateral condyle of the central trochlea. A third groove is present on the medial condyle of the central trochlea, posterior to the previous two marks, and a fourth groove is present on the medial condyle of the medial trochlea. A fifth is more centrally located on the lateral trochlea. All of these grooves have centrally oriented bevels and v-shaped floors. Whilst the penetrating marks are intact and well defined, the edges are irregular and undefined at their centres with portions of the bone surface absent. These marks are consistent with kerfs made by single-bladed, sharp lithic tools and multiple cutting actions intended to disarticulate the central phalanges (Galán and Domínguez-Rodrigo 2013).

A tibiotarsus from the same individual (USNM A605208 Figure 4) contains ossified medullary bone in the cortex, indicating that the individual was a gravid adult female. The diaphysis exhibits two depression fractures, one on the anterior fascia of the proximal surface, and another on the lateral portion of the posterior fascia at the distal surface, which may be hobbling impact marks from immobilizing the animal. A large, laterally oriented linear anthropogenic mark is also present on the medial condyle of the distal process, ending in a large undefined fragmentation of the anterior medial portion of the condyle and exposing a rough and uneven trabecular surface. Bevels are oriented centrally with an off-centre v-shaped floor biased towards the anterior. The mark penetrates through cortical tissue, leaving exposed trabeculae forming both wall aspects. Groove edges are defined at the medial limit, becoming undefined at the centre. The groove is rugose with varying relief in posterior aspect, characteristic of perimortem damage caused by a lithic tool (Galán et al. 2013), and smooth and straight in anterior aspect. The lack of undefined cracking extending away from the central extremity of the mark indicates that this kerf was made upon fresh bone, and the homogeneous colouration of the bone surface and exposed fascia also indicates that it was made before deposition. A secondary anthropogenic linear groove is present off-centre of the medial fascia oriented towards the missing anterior medial condyle with similar kerf morphology. The posterior-lateral bevel edge is defined at the anterior-medial end, and undefined from the centre to the posterior-lateral end. The morphology and orientation of the cleft and kerf are consistent with disarticulation at the intertarsal joint, including high-impact chopping actions associated with disarticulation of large animals (Garvey et al. 2011; Galán et al. 2013).

`

Figure 3: Tool marks on *Aepyornis maximus* tarsometatarsus, USNM A605209

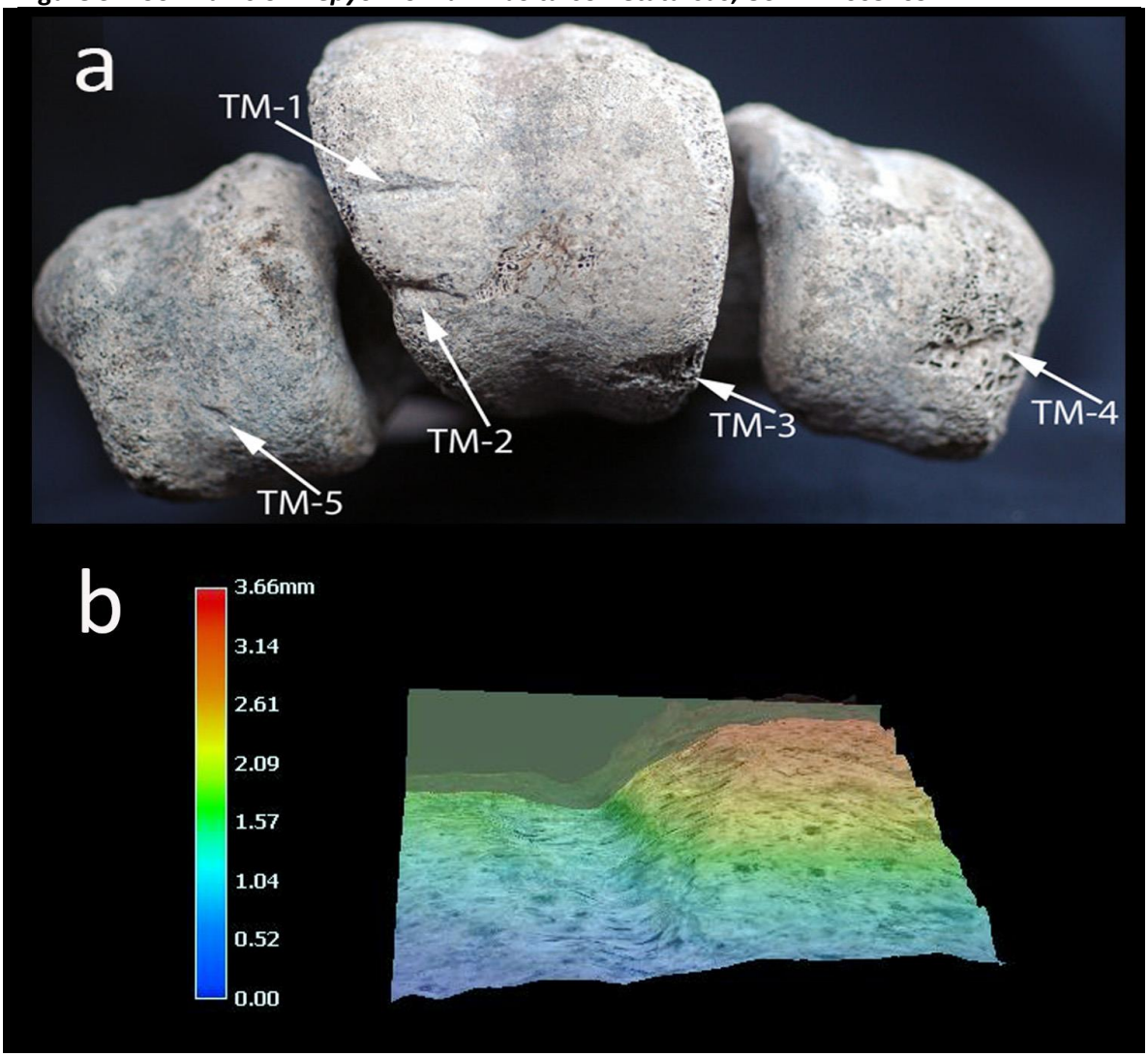

a) Distal aspect of *Aepyornis maximus* tarsometatarsus from Christmas River (USNM A605209), showing five cut marks, three (TM-1 to TM-3) on the central trochlea (digit III), one (TM-4) on the medial trochlea (digit II), and one (TM-5) on the lateral trochlea (digit IV). b) Cross-section of TM-1 at 30x magnification, illustrating depth using a topographic height colour scale.

Table 2. List of newly recognized elephant bird bones with perimortem anthropogenic modification and AMS radiocarbon dates

Specimen number	Species	Element	Location	Sample number	^{14}C age (yrs. BP)	Calibrated date (yrs. BP), ±2σ
USNM A605209	*A. maximus*	Tibiotarsus	Ilaka	UBA-31590	9,428 ± 53	10,721–10,511
USNM A605209	*A. maximus*	Tibiotarsus	Ilaka	Hela-1774	9,535 ± 70	10,721–10,511
USNM A605208	*A. maximus*	Tarsometatarsus	Ilaka	N/A	-	-
MNHN MAD6768	*M. modestus*	Tibiotarsus	Lamboharana	UBA-29726	5,597 ± 40	6,415–6,282 (93.6%)
MNHN MAD1906-16-67	*A. maximus*	Tibiotarsus	Ambolisatra	OxA-33535	1,297 ± 24	1,182–1,057 (93.7%)
MNHN MAD6662	*M. modestus*	Tarsometatarsus	unknown	UBA-19725	1,296 ± 32	1,270–1,074 (95.4%)
MNHN MAD384	*A. hildebrandti*	Tarsometatarsus	Antsirabe	N/A	FAILED	FAILED

*Same individual

`

Figure 4: Tool marks on *Aepyornis maximus* tibiotarsus, USNM A605208

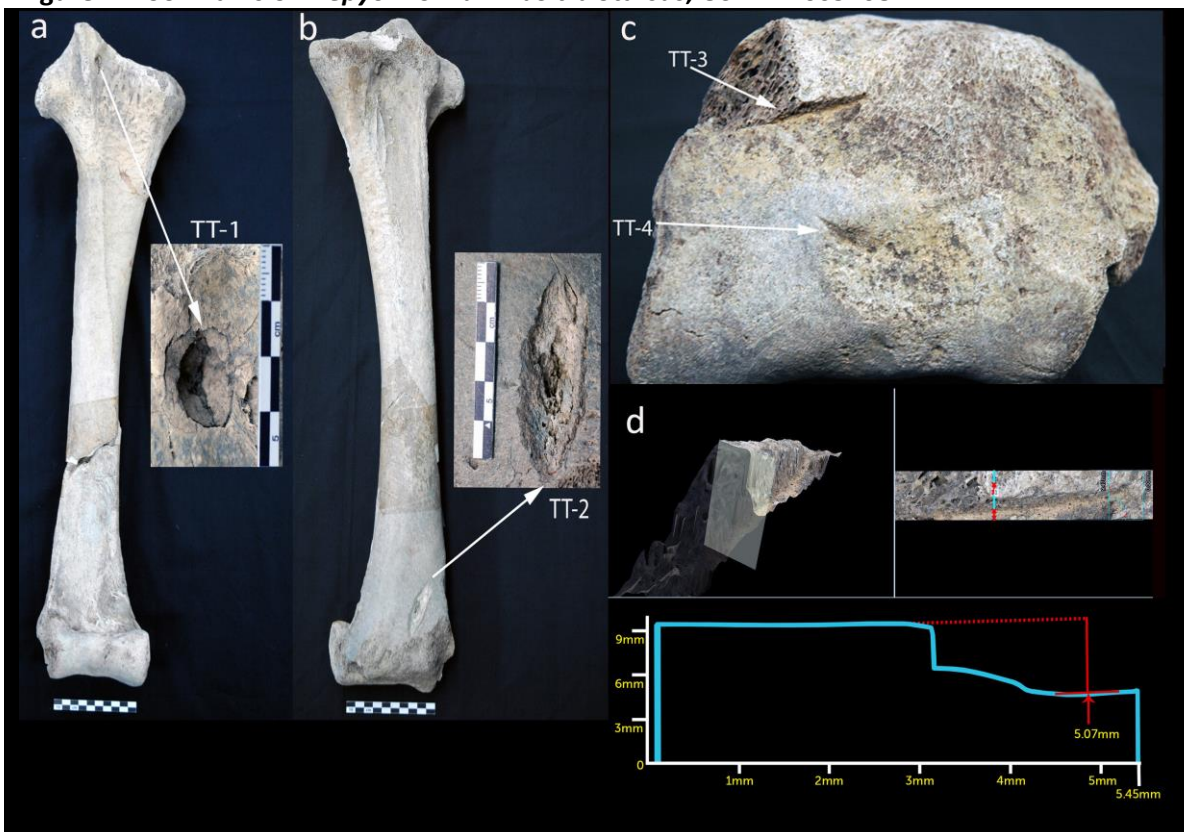

a) Depression fracture on the anterior fascia of the proximal end of *Aepyornis maximus* tibiotarsus from Christmas River (USNM A605208). b) Depression fracture on the lateral aspect of the posterior fascia. c) Distal aspect of tibiotarsus, showing two cut marks (TT-3, TT-4). d) Close-up and profile of cut mark TT-3 on the medial condyle of the distal articular process (digital thin section shows the wall and kerf floor of the mark).

Additional evidence of ancient Holocene exploitation of elephant birds is also available in historical museum collections from Madagascar that have been re-examined. A *Mullerornis* sp. tibiotarsus from Lamboharana (MNHN MAD6768) that have been AMS dated directly to 6,415–6,282 BP exhibits a shallow, laterally oriented 20×0.2 mm linear anthropogenic mark on the distal end of the posterior fascia of the diaphysis. Bevels are oriented centrally with a central v-shaped floor. The distal aspect of the groove is less regular and has more crenellations along the margin than the proximal aspect. This mark is again consistent with a kerf made by a lithic tool, with the orientation and morphology indicative of butchery (Appendix three, Figure 1). Other elephant bird specimens exhibiting distinct anthropogenic marks are dated to within Madagascar's late Holocene human settlement period, or could not be dated directly (Appendix three, Figures 2-4).

`

3.5 Discussion

This evidence for anthropogenic perimortem modification of directly dated elephant bird bones from multiple taxa and geographical localities represents the earliest known evidence of human presence in Madagascar, pre-dating all other archaeological evidence of regional anthropogenic activity (Perez et al. 2005) by approximately 6,000 years, and radically extending the island's known archaeological period. Our study therefore reveals a previously unrecognized, "cryptic" period of human presence and coexistence with now-extinct megafauna on Madagascar, which is now documented across almost the entirety of the Holocene.

These findings pose major archaeological and palaeontological questions, of crucial importance for understanding early human migrations and Quaternary megafaunal extinction dynamics. Fundamentally, evidence for long-term coexistence of humans and megafauna in Madagascar demonstrates that a radically different extinction paradigm is required to understand biodiversity loss in this island ecosystem. In contrast, the elephant birds' closest ecological analogue, the moa (Dinornithiformes) of New Zealand, probably became extinct <150 years after Polynesian settlement (Holdaway and Jacomb 2000).

This discovery of early Holocene evidence of human presence on Madagascar also raises the important question of why, if the island was occupied by prehistoric settlers continually throughout the Holocene, direct archaeological evidence of human settlement pre-dating the late Holocene has not yet been detected. Archaeological research in Madagascar has largely been focused on relatively shallow cave excavations that have not extended into early Holocene sediments(Dewar and Radimilahy 2013) and so it is possible that evidence of older human presence has so far been missed. Alternatively, early-mid Holocene human presence on Madagascar may have been restricted to transient Neolithic migration(s), presumably across the Mozambique Channel, rather than permanent island-wide settlement. New well-described excavations are required to test between these alternative potential hypotheses for prehistoric human colonization, and provide further insights into human-megafaunal interactions in Late Quaternary Madagascar.

`

`

Chapter four

`

`

Chapter four

Extinction chronology of the elephant birds

4.1 Abstract

Multidisciplinary evidence from palaeontological and archaeological excavations, geological and historical records, and contemporary ecology can be used to interpret patterns of natural and anthropogenic development of modern biomes. Insular megafauna have disproportionately large impacts on ecosystem networks through regulation of floral biomes and nutrient dispersal. Determining the timing and tempo of faunal extinction following human arrival determines the relative impact of colonisation events and defines a framework to study how ecological networks change in response to their extinction.

The extinction of Madagascar's enigmatic radiation of avian megaherbivores, the elephant birds (Aepyornithidae), has been subject to little modern critical synthesis of available data due to taxonomic confusion and the limited availability of high quality datasets. Here we review all previously published radiocarbon data for Aepyornithidae, and present a new dataset of AMS radiocarbon dates from skeletal elements held in museum collections. Extinction estimates were generated across three genera through GRWIM inference and are compared against ecological and archaeological records from the Holocene.

All extinction chronologies indicate extended periods of co-occurrence with multiple waves of human colonisation and reveal persistence after major climatic and ecological changes. Predicted extinction timing for all genera across a range of geographic locations and habitat types c.1000-1100 BP are within just a few hundred years of Bantu settlement c.1500 BP and is congruent with last occurrence records for subfossil giant lemurs and an increase in the hunting of smaller species. This evidence strongly implicates the role of humans in causing Madagascar's megafauna extinction event and promotes the need for more expansive and detailed chronological series of data. As humans were exploiting aepyornithids in the early Holocene it is vital that novel extinction studies must consider the role of changing technological and cultural dynamics of successive waves of colonists.

`

4.2 Introduction

Late Quaternary extinction studies seek to understand the processes and patterns of biodiversity loss, to inform baseline models of pristine environments for conservation targets, and to identify species at high risk of extinction (Turvey 2009; Malhi et al. 2016). Multidisciplinary evidence from palaeontological and archaeological excavations, geological and historical records, and contemporary ecology within a temporal framework, can be used to interpret patterns of natural and anthropogenic development of modern biomes (Bakker et al. 2016). To reconstruct the timing of prehistoric faunal extinction events and to identify temporally correlated natural and anthropogenic drivers of these extinctions, it is necessary to develop a robust chronology of radiocarbon or other radiometric dates, with good provenance of taxonomy and context, as well as careful extraction and pre-treatment procedures (Lister et al. 2012).

Quaternary Madagascar was host to an extraordinary megafauna of giant lemurs, giant tortoises, hippopotami, and an endemic radiation of large-bodied palaeognathus birds, the elephant birds (Aves: Aepyornithidae). The extinctions of the giant lemurs have been subject to considerable study, with AMS radiocarbon chronologies of their population declines allowing comparison with the timing of both environmental factors and anthropogenic impacts in order to identify potential extinction drivers (Burney 1998; Perez et al 2005; Crowley 2010). However, the elephant birds have so far been the focus of limited radiometric dating, which has typically consisted of site-specific studies that have aimed to answer questions related to the significance of eggshell remains in archaeological midden sites rather than objective attempts to study their extinction (Parker-Pearson et al. 1995; Parker-Pearson 2010; Douglass 2016a). No systematic attempts have yet been made to understand elephant bird extinction dynamics, either regionally or island-wide, either for single species or multi-taxon assemblages, and current reporting of extinction timing in elephant birds is inconsistent and based upon alternate sources of evidence.

Long-term environmental archives have been used to establish a Late Quaternary temporal record for ecosystem change and patterns of abundance and faunal turnover of megaherbivores (potentially including elephant birds) in Madagascar. Rapid increases in charcoal abundance from lake deposits at Ambolisatra in the south west at c.1800-1600 BP, and from speleothems from Anjohibe cave and lake sediment cores from the north, north-west, and northern central highlands at c.1300-900 BP (Burney et al. 2004; Crowley et al. 2010), are commonly interpreted

`

as signs of landscape change in response to human clearing of forest (Goodman and Jungers 2014). The long-term fungal spore record for the coprophilous fungus *Sporormiella*, which represents a quantifiable proxy of abundance (population biomass) of megafauna in an ecosystem, indicates that rapid declines in abundance of native megafauna precede the increase in fire regime in sediment records by several centuries in all regions of Madagascar, refuting hypotheses of megaherbivore extinction being caused by either widespread or regional catastrophic fires (Burney, Robinson, and Burney 2003). However, there were several large-bodied taxa in Holocene Madagascar that produce faecal matter that can be host to *Sporormiella* species, making it difficult to infer whether this proxy pattern of general megafaunal decline before the increase in fire regime reflects the specific trajectory of elephant bird populations (Wood et al. 2011; Burney et al. 2003).

The period of warming beginning island wide c. 4500 BP driving a more arid environment was initially interpreted as a major cause of megafauna extinction (Mahe and Sourdat 1972). However, δ^{15}N isotopes from vertebrate remains show no increase around the timing of island-wide peak aridity c. 1000 BP that would inform a major impact from drought (Crowley et al. 2016), driving modern hypotheses of anthropogenic driven extinction. Discussion of this lack of drought impact has not yet been assessed at a regional level, and as the aridification was focussed on the south and south west regions, naturally driven extinction is retained as an possible cause of extirpation as local peak aridity (1300 - 800 BP) (Virah-Sawmy et al. 2010) frames the decline in *Sporormiella* abundance and previously reported last occurrence dates for elephant birds (Parker-Pearson 2010; Goodman 2014). It is important to also consider that as humans settlements were prevalent in the south at this time, periods of desiccation may have led to increases in hunting in response to poor agricultural yields (Virah-Sawmy et al. 2010).

Further insights into megafaunal extinctions in Madagascar are provided by archaeological records of butchery, which reveal a shift in exploitation patterns around 1250 BP across Madagascar. Godfrey et al. (In review) described this as a “subsistence-shift” from the now-extinct giant lemurs to the small forest-dwelling species that persist today, in association with increasing human population and their dependence on agro-pastoralism. This subsistence-shift, possibly determining the functional collapse of subfossil lemur populations, post-dates peak megafaunal biomass loss as indicated by *Sporormiella* records (c.1500-1300 BP) and the initiation of the increased fire regime (c.1800-1300 BP) (Godfrey et al. 2016; Godfrey et al. 2017). The timing of this shift to smaller species is also consistent with a period of human

`

migration of predominantly males of African origin, moving south across Madagascar from c.1500 BP.

It is necessary to reconstruct the timing of decline and extinction in elephant bird populations against these broad hypotheses of faunal change across the Holocene of Madagascar. Data presented in Chapter 2 reveal that human exploitation of elephant birds, as evidenced by aepyornithid remains bearing anthropogenic tool-marks, took place across an interval of 9000 years from the early Holocene onwards, with prolonged co-occurrence between humans and megafauna. This evidence therefore excludes the possibility of rapid extinction (or "blitzkrieg") of elephant birds following first contact with humans, and indicates that extinction dynamics are poorly understood and were potentially complex. However, recent evidence of significant human migration within Madagascar c.1500 BP (Pierron et al. 2017) suggests that a delayed mass-hunting event may still have taken place during the late Holocene that caused rapid extinction of megafauna.

Other available evidence for human interaction with elephant birds, and for reconstructing their extinction chronology, is controversial. Vast deposits of fragmented elephant bird eggshell are found littered on beaches and coastal dune systems in Madagascar, as well as in midden remains of archaeological settlements, and these sites have historically been interpreted as evidence of rapid egg exploitation by early human settlers (Saint-Hilaire, 1851). Historical records demonstrate the use of these massive eggs (c. 9 litres) as liquid carriers (Strickland 1849), and several modern excavations have uncovered examples of ex-situ archaeological reworking of eggshell fragments from c. 2900 BP (Douglass, 2016). However, there is no clear evidence of human deposition associated with eggshell remains in the dune networks (Parker-Pearson 2010; Tovondrafale, Razakamanana, and Hiroko 2014), leading contemporary authors to now interpret these sites as natural deposits of nesting birds within dune networks (Douglass, 2016; Goodman, 2014). Radiocarbon dates of eggshell from archaeological midden sites also indicate greater age than their stratigraphic context (Douglass, 2016; Parker-Pearson, 2010), although this difference has been interpreted as a result of elephant birds supposedly consuming carbon from marine corals in order to ingest sufficient minerals to produce their enormous eggs, suggesting that it is therefore still possible that the eggs were harvested whilst still viable (Michael Parker Pearson 2010).

`

There are also suggestions of relatively recent elephant bird survival, until 300-400 BP during the post-European historical period on Madagascar, based upon the description of the "Voroun patra" by Etienne Flacourt in 1658: 'This is a large bird which haunts the Ampatre, it lays eggs like those of an ostrich, the people of these regions cannot catch it, as it seeks out the most deserted place'. This report consists of an unconfirmed account of a bird with large eggs (i.e. Ostrich like) from a third party that may conceivably describe an aepyornithid or alternately the extremely large and also now-extinct Madagascar crowned eagle *Stephanoaetus mahery* (Kay 2004), as without actual description of the Voroun patra, it remains unclear if it was volant or terrestrial in nature.

Two main concerns have so far prevented the development of a robust extinction chronology for elephant birds, to test between these competing possible models of human impact and faunal turnover in Madagascar. First, prior to the taxonomic revision of the Aepyornithidae in Chapter 1, there was an extremely limited framework for defining and identifying elephant bird species in the subfossil record. Whilst a small number of elephant bird skeletal remains have been radiocarbon dated, the taxonomic identity of these remains has typically either not been considered or has been inaccurately inferred or reported, and so these dates cannot be included in reliable species-specific extinction chronologies without further review. The majority of radiocarbon dates of elephant bird taxa have been taken from eggshell fragments found in dune systems, differentiated into two genera by the thickness of eggshell (thin ~2mm, *Mullerornis* sp.; thick ~4mm, *Aepyornis* sp.). Whilst the association of *Mullerornis* sp. skeletal DNA and thin eggshell DNA has been confirmed, the taxonomic identity of the thick eggshell remains confused, as *Vorombe titan* skeletal remains have had no DNA recovered to date, and DNA sequences reported as representing "*Aepyornis maximus*" have been aggregated from skeletal remains that have differing morphologies. Refinement of eggshell systematics, in association with skeletal remains, is necessary to integrate available radiocarbon data from eggshell remains into accurate species-specific extinction chronologies.

Second, reconstruction of prehistoric species extinctions typically requires extensive radiometric carbon dating of subfossil remains, to provide a robust framework for understanding contemporaneous environments and environmental change, extinction drivers, and ecosystem function loss (Perry et al. 2014). However, reported elephant bird last occurrence dates of 1000 ±150 BP; (Goodman et al. 1997) and 840 ±80 BP; Battistini et al., 1963) are both based on single, uncalibrated, pre-1980, non-AMS radiocarbon dates directly from eggshell remains

`

(Table 1). The fossil record is likely to underestimate the true chronological range of any taxon, so that last occurrence records are expected to pre-date the true time of an extinction event. The use of radiocarbon last occurrence records to infer extinction timing (with *terminus ante quem* capping using the 2σ upper confidence limit) is therefore a limited framework for understanding extinction dynamics and is vulnerable to the addition of new dates (Turvey, 2009). Non-AMS radiocarbon dates are also prone to providing unreliable extinction date estimates, and should be excluded from novel chronological analyses (Ramsey 2009).

Estimation of fossil extinction timing in the stratigraphic record can be determined more robustly through quantitative analysis of the time intervals that exist between temporally-spaced presence records (Turvey, 2009). Whilst a variety of statistical analyses are available for records with defined time points, the complex, multimodal, and non-continuous probability distributions produced from a calibrated AMS-radiocarbon date cannot be defined by a single point with confidence intervals. Gaussian-resampled inverse-weighted McInerny (GRIWM) analysis of radiocarbon data can account for probability distributions produced from a series of calibrated AMS dates (Bradshaw et al. 2012; Saltré et al. 2015). As GRIWM down-weights the intervals between dates and accounts for the uncertainties in radiocarbon estimates, models will produce well supported estimations of extinction timing, and chronological frameworks for determining the causes and impacts of their extinctions.

Here, we provide a dataset of AMS radiocarbon dates obtained from skeletal elements of multiple elephant bird genera. This novel data is combined with pre-existing, verifiable radiocarbon dates and assessed using GRWIM to obtain the most robust estimation of extinction in elephant birds. The timings of these extinction estimates are compared with available environmental and anthropogenic data to determine the likely determinants of the decline of these extraordinary birds.

`

Figure 1: Collection localities across Madagascar of radiocarbon dated specimens in this study

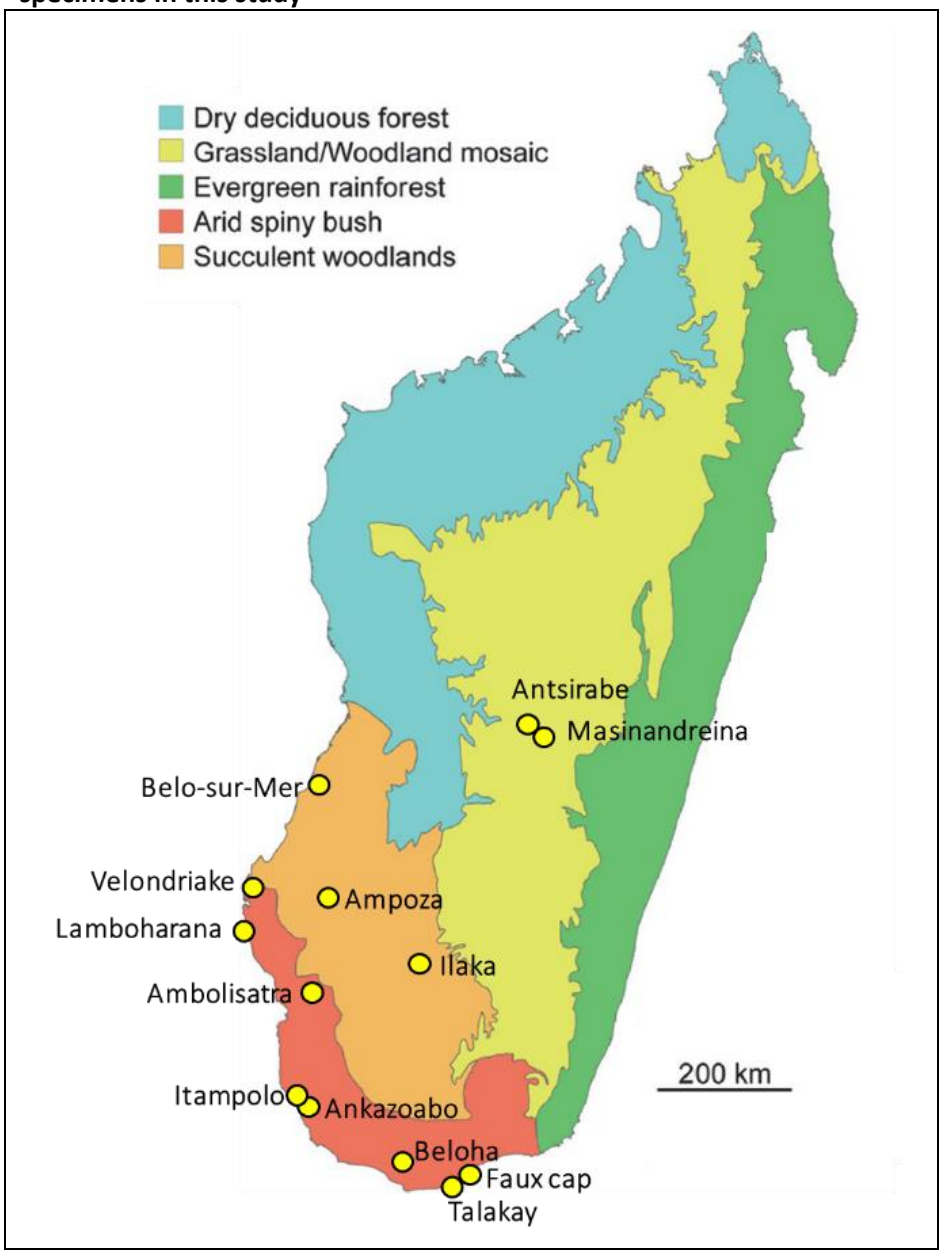

Adapted from (Yoder et al. 2016)

`

4.3 Methods

All direct radiocarbon dates from elephant bird skeletal and eggshell remains that could be located in the literature (including journal articles and grey literature), using Web of Science, Google Scholar and the ORAU radiocarbon archive, were compiled into a database. This existing date series included just one date from a *Mullerornis modestus* skeletal element. We also generated 18 new direct ultrafiltered AMS dates for previously undated elephant bird skeletal elements (6 *Aepyornis hildebrandti*, 1 *Mullerornis modestus*, and 12 *Vorombe titan*) at the Oxford Radiocarbon Accelerator Unit, UK (OxA) and the ^{14}CHRONO Centre, Queens University, Belfast (UB). Taxonomic identification of skeletal specimens was based upon morphometric classification (see Chapter 1). The database also included 24 dates associated with eggshell fragments, which we bimodally sorted by reported thickness into 19 dates from an unidentified "large taxon" (thick, ~4mm) that might represent either *Aepyornis* and/or *Vorombe*, and 5 dates from *Mullerornis modestus* (thin, ~2mm); identification of thin eggshell fragments as *Mullerornis* is supported by ancient DNA analysis of skeletal and eggshell material (Grealy et al. 2017).

Selection of radiocarbon data for analysis was based upon the auditing criteria of Stuart and Lister (Lister and Stuart 2013). Previously published radiocarbon dates of aepyornithid skeletal elements were not included if the identification of the dated elephant bird taxon could not be determined by reported sample numbers. Pre-1980 and non-ultrafiltered dates from aepyornithid remains were also excluded from our database, as collagen isolation and adequate pre-treatment cleaning were not widely implemented before 1980, and gelatine ultrafiltration is required to removes contaminants and improves reliability of date estimation. In total, seven pre-existing radiocarbon dates were rejected from our analysis (Table 1). Five of these dates were published before 1980, and two further dates from Burney et al. (1999, 2004) were associated with specimens for which taxonomic identification could not be determined based on our revised morphology-based framework (Chapter two). Remaining dates were calibrated using ShCal13 (Hogg et al. 2013) implemented in OxCal version 4.1 (Bronk Ramsey 2009). All dates are calibrated at 2σ, and date ranges are reported to their ≥95% confidence limits. The distribution of subfossil sites with dated aepyornithid remains is shown in fig. 1, and analysed dates are reported in tables 2-5 and shown as calibrated probability distributions of dates in figs 2-7.

`

GRIWM analysis of radiocarbon dates was carried out to determine the extinction dates for *Aepyornis hildebrandti*, *Mullerornis modestus* and *Vorombe titan.* Extinction date estimates were calculated in R version 3.1.3 (R Development Core Team 2011), using the approach developed by Saltré et al. (2015).

Table 1: Rejected radiocarbon dates

Laboratory number	Location	Material	Reported species	Date BP	Original source
UCLA - 1983	Fort Dauphin	Eggshell	*Aepyornis maximus*	1000 ±150	Berger et al. 1975
N/A	Irodo	Eggshell	*Aepyornis maximus*	1150 ±90	Mahe and Sourdat 1972
N/A	Manambovo	Eggshell	*Aepyornis maximus*	840 ±80	Battistini et al. 1963
N/A	S Madagascar	Eggshell	*Aepyornis maximus*	2930 ±85	Marden 1967
N/A	Tulear	Eggshell	*Aepyornis maximus*	5210 ±140	Sauer 1972
NZA-16995	Masinandreina	Bone	N/A	4496 ±40	Burney 2004
β-67659	Itampolo	Bone	N/A	1880 ±70	Burney 1999

UCLA: University of California NZA: Rafter Radiocarbon Lab (AMS), β: Beta Analytic

`

4.4 Results

Six calibrated dates are available for skeletal elements of *Aepyornis hildebrandti*, all from the central highlands near Antsirabe, which have a date range of 6179 BP to 1181 BP and a GRIWM extinction date estimate of 1121-1224 BP (Table 2, Fig. 2). Including both eggshell and skeletal elements, eight calibrated dates are available for *Mullerornis modestus* from south and southwest Madagascar, with a range of 6435-986 BP and a GRIWM extinction date estimate of 887-1144 BP (Table 3, Fig. 3). The 11 *Vorombe titan* calibrated dates available from skeletal elements from south and south west Madagascar demonstrate a range of 3680 to 1001 BP with a GRIWM extinction date estimate of 935-1108 BP (Table 4, Fig. 4). For this species, the subset of five dates from Ankazoabo has a range of 2739 to 1001 BP and a GRIWM extinction date estimate of 993-1092 BP (Fig. 5). Verifiable radiocarbon data exist for only one *Aepyornis maximus* skeletal element, which has a calibrated age of 10,721–10,511 BP; GRIWM analysis was therefore not possible for this species.

There are 19 calibrated dates for the "thick" aepyornithid eggshell specimens recovered from south and southwest Madagascar (Table 5, Fig. 6). These eggshell fragments have a range of 9545-945 BP and a GRIWM extinction date estimate of 1024-1093 BP. The subset of eight dates from the Talakay dune system of the extreme southern coast contain both the oldest and most recent examples of thick eggshell, and therefore the same total age range of all known thick eggshell specimens. The GRIWM extinction date estimate for these thick eggshell data is 1152-1228 BP (Fig.7).

Table 2: *Aepyornis hildebrandti* radiocarbon dates

Laboratory number	Location	Specimen number	Material	Date BP	Calibrated date BP	Original source
UB29724	Antsirabe	PMO A31834	Bone	5282 ±39	6179-5915	This paper
OxA-34327	Antsirabe	NHMW 2014/0238/0006	Bone	3112 ±31	3368-3177	This paper
OxA-33537	Antsirabe	NHMW 2014/0238/0037	Bone	2177 ±27	2303-2015	This paper
OxA-34758	Masinandreina	PMU 34(A46)	Bone	1537 ±25	1420-1314	This paper
OxA-34325	Antsirabe	NHMW 2014/0238/0003	Bone	1485 ±28	1376-1297	This paper
OxA-34328	Antsirabe	NHMW 2014/0238/0012	Bone	1349 ±28	1293-1181	This paper

UB: Queens University Belfast, OxA: Oxford Radiocarbon Accelerator Unit, PMO: Natural History Museum, University of Oslo, Norway, NHMW: Naturhistorisches Museum, Wien, Austria , PMU: Zoologiska Museum, Uppsala Universitet, Sweden

`

Figure 2: Calibrated radiocarbon dates for *Aepyornis hildebrandti* skeletal remains

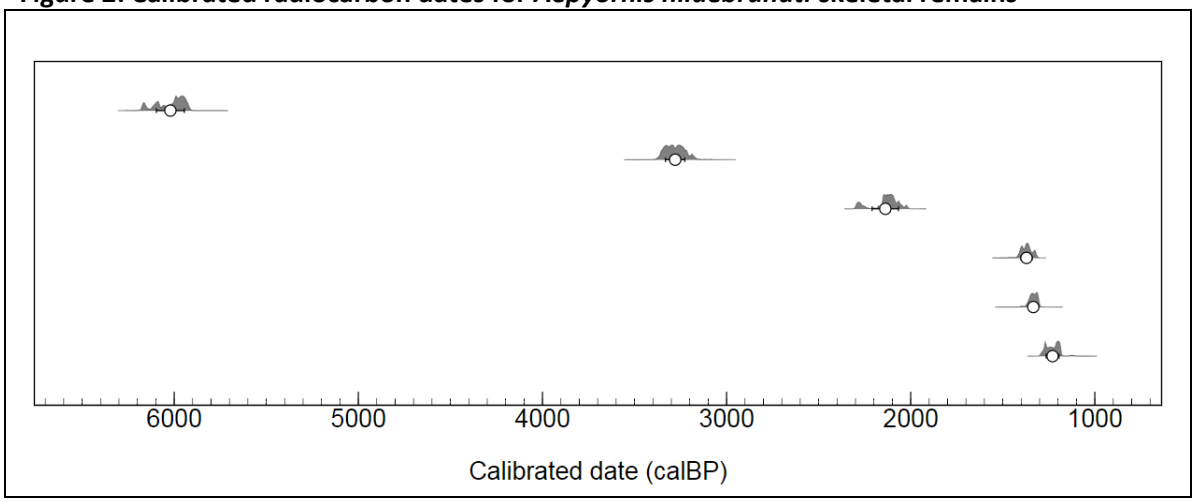

Table 3: *Mullerornis modestus* radiocarbon dates

Laboratory number	Location	Specimen number	Material	Date BP	Calibrated date BP	Original source
UB29726	Lamboharana	MAD6768	Bone	5597 ±40	6282-6435	This paper
β-55094	Anjohibe	CAMS-3547	Eggshell	2380 ±70	2158-2702	(Parker Pearson 2010)
OxA-8271	Talakay	AND 33-97	Eggshell	1825 ±30	1608-1814	(Parker Pearson 2010)
OxA-8273	Talakay	AND 2-97	Eggshell	1780 ±35	1565-1728	(Burney 1999)
OxA-34274	Velondriake	TONY10B3_S_1	Eggshell	1677 ±27	1430-1589	(Douglass, 2016)
β-103349	Belo-sur-Mer	BSM-95-10	Bone	1280 ±60	986-1285	(Burney 1999)

UB: Queens University Belfast, β: Beta Analytic, OxA: Oxford Radiocarbon Accelerator Unit,

`

Figure 3: Calibrated radiocarbon dates for *Mullerornis modestus* skeletal and eggshell remains

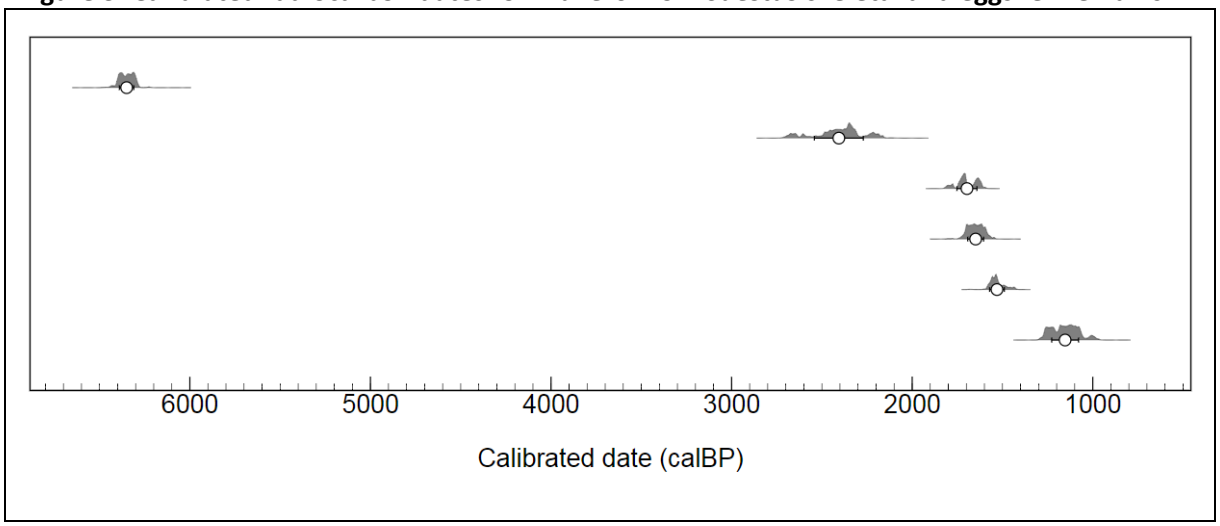

Table 4: *Vorombe titan* radiocarbon dates

Laboratory number	Location	Specimen number	Material	Date BP	Calibrated date BP	Original source
OxA-34776	Amposa	BMNH A2142	Bone	3381 ±24	3680-3478	This paper
OxA-34774	Amposa	BMNH A2145	Bone	2744 ±25	2858-2754	This paper
OxA-33534	Ankazoabo	MNHN MAD377	Bone	2540 ±26	2739-2458	This paper
OxA-34775	Amposa	BMNH A2144	Bone	2509 ±23	2714-2379	This paper
OxA-33532	Ankazoabo	MNHN MAD368	Bone	2499 ±25	2705-2363	This paper
OxA-33531	Ankazoabo	MNHN MAD 364	Bone	2470 ±24	2699-2352	This paper
OxA-33533	Ankazoabo	MNHN MAD 6770	Bone	2112 ±25	2146-1935	This paper
OxA-33572	Belo-sur-mer	MNHN MAD 8813	Bone	2047 ±29	2016-1889	This paper
OxA-33573	Belo-sur-mer	MNHN MAD 6655	Bone	1503 ±29	1404-1302	This paper
OxA-33536	Belo-sur-mer	MNHN MAD 383	Bone	1442 ±24	1351-1275	This paper
OxA-33535	Ankazoabo	MNHN 1906-16-67	Bone	1237 ±24	1182-1001	This paper

OxA: Oxford Radiocarbon Accelerator Unit, UK. BMNH: Natural History Museum, UK. MNHN: Museum National d'Histoire Naturelle, France

`

Figure 4: Calibrated radiocarbon dates for *Vorombe titan* skeletal remains

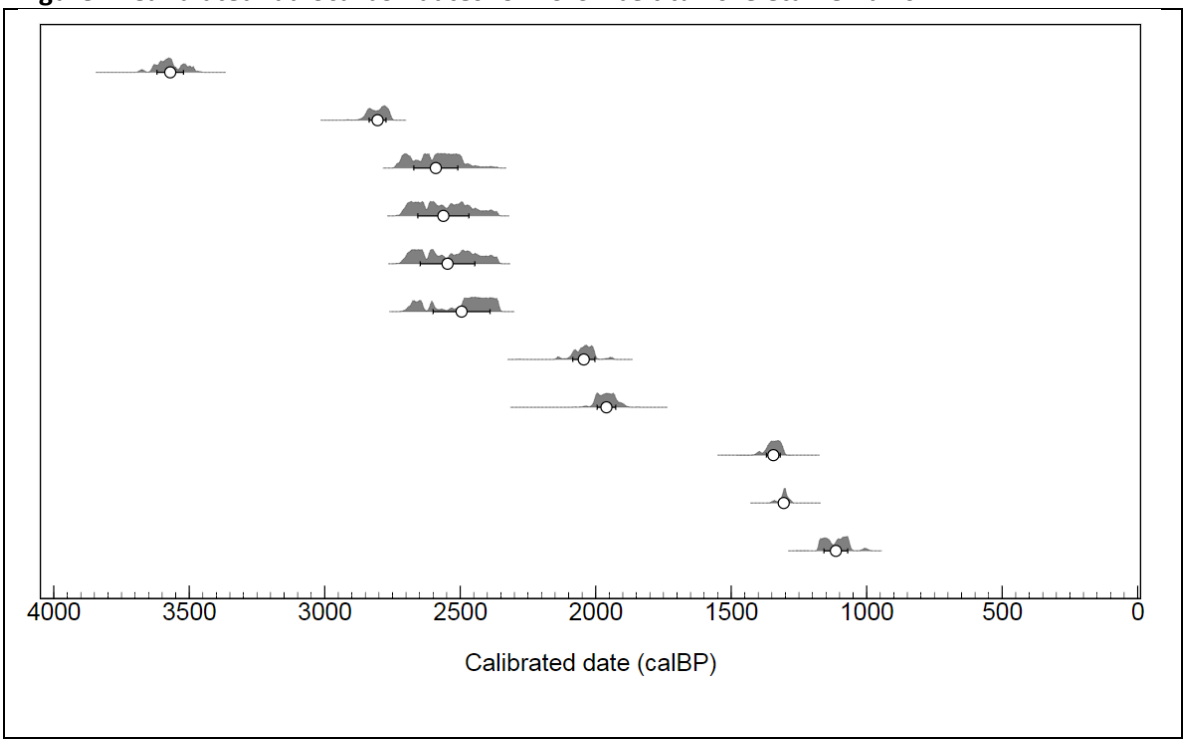

Figure 5: Calibrated radiocarbon dates for *Vorombe titan* skeletal remains at Ankazoabo

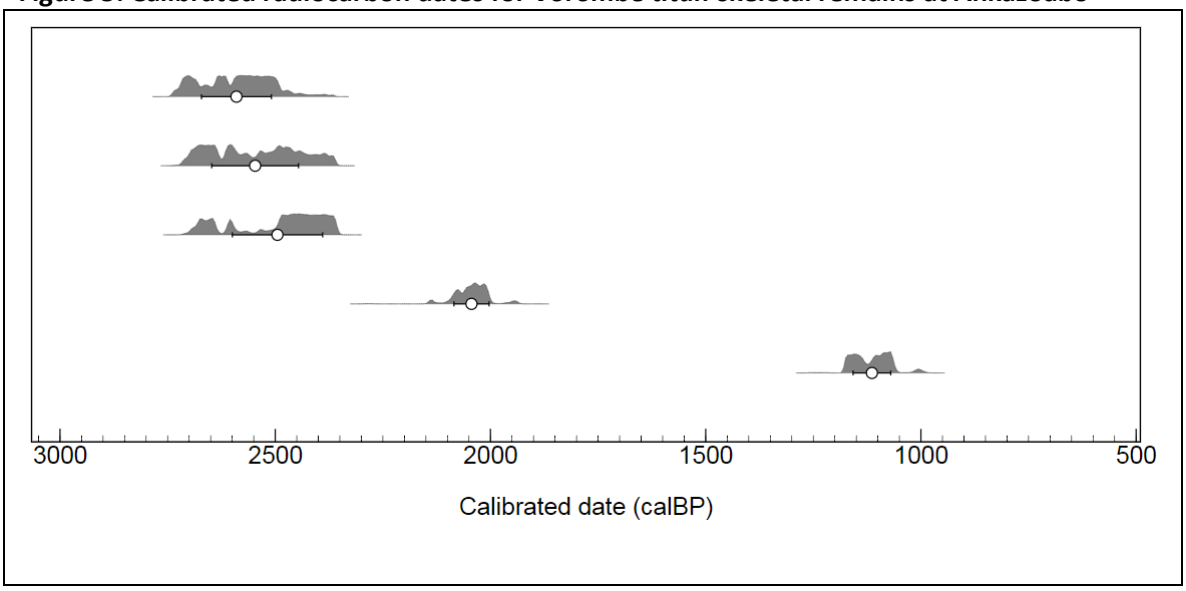

`

Table 5: Radiocarbon dates from thick eggshell

Laboratory number	Location	Specimen number	Date BP	Calibrated date BP	Original source
OxA-34217	Velondriake	TONY1SE_2_1	9420 ±83	9545-9258	(Douglass, 2016)
OxA-8279	Talakay	MAD-97/16	6238 ±45	6308-6126	(Parker Pearson 2010)
OZF856	Faux Cap	9691C	4635 ±105	4823-4441	(Clarke et al. 2006)
OZF855	Faux Cap	9691B	4510 ±98	4805-4298	(Clarke et al. 2006)
OxA-8280	Talakay	MAD-97/19	4461 ±70	4574-4295	(Parker Pearson 2010)
OZF854	Faux Cap	9691A	3447 ±63	3574-3344	(Clarke et al. 2006)
OxA-5077	Maroaloke	A2	2246 ±57	2345-2156	(Parker Pearson 2010)
OxA-8281	Talakay	MAD-97/45	2246 ±56	2344-2157	(Parker Pearson 2010)
OxA-5075	Maroaloke	A1	1941 ±48	2015-1835	(Parker Pearson 1995)
OxA-34215	Velondriake	TONY2A9_S_1	1929 ±47	2005-1836	(Douglass, 2016)
OxA-34216	Velondriake	TONY2B8_1_1	1920 ±49	2001-1835	(Douglass, 2016)
OxA-5076	Maroaloke	A8	1838 ±60	1987-1724	(Parker Pearson 2010)
OxA-8274	Talakay	AND 1-97	1716 ±56	1822-1611	(Parker Pearson 2010)
β-90099	Belo-sur-Mer	BSM-95-6	1710 ±78	1870-1566	(Burney 1999)
OxA-8269	Talakay	AND 5-97	1613 ±51	1702-1535	(Parker Pearson 2010)
OZF514	Faux Cap	9691E	1458 ±48	1541-1365	(Clarke et al. 2006)
OxA-5078	Maroaloke	A10	1281 ±40	1355-1185	(Parker Pearson et al., 1995)
OxA-8268	Bevala	AND 29-97	1234 ±40	1301-1180	(Parker Pearson 2010)
OxA-8272	Talakay	AND 4-97	1147 ±61	1270-1059	(Parker Pearson 2010)
OxA-8270	Talakay	AND 6-97	1114 ±56	1260-985	(Parker Pearson 2010)
OxA-8279	Talakay	MAD-97/16	6238 ±45	6308-6126	(Parker Pearson 2010)
OxA-8280	Talakay	MAD-97/19	4461 ±70	4574-4295	(Parker Pearson 2010)
OZF854	Faux Cap	9691A	3447 ±63	3574-3344	(Clarke et al. 2006)
OxA-8281	Talakay	MAD-97/45	2246 ±56	2344-2157	(Parker Pearson 2010)
OxA-8274	Talakay	AND 1-97	1716 ±56	1822-1611	(Parker Pearson 2010)
OxA-8269	Talakay	AND 5-97	1613 ±51	1702-1535	(Parker Pearson 2010)
OxA-8272	Talakay	AND 4-97	1147 ±61	1270-1059	(Parker Pearson 2010)
OxA-8270	Talakay	AND 6-97	1114 ±56	1260-985	(Parker Pearson 2010)

β: Beta Analytic, OxA: Oxford Radiocarbon Accelerator Unit

`

Figure 6: Calibrated radiocarbon dates for “thick” eggshell remains

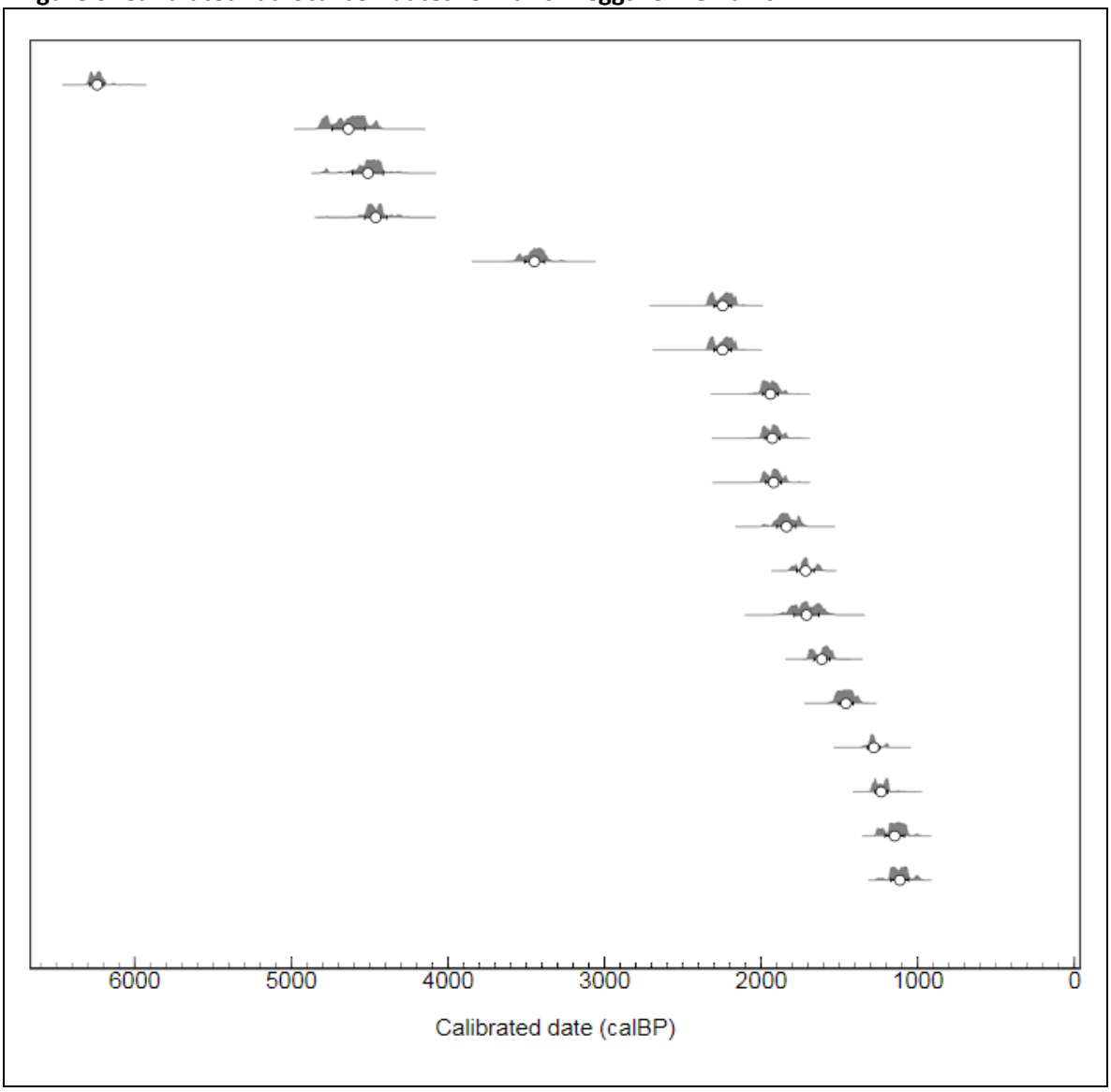

`

Figure 7: Calibrated radiocarbon dates for "thick" eggshell remains at Talakay dune system

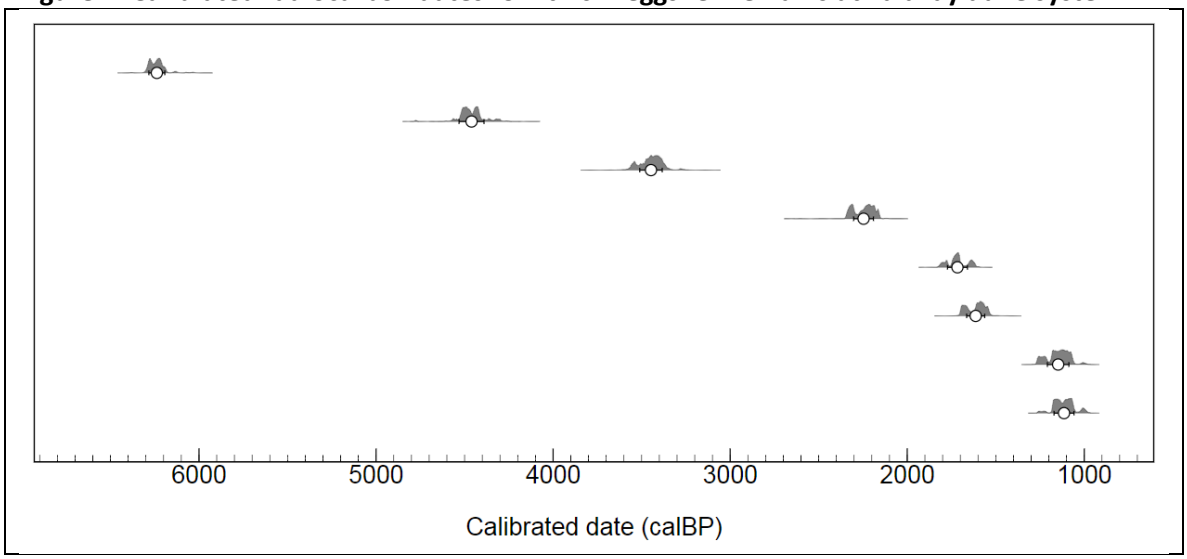

Table 6: GRIWM extinction estimates for elephant birds

Elephant bird taxon	Number of samples	GRIWM extinction date estimate
Aepyornis hildebrandti	6	1121-1224 BP
Mullerornis modestus	8	887-1144 BP
Vorombe titan	11	935-1108 BP
"thick" eggshell	19	1024-1093 BP

`

4.5 Discussion

Here we present the most robust extinction date estimates for all elephant bird genera to date (Table 6). Our findings demonstrate that the widely reported "most recent" elephant bird extinction date estimate of 840 ±80 BP which is based upon a single, non-AMS, uncalibrated radiocarbon date (Battistini et al. 1963), cannot be supported by a more extensive series of dates that meet our critical auditing criteria. GRIWM results instead demonstrate extinction date estimates around 1,000-1,100 BP for three of the four recognised elephant bird species (*Aepyornis hildebrandti, Mullerornis modestus*, and *Vorombe titan*) and for "thick" eggshell fragments. Indeed, these estimate ranges are extremely similar between all elephant bird taxa; extinction date estimates for *Mullerornis modestus*, *Vorombe titan* and "thick" eggshell fragments have overlapping confidence intervals, and the estimate for *Aepyornis hildebrandti* is only slightly older in age and overlaps with the estimate for *Mullerornis modestus*. As only one available radiocarbon date for *Aepyornis maximus* (10,721–10,511 BP), from a specimen bearing butchery marks that indicate the oldest known evidence of human presence in Madagascar (Chapter 2), a GRIWM extinction date estimate was not possible for this species. It is therefore possible that *A. maximus* went extinct earlier than other elephant birds, at the beginning of the Holocene; however, we consider it more likely that this species also survived later into the Holocene but has so far been under-represented in sampling for radiocarbon dating.

All elephant bird taxa for which we have GRIWM extinction date estimates persisted through the peak of extreme hydrological and temperature changes that Madagascar experienced during the Pleistocene-Holocene transition, and also initiation of mid-Holocene aridification that had a substantial impact in the south of Madagascar where the vast majority of aepyornithid remains have so far been recovered. These changes almost certainly had a significant impact on resource availability, particularly water availability and with all extinction estimates falling within the period of peak aridity between 1300-800 BP, there is a strong possibility that extreme drought was a significant factor in the extinction of elephant birds (Parker-Pearson 2010; Goodman and Jungers 2014).

Many Holocene faunal extinctions occurred on island ecosystems shortly after the arrival of the first human colonists, allowing relatively straightforward recognition of human involvement in their demise (Turvey 2009). The closest ecological analogue to the elephant birds, the moa of New Zealand, follow this classical extinction pattern, which is demonstrated by archaeological evidence for mass killing sites and an associated rapid "blitzkrieg" style population crash within

`

only a few centuries following Maori arrival (Holdaway et al. 2014). However, humans were present in Madagascar at least intermittently throughout the Holocene (Chapter 2), so that a hypothesis of rapid human-driven extinction following colonization by the earliest explorers and colonists of Madagascar can also be rejected. Our data suggest that elephant birds instead experienced a more delayed "sitzkrieg" (i.e. attrition) style extinction process in relation to first human arrival. Archaeological settlements demonstrate that Indonesian settlers were present in the semi-arid coastal regions of the south and south west by c.3000 BP, coexisting with elephant bird populations and exploiting other now-extinct fauna such as *Palaeopropithecus ingens* by c.2400 BP. As a butchered *Mullerornis modestus* tibiotarsus recovered from Lamboharana dates to 6,415–6,282 BP (Chapter 2), settlements may have been present much earlier than current archaeological evidence suggest as very few early Holocene contexts have been discovered. As megafauna survived well into this settlement period, hunting pressure would likely have caused at most only slow population attrition rather than an immediate population crash, possibly due to intermittent occupation of Madagascar or low-intensity hunting practices, and early human activities may not have been of sufficient impact to drive population declines.

Although GRIWM analysis to estimate extinction dates has not been conducted for any other members of Madagascar's extinct megafauna, available radiocarbon last-occurrence dates indicate survival of other megafaunal taxa until 750±370 (Burleigh and Arnold 1986). The late persistence of tortoises (750±370), and hippopotami (1215±25) (Burney et al. 2004), and elephant birds (887-1144 BP) versus *Archaeoindris* (2291±55) (Burney and Ramilisonina 1998) cannot be assessed as only one specimen has so far been dated. Regardless of data limitations to create refined chronologies, all of these megafauna cohabited Madagascar for several thousand years after colonisation.

Whilst Madagascar is an insular ecosystem, its large size and diverse array of ecosystems have led many authors to describe it as a mini-continental ecosystem (e.g. Breu et al., 2003). Its large geographical area, topographic and environmental complexity, and the presence of ground-based predators (*Cryptoprocta* spp. and other euplerid carnivores) may have slowed the extinction process of elephant birds in comparison to Moa through refugia availability and behavioural preadaptation to terrestrial predation threats. Indeed, the long human-megafauna overlap period is closer to the co-occurrence periods seen in Australia and the Americas (c. 1600 years) compared to many other island systems (Cooke et al. 2017; Gillespie et al. 2006; Johnson et al. 2013; Stuart, 2015; Trueman et al. 2005).

`

The closeness of GRIWM extinction date estimates for different elephant birds and nearly all other megafauna with adequate dating suggests that a significant change occurred c. 1000-1200 BP that led to the extinction of species with different body size, ecology and across a variety of landscape and elevations. Whilst it is important to consider the preceding anthropological and ecological dynamics, this period appears to be the most catastrophic for Malagasy megafauna.
The coincidence of megafaunal extinction timing with peak aridifcation and intensified anthropogenic factors leads to current conclusions of synergistic extinction drivers. It is vital that future research efforts must scrutinize these impacts in much greater detail and disentangle these factors to determine the primary drivers of the Malagasy megafaunal extinction event.

Recent genetic evidence demonstrates that the contemporary Malagasy human population is predominantly derived from a combination of early Austronesian settlers, who were prevalent in the coastal regions from c. 3000 BP, and a subsequent wave of African Bantu settlers who arrived in the north of Madagascar by c. 1500 BP (Pierron et al. 2017). The Bantu genotype spread through the island, predominantly through a male lineage moving south across Madagascar over a few hundred years, creating a geographic bias in the modern populace. Bantu explorers and colonists likely had significantly different subsistence strategies to the preceding Austronesian coastal dwellers. Migration and expansion of this wave of colonisation informs a hypothesis of a period of increased extinction pressure through less sustainable hunting strategies. The timing of this population expansion is broadly consistent with the "megafauna extinction window" defined by the decline in relative abundance of the coprophilous fungus *Sporormiella* in sediment records (Burney, Robinson, and Burney 2003), and our extinction estimates for all elephant bird genera follows the arrival of Bantu settlers by just a few hundred years. Whilst only four dated examples of elephant bird skeletal elements bearing butchery marks have so far been identified and dated, two of these specimens are dated to after the start of the Bantu expansion period, falling into the period between 1500-1000 BP (*M. modestus*: 1,270-1,074 BP; *Vorombe titan*: 1,182-1,057 BP; Chapter 2) and suggesting that exploitation may have increased just prior to their extinction. The "subsistence-shift" from giant lemurs to smaller forest-dwelling lemurs around c.1250 BP (Godfrey et al. 2016) and perhaps then giant tortoises (extinct c. 750 BP(Goodman and Jungers 2014)) also supports the narrative of Bantu expansion driving a rapid megafaunal extinction period.

`

4.5.1 Aepyornis hildebrandti and the central highlands

The earliest extinction for a recognised species of elephant bird is that of *Aepyornis hildebrandti*, from the central highlands region, with available dates limited to the region near Antsirabe and Masinandreina which represents the only sites for which confirmed *Aepyornis hildebrandti* specimens have so far been recovered. The GRIWM extinction date estimate for this elephant bird species of 1121-1224 BP is similar to the latest radiocarbon dates for hippopotami remains from the same area, which date to 1215±25BP (Burney et al. 2004) and whilst this may be evidence of a geographical bias in extinction, it is more likely to be an artefact of the smaller dataset for *A. hildebrandti* (n=6), and hippopotami (n=5) versus species in the south and south west regions Prior to the description of hobbling and butchery marks on an *A. hildebrandti* tarsometatarsus (MNHN MAD384; Chapter 2) there has been no reported direct evidence of humans and now-extinct animals co-occurring in this region. However, as MNHN MAD 384 failed radiocarbon dating due to low collagen content (Chapter 2), the timing of this exploitation event is unknown and cannot be used to examine the temporal duration of interaction with humans.

Sediment records from Tritrivakely crater lake inform our current understanding of ecological conditions in the central highlands region near Antsirabe for the last 40,000 years, detailing a warming cycle between 19,000 and 4000 BP when radiocarbon records for *A. hildebrandti* begin (Gasse 2000). Pollen and *Sporormiella* records indicate that there was a shifting mosaic of savannah-woodland present in the region throughout the late Quaternary with megafaunal biomass (*Sporormiella* abundance) lower to absent when forest cover or ericoid shrub land dominated between 9000-5000 BP and elevated biomass in association with increased amounts of woodland-savannah between 5000-3000 BP. The 5-metre sediment core extracted by Burney et al. (1987) in Antsirabe details a trace amount of charcoal particulates, indicating that limited fire regimes were active throughout the Holocene, which these authors attributed to limited natural regulation of plants through fire.

Most currently dated specimens of *A. hildebrandti* currently available are not contemporaneous with the periods of increased megaherbivore biomass (But see OxA-34327, Table 2) recognised in sediment core data from the central highlands (Gasse 2000). It remains unclear if this negative association of *A. hildebrandti* to total biomass is an artefact of sampling bias where viable dates are only available from the last few thousand years, or whether *A. hildebrandti* did

`

not have interspecific associations with the *Sporormiella* species that currently inform our understanding of megaherbivore abundance in Madagascar.

4.5.2 *Mullerornis modestus*

The estimated extinction date range produced by GRIWM for *Mullerornis modestus* overlaps with the upper end (most recent) of the estimated extinction date range for *A. hildebrandti* from the central highlands, although all available audited dates for this species are instead restricted to the south and south west regions of Madagascar, with no data coming from the central highlands region where *M. modestus* is also present. The estimate of 1144-887 BP is congruent with the estimated date of the wider megafaunal extinction event in Madagascar c.1100-1000 BP. Evidence of exploitation through butchery of *M. modestus* dates to over 6000 BP at Lamboharana, and the presence of peri-mortem anthropogenic marks on another dated specimen (MNHN MAD6662, not included within this study as it lacks location data) demonstrates that *M. modestus* exploitation also occurred in the late Holocene. As our data does not include specimens collected from the central highlands region, the overall narrative of *Mullerornis* extinction remains unclear; however the constrained extinction timing of megafauna in the central highlands, and the similarity to *Mullerornis* in the south and south west supports a hypothesis of cosmopolitan extinction timing.

4.5.3 Vorombe titan

The GRIWM estimate for extinction of *Vorombe titan* is within the estimated extinction range of *Mullerornis modestus*, and dated specimens come from across the same broad range of the south and south west ecoregions, excluding specimens identified as *V. titan* in the central highlands. This temporal pattern is again consistent with dates for the wider Madagascan megafauna extinction event c.1100-1000 BP and after the major drop in megafaunal activity c.1700 BP. The site-specific extinction chronology for *V. titan* at Ankazoabo included the most recent date for the taxon and shared a similar predicted extinction timing, but with a narrower confidence interval.

4.5.4 Thick eggshell

The chronology of the taxonomically indeterminate “thick” eggshell remains gathered from across the south and south west regions of Madagascar have a GRIWM extinction date estimate that is within the predicted extinction range of *V. titan.* Their extreme size, and comparable extinction chronology to *V. titan*, highlights the possibility that these are the same species,

`

rather than the other regional species with currently unidentified eggs *A. maximus*. The "thick" eggshell record is the most extensive assemblage of aepyornithid radiocarbon dates available, and as such provides the most refined timing of extinction, with an extremely small range of just 69 years. Much like *Mullerornis modestus* and *Vorombe titan* skeletal remains, this predicted extinction timing is within the period of notable megafauna extinction or "extinction window". The site-specific chronology of the Talakay dune system, whilst including the oldest and most recent examples of thick eggshell, has an older predicted extinction chronology for the taxon associated with the thick eggshells, and which is outside the range predicted by the eggshell dataset from both the south and south west ecoregions, which is likely the result of the smaller amount of data creating a less reliable estimate, and wider confidence interval.

4.5.5 Extirpation in the south and south west

Sediment records from Ambolisatra in the south west of Madagascar inform a high-resolution model of megafauna biomass through the *Sporormiella* record, and of fire regimes through relative charcoal abundance (Burney, Robinson, and Burney 2003). The estimated extinction timing of *Mullerornis modestus*, *Vorombe titan* and the "thick eggshell taxon" post-dates the start of the period of *Sporormiella* decline by approximately 700 years, and the increased fire regime by approximately 500 years. As the data used in the construction of our extinction chronology for *Mullerornis modestus* cover an extremely large geographical range across two distinct ecoregions, conclusions about the specific interactions of localised human-presence and environmental factors in driving population declines are difficult to determine. The Talakay dune system is the only currently available site-specific extinction chronology for "thick" eggshell fragments, and is not in close proximity to the Ambolisatra sedimentary records or within the same ecoregion; as such, drawing conclusions on the drivers of the extinction of the taxon associated with these eggshells may be unreliable. However, the Ankazoabo site in south west Madagascar is within close proximity and in the same ecoregion as Ambolisatra, and consideration of the local extinction chronology for Ankazoabo against Ambolisatra's sediment record demonstrates that *Vorombe titan* survived the influx of human settlements at c.3000 BP, persisting through the drop in megafaunal biomass evidenced by the drop in *Sporormiella* abundance, and also through the period of massive increase in fire regimes which would have radically transformed the environment.

`

4.5.6 The “Voroun patra”

Whilst our data are unlikely to represent the last surviving individuals of any elephant bird taxa, our GRIWM estimates represent reliable evidence from which to infer extinction timings, and allow us to assess the veracity of claims for late survival of elephant birds. Etienne Flacourt’s written account of a second-hand description of the “voroun patra” from near Fort Dauphin in the 1600s is over 500 years later than the upper confidence limits of our extinction range estimates for any of the elephant bird taxa included in this study. The restricted date series that are available for all elephant bird taxa, and the limited number of sites from which data have been collected, prevent us from determining if a small number of elephant birds may have persisted as relictual populations in remote and inaccessible regions after their extinction across the rest of Madagascar, or developed behavioural strategies to counter the impact of exploitation by humans (Reed 1999; Fisher and Blomberg 2011). However, as folk knowledge of animals may survive longer than the animals themselves (Crees and Turvey 2014), it is possible that Flacourt’s record represents a historical account of an already-extinct animal, rather than a contemporary sighting. As Flacourt was never able to verify this record with a personal sighting or biological specimen, this enigmatic potential datum remains unverified and cannot be included within a scientific framework for determining the extinction timing of any elephant bird taxon.

`

4.7 Conclusion

Our new extinction chronologies for three of the four currently recognised elephant bird species reveal extended persistence for all of these taxa following human colonisation in Madagascar and population attrition through hunting, suggesting that there is likely to be either a complex and regionally diverse synergistic explanation for the loss of elephant birds and other Malagasy megafauna, or a rapid extinction following the arrival of a novel human threat with the arrival of the Bantu populace c. 1500 BP. The growing body of archaeological evidence is driving new understanding of the succession of human colonisation periods throughout the Holocene, and the extended period of co-occurrence of humans and megafauna revealed by these findings means that future work into this extinction event must incorporate data on the varying environmental pressures posed by direct exploitation, habitat modification and agriculture as well as the impacts of natural aridification.

Previous attempts to discuss the elephant bird extinction process as a single dynamic shift driven by human presence, within a simplistic binary context of pre- and post-human arrival, have proved inadequate to explain the current extinction narrative, leading to confusion over human involvement or natural climatic change. However, available archaeological evidence indicates that Madagascar has instead experienced considerably more complex and staggered human colonisation dynamics, comparable to the arrival of humans in the Caribbean archipelago. Four phases of human arrival are known in the Caribbean (Fitzpatrick 2006; Cooke et al. 2017) — Lithic (c.7000-4000 BP), Archaic (c.5000-2000 BP), Ceramic (c.2500 BP) and European (c.500 BP) — which are associated with increasing technological advancement and more unsustainable hunting and agricultural strategies that underpin our comprehension of the region's extinction processes. With a growing body of evidence for an extended Lithic period in Holocene Madagascar (c.10,500-4500 BP) (Chapter 2, Dewar et al., 2013), followed by colonisation by Indonesian coastal dwellers (c.3000-1000 BP) (Douglass, 2016; Perez et al., 2005; Pierron et al., 2017), Bantu settlers (c.1500-1000 BP) (Pierron et al. 2017), Malagasy expansion (c.1000 BP onwards) (Pierron et al. 2017), and arrival of European colonialists (c.500 BP onwards) (Goodman and Patterson 1997), we propose that novel investigations into Malagasy megafaunal loss must refine and incorporate this staggered anthropological chronology to test extinction hypotheses. Based on currently available data for elephant bird spatial and temporal distributions and the complex series of environmental and anthropogenic events contemporary with their predicted extinction dates, it is likely that the Bantu expansion was a prominent factor in the extinction of elephant birds and other Malagasy megafauna.

`

However, it remains unclear how habitat modification and direct impacts of hunting are individually responsible for their extinction, highlighting the need for more detailed chronological studies.

The relatively restricted amount of radiocarbon data currently available for the wider Malagasy extinct megafauna – and for elephant birds in particular – still limit the analyses that can be undertaken to investigate these extinction chronologies and identify likely extinction drivers, and more data are required to create a more nuanced understanding of anthropogenic impacts in Madagascar throughout the Holocene. In comparison, the use of large numbers of radiocarbon dates has been instrumental in determining the dynamics and drivers of decline of megafaunal taxa across regions such as Eurasia, and has highlighted regional variation in patterns of extirpation in response to both natural and anthropogenic change (Turvey et al. 2013; Stuart and Lister 2012, Lister and Stuart 2013, Stuart and Lister 2014), as well as promoting interpretations of ecosystem functional loss following these extinctions. Our new data on elephant bird extinction chronologies represent an essential new step in understanding the loss of Madagascar's unique megafauna, and development of larger databases with more detailed regional chronologies from across Madagascar's ecoregions, incorporating mammalian, avian and reptilian taxa in association with archaeological data, will help to further refine this complex and intriguing narrative of megafaunal loss.

`

Chapter five

`

`

Chapter five

Reconstructing the dietary ecology of aepyornithids using stable isotope analysis

5.1 Abstract

Insular megafauna have a disproportionately large role in the development and maintenance of their surrounding biomes. The interspecific interactions of megaherbivores help define the capacity of floral species to disperse and regulation of their biomass. Understanding these interactions of recently extinct insular megafauna in relation to extant floral assemblages allows the interpretation of pristine, pre-human contact environments and ecological interactions that have become defunct following faunal extinctions. δ^{13}C isotopes in subfossil animal tissues reflect the photosynthetic pathway of plants herbivores consumed and can determine if herbivores consumed savannah grass species or not, providing vital supporting information for dietary inference.

Madagascar's extinct Holocene megafauna were diverse, including giant lemurs, hippopotami, giant tortoises and the elephant birds. In comparison to other megafauna the elephant birds have been subject to little modern research, but recent clarification of their diversity and distribution has provided a novel framework for interpreting their ecology across the variety of habitats and elevations at which they occurred. Reviewed here are all previous estimates of δ^{13}C isotopes from non-primate megafauna subfossil remains and novel values for skeletal elements of elephant birds, which are compared against contemporary regional floral compositions to infer dietary subsistence strategies.

Almost all megafauna observed here do not show signs of consumption of C4 grasses and show significant dependence upon forest plants, consistent with previous assessments of elephant birds at low elevation. *Aepyornis hildebrandti*, from the central highlands region has δ^{13}C isotope values which are significantly different from all of Madagascar's other megafauna. With a range of -13.4 to -17.1 δ^{13}C‰, it appears that *A. hildebrandti* consumed as much as 43% of their diet from C4 grasses. This new information challenges current understanding of a palaeo-grazing guild of megaherbivores in Holocene Madagascar, and hypotheses which predict extremely limited distributions of endemic C4 grasses.

`

5.2 Introduction

Late Quaternary continental and insular ecosystems were often dominated by the presence of megafauna (>44 Kg) (Malhi et al. 2016), particularly megaherbivores, which perform key ecosystem functions that shape these environments (Laundré et al. 2010; Hopcraft et al. 2010). Megaherbivores can provide a disproportionately large contribution to biogeochemical nutrient cycling (Hobbs 1996) and lateral nutrient dispersal (Wolf, Doughty, and Malhi 2013). Through consumption, digestion, urination and defecation, megafauna accelerate the nutrient cycle of plant matter that might otherwise take years to decompose (Hobbs 1996; McNaughton 1997). Megaherbivores can both suppress and propagate forest cover, through consumption of juvenile plants, or frugivory, where plants have developed coevolutionary dispersal strategies with megaherbivores (Guimarães et al. 2008; Pires et al. 2014). Understanding aspects of the past ecology of now-extinct animals is essential in order to reconstruct past ecosystem interactions and processes (Malhi et al. 2016) and determine the ecological response to their loss (Burney et al. 2003).

Subfossil and archaeological excavations indicate that Quaternary Madagascar was host to an extraordinary megafaunal assemblage including giant lemurs, hippopotami, tortoises, and the world's largest recorded birds: the elephant birds (Goodman and Jungers 2014). Research into these taxa has mainly focussed on the subfossil lemurs (Goodman and Jungers 2014), with recent studies also investigating the evolutionary history and ecological significance of the giant tortoises (Griffiths et al. 2013; Hunter et al. 2013) and hippopotami (Godfrey and Crowley 2016) . Until the last decade, elephant birds have seen remarkably little study due to poor historical museum records and extreme taxonomic and biogeographic confusion. However, new morphometric analysis of their appendicular skeletal remains (Chapter 1) indicates that elephant birds were morphologically diverse, and dispersed across a variety of habitat types.

5.2.1 Late Quaternary environmental history of Madagascar

The environment of Madagascar's insular ecosystem is comprised of distinct ecogeographic zones, created by variation in temperature, hydrological regimes and topography (Dewar and Richard 2007). Each ecogeographic zone demonstrates regional endemism in extant species (Dewar et al. 2007) and extinct megafauna (Godfrey et al. 1997; Goodman and Jungers 2014). As each zone has been subject to varying fluctuations in climate through time, understanding of the Quaternary faunal decline in Madagascar must consider how regional changes contribute to wider patterns of extinction (Goodman and Jungers 2014; Burney et al. 2003). The chronological record of sediment cores from river and lake beds (Burney et al. 2004; Crowley 2010) and cave

`

speleothems (Scroxton et al. 2017) detail these hydrological and temperature fluctuations as well as the contemporaneous abundance of charcoal particulates and pollens. Combining this information provides the basis for interpreting environmental conditions across Madagascar over the last 40,000 years (Crowley 2010; Gasse 2000).

Whilst there has been a long-held view of Madagascar having near-total forest coverage before human arrival (Bâthie 1921; Humbert 1971), endemic grasses date back as far as the Miocene and form an established part of the island's ecosystems (Bond et al. 2008; Vorontsova, Besnard, Malakasi, et al. 2016). The oldest available sediment records (c. 40,000 BP) (Gasse 2000) indicate a colder climate than today (-4°C in mean annual temperature) with extreme hydrological fluctuations at the end of the Pleistocene, with ericoid bush giving way to savannah grassland c. 17,000 BP and forest plant species dominating the highlands. By c. 9800 BP a mosaic of forest and open savannah was spread across the island (Burney et al. 2004; Crowley 2010). The period of warming and desiccation which began island-wide c. 4,500 BP converted the seasonal wetlands of the extreme south into an arid shrubland from c. 3,000 BP (Virah-Sawmy et al. 2010; Crowley 2010). Whilst deforestation has clearly impacted Madagascar significantly over the last 1000 years, little is known about the true extent and distribution of the mosaic of grassland savannah and forest cover throughout the Holocene (Klein 2002; Kull 2000).

With increasing numbers of studies investigating the phylogenetic history of Madagascar's floral communities, new information is challenging the hypothesis of rapid, widespread human-caused Holocene habitat change from forest to savannah (Godfrey and Crowley 2016; Bond et al. 2008; Vorontsova et al. 2016; Crowley and Samonds 2013; Virah-Sawmy et al. 2008; Needham et al. 2015; Quéméré et al. 2012). Botanists have proposed that natural drought caused open woodland in the extreme south to transform to grassland between 5,800 and 5,200 BP, and also caused similar shifts from humid, dense woodland to open savannah in many parts of the island (Quéméré et al. 2012). Recent studies have also suggested that grasslands may have been common within the western dry-deciduous forest ecoregion (MacPhee et al. 1985; Matsumoto and Burney 1994) before any evidence of deforestation by humans is detected, as C4 grass lineages are highly diverse in the region.

Marked increases of charcoal abundance in sediment cores indicate a shift from infrequent "background" fires to high-intensity fire regimes caused by anthropogenic deforestation starting

`

c.1,500 BP (Crowley 2010). In the absence of a high-intensity fire regime throughout the Quaternary, regulation of extensive networks of savannah grassland could have been maintained by a herbivorous grazing guild, cropping grasses and limiting seed propagation (Malhi et al. 2016; Burney et al. 2003; Godfrey and Crowley 2016). However, whilst grazing taxa are present in the Holocene subfossil record (Needham et al. 2015; Bond et al. 2008), the absence of evidence of megafaunal grazers has promoted hypotheses of endemic grasses being limited to small, low-density woodland glades (Godfrey and Crowley 2016).

5.2.2 Stable carbon isotopes and diet

Stable carbon (δ^{13}C) isotope values in animal bones correspond to their dietary niche and can provide insight into the types of plants herbivores consumed. Differences in how CO_2 is converted into sugar and fixation of carbon within leaves give plants distinct differences in values of δ^{13}C that can differentiate their photosynthetic pathways. Most trees, shrubs and herbs use a C3 (Calvin) pathway, whereas most tropical grasses use a C4 (Hatch-Slack) pathway, and succulent plants dominant in the arid southern region of Madagascar use CAM (Crassulacean Acid Metabolism). Global mean δ^{13}C isotope ratios of C3 plants are c. -26.5‰, C4 plants are c. -12.6 ‰, and CAM plants have intermediate values that vary based upon environmental conditions (Ehleringer and Monson 1993; Johnson et al. 1998).

Isotopic turnover rates in avian bone are much slower than in their eggshells, with their bone collagen reaching isotopic equilibrium with diet over months, rather than a matter of days as in eggshell (Hobson and Clark 1992; Crisp and Demarchi 2012). Studying birds and their eggshell offers an opportunity to study long-term diets through bone collagen, and "snap-shots" of their diets during oogenesis. However, interpreting these data is complicated as enrichment of δ^{13}C in animal tissues compared to their diet varies with tissue type, size, metabolic rate and body temperature. Skeletal collagen δ^{13}C values for avian and mammalian herbivores are 5‰ relatively enriched versus plants in their diets (Tykot 2004). As relative enrichment of δ^{13}C in avian eggshell is more variable than bone (Tykot 2004; Tovondrafale et al. 2014), it is particularly important to consider this factor when interpreting dietary patterns from eggshell remains, and vital to compare these data with skeletal elements.

The subfossil lemur record has been subject to the most scrutiny of past dietary niche in Madagascar. The only extinct lemur genus for which consumption of C4 grasses is likely on the basis of this evidence is *Hadropithecus stenognathus* (Archaeolemuridae), a predominantly

`

terrestrial, baboon-like lemur distributed across the south and west of Madagascar, which exhibits exceptionally low depletion of δ^{13}C isotopes, dental morphology consistent with grazing, and tooth wear patterns indicating subsistence on seeds and grasses (Crowley et al. 2012). Conversely, whilst some Madagascan giant tortoise (*Aldabrachelys*) and *Hippopotamus* species had mixed diets, available evidence suggests that neither of these groups were prodigious consumers of C4 grasses (Godfrey and Crowley 2016).

Although elephant birds are sometimes regarded as potential grazers in Madagascar (Burney et al. 2003), prior δ^{13}C isotope evidence of consumption of C4 grasses is restricted to just one radiocarbon record from a specimen described as "*Aepyornis* sp." from the central highlands (Crowley and Samonds 2013; Clarke et al. 2006; Tovondrafale, Razakamanana, and Hiroko 2014). Analysis of both skeletal and eggshell remains from the extreme south (*Aepyornis* and *Mullerornis*) (Clarke et al. 2006; Tovondrafale et al. 2014; Douglass 2016; Parker-Pearson 2010) and extreme north (*Mullerornis*) (Crowley et al. 2012) of Madagascar have shown some depletion of δ^{13}C isotopes, but within regions where C4 plants are rare and CAM plants are abundant. Assessments of floral interactions with aepyornithids have focused upon hypotheses of fruit consumption and seed dispersal. Plants with faunal-assisted dispersal strategies, such as trample-burrs (*Uncarina* spp.), show spatial congruence with the known distribution of *Aepyornis* and *Mullerornis* at low elevation (Midgley and Illing 2009; Brodkorb 1963). Morphological adaptations shown by some plants on Madagascar are also convergent with plants found within ecosystems that were dominated by Quaternary avian megafauna in New Zealand, for which a similar co-evolutionary history has been proposed (Bond and Silander 2007). The loss of the putative dispersal mechanism for these plants, or "megafauna fruit-syndrome" (Guimarães et al. 2008; Malhi et al. 2016), raises the possibility of an elevated co-extinction risk for plants that have evolved complex life-history strategies involving interspecific interactions with vulnerable megafaunal communities (de Ricqlès et al. 2016; Turvey et al. 2005).

Despite initial suggestion of C4 grass consumption in elephant birds, there has been little further investigation of elephant bird diet, or consideration of their potential as megafaunal regulators of grassland. Using the new framework for understanding elephant bird taxonomy, diversity and biogeography presented in this thesis, there is now a new opportunity to further investigate interspecific and intraspecific variation of elephant bird dietary niches inclusive of different ecogeographic zones, which can be used to test hypotheses of the possible existence of an avian megafauna grazing guild in Holocene Madagascar.

`

5.3 Methods

We assembled a database of 136 $\delta^{13}C$ isotope values obtained from previously published data for skeletal elements of *Aldabrachelys*, *Hippopotamus*, and the aepyornithids (*Aepyornis*, *Mullerornis* and *Vorombe*), as well as eggshells from *Mullerornis* and the extremely large eggs with currently undetermined genus (Table 1). Included in this database are 21 new isotope values from skeletal elements. These data are distributed across three major ecoregions of Madagascar: the arid south, the succulent forests of the west, and the temperate central highlands (Figure 1). Previously published data include isotope values obtained via AMS radiocarbon dates from bone collagen and egg collagen (stable organic fraction), and through continuous flow isotope ratio mass spectrometry. Isotope values from bone samples were compared for all non-primate megaherbivores from Madagascar using Tukey's pairwise tests within PAST version 3.15 (Hammer, Harper, and Ryan 2001).

We assessed dietary fractionation using mixing models in ISSOERROR version 1.04 (Phillips and Gregg 2001) to assess possible plant dietary niche differentiation between aepyornithid taxa, subdivided between the three distinct ecoregions in which they occur. We calculated mean % consumption of C3 vs CAM plants in the more arid ecoregions of the south and west, and C3 vs C4 plants in the comparatively wet central highlands, which do not support significant CAM plant biomass. We used regional isotope values for C3 and CAM plants and C4 grass values for the whole of Madagascar compiled by Crowley et al. (2011) as end members of the fractionation model. Carbon isotope values for subfossil individuals were corrected to account for accumulation of $\delta^{13}C$ in bone (-5%) and eggshell (-2%) (B. J. Johnson, Fogel, and Miller 1998). All specimens were corrected by -1.2% to account for $\delta^{13}C$ shifts in atmospheric CO_2 (Suess effect) (Keeling 1979). As isotope values are available for both eggshell and bone within *Mullerornis*, these values were also compared before and after adjustments, using Tukey's pairwise tests within PAST version 3.15.

`

Fig 1. Ecoregions and relief map of Madagascar, showing sampling localities for specimens included in this study

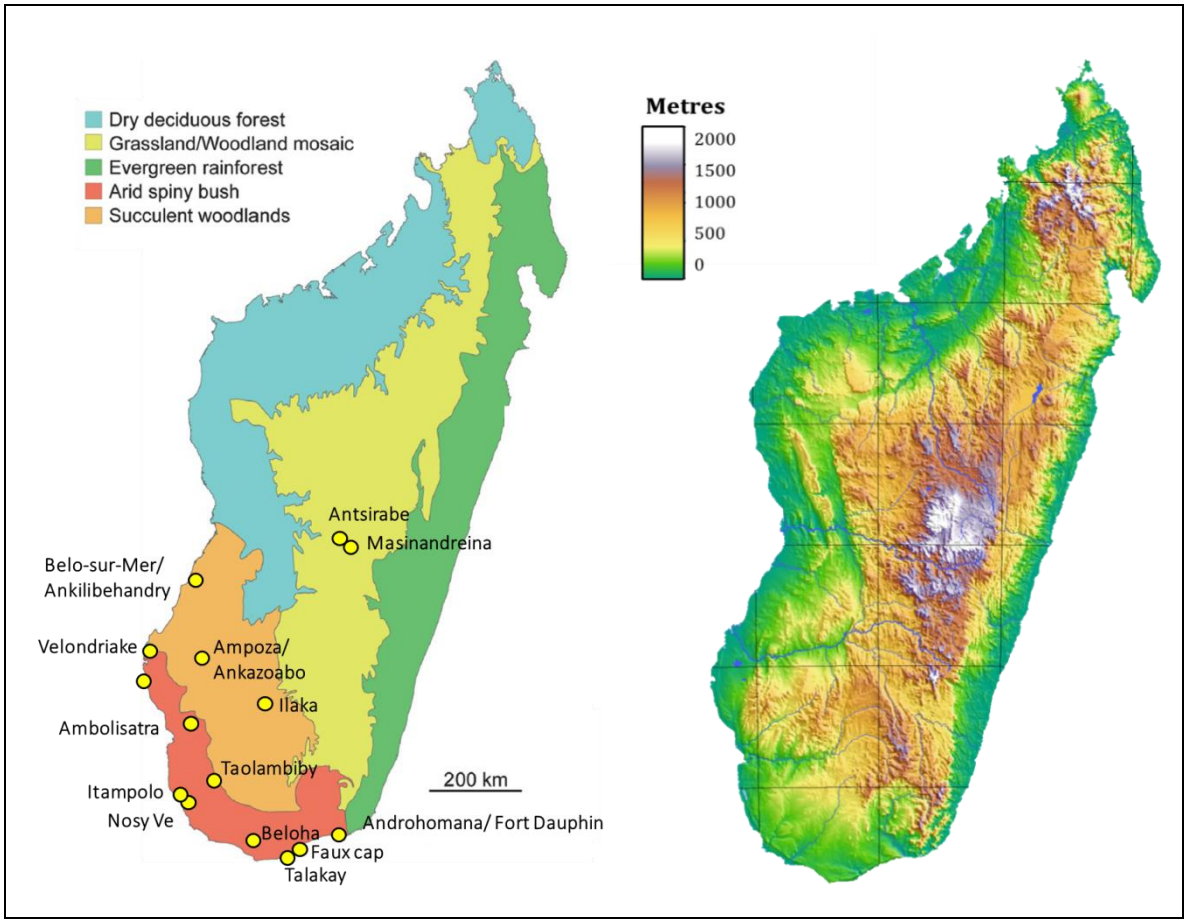

Adapted from (Yoder et al. 2016) Adapted from (L. R. Godfrey and Crowley 2016)

`

5.4 Results

Of 136 δ^{13}C isotope values obtained from skeletal and eggshell remains collated here, three are available for *Aepyornis maximus*, 6 for *Aepyornis hildebrandti*, 16 for *Mullerornis modestus* (7 eggshell, 9 skeletal), 11 for *Vorombe titan*, and 100 for thick aepyornithid eggshell for which no reliable taxonomic identification is available.

Tukey's pairwise comparisons show that nearly all sampled representatives of Madagascar's non-primate megafauna have statistically similar δ^{13}C isotope levels, indicating similar dietary ecologies (Figure 2, Table 2). The largest elephant bird species, *Vorombe titan*, has a δ^{13}C isotope range of -21.7 to -23.9 ‰. Dietary fractionation against regional CAM and C3 plant end members indicates that this species consumed almost no CAM plants, and its high levels of depletion rule out the possibility of C4 grass consumption (Table 1). *Aepyornis maximus* also shows high depletion of δ^{13}C isotopes, with a range of -21.7 to -22.7 ‰, indicating that this species also had little to no reliance on CAM plants, and with these values again ruling out the consumption of C4 plants. The unidentified aepyornithid eggshells from the south again have δ^{13}C isotopes with a wide range of depletion, from -21.4 to -26 ‰. This level of depletion indicates that CAM plants may have constituted as much as 19% of their diet.

Comparison of *Mullerornis* eggshell and skeletal remains using Tukey's pairwise comparisons showed statistically significant difference between δ^{13}C isotope values before adjustments for environmental change to δ^{13}C accumulation in bone and eggshell, with eggshell having 0.76 ‰ more mean δ^{13}C enrichment than bone (Figure 3, Table 3). There was no significant difference between eggshell and bone after their adjustment, although bone samples had a higher mean depletion than eggshell after adjustment, with 0.85 ‰ higher mean δ^{13}C values (Figure 4, Table 4). Dietary fractionation with regional CAM and C3 end members indicates that the range of *Mullerornis modestus* δ^{13}C isotope values (-19.6 to -21.6) from skeletal elements corresponds to approximately 19% of their diet being CAM plants, and that consumption of C4 grasses is unlikely. *Mullerornis* eggshell had δ^{13}C isotope values ranging from -21.8 to -22.94, which corresponded to 25% CAM diet after adjustment and fractionation (Table 1).

The only statistically distinct species is *Aepyornis hildebrandti*, which has significantly less depletion of δ^{13}C isotopes compared to all other elephant bird taxa and all other non-primate megafauna in Madagascar, with values ranging from -13.4 to -17.1 ‰ (Figure 2, Table 1). When these isotope values are compared against local flora through isotopic fractionation, the diet of

`

A. hildebrandti appears to be a mix of both C3 and C4 plants (Table 2). The only other δ^{13}C isotope values for megafauna from the same region (central highlands) are from *Hippopotamus* sp., which have comparatively high depletion of δ^{13}C isotopes, suggesting that they fed almost exclusively on C3 plants.

Figure 2. Observed δ^{13}C isotope ‰ for skeletal elements of Madagascar's non-primate megaherbivores

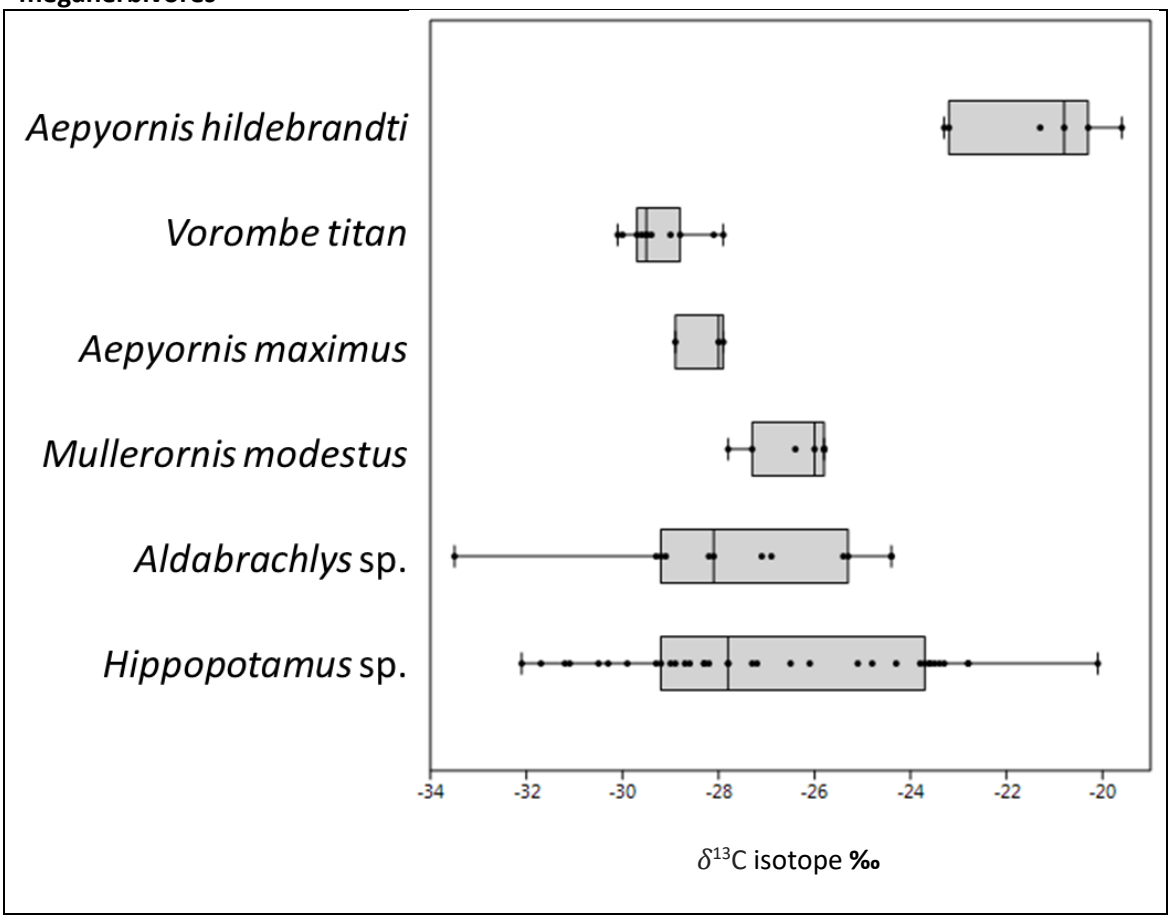

`

Table 1: Mean isotope values and dietary proportion estimates from ISOERROR 1.04 for Madagascar's non-primate megaherbivores

Source	Region	Plant site	N	Mean d13C	Std dev		C4 plant values	std dev	N	Estimated proportion of diet	standard error		C3 plant values	std dev	N	Estimated proportion of diet	standard error
Aepyornis hildebrandti	central highlands	TSI	6	-15.2	1.51		-12.195	1.33	8	0.43	0.04		-28.5	1.9	36	0.57	0.04
Hippopotamus sp.	central highlands	TSI	5	-25	0.85		-12.195	1.33	8	-0.17	0.03		-28.5	1.9	36	1.17	0.03
Source	**Region**	**Plant site**	**N**	**Mean d13C**	**Std dev**		**CAM plant values**	**std dev**	**N**	**Estimated proportion of diet**	**standard error**		**C3 plant values**	**std dev**	**N**	**Estimated proportion of diet**	**standard error**
Aepyornis maximus	west	BM P1 + P2	1	-21.8	0.71*		-15.02	1.99	87	0.07	0.05		-29.02793443	2.86	305	0.93	0.05
Vorombe titan	west	BM P1 + P2	11	-23	0.71		-15.02	1.99	87	-0.01	0.02		-29.02793443	2.86	305	1.01	0.02
Hippopotamus sp.	west	BM P1 + P2	6	-21.8	1		-15.02	1.99	87	0.07	0.03		-29.02793443	2.86	305	0.93	0.03
Aldabrachelys sp.	west	BM P1 + P2	1	-27.3	1.87*		-15.02	1.99	87	-0.32	0.13		-29.02793443	2.86	305	1.32	0.13
Source	**Region**	**Plant site**	**N**	**Mean d13C**	**Std dev**		**CAM plant values**	**std dev**	**N**	**Estimated proportion of diet**	**standard error**		**C3 plant values**	**std dev**	**N**	**Estimated proportion of diet**	**standard error**
Mullerornis modestus	south	BM P1 + P2	7	-20.2	0.82		-15.02	1.99	87	0.19	0.02		-29.02793443	2.86	305	0.81	0.02
Mullerornis modestus eggshell	south	BM P1 + P2	9	-22.36	0.48		-15.02	1.99	87	0.25	0.01		-29.02793443	2.86	305	0.75	0.01
Aepyornithid eggshell (thick)	south	BM P1 + P2	93	-23.13	0.92		-15.02	1.99	87	0.19	0.01		-29.02793443	2.86	305	0.81	0.01
Aepyornis maximus	south	BM P1 + P2	2	-22.2	0.71		-15.02	1.99	87	0.04	0.04		-29.02793443	2.86	305	0.96	0.04
Hippopotamus sp.	south	BM P1 + P2	15	-18	2		-15.02	1.99	87	0.34	0.04		-29.02793443	2.86	305	0.66	0.04
Aldabrachelys sp.	south	BM P1 + P2	11	-20.66	1.87		-15.02	1.99	87	0.15	0.04		-29.02793443	2.86	305	0.85	0.04

* Standard deviation not available. Value from alternate region used.

Table 2: Tukey's pairwise results for δ^{13}C ‰ in Madagascar's non-primate megaherbivores

	***Hippopotamus* sp.**	***Aldabrachelys* sp.**	***Mullerornis modestus***	***Aepyornis maximus***	***Vorombe titan***	***Aepyornis hildebrandti***
***Hippopotamus* sp.**		0.9967	0.9988	0.9148	0.5121	0.001288
***Aldabrachelys* sp.**	0.6819		0.9507	0.9951	0.8075	0.0003357
Mullerornis modestus	0.559	1.241		0.7267	0.283	0.004445
Aepyornis maximus	1.421	0.7394	1.98		0.9772	0.0001546
Vorombe titan	2.458	1.776	3.017	1.037		0.00013
Aepyornis hildebrandti	5.902	6.584	5.343	7.323	8.36	

`

Figure 3. Observed δ^{13}C isotopes for comparison between *Mullerornis* skeletal elements and eggshells

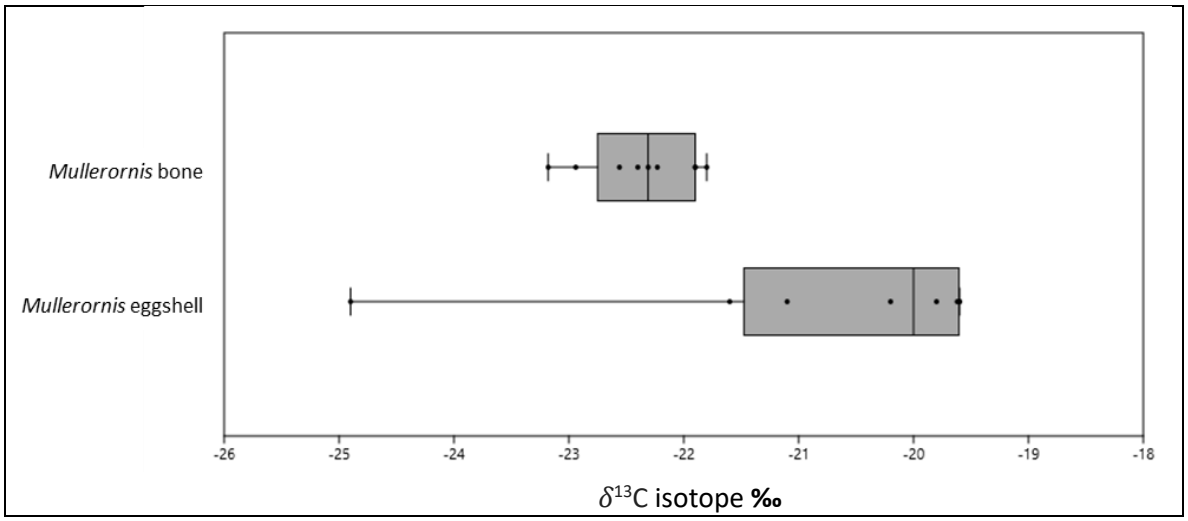

Table 3. Tukey's pairwise results: Observed δ^{13}C isotopes for *Mullerornis* skeletal elements and eggshells

Source	Number	Mean δ^{13}C ‰	Standard deviation	Tukey's Q	P-value
Mullerornis bone	7	-21.6	0.82	9.34	**≤0.0001**
Mullerornis eggshell	9	-22.36	0.48		

Figure 4. Adjusted δ^{13}C isotopes for comparison between *Mullerornis* skeletal elements and eggshells

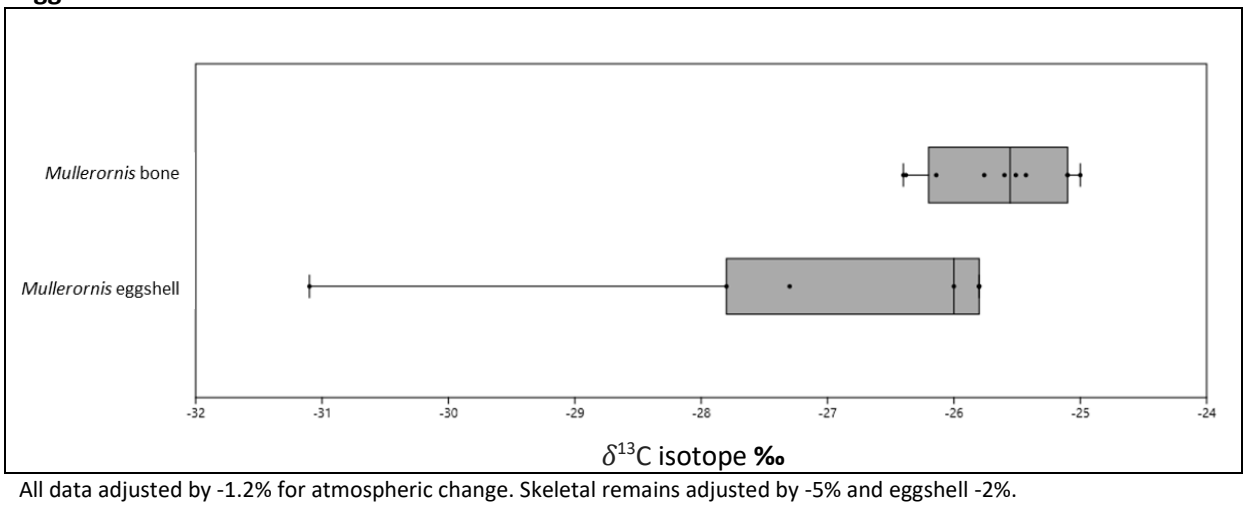

All data adjusted by -1.2% for atmospheric change. Skeletal remains adjusted by -5% and eggshell -2%.

Table 4. Tukey's pairwise results: Adjusted δ^{13}C isotopes for *Mullerornis* skeletal elements and eggshells

Source	Number	Mean δ^{13}C ‰	Standard deviation	Tukey's Q	P-value
Mullerornis bone	7	-26.41	0.82	3.734	**0.0195**
Mullerornis eggshell	9	-25.56	0.48		

`

5.5 Discussion

Presented here is the first reconstruction of dietary niche for all aepyornithid species and other non-primate Madagascan megafauna using skeletal remains, incorporating both previously published data and novel data derived for this study of δ^{13}C isotope values. Most of the megafauna assessed here do not have δ^{13}C values that support evidence of grazing ecology. However, δ^{13}C data for *Aepyornis hildebrandti* skeletal remains provide the first definitive evidence for grazing behaviour in elephant birds, with unadjusted δ^{13}C values ranging from -13.4 to -17.1 ‰, and dietary fractionation of isotopic depletion indicating that approximately 43% of their dietary carbon came from C4 tropical grasses. Dietary isotopes therefore demonstrate that this bird was the only known species of grazing megaherbivore from the Quaternary of Madagascar, meeting proposed critical δ^{13}C thresholds to identify an insular megafaunal consumer of endemic grasses (Godfrey and Crowley 2016). This evidence, compared to the statistically different dietary strategy shown by δ^{13}C isotope values for all other elephant bird species, also provides evidence of niche differentiation within the Aepyornithidae.

African hippo species have diverse ecological/dietary strategies: the common hippo (*Hippopotamus amphibius*) feeds almost entirely on grasses, whereas the pygmy hippo (*Choeropsis liberiensis*) consumes a mixture of terrestrial plants including forest plants and grasses. Madagascar's extinct hippos have remarkably low depletion of δ^{13}C isotopes in comparison to the diet of *Hippopotamus amphibius*, and they have been interpreted as consumers of herbaceous terrestrial and aquatic vegetation as well as shade loving C3 grasses in forest and swamp environments (Godfrey and Crowley 2016). Currently, data available for Madagascar's hippopotami have only been considered at the genus level, despite *H. madagascariensis* being associated with forest envionrments and *H. lemerlei* being recovered from wetland contexts. Dividing this data based upon species distinctions (Weston and Lister 2009) will likely account for the high variation in their δ^{13}C isotope values and will grant a nuanced insight into their dietary ecologies.

Although grazing behaviour has previously been inferred for *Aldabrachelys* sp. using δ^{13}C isotopes, this has been interpreted as opportunistic exploitation of introduced grasses, as this record comes from a specimen that was radiocarbon dated to just 1250 ±50 BP (Godfrey and Crowley 2016). Conversely, δ^{13}C isotopes from specimens of *A. hildebrandti* presented here range from 5282 ±39 BP to 1349 ±28 BP in age (Appendix four), indicating that grazing behaviour is not likely to coincide with late Holocene anthropogenic deforestation and

`

introduction of agricultural pasture. This evidence challenges current theories of dense forest cover with limited natural savannah in Holocene Madagascar, and highlights the need to consider the diverse array of megaherbivores in Quaternary environments to inform our understanding of ecological processes and historical baselines for anthropogenically undisturbed ecosystems.

As records of *A. hildebrandti* are limited to the Antsirabe area, it remains unclear if this spatial pattern is an artefact associated with the limited availability of Quaternary sites in the central highlands (and indeed more widely across Madagascar), or whether this species was indeed extremely limited in its geographic range and present only at high altitude (c. 1400m near Antsirabe). The *A. hildebrandti* δ^{13}C isotope record is also currently limited to specimens from the mid-late Holocene. If early Holocene and late Pleistocene records of *A. hildebrandti* can be obtained, examining dietary changes may grant insight into shifts in the mosaic of forest and savannah that was spread across the island throughout the late Quaternary (Burney et al. 2004; Crowley 2010). Currently there are no δ^{13}C isotope records for other elephant bird species found within the central highlands. As *Mullerornis modestus, Aepyornis maximus* and *Vorombe titan* are all also found in the subfossil record of the central highlands, it is unclear if the grazing behaviour demonstrated for *A. hildebrandti* can be described as sympatric niche partitioning, or if all elephant birds in the region exploited locally occurring grasses and formed a larger ecological guild adapted to regional floral communities.

Using δ^{13}C isotopes obtained from subfossil remains to interpret grazing ecology is limited to differentiating the photosynthetic pathway of the plants consumed. As both C3 and C4 grasses are present in Madagascar, it is possible that previous discussions of palaeo-grazing guilds have been subject to type II error and that consumption of grasses may have been more widespread than previously thought. Whilst approximately 43% of the diet of *A. hildebrandti* would have been C4 grasses, it therefore remains unclear if they were exclusively grazers (i.e., also consuming C3 grasses) or had mixed dietary strategies, exploiting both forest and savannah floras. Conversely, *Aepyornis maximus*, *Vorombe titan* and *Mullerornis modestus* all have δ^{13}C isotope depletion consistent with browsing of leaves and consumption of fruits from C3 plants. Although C3 grasses are present in Madagascar, they favour cooler climates such as those found in the central highlands over the hotter, more arid south and west regions. The unidentified "thick" aepyornithid eggshells also show a similar isotopic signature; these are distributed across the south and west ecoregions of Madagascar, which coincides with the known ranges

`

for *A. maximus* and *V. titan*, and so they are likely to be associated with at least one of these taxa.

Although their observed δ^{13}C values are similar, dietary analysis of "thick" eggshell determines a different dietary resource at the time of oogenesis to both *A. maximus* and *V. titan* skeletal collagen; with δ^{13}C values of -21.4 to -26 ‰, female elephant birds laying these eggs could have consumed as much as 19% of their dietary carbon from CAM plants. *Mullerornis modestus* skeletal elements have δ^{13}C isotope values of -19.6 to -21.6 ‰, which indicates their diet comprised approximately 19% CAM plants with the remainder of their diet consisting of C3 plants, most likely browsing of leaves and fruits. Their substantial difference in overall body size to co-occurring species in the south and west, *A. maximus* and *V. titan*, may have been associated with differentiation of dietary niche within an elephant bird C3 plant browsing guild, allowing them to exploit different plant resources, particularly smaller fruits and trees. Fractionation of *Mullerornis* eggshell δ^{13}C isotopes indicates that during oogenesis, *Mullerornis* females laying these eggs consumed approximately 25% of their dietary carbon from CAM plants, 6% higher than estimations from skeletal collagen data.

The 6% difference between inferred diets from eggshell and skeletal remains of *Mullerornis* could be explained by an increase in consumption of CAM plants during the period of oogenesis to consume sufficient carbon to produce their large eggs. However, given the differences between chicken and ostrich deposition rate, it seems likely that the size of eggs and their longer period of oogenesis affects their rate of δ^{13}C deposition from dietary sources. With no complete examples of *Mullerornis* eggs, there are no accurate estimations of their volume, but they are assumed to be larger than ostrich eggs (c. 0.6 litres).

All δ^{13}C ‰ data used in dietary inference are here transformed using the same environmental adjustment, but are assigned different adjustments based upon the rate of δ^{13}C deposition in bone and eggshell. A 5‰ relative difference between dietary carbon and carbon in bone collagen is well documented across all vertebrate taxa (Tykot 2004), but the relationship in eggshells is currently poorly understood. Previous authors have used a substituted rate for aepyornithids based upon a 1‰ adjustment of eggshell from experimental rates established from domestic chickens (Tovondrafale et al. 2014), and 2‰ based upon the relationship of ostrich eggshell to skeletal values (Clarke et al. 2006). Here the 2‰ value is used as ostriches

`

share more evolutionary history, have a similar ecology, and are much closer in body mass and egg size to elephant birds.

Our data suggest that an adjustment larger than 2‰ may be more appropriate for *Mullerornis* eggshells than values derived from chicken (1‰) and ostrich (2‰) data. The largest aepyornithid eggs (c. 8 litres) (Saint-Hilaire 1851) and the largest elephant birds show an even larger discrepancy between diets inferred from eggs and bones, with a difference of c. 20% predicted CAM plant diet. Without support for the thick eggshell to be assigned to either *A. maximus* or *V. titan*, it is currently difficult to assess if these are fluctuations of dietary strategy in response to increased resource requirements during oogenesis, or are a result of poor adjustment of relative δ^{13}C depletion values, skewed by the extreme size of these eggs versus those of extant birds. Further assessments of dietary ecology in the Aepyornithidae require much closer scrutiny of relative deposition of δ^{13}C in eggshell and bone, considering the possible effects of extreme egg size.

The δ^{13}C record from skeletal collagen has provided the most detailed understanding of aepyornithid dietary ecology to date. Currently most records come from the mid-late Holocene and from the south of Madagascar, and prior to this research the ecological significance of δ^{13}C data has been overlooked outside of this region. It is now clear that elephant birds had an important role in defining the natural landscapes of Madagascar at the start of the Anthropocene, and hypotheses of what constitutes a pristine Madagascar ecosystem must consider the interspecific floral interactions of these avian megafauna. Recognition of different aepyornithid taxa as representing both browsing and grazing guilds will challenge current understanding of the evolution of these environments, and studying changes in δ^{13}C isotopes of all Madagascar's fauna and flora over time will help create a more nuanced understanding of the shifting mosaic of habitats across this ecologically complex island during the late Quaternary.

`

Conclusion

`

`

Concluding remarks and future work

This thesis is the first modern study of Aepyornithidae to quantify the diversity and biogeography of skeletal remains in comparison to putative taxonomic hypotheses. Clarifying the convoluted history of historically proposed taxa underpins a modern framework for studying these enigmatic birds. The addition of a chronological sequence for their persistence provides the most reliable evidence for their species-specific extinction timings and highlights the role of anthropogenic impacts in their demise. Recording and dating evidence of butchery has provided unique and extraordinary evidence of early human settlement, and the first verifiable information on direct impacts of hunting. Dietary analysis demonstrates that these morphologically diverse family fulfilled different dietary niches and promotes new discussion into the pristine landscape of Madagascar including more expansive investigations into aepyornithid ecosystem functions. It is hoped that this thesis will catalyse and facilitate novel research into Aepyornithidae and promote understanding of their role in defining the natural state of one of the worlds most threatened ecosystems.

Chapter 1

Before this collation of museum collections of aepyornithid remains, even estimating the number of specimens available for research was not possible due to poor accession records. Analysis of morphometric data from hundreds of appendicular skeletal elements in chapter one provides the best taxonomic hypothesis available for interpreting distinct morphotypes from skeletal specimens. The comparison of museum collections of specimens with type specimens and series provides a framework for future systematic research.

To date, DNA sequences have not been collected from the full range of morphotypes identified by multivariate clustering. This data must be combined with new sampling between and across the range of clusters to clarify the systematic relationships between these groups. As interpretation of these birds is dominated by analysis of eggshell, it is critical to now match the DNA of eggs with types species based upon skeletal taxonomy, and to reassess of the bimodal differentiation of species by thickness of eggshell.

Chapter 2

Chapter two presents the oldest known evidence of human arrival in Madagascar. This data radically alters understanding of human migration and promotes the need for new

`

investigations into the human inhabitants of Madagascar throughout the Holocene and potentially the late Pleistocene. Due to resource limitations, it is likely that the true extent of butchery and hunting impacts on Aepyornithidae are currently underestimated and development of a more complete dataset will help clarify if any significant changes in the rate of exploitation had significant impact on their extinction.

Chapter 3

Auditing of available data indicates that widespread reporting of extinction in Aepyornithidae is based upon poor quality data and the GRIWM extinction estimates demonstrate that this reporting is inaccurate, with more reliable data indicating slightly earlier extinction. The timing of this extinction strongly implicates anthropogenic impacts, but also an extremely long human-megafauna overlap which is unusual for megafauna in an insular ecosystem. The number of radiocarbon dates with good provenance limits current interpretation of the extinction process. With larger, more widespread databases, supported by reliable taxonomy it will be possible to develop a more nuanced chronology than is presented in this thesis, perhaps inclusive of a truly pristine ecosystem before human arrival.

Chapter 4

Review of available dietary isotope data in *Aepyornis* has recognised that *A. hildebrandti* has a signature of a remarkably different dietary niche compared to all other megafauna in Madagascar. The recent extinction of a grazing megaherbivore challenges existing perceptions of the islands forest cover and highlights the need for more in depth research into the distribution of *A. hildebrandti.* Isotope data presented in this thesis is currently limited to the $\delta^{13}C$ record. The inclusion of nitrogen and oxygen isotopes will help progress the description of their dietary niche as well as water availability and source. This study highlights the need to include complete faunal assemblages in palaeoecological analysis and promotes the inclusion of avian, mammalian, crocodilian and reptilian megafauna in future work into reconstructing Quaternary Madagascar.

`

References

`

`

Cited references

'Amr ibn Bahr al-Jahiz, & Kopf, L. (1953). The book of Animals''(kitab Al-hayawan) of Al-Jahiz. *Actes du VIIe Congrès International d'Histoire des Sciences,* Jerusalem, 395-400.

Anderson, T. J. (2013). *Aepyornis* as moa: giant birds and global connections in nineteenth-century science. *The British Journal for the History of Science*, *46*(4), 675-693.

Andrews, C. W. (1894a). III.—Note on a New Species of Æpyornis (*Æ* Titan). *Geological Magazine*, *1*(1), 18-20.

Andrews, C. W. (1894b). On some remains of Æpyornis in the British Museum (Nat. Hist.). *Proceedings of the Zoological Society of London, 13*, 108–123.

Andrews, C. W. (1895). On Some Remains of *Aepyornis* in the Hon. Walter Rothschild's Museum at Tring. Novitates Zoologicae *2* (January), 23-25.

Andriantsaralaza, S., Pedrono, M., Tassin, J., Roger, E., Rakouth, B., & Danthu, P. (2014). The role of extinct giant tortoises in the germination of extant baobab *Adansonia rubrostipa* seeds in Madagascar. *African Journal of Ecology*, *52*(2), 246-249.

Arbour, J. H., & Brown, C. M. (2014). Incomplete specimens in geometric morphometric analyses. *Methods in Ecology and Evolution*, *5*(1), 16-26.

Bakker, E. S., Gill, J. L., Johnson, C. N., Vera, F. W., Sandom, C. J., Asner, G. P., & Svenning, J. C. (2016). Combining paleo-data and modern exclosure experiments to assess the impact of megafauna extinctions on woody vegetation. *Proceedings of the National Academy of Sciences*, *113*(4), 847-855.

Barthère, FM (1915). Observations on a bone ax, from excavations executed by the Malagasy Academy, Ampasambazimba in 1908 (Madagascar). *Bulletin of the Prehistoric Society of France*, *12* (8), 358-361.

de La Bâthie, H. P. (1921). *La végétation malgache*. Musée Colonial, Marseille.

Battistini, RP. Verin, P & Rason, R. (1963). Le Site Archaeologique de Talaky. *Annales Malgaches* (1), 111–53.

Benstead, J. P., & Goodman, S. M. (Eds.). (2003). *The natural history of Madagascar*. University of Chicago Press, Chicago.

Blench, R. M., & Walsh, M. (2010). The vocabularies of Vazimba and Beosi: do they represent the languages of the pre-Austronesian populations of Madagascar. *See http://www. rogerblench.info/Language%20data/Isolates/Vazimba%20vocabulary.pdf*

Bonaparte, CL (1853). *Ornithological classification by series*. Institute of France, Academy of Sciences, Paris.

`

Bond, W. J., Silander Jr, J. A., Ranaivonasy, J., & Ratsirarson, J. (2008). The antiquity of Madagascar's grasslands and the rise of C4 grassy biomes. *Journal of Biogeography*, *35*(10), 1743-1758.

Bond, W. J., & Silander, J. A. (2007). Springs and wire plants: anachronistic defences against Madagascar's extinct elephant birds. *Proceedings of the Royal Society of London B: Biological Sciences*, *274*(1621), 1985-1992.

Bradshaw, C. J. A., Cooper, A., Turney, C. S. M., & Brook, B. W. (2012). Robust estimates of extinction time in the geological record. *Quaternary Science Reviews*, *33*, 14-19.

Brodkorb, P. (1963). *Catalogue of Fossil Birds: Archaeopterygiformes Through Ardeiformes*. University of Florida, Gainesville.

Brucato, N., Kusuma, P., Cox, M. P., Pierron, D., Purnomo, G. A., Adelaar, A., & Ricaut, F. X. (2016). Malagasy genetic ancestry comes from an historical Malay trading post in Southeast Borneo. *Molecular biology and evolution*, *33*(9), 2396-2400.

Bunce, M., Worthy, T. H., Phillips, M. J., Holdaway, R. N., Willerslev, E., Haile, J., & Cooper, A. (2009). The evolutionary history of the extinct ratite moa and New Zealand Neogene paleogeography. *Proceedings of the National Academy of Sciences*, *106*(49), 20646-20651.

Bunce, M., Worthy, T. H., Ford, T., Hoppitt, W., Willerslev, E., Drummond, A., & Cooper, A. (2003). Extreme reversed sexual size dimorphism in the extinct New Zealand moa Dinornis. *Nature*, *425*(6954), 172.

Burckhardt, R. 1893. Über Aepyornis. *Paläontologische Abhandlungen*, *2*(6), 127-145.

Burleigh, R., & Arnold, E. N. (1986, February). Age and dietary differences of recently extinct Indian Ocean tortoises (Geochelone s. lat.) revealed by carbon isotope analysis. *Proceedings of the Royal Society of London B: Biological Sciences, 227*(1246), 137-144.

Burney, D. A. (1987). Late Quaternary stratigraphic charcoal records from Madagascar. *Quaternary Research*, 28(2), 274-280.

Burney, D. A. (1999). Rates, patterns, and processes of landscape transformation and extinction in Madagascar. In *Extinctions in near time*, ed R.D.E MacPheee (145-164). Springer, Boston, MA.

Burney, D. A., Burney, L. P., Godfrey, L. R., Jungers, W. L., Goodman, S. M., Wright, H. T., & Jull, A. T. (2004). A chronology for late prehistoric Madagascar. *Journal of Human Evolution*, *47*(1-2), 25-63.

Burney, D. A. (1998). The Kilopilopitsofy, Kidoky, and Bokyboky: Accounts of Strange Animals from Belo-sur-mer, Madagascar, and the Megafaunal "Extinction Window". *American anthropologist*, *100*(4), 957-966.

Burney, D. A., Robinson, G. S., & Burney, L. P. (2003). Sporormiella and the late Holocene extinctions in Madagascar. *Proceedings of the National Academy of Sciences*, *100*(19), 10800-10805.

`

Burns, S. J., Godfrey, L. R., Faina, P., McGee, D., Hardt, B., Ranivoharimanana, L., & Randrianasy, J. (2016). Rapid human-induced landscape transformation in Madagascar at the end of the first millennium of the Common Era. *Quaternary Science Reviews*, *134*, 92-99.

Campbell Jr, K. E., & Marcus, L. (1992). The relationship of hindlimb bone dimensions to body weight in birds. *Natural History Museum of Los Angeles County Science Series*, *36*, 395-412.

Clarke, S. J., Miller, G. H., Fogel, M. L., Chivas, A. R., & Murray-Wallace, C. V. (2006). The amino acid and stable isotope biogeochemistry of elephant bird (*Aepyornis*) eggshells from southern Madagascar. *Quaternary Science Reviews*, *25*(17-18), 2343-2356.

Clavel, J., Merceron, G., & Escarguel, G. (2014). Missing data estimation in morphometrics: how much is too much? *Systematic biology*, *63*(2), 203-218.

Cooke, S. B., Dávalos, L. M., Mychajliw, A. M., Turvey, S. T., & Upham, N. S. (2017). Anthropogenic extinction dominates Holocene declines of West Indian mammals. *Annual Review of Ecology, Evolution, and Systematics*, *48*(2), 301-327.

Corron, L., Huchet, J. B., Santos, F., & Dutour, O. (2017). Using classifications to identify pathological and taphonomic modifications on ancient bones: Do “taphognomonic” criteria exist? *Bulletins et Mémoires de la Société d'Anthropologie de Paris*, *29*(1-2), 1-18.

Cracraft, J. (1976a). Covariation patterns in the postcranial skeleton of moas (Aves, Dinornithidae): A factor analytic study. *Paleobiology*, *2*(2), 166-173.

Cracraft, J. (1976b). The Hindlimb Elements of the Moas (Aves, Dinornithidae): A Multivariate Assessment of Size and Shap. *Journal of morphology*, *150*(2), 495-526.

Crees, J. J., & Turvey, S. T. (2014). Holocene extinction dynamics of Equus hydruntinus, a late-surviving European megafaunal mammal. *Quaternary Science Reviews*, *91*, 16-29.

Crisp, M., Demarchi, B., Collins, M., Morgan-Williams, M., Pilgrim, E., & Penkman, K. (2013). Isolation of the intra-crystalline proteins and kinetic studies in Struthio camelus (ostrich) eggshell for amino acid geochronology. *Quaternary Geochronology*, 16, 110-128.

Crowley, B. E., & Samonds, K. E. (2013). Stable carbon isotope values confirm a recent increase in grasslands in northwestern Madagascar. *The Holocene*, *23*(7), 1066-1073.

Crowley, B. E. (2010). A refined chronology of prehistoric Madagascar and the demise of the megafauna. *Quaternary Science Reviews*, *29*(19-20), 2591-2603.

Crowley, B. E., & Godfrey, L. R. (2013). Why all those spines?: Anachronistic defences in the Didiereoideae against now extinct lemurs. *South African Journal of Science*, *109*(1-2), 1-7.

Crowley, B., Godfrey, L. R., Bankoff, R. J., Perry, G. H., Culleton, B. J., Kennett, D. J., & Burney, D. (2017). Island-wide aridity did not trigger recent megafaunal extinctions in Madagascar. *Ecography*, *40*(8), 901-912.

`

Crowley, B., Thorén, S., Rasoazanabary, E., Vogel, E. R., Barrett, M. A., Zohdy, S. & Wright, P. C. (2011). Explaining geographical variation in the isotope composition of mouse lemurs (*Microcebus*). *Journal of Biogeography*, *38*(11), 2106-2121.

Crowley, B., Godfrey, L. R., Guilderson, T. P., Zermeño, P., Koch, P. L., & Dominy, N. J. (2012). Extinction and ecological retreat in a community of primates. *Proceedings of the Royal Society of London B: Biological Sciences*, *279*(1742), 3597-3605.

Crowley, B., Godfrey, L. R., & Irwin, M. T. (2011). A glance to the past: subfossils, stable isotopes, seed dispersal, and lemur species loss in southern Madagascar. *American Journal of Primatology*, *73*(1), 25-37.

Crowther, A., Lucas, L., Helm, R., Horton, M., Shipton, C., Wright, H. T., & Picornell-Gelabert, L. (2016). Ancient crops provide first archaeological signature of the westward Austronesian expansion. *Proceedings of the National Academy of Sciences*, *113*(24), 6635-6640.

De Ricqlès, A., Bourdon, E., Legendre, L. J., & Cubo, J. (2016). Preliminary assessment of bone histology in the extinct elephant bird *Aepyornis* (Aves, Palaeognathae) from Madagascar. *Comptes Rendus Palevol*, *15*(1-2), 197-208.

Dewar, R. E. (1984). Extinctions in Madagascar: The loss of the subfossil fauna. In *Pleistocene extinctions: The search for a cause*, eds P.S. Martin & R.G. Klein. Yale Unversity Press, New Haven.

Dewar, R. E., Radimilahy, C., Wright, H. T., Jacobs, Z., Kelly, G. O., & Berna, F. (2013). Stone tools and foraging in northern Madagascar challenge Holocene extinction models. *Proceedings of the National Academy of Sciences*, *110*(31), 12583-12588.

Dewar, R. E., & Richard, A. F. (2007). Evolution in the hypervariable environment of Madagascar. *Proceedings of the National Academy of Sciences*, *104*(34), 13723-13727.

Dittmar, J. M., Errickson, D., & Caffell, A. (2015). The comparison and application of silicone casting material for trauma analysis on well preserved archaeological skeletal remains. *Journal of Archaeological Science: Reports*, *4*, 559-564.

Douglass, K. M. G. (2016a). *An Archaeological investigation of settlement and resource exploitation patterns in the Velondriake Marine Protected Area, Southwest Madagascar, ca. 900 BC to AD 1900*. Yale University.

Douglass, K. (2017b). The diversity of late Holocene shellfish exploitation in Velondriake, southwest Madagascar. *The Journal of Island and Coastal Archaeology*, *12*(3), 333-359.

Dowd, M., & Carden, R. F. (2016). First evidence of a Late Upper Palaeolithic human presence in Ireland. *Quaternary Science Reviews*, *139*, 158-163.

Ehleringer, J. R., & Monson, R. K. (1993). Evolutionary and ecological aspects of photosynthetic pathway variation. *Annual Review of Ecology and Systematics*, *24*(1), 411-439.

`

Fisher, D. O., & Blomberg, S. P. (2010). Correlates of rediscovery and the detectability of extinction in mammals. *Proceedings of the Royal Society of London B: Biological Sciences*, *278* (1708), 1090-1097.

Fitzpatrick, S. M. (2006). A critical approach to 14 C dating in the Caribbean: using chronometric hygiene to evaluate chronological control and prehistoric settlement. *Latin American Antiquity*, *17*(4), 389-418.

Fontoynont, M. (1909). Les Gisements fossiliferes d'Ampasambazimba. *Bulletin d'lAcademie Malgache*, *6*, 3–8.

Forsyth, M., & Alphonse, R. (1896). Fruits of Travel. *Natural Science : A Monthly Review of Scientific Progress, 9*, 225-226

Fraley, C., & Raftery, A. E. (1998). How many clusters? Which clustering method? Answers via model-based cluster analysis. *The computer journal*, *41*(8), 578-588.

Fraley, C., Raftery, A. E., Murphy, T. B., & Scrucca, L. (2012). mclust v. 4 for R: normal mixture modeling for modelbased clustering, classification, and density estimation. *Dept of Statistics, Univ. of Washington Tech. Rep*, *587*.

Freeman, S., & Jackson, W. M. (1990). Univariate metrics are not adequate to measure avian body size. *The Auk*, *107,* 69-74.

Galán, A. B., & Domínguez-Rodrigo, M. (2013). An experimental study of the anatomical distribution of cut marks created by filleting and disarticulation on long bone ends. *Archaeometry*, *55*(6), 1132-1149.

Garvey, J., Cochrane, B., Field, J., & Boney, C. (2011). Modern emu (Dromaius novaehollandiae) butchery, economic utility and analogues for the Australian archaeological ecord. *Environmental Archaeology*, *16*(2), 97-112.

Gasse, F., & Van Campo, E. (1998). A 40,000-yr pollen and diatom record from Lake Tritrivakely, Madagascar, in the southern tropics. *Quaternary Research*, *49*(3), 299-311.

Geoffroy-Saint-Hilaire, I. (1851). Note on Some Bones and Eggs Found at Madagascar, in Recent Alluvia, Belonging to a Gigantic Bird. *Comptes Rendus des Seances Hebdomadaires de l'Acadmeie des Sciences. 32,* 101–7.

Geoffroy-Saint-Hilaire, I. (1856). Sur une oeuf d'Epyornis Recemment Arrive En France. *de l'Acadmeie des Sciences. 42*, 315-316.

Gillespie, R., Brook, B. W., & Baynes, A. (2006). Short overlap of humans and megafauna in Pleistocene Australia. *Alcheringa: An Australasian Journal of Palaeontology*, *30*(1), 163-186.

Godfrey, L. R., & Crowley, B. E. (2016). Madagascar's ephemeral palaeo-grazer guild: who ate the ancient C4 grasses? *Proceedings of the Royal Society of London B: Biological Sciences., 283*(1834), 20160360.

Godfrey, L, R. (2017). Personal Communication.

`

Godfrey, L. R., Jungers, W., Reed, K. E., Simons, E. L., & Chatrath, P. S. (1997). Primate subfossils inferences about past and present primate community structure. *Natural change and human-induced change in Madagascar,* 218-256. Smithsonian Institution Press. Washington, DC.

Godfrey, L. R., Perez, V. R., Meador, L. R., Crowley, B. E., Bankoff, R. J., Culleton, B. J., & Perry, G. H. (2016). New evidence of widespread hunting of giant lemurs on Madagascar. *American journal of physical anthropology*, *159*, 156-157.

Gommery, D., Ramanivosoa, B., Faure, M., Guerin, C., Kerloc'h, P., Senegas, F., & Randrianantenaina, H. (2011). The oldest traces of human activity in Madagascar on subfossil hippopotamus bones of Anjohibe (Mahajanga Province). *Returns Palevol*, *10*(4), 271-278.

Goodman, S. M., & Jungers, W. L. (2014). *Extinct Madagascar: picturing the island's past*. University of Chicago Press. Chicago.

Goodman, S. M. (1994). Description of a new species of subfossil eagle from Madagascar-Stephanoaetus (Aves, Falconiformes) from the deposits of Ampasambazimba. *Proceedings of the Biological Society of Washington*, *107*(3), 421-428.

Goodman, S. M., & Patterson, B. D. (Eds.). (1997). *Natural change and human impact in Madagascar*. Smithsonian Institution Press, Washington D.C.

Grealy, A., Phillips, M., Miller, G., Gilbert, M. T. P., Rouillard, J. M., Lambert, D., & Haile, J. (2017). Eggshell palaeogenomics: Palaeognath evolutionary history revealed through ancient nuclear and mitochondrial DNA from Madagascan elephant bird (*Aepyornis* sp.) eggshell. *Molecular phylogenetics and evolution*, *109*, 151-163.

Griffiths, C. J., Zuel, N., Jones, C. G., Ahamud, Z., & Harris, S. (2013). Assessing the potential to restore historic grazing ecosystems with tortoise ecological replacements. *Conservation Biology*, *27*(4), 690-700.

Guimarães Jr, P. R., Galetti, M., & Jordano, P. (2008). Seed dispersal anachronisms: rethinking the fruits extinct megafauna ate. *PloS one*, *3*(3), e1745.

Hammer, Ø., Harper, D. A. T., & Ryan, P. D. (2001). Paleontological statistics software: package for education and data analysis. *Palaeontologia Electronica*, *4*(1), 1-9.

Handley, W. D., Chinsamy, A., Yates, A. M., & Worthy, T. H. (2016). Sexual dimorphism in the late Miocene mihirung Dromornis stirtoni (Aves: Dromornithidae) from the Alcoota Local Fauna of central Australia. *Journal of Vertebrate Paleontology*, *36*(5), e1180298.

Hansen, D. M., & Galetti, M. (2009). The forgotten megafauna. *Science*, *324*(5923), 42-43.

Hansford, J., Nuñez-Miño, J. M., Young, R. P., Brace, S., Brocca, J. L., & Turvey, S. T. (2012). Taxonomy-testing and the 'Goldilocks Hypothesis': morphometric analysis of species diversity in living and extinct Hispaniolan hutias. *Systematics and biodiversity*, *10*(4), 491-507.

Hobbs, N. T. (1996). Modification of ecosystems by ungulates. *The Journal of Wildlife Management*, *60*(4), 695-713.

`

Hobson, K. A., & Clark, R. G. (1992). Assessing avian diets using stable isotopes I: turnover of 13C in tissues. *The Condor*, *94*(1), 181-188.

Hockett, B., & Jenkins, D. L. (2013). Identifying stone tool cut marks and the pre-Clovis occupation of the Paisley Caves. *American Antiquity*, *78*(4), 762-778.

Hogg, A. G., Hua, Q., Blackwell, P. G., Niu, M., Buck, C. E., Guilderson, T. P., Heaton, T. J. (2013) SHCal13 Southern Hemisphere calibration, 0–50,000 years cal BP. *Radiocarbon, 55*(4), 1889-1903.

Holdaway, R. N., & Jacomb, C. (2000). Rapid extinction of the moas (Aves: Dinornithiformes): model, test, and implications. *Science*, *287*(5461), 2250-2254.

Holdaway, R. N., Allentoft, M. E., Jacomb, C., Oskam, C. L., Beavan, N. R., & Bunce, M. (2014). An extremely low-density human population exterminated New Zealand moa. *Nature Communications*, *7*(5), 5436.

Hopcraft, J. G. C., Olff, H., & Sinclair, A. R. E. (2010). Herbivores, resources and risks: alternating regulation along primary environmental gradients in savannas. *Trends in Ecology & Evolution*, *25*(2), 119-128.

Humbert, H. (1927). Destruction d'une flore insulaire par le feu. *Mémoires de l'Académie Malgache, 5*, 1–80.

Hunter, E. A., Gibbs, J. P., Cayot, L. J., & Tapia, W. (2013). Equivalency of Galápagos giant tortoises used as ecological replacement species to restore ecosystem functions. *Conservation Biology*, *27*(4), 701-709.

Huynen, L., Millar, C. D., Scofield, R. P., & Lambert, D. M. (2003). Nuclear DNA sequences detect species limits in ancient moa. *Nature, 425*(6954), 175-178.

Johnson, B. J., Fogel, M. L., & Miller, G. H. (1998). Stable isotopes in modern ostrich eggshell: a calibration for paleoenvironmental applications in semi-arid regions of southern Africa. *Geochimica et Cosmochimica Acta*, *62*(14), 2451-2461.

Johnson, C. N., Bradshaw, C. J., Cooper, A., Gillespie, R., & Brook, B. W. (2013). Rapid megafaunal extinction following human arrival throughout the New World. *Quaternary International*, *308*, 273-277.

Josse, J., & Husson, F. (2016). missMDA: a package for handling missing values in multivariate data analysis. *Journal of Statistical Software*, *70*(1), 1-31.

Kay, J. (2004). Etienne de Flacourt, L'Histoire de le Grand Ile de Madagascar (1658). *Curtis's Botanical Magazine*, *21*(4), 251-257.

Keeling, C. D. (1979). The Suess effect: 13Carbon-14Carbon interrelations. *Environment International*, *2*(4-6), 229-300.

Klein, J. (2002). Deforestation in the Madagascar highlands–established truth and scientific uncertainty. *GeoJournal*, *56*(3), 191-199.

`

Krause, D. W., O'Connor, P. M., Rogers, K. C., Sampson, S. D., Buckley, G. A., & Rogers, R. R. (2006). Late Cretaceous terrestrial vertebrates from Madagascar: implications for Latin American biogeography. *Annals of the Missouri Botanical Garden*, *93*(2), 178-208.

Kull, C. A. (2000). Deforestation, erosion, and fire: degradation myths in the environmental history of Madagascar. *Environment and History*, *6*(4), 423-450.

Kusuma, P., Cox, M. P., Pierron, D., Razafindrazaka, H., Brucato, N., Tonasso, L., & Ricaut, F. X. (2015). Mitochondrial DNA and the Y chromosome suggest the settlement of Madagascar by Indonesian sea nomad populations. *BMC genomics*, *16*(1), 191.

Lamberton, C. (1934). Contribution à l'étude anatomique des *Aepyornis. Bull. Acad. Malgache, 13, 151–174.*

Lambrecht, K. (1933). *Handbuch der palaeornithologie*, *212*. Verlag Bornträger, Berlin.

Last, J. T. (1894). On the bones of the *Aepyornis*, and on the localities and conditions in which they are found. In *Proceedings of the Zoological Society of London*, 123-129.

Laundré, J. W., Hernández, L., & Ripple, W. J. (2010). The landscape of fear: ecological implications of being afraid. *Open Ecology Journal*, *3*, 1-7.

LeMoine, J.M. (1902). "The Search for the Epyornis." *Le Naturaliste Canadien, 17*, 98-99.

Lister, A. M., & Stuart, A. J. (2013). Extinction chronology of the woolly rhinoceros Coelodonta antiquitatis: reply to Kuzmin. *Quaternary Science Reviews*, *62*, 144-146.

MacPhee, R, ed. (1999). Extinctions in Near Time. Kluwer Academic/Plenum Publishers, New York.

MacPhee, R. D., & Burney, D. A. (1991). Dating of modified femora of extinct dwarf Hippopotamus from southern Madagascar: implications for constraining human colonization and vertebrate extinction events. *Journal of Archaeological Science*, *18*(6), 695-706.

MacPhee, R. D. E., Burney, D. A., & Wells, N. A. (1985). Early Holocene chronology and environment of Ampasambazimba, a Malagasy subfossil lemur site. *International Journal of Primatology*, *6*(5), 463-489.

Mahe, J., & Sourdat, M. (1972). On the extinction of subfossil vertebrates and the aridification of climate in southwestern Madagascar. *Bulletin of the Society of Geology of France, 14*, 295-309.

Malhi, Y., Doughty, C. E., Galetti, M., Smith, F. A., Svenning, J. C., & Terborgh, J. W. (2016). Megafauna and ecosystem function from the Pleistocene to the Anthropocene. *Proceedings of the National Academy of Sciences*, *113*(4), 838-846.

Matsumoto, K., & Burneyt, D. A. (1994). Late Holocene environments at Lake Mitsinjo, northwestern Madagascar. *The Holocene*, *4*(1), 16-24.

`

McNaughton, S. J., Banyikwa, F., & McNaughton, M. (1997). Promotion of the cycling of diet-enhancing nutrients by African grazers. *Science*, *278*(5344), 1798-1800.

McPherron, S. P., Alemseged, Z., Marean, C. W., Wynn, J. G., Reed, D., Geraads, D., & Béarat, H. A. (2010). Evidence for stone-tool-assisted consumption of animal tissues before 3.39 million years ago at Dikika, Ethiopia. *Nature*, *466*(7308), 857.

Midgley, J. J., & Illing, N. (2009). Were Malagasy Uncarina fruits dispersed by the extinct elephant bird? *South African Journal of Science*, *105*(11-12), 467-469.

Milne Edwards, A., Grandidier, A. (1894). Observations sur les *Aepyornis* de Madagascar. *C. R. Hebd. Seanc. Acad. Sci*. *118*, 122–127.

Milne Edwards, A., Grandidier, A. (1866). Observations sur les caractères zoologiques et les affinités naturelles de l'*Aepyornis* de Madagascar. *Recherches sur la faune ornithologique éteinte des Îles Mascareignes et de Madagascar.* E. Martinet, Paris.

Milne Edwards, A., Grandidier, A. (1869). Nouvelles observations sur les caractères zoologiques et les affinités naturelles de l'*Aepyornis* de Madagascar. *Recherches sur la faune ornithologique éteinte des Îles Mascareignes et de Madagascar.* E. Martinet, Paris.

Mitchell, K. J., Llamas, B., Soubrier, J., Rawlence, N. J., Worthy, T. H., Wood, J., & Cooper, A. (2014). Ancient DNA reveals elephant birds and kiwi are sister taxa and clarifies ratite bird evolution. *Science*, *344*(6186), 898-900.

Monnier, L. (1913). Les *Aepyornis*. Paleontologie de Madagascar VII. In *Annales de Paleontologie, 5*, 125-172.

Muhawi, I. (2005). The Arabian Nights and the Question of Authorship. *Journal of Arabic Literature*, *36*(3), 323–37.

Muldoon, K. M., Crowley, B. E., Godfrey, L. R., Rasoamiaramanana, A., Aronson, A., Jernvall, J., & Simons, E. L. (2012). Early Holocene fauna from a new subfossil site: A first assessment from Christmas River, south central Madagascar. *Madagascar Conservation & Development*, *7*(1), 23-29.

Needham, I., Vorontsova, M. S., Banks, H., & Rudall, P. J. (2015). Pollen of Malagasy grasses as a potential tool for interpreting grassland palaeohistory. *Grana*, *54*(4), 247-262.

Olson, V. A., & Turvey, S. T. (2013). The evolution of sexual dimorphism in New Zealand giant moa (Dinornis) and other ratites. *Proceedings of the Royal Society of London B: Biological Sciences, 280*(1760), 20130401.

Oskam, C. L., Haile, J., McLay, E., Rigby, P., Allentoft, M. E., Olsen, M. E., & Walter, R. (2010). Fossil avian eggshell preserves ancient DNA. *Proceedings of the Royal Society of London B: Biological Sciences*, *277*(1690), 1991-2000.

Owen, R. (1846). Proceedings of a meeting: Owen read his second memoir on remains of Dinornis. *Proceedings of the Zoological Society (London) for 1846*, *14*, 46-49.

`

Owen, Richard. 1852. Notes on the Eggs and Young of the Apteryx, and on the Casts of the Eggs and Certain Bones of *Aepyornis* (Isid. Geoffroy), Recently Transmitted to the Zoological Society of London. *Proceedings of the Zoological Society of London, 19*, 9-13.

Parker Pearson, M. (2010). Pastoralists, Warriors and Colonists: The Archaeology of Southern Madagascar. Archaeopress, Oxford.

Parker Pearson, M., Godden, K., Ramilisonina, R., Schwenninger, J. L., & Smith, H. (1995). *The Central Androy Survey; Third Report*. University of Sheffield and Musée d'Art et d'Archéologie, Antananarivo.

Perez, V. R., Godfrey, L. R., Nowak-Kemp, M., Burney, D. A., Ratsimbazafy, J., & Vasey, N. (2005). Evidence of early butchery of giant lemurs in Madagascar. *Journal of Human Evolution*, *49*(6), 722-742.

Perry, G. L., Wheeler, A. B., Wood, J. R., & Wilmshurst, J. M. (2014). A high-precision chronology for the rapid extinction of New Zealand moa (Aves, Dinornithiformes). *Quaternary Science Reviews*, *105*, 126-135.

Phillips, D. L., & Gregg, J. W. (2001). Uncertainty in source partitioning using stable isotopes. *Oecologia*, *127*(2), 171-179.

Pierron, D., Heiske, M., Razafindrazaka, H., Rakoto, I., Rabetokotany, N., Ravololomanga, B., & Raharijesy, M. A. (2017). Genomic landscape of human diversity acrossMadagascar. *Proceedings of the National Academy of Sciences*, 201704906.

Pires, M. M., Galetti, M., Donatti, C. I., Pizo, M. A., Dirzo, R., & Guimarães, P. R. (2014). Reconstructing past ecological networks: the reconfiguration of seed-dispersal interactions after megafaunal extinction. *Oecologia*, *175*(4), 1247-1256.

Pitulko, V. V., Tikhonov, A. N., Pavlova, E. Y., Nikolskiy, P. A., Kuper, K. E., & Polozov, R. N. (2016). Early human presence in the Arctic: evidence from 45,000-year-old mammoth remains. Science, 351(6270), 260-263.

Quéméré, E., Amelot, X., Pierson, J., Crouau-Roy, B., & Chikhi, L. (2012). Genetic data suggest a natural prehuman origin of open habitats in northern Madagascar and question the deforestation narrative in this region. *Proceedings of the National Academy of Sciences*, *109*(32), 13028-13033.

Ramsey, C. B. (2009). Bayesian analysis of radiocarbon dates. *Radiocarbon*, *51*(1), 337-360.

Team, R. C. (2014). R: A language and environment for statistical computing. R Foundation for Statistical Computing. Vienna, Austria.

Reed, J. M. (1999). The role of behavior in recent avian extinctions and endangerments. *Conservation Biology*, *13*(2), 232-241.

Rosaas, T.G. (1893). Recent Discoveries of Fossils at Antsirabe. *Antananarivo Annual. 7*(17), 111–14.

`

Rowley, G. D. (1867). On the egg of *Aepyornis*, the colossal bird of Madagascar. In *Proceedings of the Zoological Society of London, 3,* 892-895.

Salemme, M., & Frontini, R. (2011). The exploitation of RHEIDAE in Pampa and Patagonia (Argentina) as recorded by chroniclers, naturalists and voyagers. *Journal of Anthropological Archaeology*, *30*(4), 473-483.

Saltré, F., Brook, B. W., Rodríguez-Rey, M., Cooper, A., Johnson, C. N., Turney, C. S., & Bradshaw, C. J. (2015). Uncertainties in dating constrain model choice for inferring extinction time from fossil records. *Quaternary Science Reviews*, *112*, 128-137.

Samonds, K. E., Parent, S. N., Muldoon, K. M., Crowley, E., & Godfrey, L. R. (2010). Rock matrix surrounding subfossil lemur skull yields diverse collection of mammalian subfossils: implications for reconstructing Madagascar's paleoenvironments. *Malagasy Nature*, *4*, 1-16.

Schwarz, G. (1978). Estimating the dimension of a model. *The Annals of Statistics*, *6*(2), 461-464.

Scroxton, N., Burns, S. J., McGee, D., Hardt, B., Godfrey, L. R., Ranivoharimanana, L., & Faina, P. (2017). Hemispherically in-phase precipitation variability over the last 1700 years in a Madagascar speleothem record. *Quaternary Science Reviews*, *164*, 25-36.

Stankiewicz, J., Thiart, C., Masters, J. C., & Wit, M. J. (2006). Did lemurs have sweepstake tickets? An exploration of Simpson's model for the colonization of Madagascar by mammals. *Journal of Biogeography*, *33*(2), 221-235.

Strauss, R. E., & Atanassov, M. N. (2006). Determining best complete subsets of specimens and characters for multivariate morphometric studies in the presence of large amounts of missing data. *Biological Journal of the Linnean Society*, *88*(2), 309-328.

Strickland, H.E. (1849). Supposed Existence of a Giant Bird in Madagascar. *The Annals and Magazine of Natural History. 2*(4), 338–39.

Stuart, A. J., & Lister, A. M. (2014). New radiocarbon evidence on the extirpation of the spotted hyaena (*Crocuta crocuta*) in northern Eurasia. *Quaternary Science Reviews*, *96*, 108-116.

Stuart, A. J., & Lister, A. M. (2012). Extinction chronology of the woolly rhinoceros Coelodonta antiquitatis in the context of late Quaternary megafaunal extinctions in northern Eurasia. *Quaternary Science Reviews*, *51*, 1-17.

Stuart, A. J. (2015). Late Quaternary megafaunal extinctions on the continents: a short review. *Geological Journal*, *50*(3), 338-363.

Tovondrafale, T., Razakamanana, T., Hiroko, K., & Rasoamiaramanan, A. (2014). Paleoecological analysis of elephant bird (Aepyornithidae) remains from the Late Pleistocene and Holocene formations of southern Madagascar. *Malagasy Nature*, *8*, 1-13.

Trueman, C. N., Field, J. H., Dortch, J., Charles, B., & Wroe, S. (2005). Prolonged coexistence of humans and megafauna in Pleistocene Australia. *Proceedings of the National Academy of Sciences of the United States of America*, *102*(23), 8381-8385.

`

Turvey, S. T., Hansford, J., Kennerley, R. J., Nunez-Mino, J. M., Brocca, J. L., & Young, R. P. (2015). A new subspecies of hutia (Plagiodontia, Capromyidae, Rodentia) from southern Hispaniola. *Zootaxa*, *3957*(2), 201-214.

Turvey, S. T., Peters, S., Brace, S., Young, R. P., Crumpton, N., Hansford, J., & Timpson, A. (2016). Independent evolutionary histories in allopatric populations of a threatened Caribbean land mammal. *Diversity and Distributions*, *22*(5), 589-602.

Turvey, S. T., Tong, H., Stuart, A. J., & Lister, A. M. (2013). Holocene survival of Late Pleistocene megafauna in China: a critical review of the evidence. *Quaternary Science Reviews*, *76*, 156-166.

Turvey, S. T. (2009). In the shadow of the megafauna: prehistoric mammal and bird extinctions across the Holocene. *Holocene Extinctions. Oxford University Press, Oxford*, 17-39.

Turvey, S. T., Green, O. R., & Holdaway, R. N. (2005). Cortical growth marks reveal extended juvenile development in New Zealand moa. *Nature*, *435*(7044), 940.

Tykot, R. H. (2004). Stable isotopes and diet: you are what you eat. In *Proceedings-International School of Physics Enrico Fermi, 154*, 433-444.

Virah-Sawmy, M., Willis, K. J., & Gillson, L. (2010). Evidence for drought and forest declines during the recent megafaunal extinctions in Madagascar. *Journal of Biogeography*, *37*(3), 506-519.

Vorontsova, M. S., Besnard, G., Forest, F., Malakasi, P., Moat, J., Clayton, W. D., & Randriatsara, F. O. (2016). Madagascar's grasses and grasslands: anthropogenic or natural? *Proceedings of the Royal Society of London B: Biological Sciences*, *283*(1823), 20152262.

Wells, H.G. (1894) *Aepyornis* island. (November) *Pall Mall Budget.* Pall Mall Gazette, London.

Weston, E. M., & Lister, A. M. (2009). Insular dwarfism in hippos and a model for brain size reduction in Homo floresiensis. *Nature*, *459*(7243), 85-88.

Willig, M. R., & Owen, R. D. (1987). Univariate analyses of morphometric variation do not emulate the results of multivariate analyses. *Systematic Zoology*, *36*(4), 398-400.

Willis, K. J., Gillson, L., & Virah-Sawmy, M. (2008). Nature or nurture: the ambiguity of C4 grasslands in Madagascar. *Journal of Biogeography*, *35*(10), 1741-1742.

Wolf, A., Doughty, C. E., & Malhi, Y. (2013). Lateral diffusion of nutrients by mammalian herbivores in terrestrial ecosystems. *PloS one*, *8*(8), e71352.

Wood, J. R., Wilmshurst, J. M., Worthy, T. H., & Cooper, A. (2011). Sporormiella as a proxy for non-mammalian herbivores in island ecosystems. *Quaternary Science Reviews*, *30*(7-8), 915-920.

Worthy, T.H., Bunce, M., Cooper, A. & Scofield, P. 2005. Dinornis– an insular oddity, a taxonomic conundrum reviewed. In Alcover, J.A. & Bover, P. (eds.): Proceedings of the International Symposium “Insular Vertebrate Evolution: the Palaeontological Approach”. *Monografies de la Societat d’Història Natural de les Balears*, *12*, 377-390.

`

Worthy, T., & Scofield, R. (2012). Twenty-first century advances in knowledge of the biology of moa (Aves: Dinornithiformes): a new morphological analysis and moa diagnoses revised. *New Zealand Journal of Zoology*, *39*(2), 87-153.

Worthy, T., & Holdaway, R. (2002). *The Lost World of the Moa*. Indiana University Press. Bloomington, Indiana.

Yoder, A. D., Campbell, C. R., Blanco, M. B., Dos Reis, M., Ganzhorn, J. U., Goodman, S. M., & Ralison, J. M. (2016). Geogenetic patterns in mouse lemurs (genus Microcebus) reveal the ghosts of Madagascar's forests past. *Proceedings of the National Academy of Sciences*, *113*(29), 8049-8056.

Yonezawa, T., Segawa, T., Mori, H., Campos, P. F., Hongoh, Y., Endo, H., & Jin, H. (2017). Phylogenomics and morphology of extinct paleognaths reveal the origin and evolution of the ratites. *Current Biology*, *27*(1), 68-77.

`

`

Appendix one

`

A. FEMORAL MEASUREMENTS

Museum	Specimen number	Genus assignment	Species assignment	Original type series	Collection locality	F1	F2	F3	F4	F5	F6	F7	F8	F9
UIO	Unnumbered	*Aepyornis*	*hildebrandti*				48.4	185	60.8	161	48.6	49.4		126.46
UIO	122.872	*Aepyornis*	*hildebrandti*				55.17	204	65.72	174	54.41	51.38	90.59	113.08
MNHN	1906-16-66	*Aepyornis*	*hildebrandti*				54.16	197	63.84	171	55.86	56.54	113.1	131.18
MNHN	Unnumbered	*Aepyornis*	*hildebrandti*			336	57.34	210	68.6	172	57.32	54.1	112.56	140.26
MNHN	1908-5	*Mullerornis*	*modestus*	*Aepyornis modestus*		255	29.9	121	41.84	112	34.9	34.54	68.54	90.66
MNHN	MAD 364	*Vorombe*	*titan*		Ankazoabo	445	70.46	267	88.36	234	72.06	72.88	139.22	184
MNHN	MAD 6648	*Mullerornis*	*modestus*				32.12	120	40.76	108	32	34.52	64.32	91.6
MNHN	MAD 441	*Mullerornis*	*modestus*		Lamboharana		28.44	114	41.52	113	34.12	34.3	63.84	96.4
MNHN	MAD 373	*Aepyornis*	*hildebrandti*	*Aepyornis gracilis*		325	53.38	172	56.56	180	55.84	55.3	95.76	123.06
MNHN	MAD 374	*Aepyornis*	*hildebrandti*			317	50.6	189	62.34	164	48.6	51.68		125.4
MNHN	MAD 369	*Vorombe*	*titan*		Antsirabe	443	73.1	284	94.62	254	72.56	73.34		200
MNHN	MAD 6754	*Aepyornis*	*hildebrandti*			322	54.58	190	61.16	175	52.54	50.26		129
MNHN	1906-16-71	*Aepyornis*	*hildebrandti*				57.16	203	66.22	152	47.4	46.96	109.3	127.5
MNHN	1906-16-65	*Aepyornis*	*hildebrandti*			321	53.06	190	60.6	153	49.1	47.8	116.88	130.72
MNHN	Unnumbered	*Aepyornis*	*hildebrandti*			312	53.32	199	65.76	171	53.38	49.4	97.5	119.04
MNHN	JH 32	*Mullerornis*	*modestus*			268	32.52	125	41.68	118	36.24	37.24		99.98
MNHN	JH 58	*Aepyornis*	*hildebrandti*			328	55.14	197	64.62	171	55.18	51.34	112.66	138.86
MNHN	JH 59	*Aepyornis*	*hildebrandti*				57.04	207	68.92	164	53.64	50.98	107	131.8
MNHN	JH 61	*Mullerornis*	*modestus*			245	31.42	116	36.8	107	35.34	32.52	71.64	92.02
MNHN	MAD 378	*Aepyornis*	*maximus*			358	65.96	237	78.64	185	51.4	58.72	112.46	
MNHN	Unnumbered	*Vorombe*	*titan*			464	71.92	277	93.18	276	69.08	67.12	154	203
MNHN	Unnumbered	*Vorombe*	*titan*			490	74.26	288	99.12			69.64	157	207
MNHN	MAD 6773	*Mullerornis*	*modestus*			264	35.54	125	42.56	114	34.42	35.14	74.22	99.52
MNHN	Unnumbered	*Aepyornis*	*hildebrandti*			328	55.1	200	66.08	149	47.28	48.04	107.24	134.72

`

Museum	Specimen number	Genus assignment	Species assignment	Original type series	Collection locality	F1	F2	F3	F4	F5	F6	F7	F8	F9
NHMW	2014/0238/039	*Aepyornis*	*hildebrandti*			329	57.18	204	65.38	177	53.52	53.82	115.28	126.48
NHMW	2014/0238/041	*Aepyornis*	*hildebrandti*			347	57.5	198	64.68	174	55.34	52.72	130.24	130.88
NHMW	2014/0238/042	*Aepyornis*	*hildebrandti*			326	48.4	188	63.58	166	51.86	52.38		126.68
NHMW	2014/0238/045	*Aepyornis*	*hildebrandti*			310	48.88	183	62.68	147	45.88	46.64	101.6	117.68
NHM	A2142	*Vorombe*	*titan*			440	70.96	275	95.12	212	66.3	74.24		187
NHM	ii.26.1254	*Aepyornis*	*hildebrandti*			316	45.88	173	55.98	154	48.42	47.54	109	122.82
NHM	Unnumbered	*Aepyornis*	*hildebrandti*			307	49.58	174	56.2	150	49.94	48.12	140.8	87.3
NHM	A696	*Aepyornis*	*hildebrandti*			337	57.54	203	67.5	167	53.76	53.14	118.08	131
NHM	A2141	*Vorombe*	*titan*			437	65.64	253	89.4	239	79.22	79.88	181	191
NHM	A465	*Aepyornis*	*hildebrandti*				50.44	188	63.64	170	52.56	53.32		124.9
CVB	Unnumbered	*Vorombe*	*titan*			440	71.2		95.36	231	77.28	76.84	162	182
UA	07AEP02	*Mullerornis*	*modestus*		Beloha	262	37.56	131	44.14	113	31.26	34.76	78.84	98.74
UA	Unnumbered	*Aepyornis*	*maximus*			363	61.42	230	79.52	220	60.98	63.24	135.52	
UA	Unnumbered	*Mullerornis*	*modestus*		Antsirafaly-soalara		35.04	124	42	110	34.9	33.1	74.64	91.72
USNHM	3013	*Aepyornis*	*hildebrandti*			317	51.14	192	64	165	54.04	49.24	112.46	125.16
ZIUU	A49b	*Aepyornis*	*maximus*		Ampoza	354	62.36	223	73.5	185	58.88	60.02	122.66	151
ZIUU	A15	*Aepyornis*	*hildebrandti*		Masinandreina	308	57.42	204	66.24	156	50.66	50.12	112.08	131.92
ZIUU	A49f	*Aepyornis*	*hildebrandti*		Masinandreina	322	55.86	200	66.06	168	53	49.86	122.2	135.52
OUMNH	4950	*Vorombe*	*titan*		Antolanbiby	446	94.1	269	66.8	247	77.6	76.7	164	
NHM	A439	*Vorombe*	*titan*	*Aepyornis titan*	Itampulu ve		71	271	91.5	232	68.6	74		203
UIO	122.946	*Mullerornis*	*modestus*		Antsirabe		42.1	155	47.65	122	42.79	44.3	89.4	
NHMW	2014/0238/038	*Aepyornis*	*hildebrandti*		Antsirabe		57.74	199	65.6	163	52.78	50.22	115.04	
NHMW	2014/0238/040	*Aepyornis*	*hildebrandti*		Antsirabe		48.6	187	63.44		51.92	51.6		132.06
NHMW	2014/0238/044	*Aepyornis*	*hildebrandti*		Antsirabe		51	192	63.54	161	51.1	48.62		

`

Museum	Specimen number	Genus assignment	Species assignment	Original type series	Collection locality	F1	F2	F3	F4	F5	F6	F7	F8	F9
MfN	MB.AV.73	*Mullerornis*	*modestus*	*Aepyornis hildebrandti*	Antsirabe		43.24	158	52.7					
CVB	Unnumbered	*Vorombe*	*titan*		Ilaka		64.42		85.24					
CVB	Unnumbered	*Vorombe*	*titan*		Ilaka		71.08	259	87.52					
CVB	Unnumbered	*Aepyornis*	*maximus*		Ilaka									
USNM	214714	*Aepyornis*	*maximus*		Itampolo		69.46	243	81.12					160
ZIUU	20	*Aepyornis*	*hildebrandti*		Masinandreina		56.76	196	66.7	169	50	52.2		
ZIUU	A16	*Aepyornis*	*maximus*		Masinandreina		56.8	208	68.68	203	60.74	58.6		150
ZIUU	A17	*Aepyornis*	*maximus*		Masinandreina		60.42	219	73.7	181				
ZIUU	17	*Aepyornis*	*maximus*				56.96	210	71.01	190	61.02	56.84		
ZIUU	14	*Aepyornis*	*hildebrandti*		Masinandreina		56.28	202	67.24					
ZIUU	3	*Aepyornis*	*hildebrandti*		Masinandreina		57.66	210	69.86					
ZIUU	5	*Aepyornis*	*maximus*		Ampoza		58.92	214	73.92	185		61.9		117.3
ZIUU	A44	*Vorombe*	*titan*		Masinandreina		70.84	283	99.48					
ZIUU	A14	*Aepyornis*	*hildebrandti*		Masinandreina		53.6	198	65.66	163	51.14	50.74		142.2
ZIUU	A43	*Aepyornis*	*maximus*		Masinandreina	383	62.66	254	89.64	203	67.64	69.94		
MNHN	1910-12-61	*Aepyornis*	*maximus*	*Aepyornis medius*		368	51.26	218	76.82	192	59.18	61.98		167

A. FEMORAL MEASUREMENTS (continued)

Specimen number	F10	F11	F12	F13	F14	F15	F16	F17	F18	F19	F20
Unnumbered	79.4	88.55	233	278	232	260		117.3	132.29	30.9	15.81
122.872		99.93			323	267	135.89	127.42	135.21	28.8	17.4
1906-16-66	87.82	99.82			302	255	149.68	122.32	148.62	30.06	15.2
Unnumbered	92.68	105.26	291	304	326	258	148.32	117.82	146.36	30.26	15.7
1908-5	55.98	63.66	223		240		96.52	75.88	95.24	23.36	11.66
MAD 364	114.82	136.88	381	392	408	325	198	169	143	36.04	27.68
MAD 6648		62.6			253	208	91.4	74.08	89.9		11.3
MAD 441		70.56			241	207	98.38	82.8	94.76	27.76	10.5
MAD 373		85.06	299	309	322	282	129.8	112.84	127.6	20.5	14.88
MAD 374		89.24	245	250	303		128.34		139.54	28.04	12.72
MAD 369		139	386	424		350	199			32.2	24.8
MAD 6754	83.78	93.88	280	298	305	262	128.1	104.94	141.4	29.92	16.62
1906-16-71	89.56	100.6			306	262	134.26	109.16	135.6	29.92	16.02
1906-16-65	87.8	99.2	278	288	303	246	135.78	110.76	126.84	22.14	17.96
Unnumbered					297		136.68	124.2	137.56	25.3	18.36
JH 32	57.28	63.18	231	262	245	208	98.12			21.18	9.17
JH 58	85.92	95.86	282	314	303	268	151.56	147.6	125.94	29.3	16.42
JH 59	88.48	92.72			311	267	138.68	115.28	133.28	34.84	16.7
JH 61	50.94	63.48	221	228	231	196	87.18	77.34	86.54	18.92	9.48
MAD 378			313	333	342	287	147.88	130.42	143.64		
Unnumbered	126.04	140.34	394	421	419	348	177	158	192	39.26	22.64
Unnumbered	124.96	142.2	426	445	453	375	183		165	44	19.56
MAD 6773	57.56	67.04	233	265	245	207	98	80.02	94.14		11.74

`

Specimen number	F10	F11	F12	F13	F14	F15	F16	F17	F18	F19	F20
Unnumbered	95.16				312	268	138	134.9	108.14	33.56	18.94
2014/0238/039	98.3	99.58	309	320	315	269	126.42	104.98	141.24	25.36	14.3
2014/0238/041		103.14	298	327	324	274	129.02	114.86	146.9	27.28	16.36
2014/0238/042		87.46	281		304			113.32	138.92	20.86	18.92
2014/0238/045	118.42	82.68	274	287	289	244	121.36	95	129.46	24.38	18.4
A2142	79.86	118.9	382	421	399	327	187	158	167		26.76
ii.26.1254	95.72	89.74	263	274	283	244	130.86	101.4	129.1	26.7	17.2
Unnumbered	90.72	92.88	264	282	293	247	133.92	125.86	102.84	24.5	17.2
A696	128.7	98.88	287	306	306	250	148.96	89.66	144.2	33.6	17.6
A2141	80.22	132.9	381	417	402	340	201	156	200	41.3	24.86
A465					285	245	125.26	126	110	20.7	18.7
Unnumbered		148.96	374	403	401	328	202	171	210	40.76	20.14
07AEP02	96.86	56.64	227	234	244	206	90.18	77.42	93.1	23.3	10.7
Unnumbered	56.68	112.4	312	328	336	290	114	132.24	163	35.94	21.06
Unnumbered	87.34	64.64				203	89.46	81.6	96.12	22.84	8.4
3013	97.4	100.08	285	303	311	265			135.52	28.36	29.18
A49b	86.54	109.96	319	332	332	350	151	132.6	160	26.26	20.86
A15	92.02	96.9	282	284	306	244	131.33	125.78	144.46	29.02	19.56
A49f	136	91.54	284	301	292	252	132.36	112.36	145.22	28.8	13.66
4950		146.9	406	435	415	344	182	165	192	43.2	20
A439		141			414	346				32	24
122.946							109.2	103.9	110.67		
2014/0238/038							122.6	107.74	126.88		
2014/0238/040		95.4				264	131.24			24.38	18.54

`

Specimen number	F10	F11	F12	F13	F14	F15	F16	F17	F18	F19	F20
2014/0238/044							123.98	109.52	138.96		
MB.AV.73							100.4				11.2
Unnumbered											29.58
Unnumbered											
Unnumbered											21
214714		110.94								28.56	13.74
20											
A16		107.9								32.88	23.5
A17											21.26
17											21.9
14											
3											17.4
5										30.16	19.24
A44										33.1	18.46
A14	89.28	98.84			308	263				28.88	17.24
A43		118.02	329	358		299				34.38	21.28
1910-12-61					364	307	151		166	27.36	21.48

`

B. TIBIOTARSAL MEASUREMENTS

Museum	Specimen number	Genus assignment	Species assignment	Original type series	Collection locality	Tt1	Tt2	Tt3	Tt4	Tt5	Tt6	Tt7	Tt8
NHM	A673	*Vorombe*	*titan*			576	34.3	143	51.1	109.7	48.2	54.8	154
UIO	A31835	*Vorombe*	*titan*			557	50.49	136	33.2	96.96	86.37	72.53	164
UIO	122.867	*Mullerornis*	*modestus*			459	46.13	134	33.18	77.03	74.1	63.84	143.9
UIO	A31833	*Mullerornis*	*modestus*			511	49.28	128	31.83	84.79	81.83	64.68	139.27
UIO	A31836	*Vorombe*	*titan*			547	48.43	135	32.19	93.66	84.7	71.84	159
UIO	122.878/.879	*Vorombe*	*titan*				43.72	122	30.01	94.17	67.73	79.67	151.69
MNHN	Unnumbered	*Mullerornis*	*modestus*	*Mullerornis agilis*	West coast		34.5	98	24.8	72.24	61.06	52.64	117.46
MNHN	Unnumbered	*Mullerornis*	*modestus*		Belo sur mer	450	34.9	97	24.14	66.7	57.26	49.86	117.56
MNHN	MAD 6733	*Aepyornis*	sp.			609	56.52	153	33.8	110.72	90.72	25.7	158
MNHN	MAD 395	*Vorombe*	*titan*			652	55.28	164	41.12	132.21	109.2	89.36	207
MNHN	[1] 1937-62	*Vorombe*	*titan*			767	72.24	199	41.76	152	119.54	104.94	225
MNHN	[3] 1937-62	*Vorombe*	*titan*			656	55.46	161	37.96	142	103.46	86	192
MNHN	[4] 1937-62	*Vorombe*	*titan*			671	63	174	39.82	136.86	114.48	96.72	
MNHN	1906-16-80	*Aepyornis*	sp.		Antsirabe	554	50.66	137	31.6				158
MNHN	1906-16-77	*Aepyornis*	sp.			560	48.16	134	30.44	103.68	73.26	87.58	158
MNHN	1906-16	*Aepyornis*	sp.		Antsirabe	544	46.26	124	28.2	105.4	82.68	67	130.58
MNHN	1906-16-82	*Aepyornis*	sp.		Amtsirabe	572	49.2	136	32.2	106.24	89.2	74.6	
MNHN	1906-16 2	*Vorombe*	*titan*			565	55.6	149	31.04	113.76	82.6	76.2	
MNHN	MAD 674	*Aepyornis*	sp.		Antsirabe	571	50.58	139	32.12	102.78	86.7	72.7	154
MNHN	1908-5	*Vorombe*	*titan*			762	66.52	196	45.1	159	125	107.8	225
MNHN	Unnumbered	*Vorombe*	*titan*		Ambolisatra	642	55.76	159	38.16	129.96	99.64	83.06	185
MNHN	1906-16	*Aepyornis*	sp.		Antsirabe	557	49.34	134	31.24	104.7	89.6	75.2	162
MNHN	MAD 6655	*Mullerornis*	*modestus*		Belo sur mer	451	33.18	95	23.78	66.72	58.74	47.36	112.4
MNHN	MAD 6747	*Mullerornis*	*modestus*		Belo sur mer	441	33.56	94	23.6	64.82	54.76	49.08	119.78

`

Museum	Specimen number	Genus assignment	Species assignment	Original type series	Collection locality	Tt1	Tt2	Tt3	Tt4	Tt5	Tt6	Tt7	Tt8
MNHN	MAD 6734	*Aepyornis*	sp.			628	49.7	142	32.42	113.24	98.06	76.72	178
MNHN	MAD 394	*Vorombe*	*titan*		Ankazoabo	723	65.1	181	42.88	151.38	116.56	100.3	197
MNHN	MAD 393	*Vorombe*	*titan*	*Aepyornis ingens*		823	67.42	214	52.46			112.94	239
MNHN	MAD 459b	*Mullerornis*	*modestus*		Beloha	474	34.66	98	23.64	64.76	56.78	47.02	123.54
MNHN	MAD 6744	*Mullerornis*	*modestus*			450	32.3	93	23.4	67.16	55.38	50.08	114.14
MNHN	MAD 440a	*Mullerornis*	*modestus*		Beloha	470	33.96	99	24.7	66.86	58.88	53.86	117.96
MNHN	MAD 6653	*Mullerornis*	*modestus*	*Mullerornis rudis*	Belo sur mer	433	32.52	95	23.72	68.58	54.48	47.6	111.9
MNHN	MAD 6741	*Aepyornis*	sp.		Antsirabe	548	47.2	132	31.38	101.7	86.32	68.4	153
MNHN	MAD 6743	*Aepyornis*	sp.			546	53.36	146	29.02	104.44	93.38	71.52	153
MNHN	Unnumbered	*Aepyornis*	sp.		Antsirabe	573	46.82	133	30.8	104.54	83.74	72.74	158
MNHN	Unnumbered	*Vorombe*	*titan*			591	51.14	143	34.4	108.76	90.38	79.98	179
NHMW	2014/0238/023	*Vorombe*	*titan*		Antsirabe	580	48.5	135	60.56	99.24	87.02	72.48	160
NHMW	2014/0238/024	*Aepyornis*	sp.		Antsirabe	569	48.82	133	3.62	107.48	92.9	76.46	159
NHM	A237	*Aepyornis*	sp.			575	30	137	49.78				167
NHM	A2143	*Vorombe*	*titan*			720	45.3	184	65.6	155	104.02	120.06	219
NHM	Unnumbered	*Vorombe*	*titan*			562	31.82	136	49.8	104.3	74.28	93.92	155
NHM	A464	*Mullerornis*	*modestus*			533	43.4	120	28.6	95.64	67.3	82.76	140.24
NHM	A506	*Vorombe*	*titan*			589	31.14	140	51.44	110.56	73.46	93.48	146.68
NHM	A4183b	*Vorombe*	*titan*			649	41.56	163	56.16	132.4	82.86	100.8	176
NHM	A462	*Vorombe*	*titan*			598	37.64	156	54.22	114.16	83.46	101.48	160
NHM	A2144	*Vorombe*	*titan*			678	45.32	178	60.58	140.62		111.16	150
NHM	A438	*Vorombe*	*titan*			814	73.52	205	56.62	67	101.42	126.62	66
NHM	A673	*Aepyornis*	sp.			575	50.92	140	31.92	107.14	75.5	88.1	167
MFN	MB.AV.70	*Mullerornis*	*modestus*	*Aepyornis hildebrandti*	Antsirabe	473	39.32	110	26.76	90.1	59.34	72.7	128.8
CVB	Unnumbered	*Vorombe*	*titan*		Ilaka	614	60.48	165	39.76	129	84.64	100.38	184

`

Museum	Specimen number	Genus assignment	Species assignment	Original type series	Collection locality	Tt1	Tt2	Tt3	Tt4	Tt5	Tt6	Tt7	Tt8
UA	08AEP10	*Vorombe*	*titan*			549	33.64	144	50.56	112.98	88.36	81.28	166
UA	08AEP14	*Mullerornis*	*modestus*		Beloha	477	24.76	99	34.78	67.48	60.42	49.54	124.92
UA	08AEP15	*Mullerornis*	*modestus*		Antsirabe	483	26.54	103	36.54	70.66	56.22	51.8	113.34
UA	08AEP08	*Vorombe*	*titan*			609	36.58	164	58.94	134.4	95.85		183
UA	08AEP18	*Mullerornis*	*modestus*			463	36.36	102	26.4	67.52	51.06	54.74	113.62
UA	08AEP09	*Vorombe*	*titan*		Beloha	557	52.6	151	38.3	119.6	78.3	89.5	174
UA	08AEP11	*Vorombe*	*titan*			578	57	152	35.08	122.24	79.18	93.06	180
UA	08AEP06	*Vorombe*	*titan*			646	56.8	165	39.22	142.04	91	110.8	
UA	08AEP07	*Vorombe*	*titan*		Beloha	618	57.6	169	38.14	131.86	88.14	105.16	
UA	08AEP16	*Mullerornis*	*modestus*		Antsirabe	483	42.42	114	26.48	88.36	57.44	70.3	132.44
UA	Unnumbered	*Vorombe*	*titan*		Beloha	618	58.44	162	39.92	131.5		98.84	172
USNM	3016	*Vorombe*	*titan*			565	27.68	132	50.54	110..42	93.54	78.18	124
ZIUU	A12	*Aepyornis*	sp.		Masinandreina	571	50.7	136	29.3	111.2	75.12	88.84	117.04
ZIUU	A49C	*Aepyornis*	sp.		Masinandreina	581	48.62	130	28.36	106.62	74.1	88.32	136.1
ZIUU	40	*Aepyornis*	sp.		Masinandreina	523	49.8	129	26.56	101.14	70.08	84.74	149.7
ZIUU	19	*Aepyornis*	sp.		Masinandreina	570	50.36	135	30.1	102.54	75	91.34	163
ZIUU	A13	*Aepyornis*	sp.		Masinandreina	564	48.68	133	30.02	104.66	75.96	93.78	155
ZIUU	12	*Aepyornis*	sp.		Masinandreina	578	53	139	31.08	107.04	75.18	88.76	156
ZIUU	14	*Vorombe*	*titan*		Masinandreina	578	50.7	133	27.68	98.2	76.68		154
ZIUU	A32	*Aepyornis*	sp.		Masinandreina	577	50.36	134	30.14	108.76	90.14	77.4	164
ZIUU	A31	*Aepyornis*	sp.		Masinandreina	553	52.36	138	30.74	108.18	87.64	74.18	172
OUMNH	4952	*Mullerornis*	*modestus*		Antolanbiby	478	25.4	99	34.9	72.9	59.5	53.5	128.2
OUMNH	4951	*Vorombe*	*titan*		Antolanbiby	724	40.2	181	64.9	148.1	112.4	98.6	215
NHM	A676	*Mullerornis*	*modestus*			435	20.5	85	28.2	61	45.5	51	91
MNHN	2	*Mullerornis*	*modestus*		Ambolisatra		32	94	25.14	69.4	54.72	47.52	103.24

`

Museum	Specimen number	Genus assignment	Species assignment	Original type series	Collection locality	Tt1	Tt2	Tt3	Tt4	Tt5	Tt6	Tt7	Tt8
MNHN	JH 9	*Aepyornis*	sp.		Antsirabe								153.48
MNHN	JH10	*Aepyornis*	sp.		Antsirabe								156.2
MNHN	JH 19	*Aepyornis*	sp.		Antsirabe								155.96
MNHN	1906-16	*Aepyornis*	sp.		Antsirabe								157.5
MNHN	85	*Aepyornis*	sp.		Antsirabe								152.7
MNHN	JH 37	*Aepyornis*	sp.		Antsirabe								157.4
MNHN	MAD 392	*Vorombe*	*titan*		Ankazoabo		71.5	199	47.62	150.68	117.9	104.72	
MNHN	MAD 396	*Vorombe*	*titan*		Ankazoabo		75.3	208	43.06				
MNHN	MAD 6656	*Mullerornis*	*modestus*		Belo sur mer	451	31.06	89	22.8	67.12	54.54	46.38	114.84
MNHN	MAD 6654	*Mullerornis*	*modestus*		Belo sur mer		32.62	88	22.06	65.6	52.36	47.8	
MNHN	1906-16, 70	*Vorombe*	*titan*		Belo sur mer		58.92	171	47.94				192
NHMW	2014/0238/007	*Aepyornis*	sp.		Antsirabe		47.94	129	22.08	106.04	84.68	71.24	
NHMW	2014/0238/010	*Aepyornis*	sp.		Antsirabe	478	39.54	122	27.56				
NHMW	2014/0238/011	*Vorombe*	*titan*		Antsirabe	538	45.88	132	31.08	99.7		71.6	
NHMW	2014/0238/014	*Aepyornis*	sp.		Antsirabe		49.48	141	32.16				
NHMW	2014/0238/018	*Aepyornis*	sp.		Antsirabe								169
NHMW	2014/0238/020	*Aepyornis*	sp.		Antsirabe		51.58	141	31.08				146.86
MFN	MB.AV.71	*Mullerornis*	*modestus*		Antsirabe					89.22	61.42	72.22	
CVB	Unnumbered	*Mullerornis*	*modestus*		Ilaka		33.58	101	24.62	61.7	45.98	52.9	
UA	08AEP13	*Vorombe*	*titan*		Antsirabe	495	26.9	110	40		76.1		114.78
UA	Unnumbered	*Mullerornis*	*modestus*		Beloha	468	35.1	101	24.1	71.14	53.42	56.7	120.2

`

Specimen number	Tt9	Tt10	Tt11	Tt12	Tt13	Tt14	Tt16	Tt17	Tt18	Tt19	Tt20	Tt21
A673	90.9	113	39.6	89.7	81.1	104.2	64.5	36.3	30.4	45.4	87.2	320
A31835	90.8	103.39	37.59	34.16	75.62	89.09	64.08	39.9	28.2	67.27	91.57	157
122.867	67.38	96.89	48.81	41.76	83.38	93.04	45.37	36.92	23.44	68.18	100.83	122.63
A31833	85.1		58.58	63.88	75.37	78.72			18.22	47.47	92.95	153
A31836	73.9	89.32	41.49	56.47	71.53	98	61.38	32.2	26.45	56.69	87.34	175
122.878/.879	83.01	90.58		71.81	75.69	90.29	35.36	56.05	22.88	38.81	83.92	161
Unnumbered	74.86			48.28	51.9	64.08	46.06	25.62	16.38	41.56		107.7
Unnumbered	74.2		50.62	40.86	64.92	62.72	44.54	31.1	14.5	30.04	70.76	108.08
MAD 6733	110.54		52.2	62.56	78.54	88.2	63.44	37.18	26.28	44.9		180
MAD 395	115		58.5	71.06	99.58	102.98	76.54	50.04	27.96	68.24	111.88	216
[1] 1937-62	114.56		61.36	95	108.5	121.48	90.14	58.44	29.56	57.4	115.3	257
[3] 1937-62	120.38		54.7	89.1	92.52	106.24	75.06	42.56	36.54	63.7	100.98	228
[4] 1937-62	119.88		67.66	77.86	100.44	112.86	82.88	51.6	30.98	78.02		230
1906-16-80	98.78		53.34	54.06	78.36	88.74	65.16	40.48	27.14	50.4	86.7	171
1906-16-77	94.94	113.8	49.38	66.8	77.1	86.4	63.04	39.76	25.2	44.8	77.38	163
1906-16	69.22	93.4	45.96	55.1			56.2	33.5	19.3	39.02	70.07	148.6
1906-16-82	77.22	100.54	31.14	65.1	69.82	78.46		28.9	22.5			151
1906-16 2	86.3	152	53.92	76.9	82.1	91.7	65.06	37.84	28.68			164
MAD 674	99.86		41.3	60.96	81.2	90.1	62.92	40.88	30.62		84.32	171
1908-5	131.96		80.16	93.5	117.64	138.64	85.84	58.7	36.8	67.4	126.54	25
Unnumbered	121.04		55.18	90.96	91.86	96.84	73.9	42.52	26.06	52.38	94.58	220
1906-16	90		38.1	59.44	77.06	85.4	63.46	42.52	25.96	42.84	76.16	148.58
MAD 6655	76.14		44.28	39.96	59.12	62.24	46.2	26.3	17.22	28.84	67.02	100.7
MAD 6747	72.3		46.72	47.08	61.2	67.08	39.62	27.44	16.76	35	76.7	93.46
MAD 6734	95.64		41.42	71.48	82.22	90.96	65.28	44.24	28.36	45.92	91.46	146.4

`

Specimen number	Tt9	Tt10	Tt11	Tt12	Tt13	Tt14	Tt16	Tt17	Tt18	Tt19	Tt20	Tt21
MAD 394	120.74		50.44	95.74	100.62	112.98	83.78	43.38	34.42	73.08	101.4	240
MAD 393	148		71.86	101.34	123.26	139	92.36	54.32	37.36	93.82	127.5	282
MAD 459b	63		42.62	42.26	55.86	63.62	43.64	29.52	17.92	35.78	82.04	97.88
MAD 6744	75.06		48.62	53.42	66.28	70.3	42.46	29.34	16.9	42.72	70.24	102.2
MAD 440a	76.62		52.7	43.5	70.9	74.76	49.1	30.76	17.4	41.1	80.76	105.5
MAD 6653			47.5	35.28			40.46	27.68	18.02	43.02	69.4	106.12
MAD 6741	95.88		40.78		71.76	83.5	58.28	31.96	25.7		74.62	146.16
MAD 6743	95.04		41.1	78.5	75.2	85.4			22.3		84.08	150
Unnumbered	91.86			54.1	75.54	83.88	60.84	42.36	27.2	38.54	80.84	148.9
Unnumbered	109.9		61.58	61.46	88.36	91.36	68.24	42.32	27.86	45.6	88048	183
2014/0238/023	100.32		39.42	83.1	75.28	88.6	60.98	42.06	56.78	40.94	79.94	155
2014/0238/024	98.56		51.48	85.94	76.66	89.4	62.7	40.42	25.92	41.5	79.86	151.5
A237	106.74	116.78	43.76	65.46	79.26	86.32	53.28	39.64	29.2	47.72	84.08	155
A2143	149.36	153	65.7			114.78	87.82	56.52	34.62	59.54	105.72	254
Unnumbered	109.68	139.38	50.7	62.8	278.84	88.7	57.98	42.34	26.08	55.62	82.88	155
A464	57.8	88.44	40.62	69.56	74.1	81.44	57.06	35.06	23.72	43.5	70.64	153
A506	109.74	153	53.08	71.26	83.02	88.84	70.6	47.28	27.7	47.62	84	153
A4183b	120.3	191	55.4	98.64	93.52	99.54	75.78	45.68	27.54	52.92	96.76	216
A462	116.5	186	62.34		80.34		63.78	41.92	32.56	42.38	89.82	149.96
A2144	144.5	191	53.04	95.62	99.5	112.94	92.36	51.22	32.4		101.12	243
A438	129.12	230	86.42	69.3	114.96	148.88	79.2	50.96	37.56	77.36	148.68	
A673	90.2	97.6	41.18	88.84	77.58	87.28	65.28	39.72	30.9	60.16	96.3	159
MB.AV.70	85.54	93.92	30.4	65.6	59.16	70.88	53.48	28.02	18.62	43.32	71.6	153
Unnumbered	96.46	196	55.6	111.86	90.2	105.42	78.94	45.2	30.9	49.74	105	225
08AEP10	86.92	148.8	38.86		75.56	79	60.18	40.4	28.64	51.12	89.3	85
08AEP14	64.52	101.86	62.18	41.18	60.33	69.38	46.9	26.6	18.88	34.36	84.92	98.1

`

Specimen number	Tt9	Tt10	Tt11	Tt12	Tt13	Tt14	Tt16	Tt17	Tt18	Tt19	Tt20	Tt21
08AEP15	59.92	99.46	51.82	58.96	65.54	72.44	40.54	28.36	17.34	40.38	72.02	99.86
08AEP08	93.3		44.92	84.36	98.34	103.14	72.26	52.56	33.96	57.92	91.9	222
08AEP18	60.42	102.8	47.84	46.34	62.72	102.24	39.4	28.34	42.72	16.68	34.98	69.4
08AEP09	90.06	161	49.3	88.2	93.96	105.48	67.94	48.02	31.5	60.22	93.06	186
08AEP11	83.58	166	50.7	78.7	84.08	91.78	65.02	38.98	24.56	56.1	88.48	171
08AEP06	104.96	138.3		90.82	103.86	107.2	87.94	50.8	28.58			200
08AEP07	105.78		54.48	88	98.6	102.18	79.28	45.7	31.62	62.36	100.88	194
08AEP16	66.46	116.92	36.06	54.38	68.82	74.48	58.42	34.66	22.24	38.48	61.38	146.36
Unnumbered	130.26	119	43.3	77.16	99.96	108.52	84.24	50.52	34.96	53.94	102.1	209
3016	97.88	169	42.4	74.06	74.96		63.26	40.4	28.66	41.16	86.14	144
A12	94.86	153	38.98		76.48		64.68	41.8	28.34	47.26	85.9	163
A49C	75.36	109.1	46.86		72.46		58.7	32.08	25.46	44.6	79.86	161
40	83.84	82.74	34.7		74.3		59.94	40.72	29.56	41.34	74.74	139
19	82.78	97.06	52.58		80.72		62.36	41.48	26.56	46.4	83.52	142
A13	85.58	99.78	46.88		82.34		62.92	41.08	29.4	45.22	87.12	144.58
12	86.09	101.92	40.16		78.2		61.34	43.8	26.12	45	83.38	140.2
14	84.32	105.64	46.34		82.86		62.78	41.34	25.14	47.7	86.94	172
A32	91.22	105.56	57.12		82.36		64.16	39.36	33.36	59.94	89.36	150
A31	92.1	107.32	59.52		82.2		66.3	43.56	29.24		88.22	149
4952	84	84.9	52.6	45.2	70.5	75	48.7	31.9	19.2	36.8	83.5	102.1
4951	109.5	149.1	58.7	104.7	102.6		73.6	73.3	30.5	65.2		255
A676	57	65	48	40.8	57.2	59.8	34	28	15.2	25	63	96
2												115.94
JH 9			47.14	81.24	75.68	84.86	58.04	36.94	22.38	43.34	77.28	
JH10	89.84		46.4	51.54	77.84	84	36	58.82			82.08	
JH 19	96.12		44.54	46.9	77.06	82.4	56.88	34.34	27.24	42.4	75.9	

`

Specimen number	Tt9	Tt10	Tt11	Tt12	Tt13	Tt14	Tt16	Tt17	Tt18	Tt19	Tt20	Tt21
1906-16	100.6		43.44	57.42	72.26	89.92	58	39.78	25.2	52.1	78.26	
85	100.8		45.04	83.8	82.74	88.2	58.72	36.34	26.4	40.2	81.68	
JH 37	92.4		52.48	35.32	68.3	70.7	54.24	28.78	23.84	46.96	80.64	
MAD 392					111.06		84.56	51.92				245
MAD 396												
MAD 6656	72			44.24	60.92	66.8	44.38	28.44				89.72
MAD 6654												
1906-16, 70	118.72				93.28		80.36	41.3	32.4			211
2014/0238/007												
2014/0238/010												132.06
2014/0238/011							45.76	63.56				150.18
2014/0238/014												159
2014/0238/018	109.84		38.48	88.92	80.9	94.48	62.96	42.62	26.66	54.44	85.5	
2014/0238/020			49.52		76		62.66	37.52	26.68	51.1	83.24	140.4
MB.AV.71												
Unnumbered												
08AEP13												
Unnumbered	61.32	102.1	50.5	38.6			45.3					98.58

`

C. TARSOMETATARSAL MEASUREMENTS

Museum	Specimen number	Genus assignment	Species assignment	Original type series	Collection locality	Tmt1	Tmt2	Tmt3	Tmt4	Tmt5	Tmt6	Tmt7	Tmt8	Tmt9	Tmt10
NHM	A2148	*Aepyornis*	*maximus*			385	28.8	69.2	54.2	140.2	48.8	54.7	87.8	150.5	108.3
UIO	122.861	*Aepyornis*	*hildebrandti*			308	25.35	56.52	46.28	109.92	43.5	45.42	60.06	113.98	85.95
MNHN	1906-16-65	*Aepyornis*	*maximus*	*Aepyornis medius*		372	31.84	64.78	48.34	125.18	58.6	49.74	79.8	140.3	
MNHN	Unnumbered	*Mullerornis*	*modestus*		Belo sur mer	324	18.2	29.6	33.62	72.26	29.16	29.7	42.84	75.88	61.38
MNHN	Unnumbered	*Mullerornis*	*modestus*		Belo sur mer	323	16.86	28.5	34.4	79.24	36.34	27.54	38.6	77.64	67.26
MNHN	Unnumbered	*Aepyornis*	*hildebrandti*			344	23.88	56.62	49.94	114.26	49.56	36.94	65.24	119.36	90.62
MNHN	Unnumbered	*Aepyornis*	*hildebrandti*			325	26.1	57.24	45.24	111.6	49.42	37.88	58.66	113.2	87.04
MNHN	1908-5, 51	*Vorombe*	*titan*			426	33.8	78.72	62.46	164	64.96	67.98	95.32	173	140.2
MNHN	MAD 6771	*Mullerornis*	*modestus*		Ankazoabo	322	15.92	27.82	31.84	74.36	37.42	25.12	32.36	65.82	65.98
MNHN	MAD 6660	*Mullerornis*	*modestus*			315	19.6	28.28	37.58	75.8	28.22	30.4	38.26	81.46	64.36
MNHN	MAD 6662	*Mullerornis*	*modestus*			303	17.62	30.62	31.3	75.66	33.12	25.74	39.54	69.48	65.94
MNHN	MAD 6658	*Mullerornis*	*modestus*	*Mullerornis rudis*	Belo sur mer	297	18.14	30.52	32.42	70.5	30.54	29.48	43.1	72.06	60.58
MNHN	MAD 387	*Aepyornis*	*maximus*			364	27.04	66.62	49.54	129.98	46.7	54.02	77.58	143.38	109.2
MNHN	MAD 385	*Aepyornis*	*maximus*	*Aepyornis cursor*	Belo sur mer	379	28.74	63.3	52.84	127.7	46.44	48.76	72.96		118.74
MNHN	MAD 6736	*Aepyornis*	*hildebrandti*			346	29.42	61.18	50.92	116.56	54.44	37.28	69.7	123.08	101.26
MNHN	1908-21	*Vorombe*	*titan*			486	35.8	87.16	62.68	177	62.88	52.92	91.22	182	153
MNHN	Unnumbered	*Aepyornis*	*hildebrandti*			312	25.24	65.04	46.02	115.94	45.88	40.9	45.94	120.8	88
MNHN	Unnumbered	*Aepyornis*	*hildebrandti*		Antsirabe	311	23.6	53.78	45.54	113.96	47.44	37.48	56.28	109.72	101.48
MNHN	1908-5	*Vorombe*	*titan*			419	31.96	76.9	59.86	167	61.56	58.92	74.68	179	139.44
MNHN	MAD 382	*Vorombe*	*titan*	*Aepyornis ingens*		466	36.98	81.76	62.14	178	67.84			173	144
MNHN	MAD 400c	*Mullerornis*	*modestus*		Beloha	307	16.56	32	33.88	73.66	27.92	28.08	44.3	72.02	59.92
MNHN	MAD 459d	*Mullerornis*	*modestus*		Beloha	308	17.7	30.82	32.5	72.7	35.3	29.64	44.68	71.68	61.26
MNHN	Unnumbered	*Aepyornis*	*hildebrandti*			314	25.1	61.36		116		55	36.94	47.8	91.02
NHMW	2014/0238/0025	*Aepyornis*	*hildebrandti*		Antsirabe	301	27.14	59.42	47.84	118.48	59.2	33.86	62.56	113.14	93.88

`

Museum	Specimen number	Genus assignment	Species assignment	Original type series	Collection locality	Tmt1	Tmt2	Tmt3	Tmt4	Tmt5	Tmt6	Tmt7	Tmt8	Tmt9	Tmt10
NHMW	2014/0238/0026	*Aepyornis*	*hildebrandti*		Antsirabe	288	24.54	50.5	45.06	105.68	50.86	35.9	52.48	105.68	81.08
NHMW	2014/0238/0027	*Aepyornis*	*hildebrandti*		Antsirabe	329	27.14	52.22	46.9	109.82	47.08	35.04	64.4	109.82	85.28
NHMW	2014/0238/0029	*Aepyornis*	*hildebrandti*		Antsirabe	291	23.46	50.48	41.44	106.3	40.12	31.64	58.14	105.38	78.14
NHMW	2014/0238/0030	*Aepyornis*	*hildebrandti*		Antsirabe	298	25.32	51.54	46	107.5	44.28	34.52	56.3	109.92	86
NHMW	2014/0238/0031	*Aepyornis*	*hildebrandti*		Antsirabe	309	27.7	52.78	45.2	107.66		39.2	57.54	111.48	85.76
NHM	A673	*Aepyornis*	*hildebrandti*			329	27.4	58.02	48.38	111.16	34.1	69.34	65.9	112.4	88.92
MNHN	Unnumbered	*Aepyornis*	*hildebrandti*			305	25.44	53.7	45.1	108.62	50	63.58	36.8	109.2	88.08
MNHN	Unnumbered	*Aepyornis*	*hildebrandti*			302	23.1	51.72	45.14	106.52	47	55.84	32.04	110.24	82.94
MFN	MB.AV.67	*Aepyornis*	*hildebrandti*			266	21.04	42.98	41.42	96.02			51.88	97.12	68.86
USNM	A605209	*Aepyornis*	*maximus*		Ilaka	352	34.66	68.18	54.54	134.9	56.24	46.42	71.8	148.66	115.1
UA	07AEP03	*Vorombe*	*titan*		Beloha	454	39	81.6	62.26	167	66.1	55.62	91.54	184	131.12
UA	08AEP01	*Aepyornis*	*hildebrandti*		Antsirabe	270	23.48	44.48	40.2	98.56	42.5	28.74	38.12	99.7	85.02
UA	07AEP06	*Mullerornis*	*modestus*		Beloha	314	20.3	32.24	34.44	74.74	39.5	24.06	30.78	76.16	65.14
UA	07AEP11	*Aepyornis*	*hildebrandti*		Antsirabe	269	22.34	44.4	39.24	94.9	46.1	28.84	35.52	99.14	77.36
UA	07AEP08	*Mullerornis*	*modestus*		Beloha	312	19.62	29.7	34.16	71.26	31.04	25.54	26.34	72.1	62.32
ZIUU	A34	*Aepyornis*	*hildebrandti*		Antsirabe	344	27.9	62.98	49.48	126.4	52.12	39.98	33.34	123.2	109.08
ZIUU	A39	*Aepyornis*	*hildebrandti*		Masinandreina	329	27	58.68	45.7	120.3	61.1	32.9	37.56	120.66	
ZIUU	A38	*Aepyornis*	*hildebrandti*		Masinandreina	327	26.58	60.88	49.42	123.74	56.58	34.78	37.54	125.04	101.16
ZIUU	A40	*Aepyornis*	*hildebrandti*		Masinandreina	325	26.88	55.36	44.58	117.26	59.86	34.48	34.96	114.48	110.6
ZIUU	A33a	*Aepyornis*	*hildebrandti*		Masinandreina	305	26.76	55.34	39.212	113.98	43.64	37.68	24.54	112.46	95.26
NHM	A676	*Mullerornis*	*modestus*			271	15	27	27.2	65	28	24		65.8	54
MNHN	MAD 6770	*Aepyornis*	*maximus*		Ankazoabo		28.06	73.3			45.6				
MNHN	MAD 383	*Aepyornis*	*maximus*		Belo sur mer		43.6	81.1	63		58.14				
MNHN	MAD 6659	*Mullerornis*	*modestus*		Ambolisatra	314	18.08	30.28	33.28	75.14	27.86				62.06
MNHN	MAD 384	*Aepyornis*	*hildebrandti*		Antsirabe	295	23.5	50.84	42.18		43.1	38.14	59.32	107.74	

`

Museum	Specimen number	Genus assignment	Species assignment	Original type series	Collection locality	Tmt1	Tmt2	Tmt3	Tmt4	Tmt5	Tmt6	Tmt7	Tmt8	Tmt9	Tmt10
MNHN	MAD 388	*Aepyornis*	*maximus*	*Aepyornis lentus*	Belo sur mer	363	28.96	67.32	45.82		48.5	44.96	56.32		
MNHN	MAD 8813	*Aepyornis*	*maximus*		Belo sur mer	536	32.58	88.06			52.58		85.8	165	
NHMW	2014/0238/0028	*Aepyornis*	*hildebrandti*		Antsirabe	309	23.04	50.6			52.6				
NHMW	2014/0238/0032	*Aepyornis*	sp.		Antsirabe	318	24.88	52.34	39.2		51.38				
NHMW	2014/0238/0033	*Aepyornis*	*maximus*		Antsirabe						55.52	40.8	38.68	125.8	
NHMW	2014/0238/0034	*Aepyornis*	*hildebrandti*		Antsirabe		23.6	52.72	49.1	118.2	46.4				95.98
NHMW	2014/0238/0035	*Aepyornis*	*hildebrandti*		Antsirabe	323	25.44	59.96	43.32	113.2	44.56				92.92
NHMW	2014/0238/0036	*Aepyornis*	*hildebrandti*									36.7	50.86	122.42	
UA	07AEP04	*Aepyornis*	*maximus*		Beloha	423	37.64	82.6	52.8	149.06	58.16	55.7	64.8	168	
UA	08AEP13	*Aepyornis*	*maximus*		Ambararata-Mahabo		43.74	85.78	62.8	167	59.92	53			150
UA	07AEP12	*Aepyornis*	*maximus*		Antsirabe		30.26	65.1			50.2			127.38	
UA	07AEP07	*Mullerornis*	*modestus*		Belo sur mer	306	19.5	31.98			32.18	30.16	27.66	79.24	66.48
UA	07AEP05	*Aepyornis*	*maximus*		Beloha	361	29.02	68.38	51.92	132.8	50.2		50.04		
UA	Unnumbered	*Aepyornis*	*maximus*		Beloha	359	30.7	69.8							
USNM	214709	*Mullerornis*	*modestus*		Itampolo	287	16.88	27.68	31.12	70.8	31.04	27.16	34.08		62.2
USNM	214713	*Aepyornis*	*maximus*		Itampolo	274	35.14	73.58	51.6	149.68	68.8	50.48	87.22		136
ZIUU	"13"	*Aepyornis*	*hildebrandti*		Masinandreina		25.54	56			46.98				
ZIUU	A36	*Aepyornis*	*hildebrandti*		Masinandreina		28.4	59.6	42.52	122.52					
ZIUU	"17"	*Aepyornis*	*hildebrandti*		Masinandreina		28.4	54.36		110.08	51.04				91.36
ZIUU	A47	*Aepyornis*	*maximus*		Ampoza	400	35.12	79.9	60.76						

`

Specimen number	Tmt11	Tmt12	Tmt13	Tmt14	Tmt15	Tmt16	Tmt17	Tmt18	Tmt19	Tmt20	Tmt21	Tmt22	Tmt23	Tmt24	Tmt25	Tmt26	Tmt27
A2148	140.1	35.9	54.2	55.5	50.7		65	59.56	65.2	56.24	50.6	53.5	70.6	61.7	54.6	65.1	67.5
122.861	109.68	25.4	46.89	38.4	35.38	47.06	48.02	42.44	46.33	43.51	35.49	36.42	52.32	47.04	46.08	50.18	55.6
1906-16-65	120.48	33	44.64	44.82		49.76	64.18	58.76	63.4	50.32	47.18	48	55.6	52.94	47.52	55.8	65.1
Unnumbered	70.66	23.64	29.5	26.78	22.9	26.82	33.92	30.2	34.06	28.4	24.2	25.7	34.62	31.3	31.8	46.82	42.92
Unnumbered	74.46	24.6	28.42	27.44	24.82	26.24	36.64	33.3	37.7	29.34	25.24	27.2	33.68	34.3	29.54	43.92	42.86
Unnumbered	108.3	29.9	41.4	44.32	39.28	47.26		47.08	53.72	46.74	40.26	41.68	55.62	48.22	50.34	52.78	62.1
Unnumbered	107.84	31.1	43.94	40.08	35.88	38.98	48.64	44.18	46.78	41.28	37.54	40.44	47.84	47.6	51.34	59.5	51.8
1908-5, 51	161	33.92	54.8	59.08	57.94	64.8	75.64	68.82	76.4	65.86	55.44	62.5	71.7	70.4	61.28	74.6	80.06
MAD 6771	74	23.36	26.4		19.7	21.9	32.46	28.36	31.92	25.7					28.92	43.22	42.08
MAD 6660	74.62	25.14	31.1	21.28	22.38	27.76	37.02	34.2	37.2	30.1	25.08	25.28	31.98	32.8	33.42	47.5	42.64
MAD 6662	75.26	22.62	27.82	22.04	20.12	21.32	31.74	28.04	33.7	26.78	24.84	26.36	29.54	30.94	28.4	36.28	39.32
MAD 6658	68.02	22.56	28.46	25.88	24.26	26.94	33.06	29.7	33.66	27.7	23.62	25.42	34.5	32.16	28.74	44.04	41.88
MAD 387	123	32.54	46.48	52.16	45.8	52.82	60.96	50.74	62.18	53.1	46.6	51.12	65.5	60.98	48.16	60.7	64.62
MAD 385	122	36.82	47.88	48.5	46.44	51.68	66.12	59.9	68.02	53.06	45.38	48.32	59.36	55.34	58.1	63.96	71.3
MAD 6736	109.36	30.86	44.02	40.12	36.52	42.18	51.92	45.64	49.34	43.02	36.58	39.06	53.66	51.38	53.4	61.5	59.68
1908-21	163	48.9	61.7										76.7	73.52	65.28	80.4	96.16
Unnumbered	108.62	25.26	46.52	45.76	38.76	44.98	51.92	43.56	50	45.4	38.64	41.36	56.3	53.18	42.46	50.7	55.62
Unnumbered	114.08	28.22	44.88	38.82	35.04	41.2	49.88	43.88	51.38	40.22	38.24	38.36	47.6	43.9	47.24	54.36	54.28
1908-5	172	35.34	60.68	59.82	54.9	57.34	77.72	69.32	77.24	65.88	58.44	63.8	62	65.32	59.18	68.64	82.44
MAD 382	173	41.08	60.96	70.86	65.36	65.1	83.12	76.84	85	63.7	59.4	55.24	81.4	67.18	61.48	85.52	85.7
MAD 400c	73.88	23.22	29.44	24.68	23.44	27.86	33.88	28.78	32.06	25.44	22.94	25.72	33.72	29.1	29.24	35.94	39.94
MAD 459d	69.76	21.06	27.28	22.2	21.12	23.36	32.16	31.52	34.84	28.16	25.56	26.42	28.16	31.42	27.1	40.86	68.76
Unnumbered	109.04			42.76	39.14	45.5	51.54			45.18	36.48	42.7	55.56	52.76	45.2	50.72	57.62
2014/0238/0025	109.08	28.9	45.16	40.26	38.36	43.86	54.24	45.98	52.98	52.6	45.82	39.72	54.12	52.48	48.16	52.18	58.02
2014/0238/0026	99.78	25.8	40.32	39.2	34.54	38.8	46.32	41.34	45.6	39.1	33.84	38.86	51.5	47.48	42	44.44	50.58

`

Specimen number	Tmt11	Tmt12	Tmt13	Tmt14	Tmt15	Tmt16	Tmt17	Tmt18	Tmt19	Tmt20	Tmt21	Tmt22	Tmt23	Tmt24	Tmt25	Tmt26	Tmt27
2014/0238/0027	104.56	21.88	38.6	43.38	37.4	41.9	52.54	45.9	51.34	39.88	35.06	40.4	52.2	49.12	46.34	52.64	54.3
2014/0238/0029	102.08	25.54	35.64	40.88	35.08	39.18	44.26	38.18	46.08	38.94	32.48	35.74	50.4	44.36	40.18	46.06	52.16
2014/0238/0030	101.16	26.3	38.64	40.28	35.68	38.9				43.1	35.68	38.26	47.48	47.4	46.32	48.86	55.52
2014/0238/0031	102.82	24.84	39.64	39.32	34.22	38.68	50.18	45.36	49.66	39.42	33.38	38.84	53.12	47.68	47.08	53.32	58.48
A673	105.46	30.72	48.5	42.18	36.62	44.4	52.62	45.76	51.82	43.86	32.96	35.88	55.44	49.2	48	53.96	57.44
Unnumbered	108	26.14	39.4	40.36	36.94	44.32	50.34	42.98	50.96	42.84	36.6	40.4	49.76	53.04	43.88	51.2	58.74
Unnumbered	104.38	28.62	36.68	40.46	36.68	41.72	50.12	45.48	51.28	40.54	35.1	40	48.04	53.62	35	42.26	55.54
MB.AV.67	96.86		40.7	32.76	31.82	36.02	44.94	40.48	45.6	36.18	31.02	33.8	42.34	40.24	37.44	42.84	45.7
TBC	134.26	33.06	51.22	49.66	43.66	53.92	65.36	62.1	67.04	53.22	48.9	48.18	64.44	54.26	53.5	60.62	71.2
07AEP03	164	39.68	60.58	81.62	73.68	66.68	64.08	70.34	88.12	80.42	89.82	70.04	61.46	65.24	63.34	76.8	87.58
08AEP01	98.44	23.38	38.96		32.56	37	41.46	36.42	41.58	36.7	31.66	35.6		44.38	41.3		46.6
07AEP06	73.9	25.88	30.22	24.86	22.32	24.86	37.22	32.46	38.22	30.96	25.84	29.9	32.2	36.3	29.2		42.1
07AEP11	89.2	25	38.5	34.96			41.9	36.8	41.64	37.68	31.74	35.74	46.72	43.98	39.08	43.16	44.6
07AEP08	68.26	21.74	34.22	24.62	27.56		35.06	32.24	36.44	27.44	23.06	24.42		30.16	32.6		42.82
A34	118.01	33.3	49.14	43.78	41.14	48.6	56.56	50.46	55.02	47.38	41.8		60.16		49.24	57.06	66.34
A39	118.16	30.2	50.26	47.5	42.42	47.96	58.94	50.3	52.76	46.5	39.18	44.58	61.34	56.74	55.74	60.24	66.36
A38	123.44	30.92	47.4	45.76	41.56	44.5	54.08	46.06	53.56	45.72	39.46	43.76	58.48	52.64	50.48	57	61.98
A40	114.06	29.78	45.81	43.02	37.66	45.01	52.4	45.58	51.06	44.74	36.2	39.08	54.26	50.38	56.16	49.4	61.18
A33a	110.82	28.16	41.38	40.38	36.96	42.14	47.68	42.8	48.54	39.02	36.54	38.88	49.1	51.24	43.96	48.52	53.32
A676	64	17.6	27	23	20	24	30	29	26.2	29.5	22	19	20	23	24.6	35	34
MAD 6770																	
MAD 383							71.7	72.8	69.9						69.96	83.6	64
MAD 6659	73.2	26.7	27.34					32.18	34.5				25.22		27.02	38.6	39.1
MAD 384		30.14	37.26				47.2	40.88	47	41.46	34.4	37.66		47.22			
MAD 388		28.96	39.8												51.1	60.06	
MAD 8813																	

`

Specimen number	Tmt11	Tmt12	Tmt13	Tmt14	Tmt15	Tmt16	Tmt17	Tmt18	Tmt19	Tmt20	Tmt21	Tmt22	Tmt23	Tmt24	Tmt25	Tmt26	Tmt27
2014/0238/0028																	
2014/0238/0032		27.08	37.1														
2014/0238/0033																	
2014/0238/0034	109.3	28.9	41.68	40.54	37.3	43.08	53.9	46.16	51.82	46.38	40.64	44.02	53.74	52.92	47.92	52.86	58.2
2014/0238/0035	95.98	28.34	39.22														
2014/0238/0036																	
07AEP04																	
08AEP13	165	40.78	60.6	63.73	57.86	62.52	84.2	72.8	83.62	67.08	59.36	66.48	81.6	73.8	62.54		80.68
07AEP12																	
07AEP07				28.52	27.7	31.02	34.16	33.02					36.68	38.1	33.08	42.84	
07AEP05		30.06	50.24		49.9	51.6	60.8	57.02	67.18	50.2	46.5				68.62	61.5	53.7
Unnumbered																	
214709	69.82	21.9	30.76	27.24	29.44	28.24	29.42	38.82	35.04	40.8	30.8	28.3	30.62	33.76	29.66	43.82	
214713	148	35.42	50.2	55.6				65.66									
"13"											40.38	43.98	52.7				
A36	115.2	29.1	51.08	40.08	38.5			47.7	58.02		38.82	43.58		53.3	51.44	60.34	62.68
"17"	110.76			39.66	36.42	42.94	51.88	48.8		42.74	35.42	40.02	52.8	48.84	46.3	48.78	59.3
A47		41.32	57.7														

`

Specimen number	Tmt28	Tmt29	Tmt30	Tmt31	Tmt32	Tmt33	Tmt34	Tmt35	Tmt36	Tmt37	Tmt38	Tmt39	Tmt40	Tmt41	Tmt42	Tmt43	Tmt44
A2148	53.6	66.1	56.4	51.7	20.2	123.3	33.4	79.62	49.2	45.4	76.9	91.7	120.26	357	372	363	377
122.861	53.96	43.04	40.6	44.58	13.78	93.43	19.58	63.81	41.98	39.79	57.95	69.25	91.77	297	267	296	295
1906-16-65	66.68	43.74	51.14	53.88	18.06	121.64	24.8	79.54	45.1	49	76.46	84.06	117.08	334	356	370	312
Unnumbered	45.66	26.34	33.2	35.28	10	61.8	11.06	43.96	27.06	26.82	48.26	51.92	65.2	298	313	315	312
Unnumbered	42.9	28.72	29.5	31.26	12.76	67.4	12.78	39.04	34.2	31.26	46.92	53.84	63.14	300	308	317	312
Unnumbered	64.26	50.44	51.82	48.14	12.5	104.5	18.02	62.82	50.54	36.7	69.9	75.84	96.34	310	327	324	331
Unnumbered	54.78	40.44	43.52	42.12	15.6	101.5		57	41.86	38.9	56.58	72.4	91.3	292	304	307	318
1908-5, 51	82.96	59.14	53.58	62.38	20.28	153.5	30.68	96.2	60.7	58.02		76.54	127	391	400	423	414
MAD 6771	41.22	24.08	28.08	31.36	7.84	56.24	11.76	32.64	23.7					290	311	304	306
MAD 6660	44.4	30.26	30.8	32.12	11.94	58.9	13.74	41.58	26.86	27.18	49.06	51.54	65	292	298	298	306
MAD 6662	38.94	26.2	26.12	30.4	11.6	56.38	13.42	32.58	19.02	18.2	38.48	49.55	53.76	279	288	287	291
MAD 6658	41.96	27.36	29.26	30.22	9.32	61.98	19.92	44.16	30.26	23.56	45.84	52.7	63.34	271	283	286	284
MAD 387	64.72	43.42	52.54	49.22	19.56	133.48	21.14	76.86	52.46	46.52	76.62	91.6	118.26	326	356	372	360
MAD 385	73.44	45.46	53.76	58.86	14.5		28.56	73.2	53.1		72.54	89.62	111.98	353	358	369	381
MAD 6736	57.8	42.5	45.02	46.12	13.4	95.5	22.6	61.6	41.86	43.56	60.88	74.66	95.6	305	333	328	334
1908-21	100.14	56.08	63.68	62.9	15.38	151.94	36.36	88.16	57.12	52.3	73.44	110.66	131.26	440	445	452	454
Unnumbered	58.76	41.28	49.2	43.94	17.06	100.68	20.18	61.04	43.02	53.24	68.1	72.46	98.14	281	304	311	302
Unnumbered	53.54	41.8	44.9	44.82	14.2	85.46	19.56	57.58	41.1	37.8	55.7	68.92	89.62	281	304	302	304
1908-5	77.2	54.22	59.14	67.58	14.06	154	26.1	99.7	69.84	57.48	87.02	101.6	134.24	405	380	415	414
MAD 382	86.26	55.78	64.32	65.5	24.6			92.62	50.78	52.8					437	456	
MAD 400c	40.18	28.8	29.34	28.08	6.78	55.96	15.38	43.72	25.22	31.42	43.54	50.34	64.14	287	294	301	296
MAD 459d			27.4	30.08	8.74	59.2	10.24	41.44	22.86	33.6	43.08	50.94	64.54	285	302	304	298
Unnumbered			46.84	43.96	17.16	98	23.46	64.62	47.46	44.7	71.4	76.2	101.1	275	296	292	306
2014/0238/0025	57.6	42.3	46.8	44.6	16.8	97.8	20.66	56.3	42.28	50.94	65.34	75.68	93.14	268	284	286	296

`

Specimen number	Tmt28	Tmt29	Tmt30	Tmt31	Tmt32	Tmt33	Tmt34	Tmt35	Tmt36	Tmt37	Tmt38	Tmt39	Tmt40	Tmt41	Tmt42	Tmt43	Tmt44
2014/0238/0026	50.5	38.38	42.66	40	12.34	90.74	17.42	60.58	38.52	40.34	58.2	65.56	82.76	259	276	278	284
2014/0238/0027	54.78	43.16	47.5	38.98	12.44	91.14	18.54	62.6	45.18	41.3	62.82	69.08	91.54	288	294	299	304
2014/0238/0029	49.48	38.18	42.96	39.58	14.64	93.28	19.78	58.18	40.62	36.72	57.64	62.44	83	279	258	278	286
2014/0238/0030	53.02	36.04	41.72	43.14	9.94	91.74	14.82	57.5	44.12	43.08	57.04	65.82	85.56	269	259	274	289
2014/0238/0031	57.12	42.38	42.48	40.92	12	94.36	19.18	61.94	44.66	42.94	62.9	70.6	90.72				
A673	60.7	44.02	40.44	43.96	8.8	98	19.82	62.1	44.14	46.64	65.96	73.88	97.22	291	308	311	309
Unnumbered	55.2	36.6	42.22	45.7	12.86	92.44	22.84	58.88	44.08	42.8	58.24	67.92	90.96	270	292	296	288
Unnumbered	52.48	55.36	42.8	42.48	11.18	92.5	25.16	61.72	42.72	46.16	61.58	68.76	90.16	260	286	288	286
MB.AV.67	45.14	34.16	41.5	36.8	13.28	80.28	19.16	52.8	38.38					252	237	261	256
TBC	68.28	47	51.22	52.82	16.8	135.3	28.62		45.94	37.88	72.5	85.8		328			355
07AEP03	88.82	58	70.64	66.6	20.8	167		90.7	69.2	82.04	93	107.54	137.02	422	447	457	459
08AEP01	47.24	33.52	39.46	35.56	12.86	87.46	7.88	55.42	41.9	44.1	55.2	61.8	80.1	255			262
07AEP06	45.04	26.26	29.14	31.1	11.2	61.16		45.62	31.8		42.7	50.94	64.34	294	301	305	304
07AEP11	46.4	35.78	37.68	37.5	14.6	86.34		55.8	40.56	42.76	54.84	58.56	82.74	242	257	262	265
07AEP08	44.36	30.16	30.88	31.6	10.52	61.82		41.08	33.18					298			
A34	66.08	46.52	44.68	44.92	15.72	102.28	20.68	72.58	49.2	56.43	67.74	79.52	99.92	295	321	329	325
A39	64.24	48.98	53.64	47.32	18.68	100.14	20.76	65.16	52.5	56.74	67.94	75.94	101.94	294	316	317	322
A38	61.04	45.04	51.06	46.66	24.94	110.02	20.6	67.1	44.56	50.64	62.8	74.68	98.96	287	314	301	323
A40	58.4	44.3	48.88	46.12		98.08								284	294	308	312
A33a	51.78	39.2	40	44.98	14	88.2	19.78	62.42	43	48.84	58.46	62.6	90.72	274	277	285	300
A676	24	20.5	27	26.8				41	29	25.2	40.2	44	56	288	261	263	265
MAD 6770					22.4	121.8	33.3										
MAD 383	69.7	56.7			24.9												
MAD 6659	40.36	26.06	28.76	28.74	14.3		17.78										
MAD 384	54.36	41.24		42.12	11.58	100.04	19.3	57.04	44.66	38.16	54.3	67.9	82.04		281		292
MAD 388					22.8												

`

Specimen number	Tmt28	Tmt29	Tmt30	Tmt31	Tmt32	Tmt33	Tmt34	Tmt35	Tmt36	Tmt37	Tmt38	Tmt39	Tmt40	Tmt41	Tmt42	Tmt43	Tmt44
MAD 8813					35.06												
2014/0238/0028							21.2										
2014/0238/0032						19.92		20.68									
2014/0238/0033							101.86		63.1	48.74	62.36	73.7	97.32				
2014/0238/0034	57.04	38.52	44.68	51.08	17.78												
2014/0238/0035					16.54												
2014/0238/0036						103.64	23.96	70.5	47.52	44.26	67.04	78.48	102.6				
07AEP04						145.3		87.82	70.98	69.32	84.6	101.18	132.5				
08AEP13	81.7	55.6	66.36	68.38													
07AEP12						107.32											
07AEP07			31.44	33.94	10.94	64.8		79.94	36.76	33.8			54.2	287	289	300	294
07AEP05		45.6	49.58	53.56	16.42	132.54											
Unnumbered																	
214709													54.84	264	273	272	282
214713						139.66											
"13"																	
A36	61.22	44.7	45.64	44.16	16.92												
"17"			44.92	43.44	27.78		22.22										
A47																	

`

Appendix two

`

`

PCA LOADINGS AND EIGENVALUES FOR MORPHOMETRIC ANALYSES

A. Unsupervised clusters of femora, <25% missing data		
Measurement number	**PC1 loadings**	**PC2 loadings**
F1	0.9857185	-0.045391197
F2	0.9472565	-0.067765936
F3	0.9828699	0.018181632
F4	0.953715	0.080898556
F5	0.9734609	-0.03204332
F6	0.9769611	-0.007694256
F7	0.9781167	0.020773356
F8	0.9461713	-0.001360694
F9	0.9664976	-0.063604966
F10	0.9858491	-0.012345429
F11	0.98249	-0.028801285
F12	0.9783639	-0.022652162
F13	0.9768762	-0.030048592
F14	0.9707743	-0.020575192
F15	0.9624025	0.011324139
F16	0.9573402	0.063518684
F17	0.9398132	0.10545931
F18	0.9261397	-0.116636652
F19	0.8357421	-0.325219429
F20	0.812738	0.511877561

Museum	**Specimen number**	**PC1 eigenvalues**	**PC2 eigenvalues**
UIO	Unnumbered	-2.0511311	-0.21962321
UIO	122.872	-0.5135119	0.13726712
MNHN	1906-16-66	-0.172591	-0.44275518
MNHN	Unnumbered	0.1864099	-0.42629677
MNHN	1908-5	-6.6750129	-0.17867059
MNHN	MAD 364	6.1840396	1.13569147
MNHN	MAD 6648	-6.9942548	-0.02912518
MNHN	MAD 441	-6.5226779	-0.67398938
MNHN	MAD 373	-1.2575163	0.24094898
MNHN	MAD 374	-1.873717	-0.62534865
MNHN	MAD 369	7.2561897	0.61216016
MNHN	MAD 6754	-0.97104	-0.31494844
MNHN	1906-16-58	0.9403054	-0.2979366
MNHN	1906-16-71	-0.8718461	-0.30989186
MNHN	1906-16-65	-1.3874851	0.67092634
MNHN	Unnumbered	-0.9573812	0.58368459
MNHN	Unnumbered	-6.1544666	-0.48735417
MNHN	Unnumbered	4.5221999	-0.023525
MNHN	Unnumbered	-0.1978221	0.10427317
MNHN	Unnumbered	-0.2533478	-0.51940059
MNHN	Unnumbered	-7.2647505	-0.20120529
MNHN	MAD 378	1.5522059	0.06267396
MNHN	Unnumbered	7.2064449	-0.52123817
MNHN	Unnumbered	8.0395316	-1.17663194
MNHN	MAD 6773	-6.110059	-0.13644699
MNHN	Unnumbered	-0.3290177	0.60730166
MNHN	Unnumbered	-0.5085531	0.20995875
NHMW	2014/0238/039	-0.4985055	-0.37289753
NHMW	2014/0238/041	0.1437468	-0.2158523
NHMW	2014/0238/042	-1.281077	0.93264767
NHMW	2014/0238/045	-2.2951568	0.56710447
NHM	Unnumbered	0.7659916	-0.25327139
NHM	A2142	6.203811	0.72625427
NHM	ii.26.1254	-2.1789808	0.20285993
NHM	Unnumbered	-1.8633018	0.74894393
NHM	A696	-0.2652592	-0.48617654
NHM	A2141	7.3257693	-0.1324806
NHM	A465	-1.6056299	1.14877818
CVB	Unnumbered	7.2852088	-0.79944015
UA	07AEP02	-6.3897649	-0.39640227
UA	Unnumbered	2.2467847	-0.20001149
UA	Unnumbered	-6.8127307	-0.68263951
USNM	3013	-0.2763862	2.06014868
ZIUU	A49b	1.9627815	0.67328935
ZIUU	A15	-0.699905	0.40326444
ZIUU	A49f	-0.7574738	-0.66069037
OUMNH	4950	7.637364	-1.53017349
NHM	A439	6.5315693	0.48624649

`

B. Supervised clusters of femora (four possible groups only), <25% missing data		
Measurement number	**PC1 loadings**	**PC2 loadings**
F1	0.9857185	-0.045391197
F2	0.9472565	-0.067765936
F3	0.9828699	0.018181632
F4	0.953715	0.080898556
F5	0.9734609	-0.03204332
F6	0.9769611	-0.007694256
F7	0.9781167	0.020773356
F8	0.9461713	-0.001360694
F9	0.9664976	-0.063604966
F10	0.9858491	-0.012345429
F11	0.98249	-0.028801285
F12	0.9783639	-0.022652162
F13	0.9768762	-0.030048592
F14	0.9707743	-0.020575192
F15	0.9624025	0.011324139
F16	0.9573402	0.063518684
F17	0.9398132	0.10545931
F18	0.9261397	-0.116636652
F19	0.8357421	-0.325219429
F20	0.812738	0.511877561

Museum	Specimen number	PC1 eigenvalues	PC2 eigenvalues
UIO	Unnumbered	-2.0511311	-0.21962321
UIO	122.872	-0.5135119	0.13726712
MNHN	1906-16-66	-0.172591	-0.44275518
MNHN	Unnumbered	0.1864099	-0.42629677
MNHN	1908-5	-6.6750129	-0.17867059
MNHN	MAD 364	6.1840396	1.13569147
MNHN	MAD 6648	-6.9942548	-0.02912518
MNHN	MAD 441	-6.5226779	-0.67398938
MNHN	MAD 373	-1.2575163	0.24094898
MNHN	MAD 374	-1.873717	-0.62534865
MNHN	MAD 369	7.2561897	0.61216016
MNHN	MAD 6754	-0.97104	-0.31494844
MNHN	1906-16-58	0.9403054	-0.2979366
MNHN	1906-16-71	-0.8718461	-0.30989186
MNHN	1906-16-65	-1.3874851	0.67092634
MNHN	Unnumbered	-0.9573812	0.58368459
MNHN	Unnumbered	-6.1544666	-0.48735417
MNHN	Unnumbered	4.5221999	-0.023525
MNHN	Unnumbered	-0.1978221	0.10427317
MNHN	Unnumbered	-0.2533478	-0.51940059
MNHN	Unnumbered	-7.2647505	-0.20120529
MNHN	MAD 378	1.5522059	0.06267396
MNHN	Unnumbered	7.2064449	-0.52123817
MNHN	Unnumbered	8.0395316	-1.17663194
MNHN	MAD 6773	-6.110059	-0.13644699
MNHN	Unnumbered	-0.3290177	0.60730166
MNHN	Unnumbered	-0.5085531	0.20995875
NHMW	2014/0238/039	-0.4985055	-0.37289753
NHMW	2014/0238/041	0.1437468	-0.2158523
NHMW	2014/0238/042	-1.281077	0.93264767
NHMW	2014/0238/045	-2.2951568	0.56710447
NHM	Unnumbered	0.7659916	-0.25327139
NHM	A2142	6.203811	0.72625427
NHM	ii.26.1254	-2.1789808	0.20285993
NHM	Unnumbered	-1.8633018	0.74894393
NHM	A696	-0.2652592	-0.48617654
NHM	A2141	7.3257693	-0.1324806
NHM	A465	-1.6056299	1.14877818
CVB	Unnumbered	7.2852088	-0.79944015
UA	07AEP02	-6.3897649	-0.39640227
UA	Unnumbered	2.2467847	-0.20001149
UA	Unnumbered	-6.8127307	-0.68263951
USNM	3013	-0.2763862	2.06014868
ZIUU	A49b	1.9627815	0.67328935
ZIUU	A15	-0.699905	0.40326444
ZIUU	A49f	-0.7574738	-0.66069037
OUMNH	4950	7.637364	-1.53017349
NHM	A439	6.5315693	0.48624649

`

C. Unsupervised clusters of femora, >25% missing data		
Measurement number	**PC1 loadings**	**PC2 loadings**
F1	0.9887578	-0.039651514
F2	0.9393263	-0.129879174
F3	0.9819048	-0.018623107
F4	0.9507536	0.030633858
F5	0.9753302	-0.019706464
F6	0.9798886	0.002866609
F7	0.9778209	0.029520495
F8	0.9541825	0.008023228
F9	0.9636019	-0.048298569
F10	0.9882925	-0.013742307
F11	0.9858418	-0.020587565
F12	0.9815946	-0.019189763
F13	0.9812347	-0.024497503
F14	0.9765094	-0.002086988
F15	0.9681366	0.019695601
F16	0.9624369	0.053267187
F17	0.9520442	0.073118044
F18	0.9352068	-0.077382961
F19	0.8454556	-0.292399108
F20	0.8066233	0.539557362

Museum	Specimen number	PC1 eigenvalues	PC2 eigenvalues
UIO	Unnumbered	-2.45994201	-0.2907373
UIO	122.872	-0.82974233	0.04015541
MNHN	1906-16-66	-0.45473173	-0.50824288
MNHN	Unnumbered	-0.08314544	-0.52839212
MNHN	1908-5	-7.37388591	-0.08574367
MNHN	MAD 364	6.28607394	1.03325016
MNHN	MAD 6648	-7.7217456	0.04842648
MNHN	MAD 441	-7.19070975	-0.59789301
MNHN	MAD 373	-1.63767568	0.25147779
MNHN	MAD 374	-2.26642766	-0.70401657
MNHN	MAD 369	7.43735083	0.52426323
MNHN	MAD 6754	-1.30955566	-0.33283503
MNHN	1906-16-71	-1.2022485	-0.43717249
MNHN	1906-16-65	-1.77602217	0.65349006
MNHN	Unnumbered	-1.30880411	0.52340765
MNHN	JH 32	-6.82194187	-0.43382739
MNHN	JH 58	-0.48934768	-0.03210094
MNHN	JH 59	-0.53509298	-0.65706683
MNHN	JH 61	-8.01492601	-0.13638034
MNHN	MAD 378	1.32914951	-0.08325926
MNHN	Unnumbered	7.39398823	-0.60609056
MNHN	Unnumbered	8.30088626	-1.40307612
MNHN	MAD 6773	-6.7879357	-0.07378688
MNHN	Unnumbered	-0.80955864	0.05960794
NHMW	2014/0238/039	-0.82030337	-0.45412752
NHMW	2014/0238/041	-0.12751915	-0.24951396
NHMW	2014/0238/042	-1.68005536	0.98621165
NHMW	2014/0238/045	-2.74225006	0.58070946
NHM	A2142	6.26974322	0.69547753
NHM	ii.26.1254	-2.60326099	0.26168729
NHM	Unnumbered	-2.26439101	0.69696304
NHM	A696	-0.55785154	-0.54012605
NHM	A2141	7.527594	-0.07237551
NHM	A465	-2.0167366	1.10421289
CVB	Unnumbered	7.49273777	-0.95312443
UA	07AEP02	-7.07940373	-0.40339214
UA	Unnumbered	2.11571513	-0.24500521
UA	Unnumbered	-7.50791653	-0.6995508
USNM	3013	-0.59750584	2.22372189
ZIUU	A49b	1.79002561	0.64632249
ZIUU	A15	-1.03204389	0.32566181
ZIUU	A49f	-1.08396595	-0.77940371
OUMNH	4950	7.89475401	-1.72122514
NHM	A439	6.64105094	0.42497339
UIO	122.946	-4.74273845	0.05789061
NHMW	2014/0238/038	-1.20409703	-0.12534605
NHMW	2014/0238/040	-1.44687131	0.64964985
NHMW	2014/0238/044	-1.61142112	-0.07150796
Berlin	MB.AV.73	-5.25862274	-0.43014589
CVB	Unnumbered	6.37888478	1.20241198
CVB	Unnumbered	5.41150487	-0.01397474

`

CVB	Unnumbered	3.02937665	0.06995185
USNM	214714	2.06854965	-0.97831687
ZIUU	20	-0.70598205	-0.04967042
ZIUU	A16	1.83681622	0.63742239
ZIUU	A17	1.67633063	0.3315491
ZIUU	17	1.46112588	0.5119236
ZIUU	14	-0.06528186	-0.01596999
ZIUU	3	0.3710719	-0.17635961
ZIUU	5	0.80533138	0.18418161
ZIUU	A44	5.58119172	-0.56949277
ZIUU	A14	-0.80376537	-0.06841565
MNHN	1910-12-61	2.10735159	0.74666871

`

D. Unsupervised clusters of tibiotarsi, <25% missing data		
Measurement number	**PC1 loadings**	**PC2 loadings**
Tt1	0.94662005	0.027442984
Tt2	0.72475441	-0.336303041
Tt3	0.98311045	-0.019111015
Tt4	0.67469045	0.43284839
Tt5	-0.26477523	0.498359911
Tt6	0.81338382	-0.166168166
Tt7	0.85348578	0.04922638
Tt8	0.73904065	-0.390676195
Tt9	0.87194351	0.135258571
Tt10	0.51241027	0.56496722
Tt11	0.53931773	0.476524543
Tt12	0.80498112	-0.159654201
Tt13	0.52860943	0.167256905
Tt14	0.88020178	0.086420905
Tt15	0.93078684	-0.098136524
Tt16	0.86450603	0.024775793
Tt17	0.69339645	-0.004401462
Tt18	0.79277335	-0.042624174
Tt19	0.04589077	-0.097774422
Tt20	0.70011896	-0.186834192

Museum	Specimen number	PC1 eigenvalues	PC2 eigenvalues
Museum	**Specimen number**	**PC1 eigenvalues**	**PC2 eigenvalues**
NHM	A673	0.12405339	-0.54673278
UIO	A31835	-0.69936455	-0.38129634
UIO	122.867	-2.19214725	0.27334351
UIO	A31833	-1.36494427	0.73844615
UIO	A31836	-1.11551545	-0.70703096
UIO	122.878/.879	-1.45661945	0.1898701
MNHN	Unnumbered	-4.42519803	0.97146741
MNHN	Unnumbered	-5.1032712	0.95652807
MNHN	MAD 6733	-0.12084217	-0.65773421
MNHN	MAD 395	3.51580072	-0.51082805
MNHN	[1] 1937-62	6.27006763	-1.05666828
MNHN	[3] 1937-62	3.43197988	-0.63122349
MNHN	[4] 1937-62	4.56098293	0.11270772
MNHN	1906-16-80	-0.01198053	-0.77541606
MNHN	1906-16-77	-0.40556675	-0.99511479
MNHN	1906-16	-2.1735439	-1.10485568
MNHN	1906-16-82	-1.41518893	-2.05870067
MNHN	1906-16 2	0.40555475	-0.10342049
MNHN	MAD 674	0.0350182	-1.18420286
MNHN	1908-5	6.47858198	0.87254882
MNHN	Unnumbered	2.56869232	-0.66521313
MNHN	1906-16	-0.5859371	-1.28393871
MNHN	MAD 6655	-5.41952954	0.7820736
MNHN	MAD 6747	-5.28253908	0.78307823
MNHN	MAD 6734	0.56782916	-1.05685776
MNHN	MAD 394	5.06720557	-1.03587632
MNHN	MAD 393	8.51938966	-0.78999364
MNHN	MAD 459b	-5.20090833	0.42745412
MNHN	MAD 6744	-4.79916603	0.99115398
MNHN	MAD 440a	-4.26316394	1.13932751
MNHN	MAD 6653	-4.51662832	1.4505661
MNHN	MAD 6741	-0.95853015	-1.25505193
MNHN	MAD 6743	-0.18860368	-1.49646814
MNHN	Unnumbered	-0.72473403	-0.65345706
MNHN	Unnumbered	1.14688292	-0.97311423
NHMW	2014/0238/023	1.04235342	0.81362271
NHMW	2014/0238/024	-0.37842734	-1.61235112
NHM	A237	-0.25174462	-0.22614605
NHM	A2143	5.91718296	1.47592956
NHM	Unnumbered	1.39431126	1.74898544
NHM	A464	-2.43470099	-0.44488714
NHM	A506	0.77640071	1.43019853
NHM	A4183b	3.26612278	1.67671139
NHM	A462	1.61085588	2.29348514
NHM	A2144	4.71923053	2.08276461

`

NHM	A438	6.70150272	4.89582129
NHM	A673	0.37535225	-1.75823235
MFN	MB.AV.70	-3.68638587	-0.56188323
CVB	Unnumbered	3.45360444	0.31261576
UA	08AEP10	-0.46229476	0.45845626
UA	08AEP14	-4.81241779	1.56371388
UA	08AEP15	-4.72993306	1.24202202
UA	08AEP08	2.50739887	0.15222628
UA	08AEP18	-4.42340476	0.9410534
UA	08AEP09	1.89612716	0.03370876
UA	08AEP11	1.00583054	-0.0899039
UA	08AEP06	3.14309311	-0.00643039
UA	08AEP07	2.85824195	-0.23397561
UA	08AEP16	-3.36592556	-0.0189154
UA	Unnumbered	3.06194213	-0.69101983
USNM	3016	-0.21728959	1.31191682
ZIUU	A12	-0.25688604	-0.07773829
ZIUU	A49C	-1.10830715	-0.96311935
ZIUU	40	-1.26174584	-2.21222876
ZIUU	19	-0.2482205	-1.28279419
ZIUU	A13	-0.31864981	-1.20999965
ZIUU	12	-0.38444895	-1.41726347
ZIUU	14	-0.64142787	-0.17302189
ZIUU	A32	0.44976541	-0.83905502
ZIUU	A31	0.33793734	-0.80815474
OUMNH	4952	-4.29582206	1.10072591
OUMNH	4951	5.4012238	0.71556925
OUMNH	A676	-6.90856114	0.61222366

`

E. Unsupervised clusters of tibiotarsi, >25% missing data		
Measurement number	**PC1 loadings**	**PC2 loadings**
Tt1	0.92576699	0.054942774
Tt2	0.71201155	-0.298324245
Tt3	0.93513571	-0.09666575
Tt4	0.69199115	0.266313414
Tt5	-0.25642698	0.553215317
Tt6	0.79217818	-0.181050262
Tt7	0.84695961	0.000327359
Tt8	0.7319112	-0.3831033
Tt9	0.85881761	0.096868323
Tt10	0.50502431	0.50001023
Tt11	0.51127358	0.576258244
Tt12	0.76849853	-0.150187324
Tt13	0.5396071	0.188985019
Tt14	0.8592628	0.166523098
Tt15	0.89854027	-0.081864152
Tt16	0.78955019	0.068300712
Tt17	0.67158524	0.030852842
Tt18	0.75950809	0.053773529
Tt19	0.04578211	-0.018615139
Tt20	0.71579869	-0.23470338

Museum	Specimen number	PC1 eigenvalues	PC2 eigenvalues
NHM	A673	0.39072713	-0.90564825
UIO	A31835	-0.54639183	-0.3060473
UIO	122.867	-2.14906905	0.55901117
UIO	A31833	-1.32017538	0.93890359
UIO	A31836	-0.99703019	-0.63921414
UIO	122.878/.879	-1.43687489	0.31958908
MNHN	Unnumbered	-4.53653504	1.03812656
MNHN	Unnumbered	-5.26019723	0.93420577
MNHN	MAD 6733	0.02011525	-0.55405128
MNHN	MAD 395	3.93276969	-0.32514691
MNHN	[1] 1937-62	6.80993458	-0.8413664
MNHN	[3] 1937-62	3.87526431	-0.48097214
MNHN	[4] 1937-62	5.02616679	0.60605128
MNHN	1906-16-80	0.09327485	-0.62118077
MNHN	1906-16-77	-0.28373964	-0.96319479
MNHN	1906-16	-2.19965499	-1.08276933
MNHN	1906-16-82	-1.41025542	-2.30354766
MNHN	1906-16 2	0.580209	0.08800844
MNHN	MAD 674	0.18500249	-1.20232707
MNHN	1908-5	7.03835037	1.73394647
MNHN	Unnumbered	2.91096015	-0.64948968
MNHN	1906-16	-0.49918421	-1.41161248
MNHN	MAD 6655	-5.58560581	0.65781504
MNHN	MAD 6747	-5.43164147	0.75698585
MNHN	MAD 6734	0.74683839	-1.09932243
MNHN	MAD 394	5.59754071	-0.9307182
MNHN	MAD 393	9.29032798	-0.18635839
MNHN	MAD 459b	-5.36270612	0.35184442
MNHN	MAD 6744	-4.90847075	1.10033408
MNHN	MAD 440a	-4.33531108	1.28742383
MNHN	MAD 6653	-4.57680312	1.61978629
MNHN	MAD 6741	-0.89160474	-1.32863212
MNHN	MAD 6743	-0.12520631	-1.54511501
MNHN	Unnumbered	-0.64076043	-0.64996785
MNHN	Unnumbered	1.40850457	-0.24673572
NHMW	2014/0238/023	1.35321797	0.5700908
NHMW	2014/0238/024	-0.29637667	-1.25202833
NHM	A237	-0.11625096	-0.47848985
NHM	A2143	6.53722417	1.36666196
NHM	Unnumbered	1.82909423	1.90350249
NHM	A464	-2.42951614	-0.46478226
NHM	A506	1.03452527	1.31131194
NHM	A4183b	3.72523212	1.49729635
NHM	A462	1.91433775	2.18863196
NHM	A2144	5.24939218	1.86406355
NHM	A438	7.39762507	5.81058528
NHM	A673	0.54640097	-1.72033536
MFN	MB.AV.70	-3.74717834	-0.84010289
CVB	Unnumbered	3.86470893	0.39087298
UA	08AEP10	-0.34282046	0.16543175
UA	08AEP14	-4.91083248	1.65995634

`

UA	08AEP15	-4.83674233	1.2509252
UA	08AEP08	2.84505004	-0.09029155
UA	08AEP18	-4.48665165	1.1385157
UA	08AEP09	2.20933369	0.19363754
UA	08AEP11	1.25075155	-0.03101033
UA	08AEP06	3.48411119	0.02298795
UA	08AEP07	3.1981011	-0.06177628
UA	08AEP16	-3.41376358	-0.14350536
UA	Unnumbered	3.42548851	-0.69546685
USNM	3016	-0.04664616	1.02138959
ZIUU	A12	-0.14648829	-0.09733461
ZIUU	A49C	-1.05638294	-0.90493763
ZIUU	40	-1.27120147	-2.27085806
ZIUU	19	-0.17208384	-1.11231737
ZIUU	A13	-0.233021	-1.1343976
ZIUU	12	-0.32899302	-1.43498623
ZIUU	14	-0.57171491	-0.02649385
ZIUU	A32	0.61617734	-0.48911924
ZIUU	A31	0.45756098	-0.50999936
OUMNH	4952	-4.36496943	1.13330174
OUMNH	4951	5.89939904	0.56349471
OUMNH	A676	-7.17947406	0.43838241
MNHN	2	-2.35288829	1.7177374
MNHN	Unnumbered	-0.4342117	-1.0028043
MNHN	Unnumbered	-0.3339402	-0.51778092
MNHN	Unnumbered	-0.78684104	-0.88088157
MNHN	1906-16	-0.23047811	-0.93524187
MNHN	85	-0.1176139	-1.0070968
MNHN	Unnumbered	-1.39157169	-0.59386261
MNHN	MAD 392	3.59824342	-0.85003154
MNHN	MAD 396	1.5144858	-1.29015882
MNHN	MAD 6656	-4.85298438	1.24614882
MNHN	MAD 6654	-1.86401855	0.75056604
MNHN	1906-16, 70	2.44201854	-1.26740586
NHMW	2014/0238/007	-0.25100731	-0.7279044
NHMW	2014/0238/010	-0.80415733	-0.51904846
NHMW	2014/0238/011	-0.24591579	1.02449189
NHMW	2014/0238/014	0.128661	-0.75326035
NHMW	2014/0238/018	0.75833051	-1.42234432
NHMW	2014/0238/020	-0.09115699	-0.73411578
MFN	MB.AV.71	-0.43455906	0.84671119
CVB	Unnumbered	-1.67595701	0.74674962
UA	08AEP13	-1.07007094	0.39755969
UA	Unnumbered	-3.79975993	1.32055178

`

F. Unsupervised clusters of tarsometatarsi, <25% missing data						
Measurement number	**PC1 loadings**	**PC2 loadings**	**Museum**	**Specimen number**	**PC1 eigenvalues**	**PC2 eigenvalues**
Tmt1	0.8548492	0.49666132	NHM	A2148	6.9796017	0.35220402
Tmt2	0.9539726	-0.097157927	UIO	122.861	-0.7042794	-1.02101699
Tmt3	0.9691305	-0.176154033	MNHN	1906-16-65	4.5415086	0.20697241
Tmt4	0.9737922	-0.085044151	MNHN	Unnumbered	-7.0245558	2.18498409
Tmt5	0.9885255	-0.064671218	MNHN	Unnumbered	-6.6388862	1.77392201
Tmt6	0.87126	-0.249700938	MNHN	Unnumbered	1.379334	0.01299087
Tmt7	0.7794771	-0.057006781	MNHN	Unnumbered	-0.2342527	-0.24423313
Tmt8	0.8052233	0.260592566	MNHN	1908-5, 51	11.1488881	0.77949977
Tmt9	0.9922544	-0.044069747	MNHN	MAD 6771	-8.393354	2.34184468
Tmt10	0.9704539	0.006618395	MNHN	MAD 6660	-6.809083	1.67047907
Tmt11	0.9813272	-0.059212433	MNHN	MAD 6662	-8.6519304	1.73057384
Tmt12	0.9181319	0.175828861	MNHN	MAD 6658	-7.6338888	1.24832952
Tmt13	0.957012	-0.14931547	MNHN	MAD 387	4.9053155	0.17079895
Tmt14	0.9751337	-0.047364004	MNHN	MAD 385	5.6142052	1.1018269
Tmt15	0.9843908	-0.013685894	MNHN	MAD 6736	1.2708043	0.21051565
Tmt16	0.9778913	-0.14414	MNHN	Unnumbered	4.8102943	-0.58531976
Tmt17	0.9716131	-0.045283048	MNHN	1908-21	13.6931545	3.15783601
Tmt18	0.9838073	0.044741171	MNHN	Unnumbered	0.5087784	-1.53469317
Tmt19	0.988939	0.051423665	MNHN	Unnumbered	-0.6999901	-0.45999081
Tmt20	0.9783936	-0.030203505	MNHN	1908-5	10.8773529	0.72685361
Tmt21	0.9459169	0.06302244	MNHN	MAD 382	13.4590335	2.14314361
Tmt22	0.9777337	-0.06265669	MNHN	MAD 400c	-7.9182718	1.67751845
Tmt23	0.934538	-0.20650968	MNHN	MAD 459d	-7.6384753	1.91556076
Tmt24	0.9560204	-0.20706829	MNHN	Unnumbered	0.8633787	-1.80776088
Tmt25	0.9348497	-0.160084854	NHMW	2014/0238/0025	0.719908	-1.84284736
Tmt26	0.9452337	0.18414817	NHMW	2014/0238/0026	-2.1305365	-1.44633146
Tmt27	0.9383795	0.113272307	NHMW	2014/0238/0027	-0.5742081	-0.71448556
Tmt28	0.9552555	0.092529438	NHMW	2014/0238/0029	-2.5161346	-0.98878689
Tmt29	0.9010956	-0.183542125	NHMW	2014/0238/0030	-1.8473703	-1.19850154
Tmt30	0.9616016	-0.144942773	NHMW	2014/0238/0031	-0.69032	-0.62051448
Tmt31	0.9782625	-0.009874792	NHM	A673	0.4936321	-0.27975266
Tmt32	0.7520898	-0.216391173	MNHN	Unnumbered	-0.5749673	-1.29677279
Tmt33	0.984007	-0.035148885	MNHN	Unnumbered	-0.9905088	-1.59439333
Tmt34	0.9079433	0.062159235	MFN	MB.AV.67	-4.0175081	-1.71059637
Tmt35	0.9671789	-0.092243185	USNM	A605209	5.4848248	0.14718904
Tmt36	0.9126302	-0.22844882	UA	07AEP03	14.5025561	1.53922551
Tmt37	0.8393997	-0.316669688	UA	08AEP01	-3.972533	-1.87943291
Tmt38	0.9572457	-0.140118361	UA	07AEP06	-6.8313716	1.50825728
Tmt39	0.9689189	0.001607305	UA	07AEP11	-3.9523886	-1.96487355
Tmt40	0.9867343	-0.093774285	UA	07AEP08	-7.3207783	1.15290707
Tmt41	0.80448	0.564692038	ZIUU	A34	2.5228445	-1.07137982
Tmt42	0.8292412	0.521351247	ZIUU	A39	2.6145	-1.76888759
Tmt43	0.8567625	0.493574046	ZIUU	A38	2.0099053	-1.69482508
Tmt44	0.8674378	0.463272267	ZIUU	A40	0.8940854	-1.55804038
			ZIUU	A33a	-1.2333413	-1.48338003
			NHM	A676	-10.294972	1.01338341

`

G. Unsupervised clusters of tarsometatarsi, >25% missing data						
Measurement number	**PC1 loadings**	**PC2 loadings**	**Museum**	**Specimen number**	**PC1 eigenvalues**	**PC2 eigenvalues**
Tmt1	0.8216996	0.382154549	NHM	A2148	5.74968038	-0.3618204
Tmt2	0.9302939	0.082055186	UIO	122.861	-1.49915292	-0.7992631
Tmt3	0.9595932	0.148137947	MNHN	1906-16-65	3.51487552	-0.9956588
Tmt4	0.968204	0.061522909	MNHN	Unnumbered	-7.5708167	0.4189729
Tmt5	0.9858789	0.066800789	MNHN	Unnumbered	-7.2398064	0.5389102
Tmt6	0.8421331	-0.029321153	MNHN	Unnumbered	0.61382784	-0.6999359
Tmt7	0.7702086	-0.274058063	MNHN	Unnumbered	-1.08269589	0.03952777
Tmt8	0.7812592	-0.160291404	MNHN	1908-5, 51	9.91715294	-0.8985983
Tmt9	0.9524358	-0.128144341	MNHN	MAD 6771	-8.90941021	0.7815541
Tmt10	0.9675275	0.159396308	MNHN	MAD 6660	-7.43176038	0.682753
Tmt11	0.9860082	0.008536182	MNHN	MAD 6662	-9.24080548	0.8345305
Tmt12	0.9161233	0.266941142	MNHN	MAD 6658	-8.29376624	0.3401908
Tmt13	0.9632588	0.040077678	MNHN	MAD 387	3.91053628	-1.097052
Tmt14	0.9519701	-0.253220265	MNHN	MAD 385	4.54368652	-0.381454
Tmt15	0.9582675	-0.240559593	MNHN	MAD 6736	0.35868601	0.1187305
Tmt16	0.9815123	-0.073468255	MNHN	1908-21	12.22866488	0.2795847
Tmt17	0.9734804	0.141539727	MNHN	Unnumbered	-0.342417	-0.9503902
Tmt18	0.9807622	0.053231004	MNHN	Unnumbered	-1.50769822	-0.2368387
Tmt19	0.9900783	-0.043087497	MNHN	1908-5	9.85492291	-1.91285
Tmt20	0.9065055	-0.391956759	MNHN	MAD 382	11.87430841	0.4855175
Tmt21	0.8321183	-0.496280439	MNHN	MAD 400c	-8.45769794	0.1922359
Tmt22	0.9719048	-0.176518846	MNHN	MAD 459d	-8.11625217	-0.02077279
Tmt23	0.9162783	0.26617256	MNHN	Unnumbered	-0.55486999	-0.6974048
Tmt24	0.9616487	0.102064615	NHMW	2014/0238/0025	-0.16238773	-0.987081
Tmt25	0.9203827	0.184820395	NHMW	2014/0238/0026	-2.8467715	-0.9100674
Tmt26	0.9378805	0.251765197	NHMW	2014/0238/0027	-1.34452134	-0.7641149
Tmt27	0.9398531	-0.025491003	NHMW	2014/0238/0029	-3.30671728	-0.6468975
Tmt28	0.9598786	0.121359638	NHMW	2014/0238/0030	-2.48273024	-1.212643
Tmt29	0.9239146	0.115439773	NHMW	2014/0238/0031	-1.55279201	-0.6937974
Tmt30	0.96422	-0.099170816	NHM	A673	-0.24936237	-1.088272
Tmt31	0.9831541	-0.045327304	MNHN	Unnumbered	-1.37619613	-1.006295
Tmt32	0.5794188	0.689604524	MNHN	Unnumbered	-1.76805449	-1.073922
Tmt33	0.9307629	-0.326271946	MFN	MB.AV.67	-4.75506813	-0.8910916
Tmt34	0.5548102	0.785485695	USNM	A605209	4.31859242	-0.5061484
Tmt35	0.8917134	-0.331213822	UA	07AEP03	13.00646689	-3.518837
Tmt36	0.9155208	-0.084925267	UA	08AEP01	-4.50762166	-1.187922
Tmt37	0.7780729	-0.299619467	UA	07AEP06	-7.40561053	0.4928956
Tmt38	0.9331512	-0.284717084	UA	07AEP11	-4.66504107	-0.8615665
Tmt39	0.9594884	-0.177479334	UA	07AEP08	-7.8307617	0.4130698
Tmt40	0.9661743	-0.179588643	ZIUU	A34	1.6600313	-0.5103739
Tmt41	0.828099	0.083719368	ZIUU	A39	1.72694398	-0.2988614
Tmt42	0.8325239	0.260783217	ZIUU	A38	0.99554626	0.01476674
Tmt43	0.8679176	0.139070692	ZIUU	A40	0.11273537	0.05393988
Tmt44	0.8712323	0.212502303	ZIUU	A33a	-2.02108643	-0.5947444
			NHM	A676	-10.7855207	-0.9403179
			MNHN	MAD 6770	5.23105368	0.6524448
			MNHN	MAD 383	7.53783087	3.016973

`

MNHN	MAD 6659	-8.94043054	1.444323
MNHN	MAD 6772	-0.21404596	-4.78606E-05
MNHN	MAD 384	-2.43887458	-0.64147
MNHN	MAD 388	0.19107377	1.887738
MNHN	MAD 8813	10.70681655	4.53021
NHMW	2014/0238/0028	-2.7077909	0.1670587
NHMW	2014/0238/0032	-7.18190704	6.129741
NHMW	2014/0238/0033	8.21237279	8.905568
NHMW	2014/0238/0034	-0.03053473	-0.3390246
NHMW	2014/0238/0035	-2.015995	0.6954782
NHMW	2014/0238/0036	1.44345699	-0.1830588
UA	07AEP04	9.95052776	-1.155404
UA	08AEP13	11.6398452	-0.2838738
UA	07AEP12	2.65954752	0.6836786
UA	07AEP07	-6.38936503	-0.6833361
UA	07AEP05	3.77042398	-0.949417
UA	Unnumbered	3.87390606	-0.100659
USNM	214709	-7.85520431	-1.317022
USNM	214713	5.85903795	-2.12629
ZIUU	"13"	0.40152354	-0.5522538
ZIUU	A36	0.82405524	0.06897192
ZIUU	"17"	-0.68399932	0.9897771
ZIUU	A47	9.07741046	0.2177082

`

`

Appendix three

`

`

Appendix three: Additional descriptions and figures of anthropogenic tool marks on bones of Aepyornithidae

Appendix 3 figure 1: A *Mullerornis* sp. tibiotarsus from Lamboharana (MNHN MAD6768) dated to 6,415–6,282 BP, exhibiting a shallow, laterally oriented linear anthropogenic mark on the distal end of the posterior fascia of the diaphysis. The specimen also exhibits damage from scavenging by an endemic large carnivore (*Cryptoprocta* sp.); plurifocal overlaid furrows with undefined margins are present on the remaining portion of the proximal epiphysis, with two non-boring round puncture marks 3.5 mm and 2.68 mm in diameter present 29 mm apart on the medial fascia.

`

Appendix 3 figure 2: An *Aepyornis maximus* tibiotarsus from Ambolisatra (MNHN 1906-16-67) directly dated to 1,182–1,057 BP, exhibiting four linear anthropogenic marks disseminated across the proximal epiphysis. The centrally-oriented bevelled grooves with v-shaped floors all share similar characteristics of approximate size and cross section (maximum length×width: 1, 20×3 mm; 2, 16×5 mm; 3, 14.2×4 mm; 20×1.5 mm), but show both defined and undefined periosteal fracturing surrounding the marks due to penetration of cortical bone creating marginal post-mortem periosteal instability. The marks are not parallel (grooves 2–4 are clustered around the lateral articular surface). These marks are consistent with deep clefts made by chopping actions from a sharp, hard tool on fresh bone, with their presence on the proximal epiphysis representing evidence of disarticulation at the knee joint.

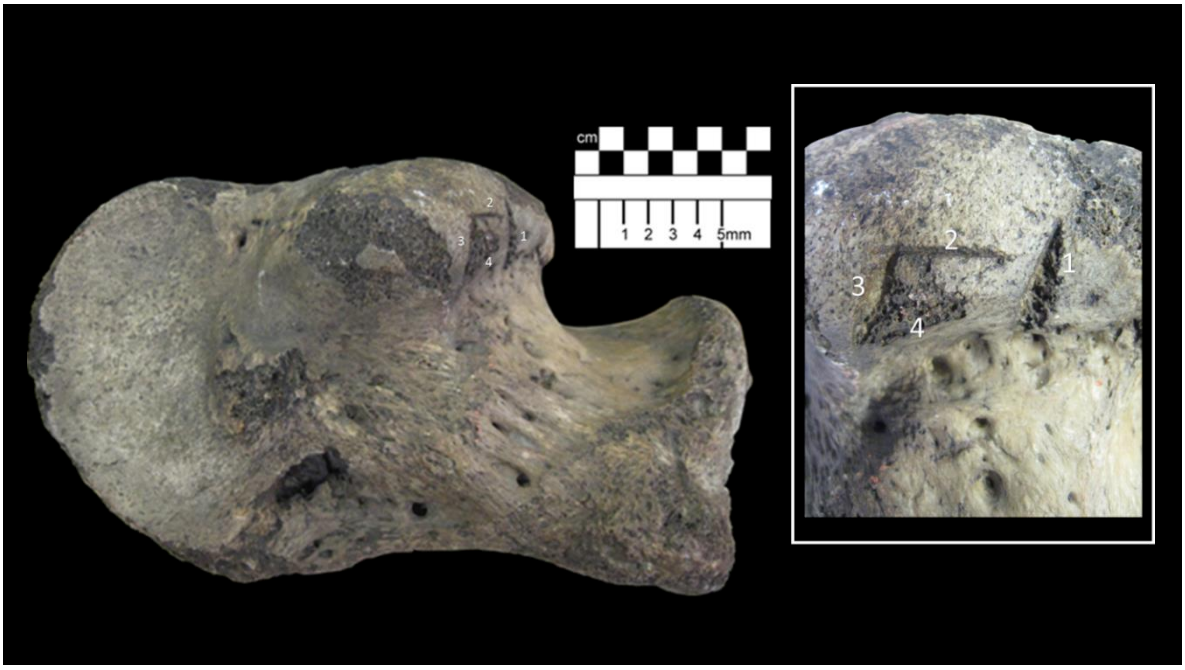

`

Appendix 3 figure 3: A *Mullerornis* sp. tarsometatarsus from an unknown locality on Madagascar (MNHN MAD6662) directly dated to 1,270–1,054 BP, exhibiting an open-ended linear anthropogenic groove on the lateral portion of the distal epiphysis (1) (16 mm length, 2.5 mm maximum depth, 3 mm maximum width), oriented laterally across the articular surface and angled towards the posterior distal epiphysis of the central condyle. The bevel of the proximal aspect has an even surface with no relief, the distal aspect and margin is more rugose, and the floor is an off-centre v-shape with a distal bias. This mark is consistent with a kerf made by a single-edged, sharp, hard blade cutting into fresh bone. The orientation and morphology of this kerf is consistent with a perimortem disarticulation of the lateral phalanges through a cut with an acute angle of incidence on fresh bone.

`

Appendix 3 figure 4: An *Aepyornis hildebrandti* tarsometatarsus from Antsirabe (MNHN MAD384), which failed AMS dating due to low collagen yield. This specimen exhibits a missing large triangular portion bisecting the medial tarsal diaphysis on its medial fascia (1). The distal fascia is uneven and shows signs of breakage. The proximal fascia of the cleft is even and straight with no relief, and extends past the limit of the distal fascia ending in a groove with a v-shaped floor. Two additional grooves with centrally oriented bevels and v-shaped floors are present; one parallel and adjacent to the distal edge of the cleft, the other on the posterior fascia of the medial condyle. The lateral toe is missing a small portion of the distal process (2). The exposed fascia is even and straight with well-defined limits and few striations. The morphology and orientation of the distal cleft is similar to chop marks found on long bones of lemurs(Perez et al. 2005) and may be further evidence of immobilizing the animals through hobbling (striking at their legs), as part of hunting. The morphology and orientation of the kerf found on the toe are consistent with disarticulation of the phalanges using a very sharp, bladed tool.

`

Appendix four

`

`

Appendix four: δ13C isotope records for Holocene megaherbivores of Madagascar

14C Lab number	Location	Region	Sample ID	Material	Species	14C Age Before Present ± 1σ	d13C (‰)	d13C Corrected for atmospheric CO2 changes (‰)	d13C Corrected for tissue differences (‰)	Reference
CAMS 143065	Antsirabe	Central highlands	NHMW uncatalogued5	Bone	*Hippopotamus* sp.	1215 ± 25	-25.5	-26.7	-31.7	1
CAMS 142540	Antsirabe	Central highlands	NHMW uncatalogued1	Bone	*Hippopotamus* sp.	1260 ± 25	-25	-26.2	-31.2	1
CAMS 143150	Antsirabe	Central highlands	NHMW uncatalogued2	Bone	*Hippopotamus* sp.	1800 ± 35	-24.9	-26.1	-31.1	1
CAMS 142638	Taolambiby	South	David Burney Collection uncatalogued	Bone	*Aldabrachelys* sp.	2535 ± 30	-23.1	-24.3	-29.3	1
CAMS 143050	Taolambiby	South	David Burney Collection uncatalogued	Bone	*Aldabrachelys* sp.	2500 ± 25	-23	-24.2	-29.2	1
CAMS 143099	Taolambiby	South	David Burney Collection uncatalogued	Bone	*Aldabrachelys* sp.	2605 ± 30	-22.9	-24.1	-29.1	1
CAMS 243052	Ampoza	West	UA uncatalogued (B3-13)	Bone	*Hippopotamus* sp.	2660 ± 40	-22.4	-23.6	-28.6	1
CAMS 142884	Amparihingidro	North	David Burney Collection (APG-3 320-330 cm)	Bone	*Aldabrachelys* sp.	6300 ± 50	-22	-23.2	-28.2	1
CAMS 143098	Taolambiby	South	David Burney Collection uncatalogued	Bone	*Aldabrachelys* sp.	3025 ± 35	-21	-21.9	-26.9	1

`

CAMS 142734	Taolambiby	South	David Burney Collection	Bone	*Hippopotamus* sp.	1440 ± 30	-20.3	-21.5	-26.5	1
CAMS 142636	Ankilibehandry	West	David Burney Collection (SQ 234. Oh)	Bone	*Hippopotamus* sp.	2275 ± 35	-19.9	-21.1	-26.1	1
CAMS 143108	Taolambiby	South	David Burney Collection uncatalogued	Bone	*Aldabrachelys* sp.	1745 ± 30	-19.1	-20.3	-25.3	1
CAMS 143060	Taolambiby	South	David Burney Collection	Bone	*Hippopotamus* sp.	2300 ± 50	-18.9	-20.1	-25.1	1
CAMS 142896	Taolambiby	South	David Burney Collection	Bone	*Hippopotamus* sp.	2905 ± 40	-18.6	-19.8	-24.8	1
CAMS 143059	Taolambiby	South	David Burney Collection	Bone	*Hippopotamus* sp.	2855 ± 35	-18.1	-19.3	-24.3	1
CAMS 142567	Taolambiby	South	David Burney Collection	Bone	*Hippopotamus* sp.	2470 ± 25	-17.6	-18.8	-23.8	1
CAMS 143057	Taolambiby	South	David Burney Collection uncatalogued	Bone	*Hippopotamus* sp.	1540 ± 45	-17.5	-18.7	-23.7	1
CAMS 142566	Taolambiby	South	David Burney Collection	Bone	*Hippopotamus* sp.	2550 ± 30	-17.3	-18.5	-23.5	1
CAMS 142640	Taolambiby	South	David Burney Collection	Bone	*Hippopotamus* sp.	2745 ± 40	-17.1	-18.3	-23.3	1
CAMS 143072	Andrahomana	South	David Burney Collection (AHA Vicinity G "D")	Bone	*Hippopotamus* sp.	1755 ± 25	-16.6	-17.8	-22.8	1
BM-1628	Ampoza	West	NHM (P) R5890	Bone	*Aldabrachelys* sp.	2035 ± 35	-27.3	-28.5	-33.5	2
BM-2125	Andolonomby	South	MNHN (Paléontologie) 1884-30	Bone	*Aldabrachelys* sp.	750 ± 370	-20.9	-22.1	-27.1	2

`

BM-1399	SW Madagascar, near Nosy Ve	South	BMNH (Z) 1984.1282	Bone	*Hippopotamus* sp.	1250 ± 50	-13.9	-15.1	-20.1	2
CAMS 143194	Anjohibe	North	UA 3591 (Field No. 92-M-396)	Bone	*Hippopotamus* sp.	4055 ± 40	-24.3	-25.5	-30.5	3
CAMS 144110	Anjohibe	North	UA 9570	Bone	*Hippopotamus* sp.	4815 ± 40	-24.1	-25.3	-30.3	3
CAMS 143120	Anjohibe	North	UA uncatalogued (Field No. 1992-M-395)	Bone	*Hippopotamus* sp.	3095 ± 30	-23.1	-24.3	-29.3	3
CAMS 142559	Anjohibe	North	UA 4917	Bone	*Hippopotamus* sp.	6310 ± 60	-23	-24.2	-29.2	3
CAMS 143195	Anjohibe	North	UA 3560 (Field No. 92-M-397)	Bone	*Hippopotamus* sp.	3455 ± 25	-21.6	-22.8	-27.8	3
CAMS 143068	Anjohibe	North	UA 3558 (Field No. 92-M-366)	Bone	*Hippopotamus* sp.	2890 ± 40	-21.1	-22.3	-27.3	3
CAMS 143193	Anjohibe	North	UA uncatalogued	Bone	*Hippopotamus* sp.	2635 ± 40	-21	-22.2	-27.2	3
NZA-16996 R-28139/7	Ampoza	West	David Burney Collection (Field No. AMO-1)	Bone	*Hippopotamus* sp.	2517 ± 40	-21.6	-22.8	-27.8	4
NZA-18525 R-28331/10a	Mananjary	North	AM uncatalogued	Bone	*Hippopotamus* sp.	2327 ± 40	-17.2	-18.4	-23.4	4
OZF856	Faux cap	South	9691C	Eggshell	"Thick" eggshell	4140 ± 50	-24.1	-25.3	-27.3	5
OZF855	Faux cap	South	9691B	Eggshell	"Thick" eggshell	4060 ± 50	-23.3	-24.5	-26.5	5
OZF854	Faux cap	South	9691A	Eggshell	"Thick" eggshell	3260 ± 50	-23.6	-24.8	-26.8	5
OZF514	Faux cap	South	9691E	Eggshell	"Thick" eggshell	1610 ± 40	-24	-25.2	-27.2	5
	Faux cap	South	9691D	Eggshell	"Thick" eggshell		-24.9	-26.1	-28.1	5
	Songoritelo	South	521007	Eggshell	"Thick" eggshell		-22.2	-23.4	-25.4	5

`

	Songoritelo	South	521008	Eggshell	"Thick" eggshell		-23.1	-24.3	-26.3	5
	Songoritelo	South	521009	Eggshell	"Thick" eggshell		-22.4	-23.6	-25.6	5
	Songoritelo	South	521010	Eggshell	"Thick" eggshell		-22.8	-24	-26	5
	Songoritelo	South	521011	Eggshell	"Thick" eggshell		-23	-24.2	-26.2	5
	Songoritelo	South	521012	Eggshell	"Thick" eggshell		-22.8	-24	-26	5
	Songoritelo	South	521013	Eggshell	"Thick" eggshell		-22.8	-24	-26	5
	Songoritelo	South	521014	Eggshell	"Thick" eggshell		-22.9	-24.1	-26.1	5
	Songoritelo	South	521015	Eggshell	"Thick" eggshell		-23.6	-24.8	-26.8	5
	Songoritelo	South	521016	Eggshell	"Thick" eggshell		-22.5	-23.7	-25.7	5
	Songoritelo	South	521017	Eggshell	"Thick" eggshell		-22.6	-23.8	-25.8	5
	Songoritelo	South	521018	Eggshell	"Thick" eggshell		-24.1	-25.3	-27.3	5
	Songoritelo	South	521019	Eggshell	"Thick" eggshell		-23.5	-24.7	-26.7	5
	Songoritelo	South	521020	Eggshell	"Thick" eggshell		-22.5	-23.7	-25.7	5
	Songoritelo	South	521021	Eggshell	"Thick" eggshell		-22.6	-23.8	-25.8	5
	Songoritelo	South	521022	Eggshell	"Thick" eggshell		-22.6	-23.8	-25.8	5
	Nasua	South	521023	Eggshell	"Thick" eggshell		-22.9	-24.1	-26.1	5
	Nasua	South	521024	Eggshell	"Thick" eggshell		-22.3	-23.5	-25.5	5
	Nasua	South	521025	Eggshell	"Thick" eggshell		-23.6	-24.8	-26.8	5
	Nasua	South	521026	Eggshell	"Thick" eggshell		-24.3	-25.5	-27.5	5
	Nasua	South	521027	Eggshell	"Thick" eggshell		-23.1	-24.3	-26.3	5
	Nasua	South	521028	Eggshell	"Thick" eggshell		-23.4	-24.6	-26.6	5
	Nasua	South	521029	Eggshell	"Thick" eggshell		-23	-24.2	-26.2	5
	Nasua	South	521030	Eggshell	"Thick" eggshell		-21.8	-23	-25	5
	Nasua	South	521031	Eggshell	"Thick" eggshell		-23.3	-24.5	-26.5	5
	Nasua	South	521032	Eggshell	"Thick" eggshell		-23.6	-24.8	-26.8	5

`

	Nasua	South	521033	Eggshell	"Thick" eggshell		-24.4	-25.6	-27.6	5
	Nasua	South	521034	Eggshell	"Thick" eggshell		-24.6	-25.8	-27.8	5
	Nasua	South	521035	Eggshell	"Thick" eggshell		-23.2	-24.4	-26.4	5
	Nasua	South	521036	Eggshell	"Thick" eggshell		-22.5	-23.7	-25.7	5
	Nasua	South	521037	Eggshell	"Thick" eggshell		-22.4	-23.6	-25.6	5
	Nasua	South	521038	Eggshell	"Thick" eggshell		-22.3	-23.5	-25.5	5
	Table Mountain	South	10500	Eggshell	"Thick" eggshell		-22.5	-23.7	-25.7	5
	Table Mountain	South	10501	Eggshell	"Thick" eggshell		-23.6	-24.8	-26.8	5
	Table Mountain	South	10502	Eggshell	"Thick" eggshell		-23.3	-24.5	-26.5	5
	Table Mountain	South	10503	Eggshell	"Thick" eggshell		-21.4	-22.6	-24.6	5
	Table Mountain	South	10504	Eggshell	"Thick" eggshell		-23.5	-24.7	-26.7	5
	Table Mountain	South	10505	Eggshell	"Thick" eggshell		-24.1	-25.3	-27.3	5
	Table Mountain	South	10506	Eggshell	"Thick" eggshell		-23.2	-24.4	-26.4	5
	Table Mountain	South	10507	Eggshell	"Thick" eggshell		-26	-27.2	-29.2	5
	Table Mountain	South	10508	Eggshell	"Thick" eggshell		-25	-26.2	-28.2	5
	Table Mountain	South	10509	Eggshell	"Thick" eggshell		-23.8	-25	-27	5
	Table Mountain	South	10510	Eggshell	"Thick" eggshell		-22.5	-23.7	-25.7	5
	Table Mountain	South	10511	Eggshell	"Thick" eggshell		-21.8	-23	-25	5
	Table Mountain	South	10512	Eggshell	"Thick" eggshell		-23.7	-24.9	-26.9	5
	Table Mountain	South	10513	Eggshell	"Thick" eggshell		-23	-24.2	-26.2	5
	Table Mountain	South	10514	Eggshell	"Thick" eggshell		-23.4	-24.6	-26.6	5
	Table Mountain	South	10515	Eggshell	"Thick" eggshell		-21.7	-22.9	-24.9	5
	Faux Cap	South	04EG01	Eggshell	"Thick" eggshell		-22.7	-23.9	-25.9	5
	Faux Cap	South	04EG02	Eggshell	"Thick" eggshell		-23.73	-24.9	-26.9	5
	Faux Cap	South	04EG03	Eggshell	"Thick" eggshell		-22.95	-24.2	-26.2	5

`

	Faux Cap	South	04EG04	Eggshell	"Thick" eggshell		-22.8	-24	-26	5
	Faux Cap	South	04EG05	Eggshell	"Thick" eggshell		-22.61	-23.8	-25.8	5
	Faux Cap	South	04EG06	Eggshell	"Thick" eggshell		-22.25	-23.5	-25.5	5
	Faux Cap	South	04EG07	Eggshell	"Thick" eggshell		-23.19	-24.4	-26.4	5
	Faux Cap	South	04EG08	Eggshell	"Thick" eggshell		-24.19	-25.4	-27.4	5
	Faux Cap	South	04EG09	Eggshell	"Thick" eggshell		-23.16	-24.4	-26.4	5
	Faux Cap	South	02EG01	Eggshell	"Thick" eggshell		-23.08	-24.3	-26.3	5
	Faux Cap	South	02EG02	Eggshell	"Thick" eggshell		-22.68	-23.9	-25.9	5
	Faux Cap	South	02EG05	Eggshell	"Thick" eggshell		-22.39	-23.6	-25.6	5
	Toliara	South	06EG02	Eggshell	"Thick" eggshell		-24	-25.2	-27.2	5
	Toliara	South	06EG03	Eggshell	"Thick" eggshell		-21.62	-22.8	-24.8	5
	Toliara	South	06EG04	Eggshell	"Thick" eggshell		-21.58	-22.8	-24.8	5
	Toliara	South	06EG05	Eggshell	"Thick" eggshell		-22.16	-23.4	-25.4	5
	Faux Cap	South	07MD30	Eggshell	"Thick" eggshell		-24	-25.2	-27.2	5
	Faux Cap	South	07MD31	Eggshell	"Thick" eggshell		-22.8	-24	-26	5
	Faux Cap	South	07MD32	Eggshell	"Thick" eggshell		-24.1	-25.3	-27.3	5
	Faux Cap	South	07MD34	Eggshell	"Thick" eggshell		-25.3	-26.5	-28.5	5
	Faux Cap	South	07MD36	Eggshell	"Thick" eggshell		-23.2	-24.4	-26.4	5
	Faux Cap	South	07MD05	Eggshell	"Thick" eggshell		-23.21	-24.4	-26.4	5
	Faux Cap	South	07MD06	Eggshell	"Thick" eggshell		-23	-24.2	-26.2	5
	Faux Cap	South	07MD07	Eggshell	"Thick" eggshell		-25	-26.2	-28.2	5
	Faux Cap	South	07MD08	Eggshell	"Thick" eggshell		-24.72	-25.9	-27.9	5
	Faux Cap	South	07MD09	Eggshell	"Thick" eggshell		-22.01	-23.2	-25.2	5
	Faux Cap	South	07MD19	Eggshell	"Thick" eggshell		-24.9	-26.1	-28.1	5
	Faux Cap	South	07MD28	Eggshell	"Thick" eggshell		-23.34	-24.5	-26.5	5

`

	Faux Cap	South	07MD47	Eggshell	"Thick" eggshell		-22.4	-23.6	-25.6	5
	Faux Cap	South	07MD49	Eggshell	"Thick" eggshell		-23.5	-24.7	-26.7	5
	Faux Cap	South	07MD20	Eggshell	"Thick" eggshell		-22.69	-23.9	-25.9	5
	Faux Cap	South	07MD22	Eggshell	"Thick" eggshell		-22.76	-24	-26	5
	Faux Cap	South	07MD23	Eggshell	"Thick" eggshell		-22.91	-24.1	-26.1	5
	Faux Cap	South	07MD26	Eggshell	"Thick" eggshell		-23.42	-24.6	-26.6	5
	Faux Cap	South	07MD67	Eggshell	"Thick" eggshell		-22	-23.2	-25.2	5
	Faux Cap	South	07MD77	Eggshell	"Thick" eggshell		-21.6	-22.8	-24.8	5
	Faux Cap	South	07MD50	Eggshell	"Thick" eggshell		-23.5	-24.7	-26.7	5
	Faux Cap	South	07MD57	Eggshell	"Thick" eggshell		-22	-23.2	-25.2	5
	Faux Cap	South	07MD01	Eggshell	"Thick" eggshell		-22.81	-24	-26	5
	Faux Cap	South	07MD02	Eggshell	"Thick" eggshell		-21.4	-22.6	-24.6	5
	Antsirabe	Central highlands	NHMW uncatalogued3	Bone	*Hippopotamus* sp.		-25.9	-27.1	-32.1	6
	Antsirabe	Central highlands	NHMW uncatalogued4	Bone	*Hippopotamus* sp.		-23.7	-24.9	-29.9	6
	Ampoza	West	UA uncatalogued (B2-25)	Bone	*Hippopotamus* sp.		-22.8	-24	-29	6
CAMS 150585	Taolambiby	South	David Burney Collection	Bone	*Hippopotamus* sp.	2620 ± 110	-22.7	-23.9	-28.9	6
	Anjohibe	North	UA uncatalogued (Field No. 1992-M-395)	Bone	*Hippopotamus* sp.		-22.5	-23.7	-28.7	6
	Anjohibe	North	UA uncatalogued	Bone	*Hippopotamus* sp.		-22.1	-23.3	-28.3	6
	Ampoza	West	UA uncatalogued (B3-117-P)	Bone	*Hippopotamus* sp.		-22.1	-23.3	-28.3	6

`

	Ampoza	West	UA uncatalogued (D3-4)	Bone	*Hippopotamus* sp.		-22	-23.2	-28.2	6
	Andrahomana	South	David Burney Collection (AHA -I C2)	Bone	*Aldabrachelys* sp.		-21.9	-23.1	-28.1	6
	Andrahomana	South	David Burney Collection (AHA-I layer 1 SQC4)	Bone	*Aldabrachelys* sp.		-19.2	-20.4	-25.4	6
	Andrahomana	South	David Burney Collection (AHA-H surface)	Bone	*Aldabrachelys* sp.		-18.2	-19.4	-24.4	6
	Andrahomana	South	David Burney Collection (AHA-J surface)	Bone	*Aldabrachelys* sp.		-18.2	-19.4	-24.4	6
	Andrahomana	South	David Burney Collection (AHA-I Old Spoil NE excavation)	Bone	*Hippopotamus* sp.		-17.4	-18.6	-23.6	6
	Andrahomana	South	David Burney Collection (AHA Vicinity G "C")	Bone	*Hippopotamus* sp.		-17.4	-18.6	-23.6	6
	Andrahomana	South	David Burney Collection (AHA Vicinity G "B")	Bone	*Hippopotamus* sp.		-16.6	-17.8	-22.8	6
	Beloha	South	07AEP02	Bone	*Mullerornis modestus*		-19.62	-20.8	-25.8	7
	Beloha	South	07AEP03	Bone	*Mullerornis modestus*		-21.1	-22.3	-27.3	7
	Beloha	South	07AEP06	Bone	*Mullerornis modestus*		-19.8	-21	-26	7

`

	Beloha	South	07AEP08	Bone	*Mullerornis modestus*		-19.6	-20.8	-25.8	7
	Beloha	South	07AEP09	Bone	*Mullerornis modestus*		-19.6	-20.8	-25.8	7
	Toliara	South	06EG06	Eggshell	*Mullerornis* eggshell		-22.31	-23.5	-25.5	7
	Toliara	South	06EG07	Eggshell	*Mullerornis* eggshell		-22.56	-23.8	-25.8	7
	Faux Cap	South	07MD29	Eggshell	*Mullerornis* eggshell		-21.9	-23.1	-25.1	7
	Faux Cap	South	07MD44	Eggshell	*Mullerornis* eggshell		-21.9	-23.1	-25.1	7
	Faux Cap	South	07MD21	Eggshell	*Mullerornis* eggshell		-22.23	-23.4	-25.4	7
	Faux Cap	South	07MD24	Eggshell	*Mullerornis* eggshell		-23.18	-24.4	-26.4	7
	Faux Cap	South	07MD25	Eggshell	*Mullerornis* eggshell		-22.94	-24.1	-26.1	7
	Faux Cap	South	07MD69	Eggshell	*Mullerornis* eggshell		-22.4	-23.6	-25.6	7
	Faux Cap	South	07MD63	Eggshell	*Mullerornis* eggshell		-21.8	-23	-25	7
	Beloha	South	07AEP04	Bone	*Aepyornis maximus*		-22.7	-23.9	-28.9	7
	Beloha	South	07AEP10	Bone	*Aepyornis maximus*		-21.7	-22.9	-27.9	7
UB31590	Ilaka	West	USNM A605209	Bone	*Aepyornis maximus*	9345 ± 66	-21.8	-23	-28	This paper
OxA-34776	Amposa	West	NHM A2142	Bone	*Vorombe titan*	3381 ± 24	-23.3	-24.5	-29.5	This paper
OxA-34774	Amposa	West	NHM A2145	Bone	*Vorombe titan*	2744 ± 25	-22.6	-23.8	-28.8	This paper
OxA-33534	Ankazoabo	West	MAD377	Bone	*Vorombe titan*	2540 ± 26	-23.3	-24.5	-29.5	This paper

`

OxA-34775	Amposa	West	NHM A2144	Bone	*Vorombe titan*	2509 ± 23	-23.8	-25	-30	This paper
OxA-33532	Ankazoabo	West	MAD368	Bone	*Vorombe titan*	2499 ± 25	-22.8	-24	-29	This paper
OxA-33531	Ankazoabo	West	MAD 364	Bone	*Vorombe titan*	2470 ± 24	-23.2	-24.4	-29.4	This paper
OxA-33533	Ankazoabo	West	MAD 6770	Bone	*Vorombe titan*	2112 ± 25	-23.9	-25.1	-30.1	This paper
OxA-33572	Belo sur mer	West	MAD 8813	Bone	*Vorombe titan*	2047 ± 29	-23.4	-24.6	-29.6	This paper
OxA-33573	Belo sur mer	West	MAD 6655	Bone	*Vorombe titan*	1503 ± 29	-21.7	-22.9	-27.9	This paper
OxA-33536	Belo sur mer	West	MAD 383	Bone	*Vorombe titan*	1442 ± 24	-23.5	-24.7	-29.7	This paper
OxA-33535	Ankazoabo	West	JH 63	Bone	*Vorombe titan*	1237 ± 24	-21.9	-23.1	-28.1	This paper
UB29726	Lamboharana	South	MAD6768	Bone	*Mullerornis modestus*	5597 ± 40	-20.2	-21.4	-26.4	This paper
UB29725	South west coast	South	MAD6662	Bone	*Mullerornis modestus*	1296 ± 32	-21.6	-22.8	-27.8	This paper
UB29724	Antsirabe	Central highlands	A31834	Bone	*Aepyornis hildebrandti*	5282 ± 39	-14.1	-15.3	-20.3	This paper
OxA-34327	Antsirabe	Central highlands	2014/0238/0006	Bone	*Aepyornis hildebrandti*	3112 ± 31	-14.6	-15.8	-20.8	This paper
OxA-33537	Antsirabe	Central highlands	2014/0238/0037	Bone	*Aepyornis hildebrandti*	2177 ± 27	-15.1	-16.3	-21.3	This paper
OxA-34758	Masinandreina	Central highlands	PMU 34(A46)	Bone	*Aepyornis hildebrandti*	1537 ± 25	-17.1	-18.3	-23.3	This paper
OxA-34326	Antsirabe	Central highlands	2014/0238/0003	Bone	*Aepyornis hildebrandti*	1461 ± 28	-13.4	-14.6	-19.6	This paper
OxA-34328	Antsirabe	Central highlands	2014/0238/0012	Bone	*Aepyornis hildebrandti*	1349 ± 28	-17	-18.2	-23.2	This paper

1. Crowley, B. E. (2010). A refined chronology of prehistoric Madagascar and the demise of the megafauna. *Quaternary Science Reviews*, *29*(19-20), 2591-2603.
2 Burleigh, R., & Arnold, E. N. (1986, February). Age and dietary differences of recently extinct Indian Ocean tortoises (Geochelone s. lat.) revealed by carbon isotope analysis. In *Proc. R. Soc. Lond. B 227*(1246),137-144).
3. Samonds, K. E., Parent, S. N., Muldoon, K. M., Crowley, E., & Godfrey, L. R. (2010). Rock matrix surrounding subfossil lemur skull yields diverse collection of

`

mammalian subfossils: implications for reconstructing Madagascar’s paleoenvironments. *Malagasy Nature*, *4*, 1-16.

4. Burney, D. A., Burney, L. P., Godfrey, L. R., Jungers, W. L., Goodman, S. M., Wright, H. T., & Jull, A. T. (2004). A chronology for late prehistoric Madagascar. *Journal of Human Evolution*, *47*(1-2), 25-63.

5. Clarke, S. J., Miller, G. H., Fogel, M. L., Chivas, A. R., & Murray-Wallace, C. V. (2006). The amino acid and stable isotope biogeochemistry of elephant bird (*Aepyornis*) eggshells from southern Madagascar. *Quaternary Science Reviews*, *25*(17-18), 2343-2356.

6. Godfrey, L. R., & Crowley, B. E. (2016, July). Madagascar's ephemeral palaeo-grazer guild: who ate the ancient C4 grasses?. In *Proc. R. Soc. 283*(1834),20160360.

7. Tovondrafale, T., Razakamanana, T., Hiroko, K., & Rasoamiaramanan, A. (2014). Paleoecological analysis of elephant bird (Aepyornithidae) remains from the Late Pleistocene and Holocene formations of southern Madagascar. *Malagasy Nat*, *8*, 1-13.